Publishing House ASV

begell house, inc. publishers

Scientific coordination is carried out by the Russian Academy of Architecture and Construction Sciences (RAACS)

Volume 14 • Issue 3 • 2018

ISSN 2588-0195 (Online)
ISSN 2587-9618 (Print) Continues ISSN 1524-5845

International Journal for

Computational Civil and Structural Engineering

Международный журнал по расчету гражданских и строительных конструкций

http://raasn.ru/public.php
http://ijccse.iasv.ru/index.php/IJCCSE

DOI: 10.22337/2587-9618
GICID: 71.0000.1500.2830

EXECUTIVE EDITOR

Vladimir I. Travush,
Full Member of RAACS, Professor, Dr.Sc.,
Vice-President of the Russian Academy
of Architecture and Construction Sciences;
Urban Planning Institute
of Residential and Public Buildings;
24, Ulitsa Bolshaya Dmitrovka, 107031, Moscow, Russia

EDITOR-IN-CHIEF

Vladimir N. Sidorov,
Corresponding Member of RAACS, Professor, Dr.Sc.,
Russian University of Transport (RUT – MIIT);
Russian University of Friendship of Peoples;
Moscow Institute of Architecture (State Academy);
Perm National Research Polytechnic University;
Kielce University of Technology (Poland);
9b9, Obrazcova Street, Moscow, 127994, Russia

EDITORIAL DIRECTOR

Valery I. Telichenko,
Full Member of RAACS, Professor, Dr.Sc.,
The First Vice-President of the Russian Academy
of Architecture and Construction Sciences;
National Research Moscow State University
of Civil Engineering;
24, Ulitsa Bolshaya Dmitrovka, 107031, Moscow, Russia

MANAGING EDITOR

Nadezhda S. Nikitina,
Professor, Ph.D.,
Director of ASV Publishing House;
National Research Moscow State University
of Civil Engineering;
26, Yaroslavskoe Shosse, 129337, Moscow, Russia

ASSOCIATE EDITORS

Pavel A. Akimov,
Full Member of RAACS, Professor, Dr.Sc.,
Executive Scientific Secretary of the Russian Academy
of Architecture and Construction Sciences;
Scientific Research Center "STADYO";
Tomsk State University of Architecture and Building;
Russian University of Friendship of Peoples;
24, Ul. Bolshaya Dmitrovka, 107031, Moscow, Russia

Alexander M. Belostotsky,
Corresponding Member of RAACS, Professor, Dr.Sc.,
Research & Development Center "STADYO";
Russian University of Transport (RUT – MIIT);
Russian University of Friendship of Peoples;
Perm National Research Polytechnic University;
Tomsk State University of Architecture and Building;
8th Floor, 18, ul. Tretya Yamskogo Polya,
125040, Moscow, Russia

Vladimir Belsky, Ph.D.,
Dassault Systèmes Simulia;
1301 Atwood Ave Suite 101W
02919 Johnston, RI, United States

Mikhail Belyi, Professor, Dr.Sc.,
Dassault Systèmes Simulia;
1301 Atwood Ave Suite 101W
02919 Johnston, RI, United States

Vitaly Bulgakov, Professor, Dr.Sc.,
SemanticPro;
Boston, USA

Nikolai P. Osmolovskii, Professor, Dr.Sc.,
Systems Research Institute, Polish Academy of
Sciences; Kazimierz Pulaski University
of Technology and Humanities in Radom;
29, ul. Malczewskiego, 26-600, Radom, Poland

Gregory P. Panasenko, Professor, Dr.Sc.,
Equipe d'Analise Numerique; NMR CNRS 5585
University Gean Mehnet;
23 rue. P.Michelon 42023, St.Etienne, France

Leonid A. Rozin, Professor, Dr.Sc.,
Peter the Great Saint-Petersburg
Polytechnic University;
29, Ul. Politechnicheskaya,
195251 Saint-Petersburg, Russia

Scientific coordination is carried out by the Russian Academy of Architecture and Construction Sciences (RAACS)

PUBLISHER

ASV Publishing House
(ООО «Издательство АСВ»)
19/1,12, Yaroslavskoe Shosse, 120338, Moscow, Russia
Tel. +7(925)084-74-24; E-mail: iasv@iasv.ru; Интернет-сайт: http://iasv.ru/

ADVISORY EDITORIAL BOARD

Robert M. Aloyan,
Corresponding Member
of RAACS, Professor, Dr.Sc.,
Ivanovo State Polytechnic
University; 20, Ulitsa 8 Marta,
Ivanovo, 153037, Russia

Vladimir I. Andreev,
Full Member of RAACS,
Professor, Dr.Sc.,
National Research Moscow State
University of Civil Engineering;
Yaroslavskoe Shosse 26,
Moscow, 129337, Russia

Mojtaba Aslami, Ph.D,
Fasa University; Daneshjou blvd,
Fasa, Fars Province, Iran

Klaus-Jurgen Bathe, Professor
Massachusetts Institute
of Technology;
Cambridge, MA 02139, USA

Yuri M. Bazhenov,
Full Member of RAACS,
Professor, Dr.Sc.,
National Research Moscow State
University of Civil Engineering;
Yaroslavskoe Shosse 26,
Moscow, 129337, Russia

Alexander T. Bekker,
Corresponding Member
of RAACS, Professor, Dr.Sc.,
Far Eastern Federal University;
Russian Academy of Architecture
and Construction Sciences;
8, Sukhanova Street, Vladivostok,
690950, Russia

Tomas Bock, Professor, Dr.-Ing.,
Technical University of Munich,
Arcisstrasse 21, D-80333
Munich, Germany

Jan Buynak, Professor, Ph.D.,
University of Žilina;
1, Univerzitná, Žilina, 010 26,
Slovakia

Evgeniy M. Chernishov,
Full Member of RAACS,
Professor, Dr.Sc.,
Voronezh State Technical
University; 14, Moscow Avenue,
Voronezh, 394026, Russia

Vladimir T. Erofeev,
Full Member of RAACS,
Professor, Dr.Sc.,
Ogarev Mordovia State
University; 68, Bolshevistskaya
Str., Saransk 430005, Republic of
Mordovia, Russia

Victor S. Fedorov,
Full Member of RAACS,
Professor, Dr.Sc.,
Russian University of Transport
(RUT – MIIT);
9b9 Obrazcova Street, Moscow,
127994, Russia

Sergey V. Fedosov,
Full Member of RAACS,
Professor, Dr.Sc.,
Ivanovo State Polytechnic
University;
20, Ulitsa 8 Marta, Ivanovo,
153037, Russia

Sergiy Yu. Fialko,
Professor, Dr.Sc.,
Cracow University of
Technology;
24, Warszawska Street, Kraków,
31-155, Poland

Vladimir G. Gagarin,
Corresponding Member
of RAACS, Professor, Dr.Sc.,
Research Institute of Building
Physics of Russian Academy
of Architecture and Construction
Sciences;
21, Lokomotivny Proezd,
Moscow, 127238, Russia

Alexander S. Gorodetsky,
Foreign Member of RAACS,
Professor, Dr.Sc.,
LIRA SAPR Ltd.;
7a Kiyanovsky Side Street
(Pereulok), Kiev, 04053, Ukraine

Vyatcheslav A. Ilyichev,
Full Member of RAACS,
Professor, Dr.Sc.,
Russian Academy of Architecture
and Construction Sciences;
Podzemproekt Ltd.;
24, Ulitsa Bolshaya Dmitrovka,
Moscow, 107031, Russia

Marek Iwański,
Professor, Dr.Sc.,
Kielce University of Technology;
7, al. Tysiąclecia Państwa
Polskiego Kielce, 25 – 314,
Poland

Sergey Yu. Kalashnikov,
Advisor of RAACS,
Professor, Dr.Sc.,
Volgograd State Technical
University; 28, Lenin avenue,
Volgograd, 400005, Russia

Semen S. Kaprielov,
Corresponding Member
of RAACS, Professor, Dr.Sc.,
Research Center of Construction;
6, 2nd Institutskaya St., Moscow,
109428, Russia

Nikolay I. Karpenko,
Full Member of RAACS,
Professor, Dr.Sc.,
Research Institute of Building
Physics of Russian Academy
of Architecture and Construction
Sciences; Russian Academy of
Architecture and Construction
Sciences; 21, Lokomotivny
Proezd, Moscow, 127238, Russia

Vladimir V. Karpov,
Professor, Dr.Sc.,
Saint Petersburg State University
of Architecture and Civil
Engineering;
4, 2-nd Krasnoarmeiskaya Steet,
Saint Petersburg, 190005, Russia

Galina G. Kashevarova,
Corresponding Member
of RAACS, Professor, Dr.Sc.,
Perm National Research
Polytechnic University;
29 Komsomolsky pros., Perm,
Perm Krai, 614990, Russia

John T. Katsikadelis,
Professor, Dr.Eng, PhD, Dr.h.c.,
National Technical University of
Athens; Zografou Campus
9, Iroon Polytechniou str
15780 Zografou, Greece

Vitaly I. Kolchunov,
Full Member of RAACS,
Professor, Dr.Sc.,
Southwest State University;
Russian Academy of Architecture
and Construction Sciences;
94, 50 let Oktyabrya, Kursk,
305040, Russia

Markus König, Professor
Ruhr-Universität Bochum;
150, Universitätsstraße, Bochum,
44801, Germany

Sergey B. Kositsin,
Professor, Dr.Sc.,
Russian University of Transport
(RUT – MIIT); 9b9 Obrazcova
Street, Moscow, 127994, Russia

Sergey B. Krylov,
Corresponding Member
of RAACS, Professor, Dr.Sc.,
Research Center of Construction;
6, 2nd Institutskaya St., Moscow,
109428, Russia

Sergey V. Kuznetsov,
Professor, Dr.Sc.,
Ishlinsky Institute for Problems
in Mechanics of the Russian
Academy of Sciences;
101-1, Prosp. Vernadskogo,
Moscow, 119526, Russia

Vladimir V. Lalin,
Professor, Dr.Sc.,
Peter the Great Saint-Petersburg
Polytechnic University;
29, Ul. Politechnicheskaya,
Saint-Petersburg, 195251, Russia

Leonid S. Lyakhovich,
Full Member of RAACS,
Professor, Dr.Sc.,
Tomsk State University
of Architecture and Building;
2, Solyanaya Sq., Tomsk,
634003, Russia

Rashid A. Mangushev,
Corresponding Member
of RAACS, Professor, Dr.Sc.,
Saint Petersburg State University
of Architecture and Civil
Engineering;
4, 2-nd Krasnoarmeiskaya Steet,
Saint Petersburg, 190005, Russia

Ilizar T. Mirsayapov,
Advisor of RAACS,
Professor, Dr.Sc., Kazan State
University of Architecture and
Engineering; 1, Zelenaya Street,
Kazan, 420043, Republic
of Tatarstan, Russia

Vladimir L. Mondrus,
Corresponding Member
of RAACS, Professor, Dr.Sc.,
National Research Moscow State
University of Civil Engineering;
Yaroslavskoe Shosse 26,
Moscow, 129337, Russia

Valery I. Morozov,
Corresponding Member
of RAACS, Professor, Dr.Sc.,
Saint Petersburg State University
of Architecture and Civil
Engineering;
4, 2-nd Krasnoarmeiskaya Steet,
Saint Petersburg, 190005, Russia

Anatoly V. Perelmuter,
Foreign Member of RAACS,
Professor, Dr.Sc., SCAD Soft;
Office 1,2, 3a Osvity street,
Kiev, 03037, Ukraine

Alexey N. Petrov,
Advisor of RAACS, Professor,
Dr.Sc., Petrozavodsk State
University; 33, Lenina Prospect,
Petrozavodsk, 185910,
Republic of Karelia, Russia

Vladilen V. Petrov,
Full Member of RAACS,
Professor, Dr.Sc.,
Yuri Gagarin State Technical
University of Saratov;
77 Politechnicheskaya Street,
Saratov, 410054, Russia

Jerzy Z. Piotrowski,
Professor, Dr.Sc.,
Kielce University of Technology;
al. Tysiąclecia Państwa Polskiego
7, Kielce, 25 – 314, Poland

Chengzhi Qi, Professor, Dr.Sc.,
Beijing University of Civil
Engineering and Architecture;
1, Zhanlanlu, Xicheng District,
Beijing, China

Vladimir P. Selyaev,
Full Member of RAACS,
Professor, Dr.Sc., Ogarev
Mordovia State University;
68, Bolshevistskaya Str., Saransk
430005, Republic of Mordovia,
Russia

Eun Chul Shin,
Professor, Ph.D.,
Incheon National University;
(Songdo-dong)119 Academy-ro,
Yeonsu-gu, Incheon, Korea

D.V. Singh,
Professor, Ph.D,
University of Roorkee;
Roorkee, India, 247667

Wacław Szcześniak,
Foreign Member of RAACS,
Professor, Dr.Sc.,
Lublin University of Technology;
Ul. Nadbystrzycka 40,
20-618 Lublin, Poland

Tadatsugu Tanaka,
Professor, Dr.Sc.,
Tokyo University; 7-3-1 Hongo,
Bunkyo, Tokyo, 113-8654, Japan

Josef Vican,
Professor, Ph.D,
University of Žilina;
1, Univerzitná, Žilina, 010 26,
Slovakia

Zbigniew Wojcicki,
Professor, Dr.Sc.,
Wroclaw University
of Technology;
11 Grunwaldzki Sq., 50-377,
Wrocław, Poland

Artur Zbiciak, Ph.D.,
Warsaw University of
Technology;
Pl. Politechniki 1, 00-661
Warsaw, Poland

Segrey I. Zhavoronok, Ph.D.,
Institute of Applied Mechanics of
Russian Academy of Sciences;
Moscow Aviation Institute
(National Research University);
7, Leningradsky Prt.,
Moscow, 125040, Russia

Askar Zhussupbekov,
Professor, Dr.Sc.,
Eurasian National University;
5, Munaitpassov street, Astana,
010000, Kazakhstan

TECHNICAL EDITOR

Taymuraz B. Kaytukov,
Advisor of RAACS,
Associate Professor, Ph.D.,
Deputy Executive Scientific
Secretary of the Russian
Academy of Architecture and
Construction Sciences;
24, Ul. Bolshaya Dmitrovka,
107031, Moscow, Russia

EDITORIAL TEAM

Alexander V. Kuzmin,
Full Member of RAACS,
President of the Russian Academy of Architecture and Construction Sciences;
Research Center of Construction;
24, Ulitsa Bolshaya Dmitrovka,
107031, Moscow, Russia

Vadim K. Akhmetov, Professor, Dr.Sc., National Research Moscow State University of Civil Engineering; 26, Yaroslavskoe Shosse, 129337 Moscow, Russia

Pavel A. Akimov,
Full Member of RAACS,
Professor, Dr.Sc., Executive Scientific Secretary of the Russian Academy of Architecture and Construction Sciences;
Scientific Research Center "STADYO"; Tomsk State University of Architecture and Building; Russian University of Friendship of Peoples;
24, Ul. Bolshaya Dmitrovka,
107031, Moscow, Russia

Alexander M. Belostotsky,
Corresponding Member of RAACS, Professor, Dr.Sc.,
Research & Development Center "STADYO"; Russian University of Transport (RUT – MIIT); Russian University of Friendship of Peoples; Perm National Research Polytechnic University; Tomsk State University of Architecture and Building;
8th Floor, 18, ul. Tretya Yamskogo Polya,
125040, Moscow, Russia

Vladimir Belsky, Ph.D.,
Dassault Systèmes Simulia;
1301 Atwood Ave Suite 101W
02919 Johnston, RI, United States

Mikhail Belyi, Professor, Dr.Sc.,
Dassault Systèmes Simulia;
1301 Atwood Ave Suite 101W
02919 Johnston, RI, United States

Vitaly Bulgakov, Professor,
Dr.Sc., SemanticPro; Boston, USA

Charles El Nouty, Professor,
Dr.Sc., LAGA Paris-13 Sorbonne Paris Cite; 99 avenue J.B. Clément,
93430 Villetaneuse, France

Natalya N. Fedorova, Professor,
Dr.Sc., Novosibirsk State University of Architecture and Civil Engineering (SIBSTRIN);
113 Leningradskaya Street,
Novosibirsk, 630008, Russia

Darya Filatova, Professor,
Dr.Sc., Kielce University of Tecnology; 7, al. Tysiąclecia Państwa Polskiego, Kielce, 25-314, Poland

Vladimir Ya. Gecha, Professor,
Dr.Sc., Research and Production Enterprise All-Russia Scientific-Research Institute of Electromechanics with Plant Named after A.G. Iosiphyan;
30, Volnaya Street, Moscow,
105187, Russia

Taymuraz B. Kaytukov,
Advisor of RAACS, Ph.D,
Deputy Executive Scientific Secretary of the Russian Academy of Architecture and Construction Sciences;
24, Ul. Bolshaya Dmitrovka,
107031, Moscow, Russia

Amirlan A. Kusainov,
Foreign Member of RAACS,
Professor, Dr.Sc.,
Kazakh-American University,
9, Toraighyrov Str., Almaty,
050043, Republic of Kazakhstan

Nadezhda S. Nikitina,
Professor, Ph.D., Director of ASV Publishing House;
National Research Moscow State University of Civil Engineering;
26, Yaroslavskoe Shosse, 129337 Moscow, Russia

Nikolai P. Osmolovskii,
Professor, Dr.Sc.,
Systems Research Institute Polish Academy of Sciences;
Kazimierz Pulaski University of Technology and Humanities in Radom; 29, ul. Malczewskiego, 26-600, Radom, Poland

Gregory P. Panasenko, Professor,
Dr.Sc., Equipe d'Analise Numerique NMR CNRS 5585 University Gean Mehnet;
23 rue. P.Michelon 42023,
St.Etienne, France

Leonid A. Rozin,
Professor, Dr.Sc.,
Peter the Great Saint-Petersburg Polytechnic University;
29, Ul. Politechnicheskaya,
195251 Saint-Petersburg, Russia

Marina V. Shitikova,
Professor, Dr.Sc.,
Voronezh State Technical University;
14, Moscow Avenue,
Voronezh, 394026, Russia

Igor L. Shubin,
Corresponding Member of RAACS, Professor, Dr.Sc.,
Research Institute of Building Physics of Russian Academy of Architecture and Construction Sciences;
21, Lokomotivny Proezd,
Moscow, 127238, Russia

Vladimir N. Sidorov,
Advisor of RAACS,
Professor, Dr.Sc.,
Russian University of Transport (RUT – MIIT); Russian University of Friendship of Peoples; Moscow Institute of Architecture (State Academy); Perm National Research Polytechnic University; Kielce University of Technology (Poland);
9b9 Obrazcova Street, Moscow,
127994, Russia

Valery I. Telichenko,
Full Member of RAACS,
Professor, Dr.Sc.,
The First Vice-President of the Russian Academy of Architecture and Construction Sciences;
National Research Moscow State University of Civil Engineering;
24, Ulitsa Bolshaya Dmitrovka,
107031, Moscow, Russia

Vladimir I. Travush,
Full Member of RAACS,
Professor, Dr.Sc.,
Vice-President of the Russian Academy of Architecture and Construction Sciences;
Urban Planning Institute of Residential and Public Buildings;
24, Ulitsa Bolshaya Dmitrovka,
107031, Moscow, Russia

INVITED REVIEWERS

Akimbek A. Abdikalikov, Professor, Dr.Sc.,
Kyrgyz State University of Construction, Transport and Architecture n.a. N. Isanov;
34 Maldybayeva Str., Bishkek, 720020, Biskek, Kyrgyzstan

Irina N. Afanasyeva, Ph.D.,
University of Florida; Gainesville, FL 32611, USA

Ján Čelko, Professor, PhD, Ing.,
University of Žilina; Univerzitná 1, 010 26, Žilina, Slovakia

Tatyana L. Dmitrieva, Professor, Dr.Sc.,
Irkutsk National Research Technical University; 83, Lermontov street, Irkutsk, 664074, Russia

Petr P. Gaidzhurov, Professor, Dr.Sc.,
Don State Technical University; 1, Gagarina Square, Rostov-on-Don, 344000, Russia

Jacek Grosel, Associate Professor, Dr inz.
Wroclaw University of Technology; 11 Grunwaldzki Sq., 50-377, Wrocław, Poland

Stanislaw Jemioło, Professor, Dr.Sc.,
Warsaw University of Technology; 1, Pl. Politechniki, 00-661, Warsaw, Poland

Konstantin I. Khenokh, M.Ing., M.Sc.,
General Dynamics C4 Systems; 8201 E McDowell Rd, Scottsdale, AZ 85257, USA

Christian Koch, Dr.-Ing.,
Ruhr-Universität Bochum;
Lehrstuhl für Informatik im Bauwesen, Gebäude IA, 44780, Bochum, Germany

Gaik A. Manuylov, Professor, Ph.D.,
Moscow State University of Railway Engineering; 9, Obraztsova Street, Moscow, 127994, Russia

Marina L. Mozgaleva, Professor, Dr.Sc.,
National Research Moscow State University of Civil Engineering;
26, Yaroslavskoe Shosse, Moscow, 129337, Russia

Alexander S. Noskov, Professor, Dr.Sc.,
Ural Federal University named after the first President of Russia B.N. Yeltsin;
19 Mira Street, Ekaterinburg, 620002, Russia

Grzegorz Świt, Professor, Dr.hab. Inż.,
Kielce University of Technology; 7, al. Tysiąclecia Państwa Polskiego, Kielce, 25 – 314, Poland

AIMS AND SCOPE

The aim of the Journal is to advance the research and practice in structural engineering through the application of computational methods. The Journal will publish original papers and educational articles of general value to the field that will bridge the gap between high-performance construction materials, large-scale engineering systems and advanced methods of analysis.

The scope of the Journal includes papers on computer methods in the areas of structural engineering, civil engineering materials and problems concerned with multiple physical processes interacting at multiple spatial and temporal scales. The Journal is intended to be of interest and use to researches and practitioners in academic, governmental and industrial communities.

ОБЩАЯ ИНФОРМАЦИЯ О ЖУРНАЛЕ

International Journal for Computational Civil and Structural Engineering

(Международный журнал по расчету гражданских и строительных конструкций)

Международный научный журнал "International Journal for Computational Civil and Structural Engineering (Международный журнал по расчету гражданских и строительных конструкций)" (IJCCSE) является ведущим научным периодическим изданием по направлению «Инженерные и технические науки», издаваемым, начиная с 1999 года (ISSN 2588-0195 (Online); ISSN 2587-9618 (Print) Continues ISSN 1524-5845). В журнале на высоком научно-техническом уровне рассматриваются проблемы численного и компьютерного моделирования в строительстве, актуальные вопросы разработки, исследования, развития, верификации, апробации и приложений численных, численно-аналитических методов, программно-алгоритмического обеспечения и выполнения автоматизированного проектирования, мониторинга и комплексного наукоемкого расчетно-теоретического и экспериментального обоснования напряженно-деформированного (и иного) состояния, прочности, устойчивости, надежности и безопасности ответственных объектов гражданского и промышленного строительства, энергетики, машиностроения, транспорта, биотехнологий и других высокотехнологичных отраслей.

В редакционный совет журнала входят известные российские и зарубежные деятели науки и техники (в том числе академики, члены-корреспонденты, иностранные члены, почетные члены и советники Российской академии архитектуры и строительных наук). Основной критерий отбора статей для публикации в журнале − их высокий научный уровень, соответствие которому определяется в ходе высококвалифицированного рецензирования и объективной экспертизы, поступающих в редакцию материалов.

Журнал входит в Перечень ВАК РФ ведущих рецензируемых научных изданий, в которых должны быть опубликованы основные научные результаты диссертаций на соискание ученой степени кандидата наук, на соискание ученой степени доктора наук по отраслям науки

- 01.00.00 Физико-математические науки;
- 05.00.00 Технические науки

и группам специальностей

- 01.02.00 Механика
- 05.13.00 Информатика, вычислительная техника и управление
- 05.23.00 Строительство и архитектура.

В Российской Федерации журнал индексируется Российским индексом научного цитирования (РИНЦ).

Журнал входит в базу данных Russian Science Citation Index (RSCI), полностью интегрированную с платформой Web of Science. Журнал имеет международный статус и высылается в ведущие библиотеки и научные организации мира.

Издатели журнала – *Издательство Ассоциации строительных высших учебных заведений /АСВ/* (Россия, г. Москва) и до 2017 года *Издательский дом Begell House Inc.* (США, г. Нью-Йорк). Официальными партнерами издания является *Российская академия архитектуры и строительных наук* (*РААСН*), осуществляющая научное курирование издания, и *Научно-исследовательский центр СтаДиО* (ЗАО НИЦ СтаДиО).

Цели журнала – демонстрировать в публикациях российскому и международному профессиональному сообществу новейшие достижения науки в области вычислительных методов решения фундаментальных и прикладных технических задач, прежде всего в области строительства.

Задачи журнала:

- предоставление российским и зарубежным ученым и специалистам возможности публиковать результаты своих исследований;
- привлечение внимания к наиболее актуальным, перспективным, прорывным и интересным направлениям развития и приложений численных и численно-аналитических методов решения фундаментальных и прикладных технических задач, совершенствования технологий математического, компьютерного моделирования, разработки и верификации реализующего программно-алгоритмического обеспечения;
- обеспечение обмена мнениями между исследователями из разных регионов и государств.

Тематика журнала. К рассмотрению и публикации в журнале принимаются аналитические материалы, научные статьи, обзоры, рецензии и отзывы на научные публикации по фундаментальным и прикладным вопросам технических наук, прежде всего в области строительства. В журнале также публикуются информационные материалы, освещающие научные мероприятия и передовые достижения Российской академии архитектуры и строительных наук, научно-образовательных и проектно-конструкторских организаций.

Тематика статей, принимаемых к публикации в журнале, соответствует его названию и охватывает направления научных исследований в области разработки, исследования и приложений численных и численно-аналитических методов, программного обеспечения, технологий компьютерного моделирования в решении прикладных задач в области строительства, а также соответствующие профильные специальности, представленные в диссертационных советах профильных образовательных организациях высшего образования.

Редакционная политика. Политика редакционной коллегии журнала базируется на современных юридических требованиях в отношении авторского права, законности, плагиата и клеветы, изложенных в законодательстве Российской Федерации, и этических принципах, поддерживаемых сообществом ведущих издателей научной периодики.

За публикацию статей плата с авторов не взымается. Публикация статей в журнале бесплатная. На платной основе в журнале могут быть опубликованы материалы рекламного характера, имеющие прямое отношение к тематике журнала.

Журнал предоставляет непосредственный открытый доступ к своему контенту, исходя из следующего принципа: свободный открытый доступ к результатам исследований способствует увеличению глобального обмена знаниями.

Индексирование. Публикации в журнале входят в системы расчетов индексов цитирования авторов и журналов. «Индекс цитирования» — числовой показатель, характеризующий значимость данной статьи и вычисляющийся на основе последующих публикаций, ссылающихся на данную работу.

Авторам. Прежде чем направить статью в редакцию журнала, авторам следует ознакомиться со всеми материалами, размещенными в разделах сайта журнала (интернет-сайт Российской академии архитектуры и строительных наук (http://raasn.ru); подраздел «Издания РААСН» или интернет-сайт Издательства АСВ (http://iasv.ru); подраздел «Журнал IJCCSE»): с основной информацией о журнале, его целями и задачами, составом редакционной коллегии и редакционного совета, редакционной политикой, порядком рецензирования направляемых в журнал статей, сведениями о соблюдении редакционной этики, о политике авторского права и лицензирования, о представлении журнала в информационных системах (индексировании), информацией о подписке на журнал, контактными данными и пр. Журнал работает по лицензии Creative Commons типа cc by-nc-sa (Attribution Non-Commercial Share Alike) – Лицензия «С указанием авторства – Некоммерческая – Копилефт».

Рецензирование. Все научные статьи, поступившие в редакцию журнала, проходят обязательное двойное слепое рецензирование (рецензент не знает авторов рукописи, авторы рукописи не знаю рецензентов).

Заимствования и плагиат. Редакционная коллегия журнала при рассмотрении статьи проводит проверку материала с помощью системы «Антиплагиат». В случае обнаружения многочисленных заимствований редакция действует в соответствии с правилами COPE.

Подписка. Журнал зарегистрирован в Федеральном агентстве по средствам массовой информации и охраны культурного наследия Российской Федерации. Индекс в общероссийском каталоге РОСПЕЧАТЬ − 18076.

По вопросам подписки на международный научный журнал “International Journal for Computational Civil and Structural Engineering (Международный журнал по расчету гражданских и строительных конструкций)” обращайтесь в Агентство «Роспечать» (Официальный сайт в сети Интернет: http://www.rosp.ru/) или в издательство Ассоциации строительных вузов (АСВ) в соответствии со следующими контактными данными:

ООО «Издательство АСВ»

Юридический адрес: 129337, Россия, г. Москва, Ярославское ш., д. 26, офис 705;

Фактический адрес: 129337, Россия, г. Москва, Ярославское ш., д. 19, корп. 1, 5 этаж, офис 12 (ТЦ Мебель России);

Телефоны: +7 (925) 084-74-24, +7 (926) 010-91-33

Интернет-сайт: www.iasv.ru. Адрес электронной почты: iasv@iasv.ru.

Контактная информация. По всем вопросам работы редакции, рецензирования, согласования правки текстов и публикации статей следует обращаться к главному редактору журнала члену-корреспонденту РААСН *Сидорову Владимиру Николаевичу* (адреса электронной почты: sidorov.vladimir@gmail.com, sidorov@iasv.ru, iasv@iasv.ru, sidorov@raasn.ru) или к техническому редактору журнала советнику РААСН *Кайтукову Таймуразу Батразовичу* (адреса электронной почты: tkaytukov@gmail.com; Kaytukov@raasn.ru). Кроме того, по указанным вопросам, а также по вопросам размещения в журнале рекламных материалов можно обращаться к генеральному директору ООО «Издательство АСВ» *Никитиной Надежде Сергеевне* (адреса электронной почты: iasv@iasv.ru, nsnikitina@mail.ru, ijccse@iasv.ru).

Журнал становится технологичнее. Издательство АСВ с сентября 2016 года является членом Международной ассоциации издателей научной литературы (Publishers International Linking Association (PILA)), осуществляющей свою деятельность на платформе CrossRef. Оригинальным статьям, публикуемым в журнале, будут присваиваться уникальные номера (индексы DOI – Digital Object Identifier), что значительно облегчит поиск метаданных и местонахождение полнотекстового произведения. DOI – это система определения научного контента в сети Интернет.

С октября 2016 года стал возможен прием статей на рассмотрение и рецензирование через онлайн систему приема статей Open Journal Systems на сайте журнала (электронная редакция): http://ijccse.iasv.ru/index.php/IJCCSE.

Автор имеет возможность следить за продвижением статьи в редакции журнала в личном кабинете Open Journal Systems и получать соответствующие уведомления по электронной почте.

В феврале 2018 года журнал был зарегистрирован в Directory of open access journals (DOAJ) – это один из самых известных поисковых сервисов в мире, который предоставляет открытый доступ к материалам и индексирует не только заголовки журналов, но и научные статьи.

International Journal for
Computational Civil and Structural Engineering
(Международный журнал по расчету гражданских и строительных конструкций)
Volume 14, Issue 3 ***2018***

Scientific coordination is carried out by the Russian Academy of Architecture and Construction Sciences (RAACS)

CONTENTS

About Methods of Seismic Analysis of Underground Structures 14
Alexander M. Belostotsky, Pavel A. Akimov, Dmitry S. Dmitriev

Universal Software System "STADYO" for the Numerical Solution of Linear and Nonlinear Problems of the Field Theory, Statics, Stability and Dynamics of Spatial Combined Systems: General Parameters and Superelemental Features 26
Alexander M. Belostotsky, Alexey L. Potapenko, Pavel A. Akimov

Moisture Regime Calculation for Single-Layer Enclosing Structures Using Discrete-Continual Mathematical Model 42
Vladimir G. Gagarin, Kirill P. Zubarev

The Comparative Analysis of the Results of Real and Numerical Experiments for Defining the Ultimate Bearing Capacity of Light Gauge Steel Studs "Atlant" 50
Galina G. Kashevarova, Pavel A. Kosykh

Determination of Elastic Properties of Cement-Sand Composition Using Structural Simulation Modeling 59
Yuri E. Kurbatov, Galina G. Kashevarova

Architectural Modelling of "Sound" Pergola 68
Valery S. Lesovik, Irina L. Pershina, Dmitry Yu. Popov, Andrey V. Shevchenko

About Wavelet-Based Multigrid Numerical Method of Structural Analysis with the Use of Discrete Haar Basis 83
Marina L. Mozgaleva, Pavel A. Akimov, Taymuraz B. Kaytukov

About the Problem of Analysis Resistance Bearing Systems in Failure of a Structural Element 103
Anatoly V. Perelmuter, Oleg V. Kabantsev

About the Free-Vibration Mode Shapes of Elastoplastic Dissipative Systems 114
Aleksander N. Potapov

Computer Modelling of the Stress-Strain State of Plug-In Connections of Reinforced Concrete Columns with the Coverage Plates Under the Out-of-Square Eccentric Compression 126
Boris S. Sokolov, Evgeniy O. Troshkov

Bolts Pulling Test. Reverser for Bolts Testing 136
Mark P. Son

Reliability Analysis of Reinforced Concrete Elements with Normal Cracks (On RC Beam Example) 142
Vladimir S. Utkin, Sergey A. Solovyev

Study and Simulation of Heat Transfer Processes During Foam Glass High Temperature Processing 153
Sergey V. Fedosov, Maksim O. Bakanov, Sergey N. Nikishov

Mathematical Modelling of Diffusion Processes of Mass Transfer of "Free Calcium Hydroxide" During Corrosion of Cement Concretes 161
Sergey V. Fedosov, Varvara Eu. Roumyantseva, Viktoriya S. Konovalova, Svetlana A. Loginova

To the Anniversary of Prof. Vitaly I. Solomin 169

About the General Meeting of Members of the Russian Academy of Architecture and Construction Sciences in 2019 170

International Journal for
Computational Civil and Structural Engineering
(Международный журнал по расчету гражданских и строительных конструкций)
Volume 14, Issue 3 ***2018***

Scientific coordination is carried out by the Russian Academy of Architecture and Construction Sciences (RAACS)

СОДЕРЖАНИЕ

О методах сейсмического расчета подземных сооружений 14
А.М. Белостоцкий, П.А. Акимов, Д.С. Дмитриев

Универсальный программный комплекс «СТАДИО» для численного решения линейных и нелинейных задач теории поля, статики, устойчивости и динамики пространственных комбинированных систем: общая характеристика и суперэлементные возможности 26
А.М. Белостоцкий, А.Л. Потапенко, П.А. Акимов

Расчет влажностного режима однослойных ограждающих конструкций с использованием дискретно-континуальной математической модели 42
В.Г. Гагарин, К.П. Зубарев

Сравнительный анализ результатов натурного и численного экспериментов по определению предельной несущей способности тонкостенных профилей «Атлант» 50
Г.Г. Кашеварова, П.А. Косых

Определение упругих характеристик цементно-песчаной композиции методом структурно-имитационного моделирования 59
Ю.Е. Курбатов, Г.Г. Кашеварова

Архитектурное моделирование «звуковой» перголы 68
В.С. Лесовик, И.Л. Першина, Д.Ю. Попов, А.В. Шевченко

О численной реализации многосеточного численного метода расчета конструкций на основе дискретного базиса Хаара 83
М.Л. Мозгалева, П.А. Акимов, Т.Б. Кайтуков

Об анализе сопротивления несущих систем при отказе конструктивного элемента 103
А.В. Перельмутер, О.В. Кабанцев

О формах собственных колебания упругопластических диссипативных систем 114
А.Н. Потапов

Компьютерное моделирование напряженно-деформированного состояния штепсельных стыков железобетонных колонн с плитами перекрытия при косом внецентренном сжатии 126
Б.С. Соколов, Е.О. Трошков

Испытание болтов на растяжение. Реверсор для испытания болтов 136
М.П. Сон

Расчет надежности железобетонных элементов с нормальными трещинами на примере железобетонной балки 142
В.С. Уткин, С.А. Соловьев

Исследование и моделирование процессов теплопереноса при высокотемпературной обработке пеностекла 153
С.В. Федосов, М.О. Баканов, С.Н. Никишов

Математическое моделирование диффузионных процессов массопереноса «свободного гидроксида кальция» при коррозии цементных бетонов 161
С.В. Федосов, В.Е. Румянцева, В.С. Коновалова, С.А. Логинова

К Юбилею Виталия Ивановича Соломина 169

О проведении Общего собрания членов Российской академии архитектуры и строительных наук в 2019 года 170

DOI:10.22337/2587-9618-2018-14-3-14-25

ABOUT METHODS OF SEISMIC ANALYSIS OF UNDERGROUND STRUCTURES

Alexander M. Belostotsky [1, 2, 3, 4, 5]***, Pavel A. Akimov*** [1, 2, 3, 6]***, Dmitry S. Dmitriev*** [1]

[1] Scientific Research Center "StaDyO", Moscow, RUSSIA
[2] Tomsk State University of Architecture and Building, Tomsk, RUSSIA
[3] Peoples' Friendship University of Russia, Moscow, RUSSIA
[4] Russian University of Transport» (RUT – MIIT), Moscow, RUSSIA
[5] Perm National Research Polytechnic University, Perm, RUSSIA
[6] Russian Academy of Architecture and Construction Sciences, Moscow, RUSSIA

Abstract: As is known, underground facilities are an integral part of the infrastructure of modern society. These objects have some specific characteristics such as complex construction, high cost, long life cycle, etc. Once it is destroyed, the direct and indirect losses are more seriousness than the general structure in the ground. Underground facilities built in areas subject to earthquake activity must withstand both seismic and static loading. Therefore, it is very important to carry on the seismic design of the underground structure in a safe and economical way. The distinctive paper presents a summary of the current state of seismic analysis for underground structures. Classification and brief overview of methods of seismic analysis of underground structures (force-based methods, displacement-based methods, numerical methods of seismic analysis of coupled system "soil – underground structure") are presented, problems of soil-structure interaction are under consideration as well. So-called static finite element method with substructure technique for seismic analysis of underground structures is described.

Keywords: seismic analysis, numerical methods, underground structures, finite element method, force-based methods, displacement-based methods, coupled system "soil – underground structure", static finite element method, substructure technique

О МЕТОДАХ СЕЙСМИЧЕСКОГО РАСЧЕТА ПОДЗЕМНЫХ СООРУЖЕНИЙ

А.М. Белостоцкий [1, 2, 3, 4, 5]***, П.А. Акимов*** [1, 2, 3, 6]***, Д.С. Дмитриев*** [1]

[1] Научно-исследовательский центр СтаДиО, г. Москва, РОССИЯ
[2] Томский государственный архитектурно-строительный университет, г. Томск, РОССИЯ
[3] Российский университет дружбы народов, г. Москва, РОССИЯ
[4] Российский университет транспорта (МИИТ), г. Москва, РОССИЯ
[5] Пермский национальный исследовательский политехнический университет, г. Пермь, РОССИЯ
[6] Российская академия архитектуры и строительных наук, г. Москва, РОССИЯ

Аннотация: Как известно, в настоящее время подземные сооружения являются, по существу, важнейшей составляющей современной инфраструктуры. Подземные объекты характеризуются целым рядом специфических особенностей, в числе которых можно указать, в частности, трудоемкость возведения, высокую стоимость, достаточно продолжительный жизненный цикл. Очевидно, что в случае разрушения подземного сооружения соответствующие прямые и непрямые потери будут более существенны, чем при разрушении надземного здания или сооружения. Подземные объекты, возведенные в сейсмоопасных районах, разумеется, должны воспринимать без разрушения как сейсмические, так и статические нагрузки. Таким образом, задача экономически обоснованного проектирования безопасных сейсмостойких подземных сооружений является исключительно актуальной. В настоящей статье рассматриваются современные методы сейсмического расчета подземных сооружений. В частности, приведены классификация и краткий анализ последних (методы, основанные на задании эквивалентных нагрузок; методы, основанные на задании эквивалентных перемещений; численные методы расчета связанных систем типа «сооружение – основание»), затронуты проблемы моделирования взаимодействия подземного сооружения с

окружающим грунтовым массивом, представлено описание так называемого статического метода конечных элементов для расчета подземных сооружений, основанного на технике метода подконструкций.

Ключевые слова: сейсмический расчет, численные методы, подземные сооружения, метод конечных элементов, эквивалентные нагрузки, эквивалентные перемещения, связанная система типа «сооружение – основание», статический метод конечных элементов, метод подконструкций

INTRODUCTION

As is known, underground facilities are an integral part of the infrastructure of modern society [1,2]. Underground structures, tunnels, subways, metro stations and parking lots, are crucial components of the build environment and transportation networks. They are more and more frequently constructed especially in densely populated urban areas to facilitate different needs. These objects have some specific characteristics such as complex construction, high cost, long life cycle, etc. Once it is destroyed, the direct and indirect losses are more seriousness than the general structure in the ground [3-5]. Thus, considering importance of underground structures for life save and economy, their appropriate seismic design is of prior significance [6-17]. However, underground facilities built in areas subject to earthquake activity must withstand both seismic and static loading [18]. Therefore, it is very important to carry on the seismic design of the underground structure in a safe and economical way.

A review of the past performance of hundreds underground openings during earthquakes indicated that underground structures in general are less severely affected than surface structures at the same geographic location. However, some severe damage, including collapse has been reported. We should mention here, in particular, that some underground structures have experienced significant damage in recent large earthquakes, including the 1995 Kobe, Japan earthquake, the 1999 Chi-Chi, Taiwan earthquake and the 1999 Kocaeli, Turkey earthquake (Figure 1).

Ground shaking due to wave propagation and permanent ground displacements due to lateral spreading, landslides and fault rupture are affecting underground structures during a strong earthquake [5]. The deformation modes dominating the seismic response are somehow different from aboveground structures (Figure 2).

These recent damages revealed some important weaknesses in the current seismic design practices. For instance, stability of tunnels during seismic motion is affected by peak ground parameters, earthquake duration, type of support, ground conditions and in situ stresses. Moreover, underground structures are quite vulnerable to ground failures associated with large permanent deformations, caused by ground liquefaction, slope instability and fault movements [20].

The distinctive paper presents a summary of the current state of seismic analysis for underground structures. The complexity of the problem and the conscience on the various shortcomings of the available methods lead often to an overdesign of the new structures. The lack of knowledge is attributed, to a certain degree, to the relatively few well documented cases of important damages during strong earthquakes. Several questions regarding their real seismic behavior during shaking remain still non-responded.

In densely populated urban areas, tunnels and other underground structures are often passing beneath high-rise buildings or they are located close to them. The existence of these structures may create complex interaction effects with the underground structures usually referred as “city effects” [5]. These effects can affect the seismic wave propagation field, altering the seismic input motion with respect to the free field case [6, 14]. In this sense, they may modify considerably the seismic response of the underground structure, while at the same time the existence of the embedded structure, close to the surface and buildings foundations may alter the response of the buildings themselves.

a)  b) 

Figure 1. Daikai Station that collapsed during the major Hyogoken-Nambu earthquake (1995). (a) Settlements of the overlaying roadway caused by the subway collapse. (b) collapse of the central columns of the station [19].

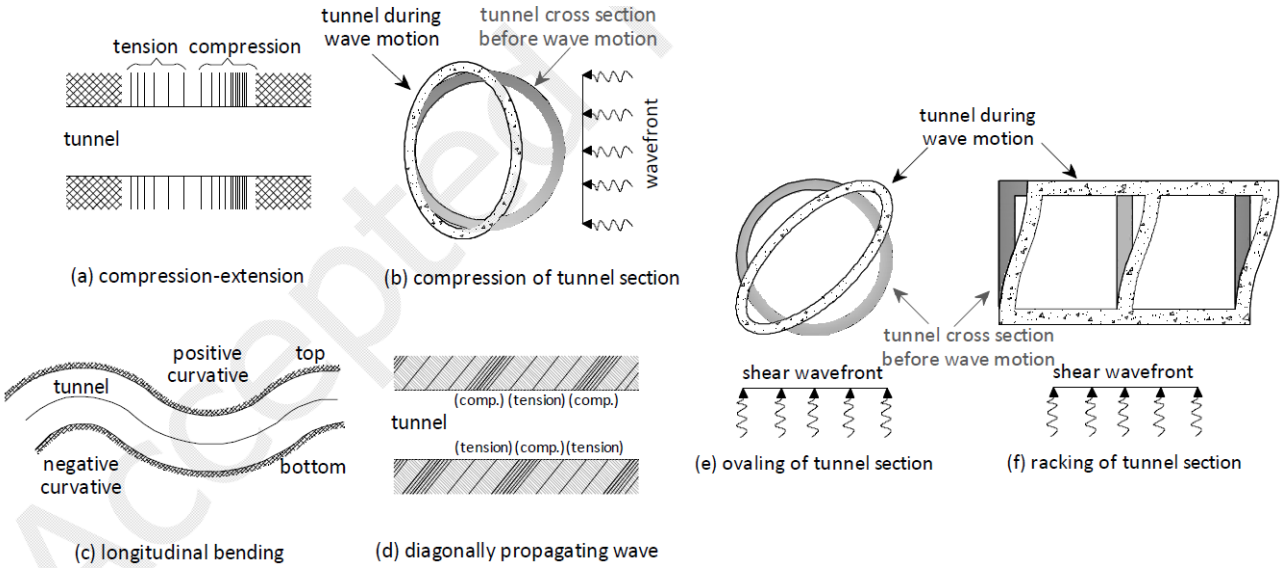


Figure 2. Simplified deformation modes of tunnels due to seismic waves [18].

1. CLASSIFICATION OF METHODS OF SEISMIC ANALYSIS OF UNDERGROUND STRUCTURES

As is known, several methods have been proposed in the literature and used in practice for the seismic design of tunnels and large underground structures. From simple analytical elastic solutions, to pseudo-static or equivalent static solutions, and from hybrid methods, which try to take into account the relative stiffness of the ground and the structures and the soil-structure interaction (SSI) effects, to more sophisticated and a priori accurate models using full dynamic numerical analysis of the soil-structure system.

Generally, several methods are available in the literature for the seismic design of tunnels and large underground structures [3,5,8,22,25]. These methods can be classified in three general categories.

1.1. Force-based methods.

According to these methods, the seismic load is introduced in terms of equivalent forces acting on the structure in a static way. The structure is commonly simulated as a frame model using beam elements. The main differences between the methods are related to the way that the equivalent forces are estimated and the way the soil-structure interaction is modeled, if accounted. It should be noted that the real

seismic loading on tunnels and underground structures is applied through the seismic wave propagation and the associated ground distortions imposed on the underground structure. So, displacement-based design is appropriate and consistent with the physics of the problem. Besides, the displacement-based methods are also more appropriate for the efficient seismic design of reinforced concrete (RC) underground structures with ductility higher that unity.

1.2. Displacement-based methods.

Contrary to the force-based methods, in the displacement-based methods the seismic load is introduced in terms of seismic displacements, an assumption, which is closer to the problem's physics. Once again, the main differences between the methods are related to the way that the seismic displacements are computed and the way in which the soil-structure interaction is modeled, if accounted. Force-based design, despite several drawbacks, remains always familiar to the engineering community and simpler to apply (in comparison with displacement-based design). Several arguments, in favor of the inconsistency of force-based design, as discussed by [23, 24] are also valid in the case of large space underground structures and tunnels.

1.3. Numerical methods of seismic analysis of coupled system "soil – underground structure".

Full dynamic time history analysis is considered to be the most sophisticated and accurate method for the seismic analysis of underground structures [22] (finite element or finite difference techniques are always used). However, complex and time consuming computer analysis is required and uncertainty of design seismic input parameters may be several times the uncertainty of the analysis [18]. These analyses involve setting artificial boundaries and soil dynamic constitutive and other issues, and it is difficult widely used in engineering. However, numerical methods can efficiently describe the kinematic and inertial aspects of the soil-structure interaction and the complex geometry of the soil deposit. Moreover, the nonlinear behavior of both the structure and the soils can be efficiently simulated using appropriate constitutive laws.

1.4. About soil-structure interaction.

First of all it should be noted that interface characteristics underground structure and the surrounding soil affect considerably the seismic behavior of the corresponding system [19,25].

With the exception of the third one, where the soil-structure interaction effects are inherently considered in the model, methods belonging in the other two general categories can be also classified accounting or not for soil-structure interaction. For the methods where the soil-structure interaction is not considered (free field deformation methods), it is assumed that the structure will undergo the free field ground deformations, whereas for the soil-structure interaction methods, the input motion (in terms of ground displacements or equivalent forces) is modified to account of the existence of the structure.

It should be noted that pseudo-static formulations [4,26] are relatively simple, and they lead to static calculation methods which can obtain the effect of underground structures under earthquake action. These formulations are widely used in engineering and specifications.

Conventional free field deformation approach [18] may overestimate or underestimate structure deformations depending on the rigidity of the structure relative to the ground. It should be noted that the term "free-field deformations" describes ground strains caused by seismic waves in the absence of structures or excavations. These deformations ignore the interaction between the underground structure and the surrounding ground, but can provide a first-order estimate of the anticipated deformation of the structure. A designer may choose to impose these deformations directly on the structure. The free field deformation approach is conservative for underground

structures stiffer than ground (and overly conservative for underground structures significantly stiffer than ground), non-conservative for underground structures more flexible than ground and can be applied for underground structures with equal stiffness to ground. On the one hand it is comparatively easy to formulate this approach and free field deformation approach was widely used with reasonable results in the past. On the other hand it provides less precision with highly variable ground conditions.

2. STATIC FINITE ELEMENT METHOD FOR SEISMIC ANALYSIS OF UNDERGROUND STRUCTURES (SFEM)

Application of static finite element method (SFEM) with substructure technique [27] for seismic analysis of underground structures was presented in [4]. In accordance with [4] the dynamic soil-structure interaction system can be decomposed into three sub-structures: structure, near-field and far-field soil (Figure 3) [9].
Thus we can obtain the basic soil-structure interaction equations:

$$\begin{bmatrix} S_{ss} & S_{sn} & \\ S_{ns} & S_{nn} & S_{nb} \\ & S_{bn} & S_{bb}^{g} + S_{bb} \end{bmatrix} \begin{Vmatrix} \bar{u}_s \\ \bar{u}_n \\ \bar{u}_b \end{Vmatrix} = \begin{bmatrix} 0 \\ 0 \\ S_{bb}^{g} \bar{u}_b^{g} \end{bmatrix}, \quad (1)$$

where S is the stiffness matrix; $\bar{u}$ is the displacement vector; s, n, b are subscripts, which denote structure, near-field and far-field, respectively; g is superscript, which denotes excavated soil.
If we suppose that the excavated soil is a structure, we can get the following equation:

$$(S_{bb}^{e} + S_{bb}^{g})\bar{u}_b^{f} = S_{bb}^{g}\bar{u}_b^{g}, \quad (2)$$

where e, f are subscripts, which denote excavated soil and free field, respectively.

Combining (1) and (2) we get:

$$\begin{bmatrix} S_{ss} & S_{sn} & \\ S_{ns} & S_{nn} & S_{nb} \\ & S_{bn} & S_{bb}^{g} + S_{bb} \end{bmatrix} \begin{Vmatrix} \bar{u}_s \\ \bar{u}_n \\ \bar{u}_b \end{Vmatrix} = \begin{bmatrix} 0 \\ 0 \\ S_{bb}^{e}\bar{u}_b^{f} + S_{bb}^{g}\bar{u}_b^{f} \end{bmatrix}. \quad (3)$$

Dynamic stiffness matrix can be defined by formula:

$$S = K + i\omega C - \omega^2 M, \quad (4)$$

where K is the stiffness matrix; M is the mass matrix; C is the damping matrix; ω is predominant circular frequency.
The ground dynamic stiffness matrix equation (4) is rewritten as (for simplicity):

$$S_{bb}^{g} = K_{bb}^{g} + i\omega C_{bb}^{g}. \quad (5)$$

In order to use the free field seismic response analysis data or the soil layers seismic response analysis data to solve the underground structure seismic response two main assumptions are made. In accordance with the first assumption the accelerations of the structure and the near-field are the same as those of the free field at the same location. In accordance with the second assumption the velocity of the structure and the near-field are the same as those of the free field at the same location [21].
The key of SFEM is that the stress state of the maximum moment of the dynamic time history analysis of the underground structure is replaced by the static state, and the computed parameters are obtained from the free field seismic response analysis. So, assumptions are to facilitate the use of the results of the free field seismic response analysis to approximate the seismic response of the underground structure. Thus the seismic response of the underground structure can be obtained by the free field seismic response [21].

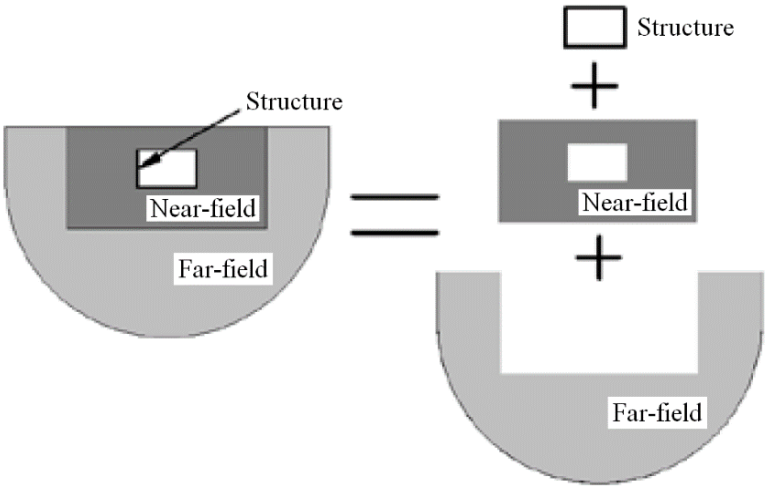


Figure 3. Substructure decomposition of the soil-structure system.

The formula (4) and (5) are brought into the formula (3), and taking into account the above two hypotheses, we can get the formula (6) as following [4]

$$\begin{aligned}
&\begin{bmatrix} K_{ss} & K_{sn} & \\ K_{ns} & K_{nn} & K_{nb} \\ & K_{bn} & K_{bb}^{g}+K_{bb} \end{bmatrix}\begin{Bmatrix} \bar{u}_s^f \\ \bar{u}_n^f \\ \bar{u}_b^f \end{Bmatrix} = \\
&=\begin{bmatrix} M_{ss} & M_{sn} & \\ M_{ns} & M_{nn} & M_{nb} \\ & M_{bn} & M_{bb}^{g}+M_{bb} \end{bmatrix}\begin{Bmatrix} \ddot{\bar{u}}_s^f \\ \ddot{\bar{u}}_n^f \\ \ddot{\bar{u}}_b^f \end{Bmatrix} - \\
&-\begin{bmatrix} C_{ss} & C_{sn} & \\ C_{ns} & C_{nn} & C_{nb} \\ & C_{bn} & C_{bb}^{g}+C_{bb} \end{bmatrix}\begin{Bmatrix} \dot{\bar{u}}_s^f \\ \dot{\bar{u}}_n^f \\ \dot{\bar{u}}_b^f \end{Bmatrix} + \\
&+\begin{bmatrix} 0 \\ 0 \\ M_{bb}^{e}\ddot{\bar{u}}_f^f + C_{bb}^{e}\dot{\bar{u}}_b^f + K_{bb}^{e}\bar{u}_b^f \end{bmatrix}.
\end{aligned} \tag{6}$$

The left hand side of formula (6) represents the soil-structure interaction system reaction, the first term and the second term of the right of the equal sign represent internal force of the underground structure and the near-field soil (inertial force and damping force), the third term represents the boundary condition.

By the formula (6) we can get the computational model of the generalized static finite element method shown in Figure 3 [21]. It includes two parts: the internal force of the structure and the soil and the boundary conditions (boundary constraints and boundary loads).

According to the equation (6) the internal force of the structure and the soil is mainly includes the damping force and the inertia force. This part can be solved by the conventional methods [6]. However, it is necessary to improve (correct) boundary conditions [9]. Let us consider correction of boundary constraints (K_{bb}^{e}).

The side and the bottom boundary are constrained by the viscoelastic boundary. Since static calculation, the boundary constraint only imposed by spring, shown in Figure 2. The value of the spring coefficient adopts the spring stiffness of the viscoelastic boundary value [4], such as the formula

$$K_N = G/(2R); \quad K_T = G/R, \tag{7}$$

where K_N is the normal spring coefficient; K_T is the and tangential spring coefficient; G is the shear modulus of the soil; R is the distance between structure and boundary points.

In accordance with (6), the boundary load includes four parts: the free field displacement ($\bar{u}_b^f$), the inertia force of the near field soil boundary ($M_{bb}^{e}\ddot{\bar{u}}_f^f$), the damping force of the near field ($C_{bb}^{e}\dot{\bar{u}}_b^f$) and the equivalent load of the free field displacement ($K_{bb}^{e}\bar{u}_b^f$).

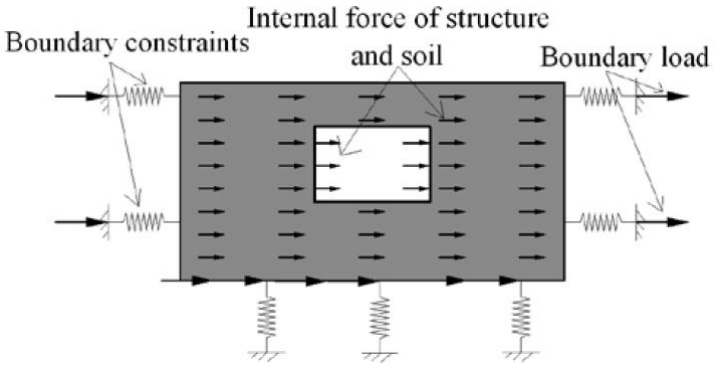


Figure 4. Generalized computational model of SFEM.

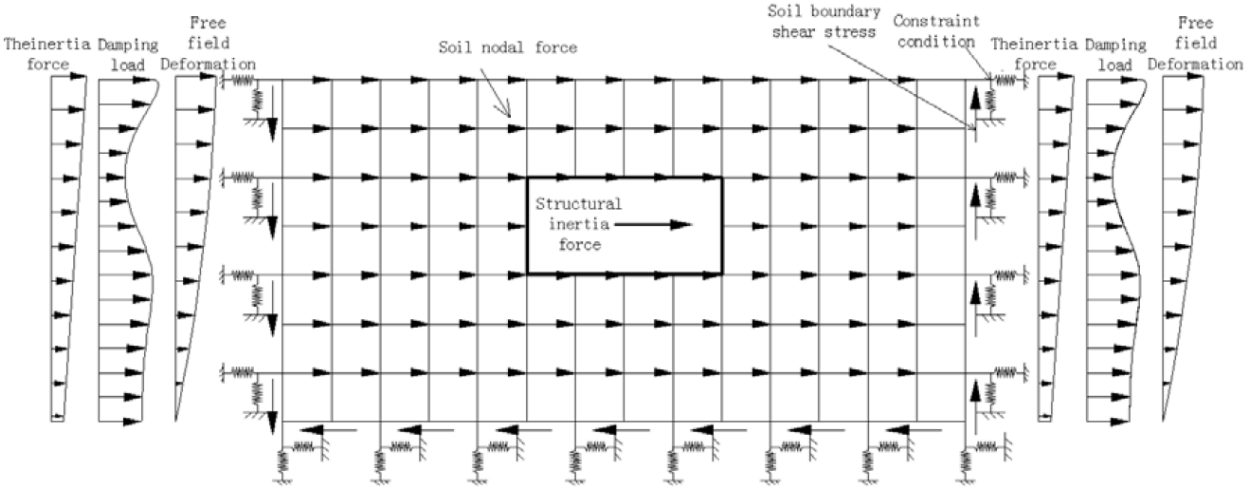


Figure 5. Computational model of SFEM [4].

Let us consider the method of correction of corresponding boundary loads.

The free field displacement ($\bar{u}_b^f$) can be obtained by the specialized well-known soil layers seismic response analysis software [18].

The inertia force of the near field soil boundary ($M_{bb}^e \ddot{\bar{u}}_f^f$) can be computed with the use of the free field acceleration (can be obtained by the soil layers seismic response analysis programs) and the near field soil mass (it is also relatively easy to obtain).

The damping force of the near field ($C_{bb}^e \dot{\bar{u}}_b^f$) can be computed with the use of the following formula for boundary damping force based on relationship between the Rayleigh damping and the damping coefficient

$$f_{ci} = c_i \dot{u}_i; \quad c_i = 2 m_i w_i \xi_i; \quad \xi_i = 0.5 \cdot (\alpha_0 / w_i + \alpha_1 w_i), \quad (8)$$

where f_{ci} is the damping force; c_i is the damping coefficient; $\dot{u}_i$ is the node speed; m_i is the assigned node mass; w_i is the frequency; ξ_i is the damping ratio; α_0, α_1 are two Rayleigh damping coefficients, respectively.

The equivalent load of the free field displacement ($K_{bb}^e \bar{u}_b^f$) can be equivalent to the same location soil stress of the free field, which can be obtained by the well-known soil layers seismic response analysis software.

Therefore, the computational model of SFEM is shown in Figure 5 [4].

3. CONCLUSION

Thus SFEM includes the three main stages.

The first stage is solving the free field shear stress, acceleration, velocity and displacement, when the moment that the relative displacement of the soil that the underground structure located in reaches the maximum.
The second stage is computing of internal forces and parameters of boundary conditions (the spring parameters, the inertia force, the damping force, the equivalent load of the free field displacement).
The third stage is construction of the static finite element model and imposing the loads and constrains computed at the second stage as shown in Figure 4, and then making a static analysis.
Verification samples [9] show good agreement of SFEM and dynamic FEM, meaning that SFEM has good accuracy. Besides, SFEM is less affected by the size of the model, but the boundary of the model must have more than one times the width of the structure distance from the side wall.
Full dynamic time-history analysis, using three-dimensional finite elements, finite difference or lumped mass models [22], is by far the most adequate method to design large and long underground structures. With this method, both the transversal and the longitudinal directions of the structure can be modeled and analyzed simultaneously, taking into account the complicated soil deposit geometry, the non-linear behavior of the soil and the structure, using appropriate constitutive relationships, and the behavior of the soil-structure interface. While the input motion definition remains a decisive and constantly debated parameter, the main shortcoming of the method is the high computational cost, which makes its use difficult for parametric analysis, usually needed during the design phases of underground structures. To this end, full dynamic three-dimensional analysis is practically used in cases of structures of significant importance (i.e. nuclear station underground ducts). Several issues, such as the appropriate simulation of the soil-tunnel interface or of the incoherence and spatial variation of the seismic input motion are still open [28, 29].

ACKNOWLEDGEMENTS

The Reported study was funded by Government Program of the Russian Federation "Development of science and technology" (2013-2020) within Program of Fundamental Researches of Ministry of Construction, Housing and Utilities of the Russian Federation and Russian Academy of Architecture and Construction Sciences, the Research Projects 7.1.1 and 7.1.2".

REFERENCES

1. **Belostotsky A.M., Akimov P.A., Afanasyeva I.N., Kaytukov T.B.** Contemporary problems of numerical modelling of unique structures and buildings. // International Journal for Computational Civil and Structural Engineering, 2017, Volume 13, Issue 2, pp. 9-34.
2. **Belostotsky A.M., Akimov P.A.** Nauchno-issledovatelsky tsentr StaDyO. 25 let na fronte chislennogo modelirovaniys [25-th Anniversary of scientific research centre StaDyO]. // International Journal for Computational Civil and Structural Engineering, 2016, Volume 12, Issue 1, pp. 9-34.
3. AFPS/AFTES. Guidelines on Earthquake Design and Protection of Underground Structures. Working Group of the French Association for Seismic Engineering (AFPS) and French Tunneling Association (AFTES). Version 1, 2001.
4. **Jia B., Li-ping J., Yong-qiang L.** Seismic Analysis of Underground Structures Based on the Static Finite Element Method. // The Electronic Journal of Geotechnical Engineering, 2016, No. 21(06), pp. 2307-2315.

5. **Wang J.N.** Seismic Design of Tunnels: A Simple State-of-the-art Design Approach. New York, Parsons Brinckerhoff Quade and Douglas Inc., 1993, 159 p.
6. **Baziar M.H., Moghadam M.R., Kim D.-S., Choo Y.W.** Effect of underground tunnel on the ground surface acceleration. // Tunnelling and Underground Space Technology, 2014, Vol. 44, pp. 10-22.
7. **Debiasi E., Gajo A., Zonta D.** On the seismic response of shallow-buried rectangular structures. // Tunnelling and Underground Space Technology, 2013, Vol. 38, pp. 99-113.
8. **Fabozzi S., Licata V., Autuori S., Bilotta E., Russo G., Silvestri F.** Prediction of the seismic behavior of an underground railway station and a tunnel in Napoli (Italy). // Underground Space, 2017, Vol. 2, Issue 2, pp. 88-105.
9. **Fuentes R.** Internal forces of underground structures from observed displacements. // Tunnelling and Underground Space Technology, 2015, Vol. 49, pp. 50-66.
10. **Kawamata Y., Nakayama M., Towhata I., Yasuda S.** Dynamic behaviors of underground structures in E-Defense shaking experiments. // Soil Dynamics and Earthquake Engineering, 2016, Vol. 82, pp. 24-39.
11. **Romero A., Galvin P., Antonio J., Dominguez J., Tadeu A.** Modelling of acoustic and elastic wave propagation from underground structures using a 2.5D BEM-FEM approach. // Engineering Analysis with Boundary Elements, 2017, Vol. 76, pp. 26-39.
12. **Sandoval E., Bobet A.** Effect of frequency and flexibility ratio on the seismic response of deep tunnels. // Underground Space, 2017, Vol. 2, Issue 2, pp. 125-133.
13. **Wang H.-F., Lou M.-L., Chen X., Zhai Y.-M.** Structure – soil – structure interaction between underground structure and ground structure. // Soil Dynamics and Earthquake Engineering, 2013, Vol. 54, pp. 31-38.
14. **Wang H.-F., Lou M.-L., Zhang R.-L.** Influence of presence of adjacent surface structure on seismic response of underground structure. // Soil Dynamics and Earthquake Engineering, 2017, Vol. 100, pp. 131-143.
15. **Wang S.** Evaluation of underground pipe-structure interface for surface impact load. // Nuclear Engineering and Design, 2017, Vol. 317, pp. 59-68.
16. **Wang X., Cai M.** Numerical modeling of seismic wave propagation and ground motion in underground mines. // Tunnelling and Underground Space Technology, 2017, Vol. 68, pp. 211-230.
17. **Zou Y., Liu H., Jing L., Cui J.** A pseudo-static method for seismic responses of underground frame structures subjected to increasing excitations. // Tunnelling and Underground Space Technology, 2017, Vol. 65, pp. 106-120.
18. **Hashasha Y.M.A., Hooka J.J., Schmidt B., Yaoa J.I-C.** Seismic Design and Analysis of Underground Structures. // Tunnelling and Underground Space Technology, 2001, No. 16, pp. 247-293.
19. **Huo H., Bodet A., Fernandez G., Ramirez J.** Load Transfer Mechanisms between Underground Structure and Surrounding Ground: Evaluation of the Failure of the Daikai Station. // J. Geotech Geoenviron, 2005, No. 131(12), pp. 1522-1533.
20. **Zeghal M., Elgamal A.W.** Analysis of Site Liquefaction Using Earthquake Records. // J. Geotech. Eng. ASCE, 1994, No. 120(6), pp. 996-1017.
21. FHWA. Technical Manual for Design and Construction of Road Tunnels – Civil Elements. U.S. Department of Transportation. Federal Highway Administration. Publication No. FHWA-NHI-10-034, 2009. 702 p.
22. ISO 23469. Bases for Design of Structures – Seismic Actions for Designing Geotechnical Works. ISO International Standard. ISO TC 98/SC3/WG10, 2005.

23. **Calvi G.M., Sullivan T.J.** A Model Code for Displacement-Based Seismic Design of Structures. Pavia, IUSS Press, 2009.
24. **Priestley M.J.N.** Myths and Fallacies in Earthquake Engineering – Conflict between Design and Reality. // Bull. Natl. Soc. Earthq. Eng. NZSEE, 1993, No. 26(3), pp. 329-341.
25. **Sedarat H., Kozak A., Hashash Y.M.A., Shamsabadi A., Krimotat A.** Contact Interface in Seismic Analysis of Circular Tunnels. // Tunn. Undergr. Space Technol, 2009, No. 24(4), pp. 482-490.
26. **Tateishi A.**, 2005. A Study on Seismic Analysis Methods in the Cross Section of Underground Structures Using Static Finite Element Method. Structural Engineering // Earthquake Engineering, JSCE., 2005, No. 22(1), pp. 41-53.
27. **Belostotsky A.M., Akimov P.A., Dmitriev D.S.** O sovremennikh metodakh redutsirovaniya vichislitelnoy razmernosti zadach rascheta konstruktsiy, zdaniy i sooruzheniy v ramkakh metoda konechnikh elementov [About Contemporary Approaches to Reduction of Computational Dimension of Problems of Structural Analysis within Finite Element Method]. // International Journal for Computational Civil and Structural Engineering, 2017, Volume 13, Issue 3, pp. 19-33.
28. **Ghergu M., Ionescum I.R.** Structure – Soil – Structure Coupling in Seismic Excitation and "City Effect". // Int. J. Eng. Sci., 2009, No. 47, pp. 347-354.
29. **Semblat J.F., Kham M., Bard P.Y.** Seismic-Wave Propagation in Alluvial Basins and Influence of Site-City Interaction. // Bull. Seismol. Soc. Am., 2008, No. 98(6), pp. 2665-2678.

СПИСОК ЛИТЕРАТУРЫ

1. **Белостоцкий А.М., Акимов П.А., Афанасьева И.Н., Кайтуков Т.Б.** Contemporary problems of numerical modelling of unique structures and buildings. // International Journal for Computational Civil and Structural Engineering, 2017, Volume 13, Issue 2, pp. 9-34.
2. **Белостоцкий А.М., Акимов П.А.** Научно-исследовательский центр СтаДиО. 25 лет на фронте численного моделирования. // International Journal for Computational Civil and Structural Engineering, 2016, Volume 12, Issue 1, pp. 9-34.
3. AFPS/AFTES. Guidelines on Earthquake Design and Protection of Underground Structures. Working Group of the French Association for Seismic Engineering (AFPS) and French Tunneling Association (AFTES). Version 1, 2001.
4. **Jia B., Li-ping J., Yong-qiang L.** Seismic Analysis of Underground Structures Based on the Static Finite Element Method. // The Electronic Journal of Geotechnical Engineering, 2016, No. 21(06), pp. 2307-2315.
5. **Wang J.N.** Seismic Design of Tunnels: A Simple State-of-the-art Design Approach. New York, Parsons Brinckerhoff Quade and Douglas Inc., 1993, 159 p.
6. **Baziar M.H., Moghadam M.R., Kim D.-S., Choo Y.W.** Effect of underground tunnel on the ground surface acceleration. // Tunnelling and Underground Space Technology, 2014, Vol. 44, pp. 10-22.
7. **Debiasi E., Gajo A., Zonta D.** On the seismic response of shallow-buried rectangular structures. // Tunnelling and Underground Space Technology, 2013, Vol. 38, pp. 99-113.
8. **Fabozzi S., Licata V., Autuori S., Bilotta E., Russo G., Silvestri F.** Prediction of the seismic behavior of an underground railway station and a tunnel in Napoli (Italy). // Underground Space, 2017, Vol. 2, Issue 2, pp. 88-105.
9. **Fuentes R.** Internal forces of underground structures from observed displacements. // Tunnelling and Underground Space Technology, 2015, Vol. 49, pp. 50-66.

10. **Kawamata Y., Nakayama M., Towhata I., Yasuda S.** Dynamic behaviors of underground structures in E-Defense shaking experiments. // Soil Dynamics and Earthquake Engineering, 2016, Vol. 82, pp. 24-39.
11. **Romero A., Galvin P., Antonio J., Dominguez J., Tadeu A.** Modelling of acoustic and elastic wave propagation from underground structures using a 2.5D BEM-FEM approach. // Engineering Analysis with Boundary Elements, 2017, Vol. 76, pp. 26-39.
12. **Sandoval E., Bobet A.** Effect of frequency and flexibility ratio on the seismic response of deep tunnels. // Underground Space, 2017, Vol. 2, Issue 2, pp. 125-133.
13. **Wang H.-F., Lou M.-L., Chen X., Zhai Y.-M.** Structure – soil – structure interaction between underground structure and ground structure. // Soil Dynamics and Earthquake Engineering, 2013, Vol. 54, pp. 31-38.
14. **Wang H.-F., Lou M.-L., Zhang R.-L.** Influence of presence of adjacent surface structure on seismic response of underground structure. // Soil Dynamics and Earthquake Engineering, 2017, Vol. 100, pp. 131-143.
15. **Wang S.** Evaluation of underground pipe-structure interface for surface impact load. // Nuclear Engineering and Design, 2017, Vol. 317, pp. 59-68.
16. **Wang X., Cai M.** Numerical modeling of seismic wave propagation and ground motion in underground mines. // Tunnelling and Underground Space Technology, 2017, Vol. 68, pp. 211-230.
17. **Zou Y., Liu H., Jing L., Cui J.** A pseudo-static method for seismic responses of underground frame structures subjected to increasing excitations. // Tunnelling and Underground Space Technology, 2017, Vol. 65, pp. 106-120.
18. **Hashasha Y.M.A., Hooka J.J., Schmidt B., Yaoa J.I-C.** Seismic Design and Analysis of Underground Structures. // Tunnelling and Underground Space Technology, 2001, No. 16, pp. 247-293.
19. **Huo H., Bodet A., Fernandez G., Ramirez J.** Load Transfer Mechanisms between Underground Structure and Surrounding Ground: Evaluation of the Failure of the Daikai Station. // J. Geotech Geoenviron, 2005, No. 131(12), pp. 1522-1533.
20. **Zeghal M., Elgamal A.W.** Analysis of Site Liquefaction Using Earthquake Records. // J. Geotech. Eng. ASCE, 1994, No. 120(6), pp. 996-1017.
21. FHWA. Technical Manual for Design and Construction of Road Tunnels – Civil Elements. U.S. Department of Transportation. Federal Highway Administration. Publication No. FHWA-NHI-10-034, 2009. 702 p.
22. ISO 23469. Bases for Design of Structures – Seismic Actions for Designing Geotechnical Works. ISO International Standard. ISO TC 98/SC3/WG10, 2005.
23. **Calvi G.M., Sullivan T.J.** A Model Code for Displacement-Based Seismic Design of Structures. Pavia, IUSS Press, 2009.
24. **Priestley M.J.N.** Myths and Fallacies in Earthquake Engineering – Conflict between Design and Reality. // Bull. Natl. Soc. Earthq. Eng. NZSEE, 1993, No. 26(3), pp. 329-341.
25. **Sedarat H., Kozak A., Hashash Y.M.A., Shamsabadi A., Krimotat A.** Contact Interface in Seismic Analysis of Circular Tunnels. // Tunn. Undergr. Space Technol, 2009, No. 24(4), pp. 482-490.
26. **Tateishi A.**, 2005. A Study on Seismic Analysis Methods in the Cross Section of Underground Structures Using Static Finite Element Method. Structural Engineering // Earthquake Engineering, JSCE., 2005, No. 22(1), pp. 41-53.
27. **Белостоцкий А.М., Акимов П.А., Дмитриев Д.С.** О современных методах редуцирования вычислительной размерности задач расчета конструкций, зданий и сооружений в

рамках метода конечных элементов. // International Journal for Computational Civil and Structural Engineering, 2017, Volume 13, Issue 3, pp. 19-33.
28. **Ghergu M., Ionescum I.R.** Structure – Soil – Structure Coupling in Seismic Excitation and "City Effect". // Int. J. Eng. Sci., 2009, No. 47, pp. 347-354.
29. **Semblat J.F., Kham M., Bard P.Y.** Seismic-Wave Propagation in Alluvial Basins and Influence of Site-City Interaction. // Bull. Seismol. Soc. Am., 2008, No. 98(6), pp. 2665-2678.

Alexander M. Belostotsky, Corresponding Member of the Russian Academy of Architecture and Construction Sciences, Professor, Dr.Sc.; Director of Scientific Research Center "StaDyO"; Professor of Department of Structures, Buildings and Facilities, Russian University of Transport» (RUT – MIIT); Professor of Department of Architecture and Construction, Peoples' Friendship University; Professor of Department of Building Structures and Computational Mechanics, Peoples' Friendship University of Russia; office 810, 18, 3ya Ulitsa Yamskogo Polya, Moscow, 125040, Russia; phone +7 (499) 706-88-10;
E-mail: amb@stadyo.ru.

Pavel A. Akimov, Full Member of the Russian Academy of Architecture and Construction Sciences, PhD, Professor; Executive Scientific Secretary of Russian Academy of Architecture and Construction Sciences; Vice-Director for Science Activities, Scientific Research Center "StaDyO"; Professor of Department of Architecture and Construction, Peoples' Friendship University of Russia; Professor of Department of Structural Mechanics, Tomsk State University of Architecture and Building; 24, Ul. Bolshaya Dmitrovka, 107031, Moscow, Russia;
phone +7(495) 625-71-63; fax: +7 (495) 650-27-31;
E-mail: akimov@raasn.ru, pavel.akimov@gmail.com.

Dmitry S. Dmitriev, Engineer, StaDyO Research & Engineering Center; office 810, 18, 3-ya Ulitsa Yamskogo Polya, Moscow, 125040, Russia;
phone +7 (495) 706-88-10; e-mail: stadyo@stadyo.ru.

Белостоцкий Александр Михайлович, член-корреспондент РААСН, профессор, доктор технических наук; генеральный директор ЗАО «Научно-исследовательский центр СтаДиО»; профессор кафедры «Строительные конструкции, здания и сооружения» Российского университета транспорта (МИИТ); профессор Департамента архитектуры и строительства Российского университета дружбы народов; профессор кафедры строительных конструкций и вычислительной механики Пермского национального исследовательского политехнического университета; 125040, Россия, Москва, ул. 3-я Ямского Поля, д.18, офис 810; тел. +7 (499) 706-88-10;
E-mail: amb@stadyo.ru.

Акимов Павел Алексеевич, академик РААСН, профессор, доктор технических наук; главный ученый секретарь Российской академии архитектуры и строительных наук; заместитель генерального директора по науке ЗАО «Научно-исследовательский центр СтаДиО»; профессор Департамента архитектуры и строительства Российского университета дружбы народов; профессор кафедры строительной механики Томского государственного архитектурно-строительного университета; 107031, г. Москва, ул. Большая Дмитровка, д. 24, стр. 1; тел. +7(495) 625-71-63;
факс +7 (495) 650-27-31; Email: akimov@raasn.ru, pavel.akimov@gmail.com.

Дмитриев Дмитрий Сергеевич, ведущий инженер-расчетчик Отдела расчетных исследований, ЗАО «Научно-исследовательский центр СтаДиО»; 125040, Россия, г. Москва ул. 3-я Ямского Поля, д.18, 8 этаж, офис 810, тел. +7 (495) 706-88-10,
e-mail: stadyo@stadyo.ru.

UNIVERSAL SOFTWARE SYSTEM "STADYO" FOR THE NUMERICAL SOLUTION OF LINEAR AND NONLINEAR PROBLEMS OF THE FIELD THEORY, STATICS, STABILITY AND DYNAMICS OF SPATIAL COMBINED SYSTEMS: GENERAL PARAMETERS AND SUPERELEMENTAL FEATURES

Alexander M. Belostotsky [1, 2, 3, 4, 5]***, Alexey L. Potapenko*** [1]***,***
Pavel A. Akimov [1, 2, 3, 6]

[1] Scientific Research Center "StaDyO", Moscow, RUSSIA
[2] Tomsk State University of Architecture and Civil Engineering, Tomsk, RUSSIA
[3] Peoples' Friendship University of Russia, Moscow, RUSSIA
[4] Russian Transport University (MIIT), Moscow, RUSSIA
[5] Perm National Research Polytechnic University, Perm, RUSSIA
[6] Russian Academy of Architecture and Building Sciences, Moscow, RUSSIA

Abstract: The distinctive paper presents the general papers of the science-based universal software system "STADYO" intended for the numerical solution of stationary and nonstationary problems of field theory, analysis of static, temperature and dynamic stress-strain state (SSS), stability and strength of arbitrary combined mechanical systems (massive-shell-lamellar-membrane-rod with "rigid" bodies, fluid cavities and internal bonds, isotropic and orthotropic materials) into a flat axis, axisymmetric and three-dimensional linear and nonlinear formulations. The composition of the "STADYO" software system is briefly described; in terms of its theoretical foundations, the main provisions and matrix relationships of the superelement method (which is known to be one of the most effective ways to increase the universality and increase the computational efficiency of finite element algorithms) are presented, as well as methods for dynamic synthesis of substructures and submodelling. The superelement algorithm is also extended to solving a system of linear equations at each step of the implicit scheme of direct integration of the equations of motion, and at each iteration in the calculation of natural oscillations; however, an alternative and more efficient approach consists in constructing special superelement algorithms based on the direct condensation of the equations of motion and ideologically close to the method of dynamic synthesis of substructures. The submodelling options, in particular, are important for the refined analysis of the three-dimensional SSS of heavily loaded component parts of the objects under consideration. In general, the presentation of the global design model of the system as a set of substructures is also very convenient for its description and creates the prerequisite for the creation (application) of effective pre- and postprocessor software. The paper also provides information on verification and experience in the use of the "STADYO" software system, as well as prospects for development.

Keywords: buildings, dynamic substructure synthesis method, finite element method, mathematical modelling, submodelling, substructure method, superelement method, "STADYO" software system, structures

УНИВЕРСАЛЬНЫЙ ПРОГРАММНЫЙ КОМПЛЕКС СТАДИО ДЛЯ ЧИСЛЕННОГО РЕШЕНИЯ ЛИНЕЙНЫХ И НЕЛИНЕЙНЫХ ЗАДАЧ ТЕОРИИ ПОЛЯ, СТАТИКИ, УСТОЙЧИВОСТИ И ДИНАМИКИ ПРОСТРАНСТВЕННЫХ КОМБИНИРОВАННЫХ СИСТЕМ: ОБЩАЯ ХАРАКТЕРИСТИКА И СУПЕРЭЛЕМЕНТНЫЕ ВОЗМОЖНОСТИ

Universal Software System “STADYO” for the Numerical Solution of Linear and Nonlinear Problems of the Field Theory, Statics, Stability and Dynamics of Spatial Combined Systems: General Parameters and Superelemental Features

А.М. Белостоцкий [1, 2, 3, 4, 5]***, А.Л. Потапенко*** [1]***, П.А. Акимов*** [1, 2, 3, 6]

[1] Научно-исследовательский центр СтаДиО, г. Москва, РОССИЯ
[2] Томский государственный архитектурно-строительный университет, г. Томск, РОССИЯ
[3] Российский университет дружбы народов, г. Москва, РОССИЯ
[4] Российский университет транспорта (МИИТ), г. Москва, РОССИЯ
[5] Пермский национальный исследовательский политехнический университет, г. Пермь, РОССИЯ
[6] Российская академия архитектуры и строительных наук, г. Москва, РОССИЯ

Аннотация: В настоящей статье представлена общая характеристика наукоемкого универсального программного комплекса СТАДИО, предназначенного для численного решения стационарных и нестационарных задач теории поля, расчетов статического, температурного и динамического напряженно-деформированного состояния (НДС), устойчивости и прочности произвольных комбинированных механических систем (массивно-оболочечно-пластинчато-мембранно-стержневых с «жесткими» телами, полостями жидкости и внутренними связями, изо- и ортотропными материалами) в плоской, осесимметричной и трехмерной линейной и нелинейной постановках. Кратко описан состав программного комплекса СТАДИО, в части его теоретических основ приведены основные положения и матричные соотношения метода суперэлементов (являющегося, как известно, одним из наиболее действенных способов повышения универсальности и увеличения вычислительной эффективности конечноэлементных алгоритмов), а также методов динамического синтеза подконструкций и субмоделирования. Суперэлементный алгоритм распространен также на решение системы линейных уравнений на каждом шаге неявной схемы прямого интегрирования уравнений движения и на каждой итерации при расчете собственных колебаний, однако альтернативный и более эффективный подход состоит в построении специальных суперэлементных алгоритмов, основанных на непосредственной конденсации уравнений движения и идеологически близких методу динамического синтеза подконструкций. Опции субмоделирования, в частности, являются важными для уточненного анализа трехмерного НДС тяжело нагруженных узлов-деталей рассматриваемых объектов. В целом, представление глобальной расчетной модели системы в виде совокупности подконструкций является также очень удобным для ее описания и создает предпосылку для создания (применения) эффективных пре- и постпроцессорных программных средств. В статье также приведены сведения о верификации и опыте использования программного комплекса СТАДИО, а также рассмотрены перспективы развития.

Ключевые слова: математическое моделирование, метод конечных элементов, метод суперэлементов, метод подконструкций, метод динамического синтеза подконструкций, субмоделирование, программный комплекс СТАДИО, конструкции, здания, сооружения

1. GENERAL CHARACTERISTICS OF “STADYO” SOFTWARE SYSTEM

Founded in far 1975, the Russian multipurpose software system “STADYO” ™ provides a numerical solution of stationary and nonstationary field theory problems, analysis of the static, temperature and dynamic stress-strain state (SSS), stability and strength of arbitrary combined mechanical systems (massively shell-lamellar-membrane-rod with “rigid” bodies, fluid cavities and internal bonds, isotropic and orthotropic materials) in a plane, axisymmetric and three-dimensional linear and nonlinear statements [1, 2, 8].

In the “STADYO” software product, a representative library of straight- and curvilinear rod, flexural-membrane, curved super- (thin- and medium-walled shells) and isoparametric volumetric finite elements (total more than 120 types), elements with given stiffness, inertia and damping matrices see, for example, Figure 1), modern optimized numerical algorithms (the methods of Cholesky and the preconditioned conjugate gradient, block method of Lanczos and method of iterations of the subspace, explicit and implicit difference schemes of integration: central differences, Newmark, Wilson and Crank - Nicholson, finite-element and superelement schemes, etc.) and developed service provision are implemented.

The main quantitative possibilities for the version of the complex on IBM-compatible PCs (the main programming language of the computational modules is Intel Visual Fortran) are presented in Table 1.

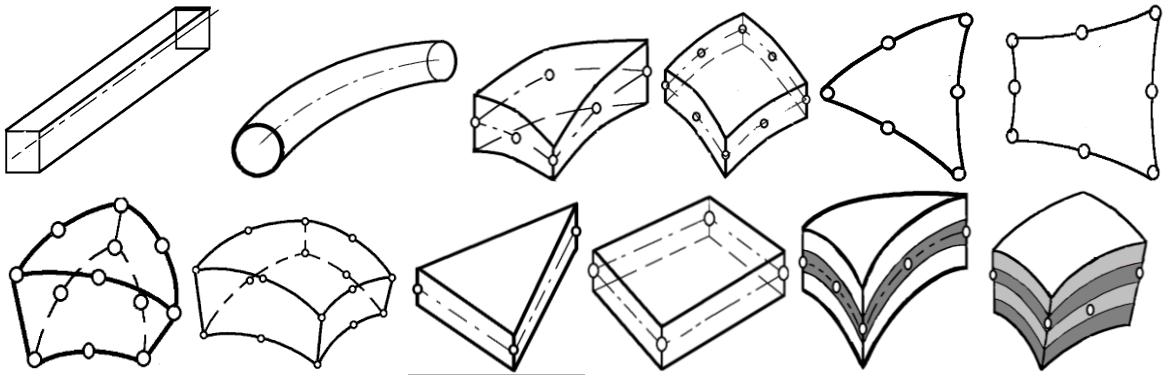


Figure 1. Some implemented types of finite elements.

Table 1. The main quantitative capabilities of "STADYO" software system.

Parameter for system / superelement	Limiting value
Degrees of freedom	**24 000 000**
Grid station	**4 000 000**
Finite elements	**4 000 000**
Fabric (environment)	**4 000 000**
Eigenfrequencies and forms	**4 000**

The hierarchy and degree of "nesting" of substructures (for the superelement "branch" of the software system) are arbitrary.

2. COMPOSITION OF THE "STADYO" SOFTWARE SYSTEM

"STADYO" software system consists of the following program modules (Figure 2):

- *STADYO-STATN* – solution of stationary problems of thermal conductivity, filtration, flow of an ideal fluid, and other problems of field theory with arbitrary boundary conditions;
- *STADYO-NSTATN* – solution of non-stationary problems of field theory (with the possibility of memorizing and using results for the subsequent solution of elastic problems);
- *STADYO-STAT* – linearly elastic calculation for stationary loads (volumetric, surface, linearly distributed, concentrated forces and moments, temperature, initial strains and stresses), including multiple-choice calculations, taking into account the stage-by-stage construction;
- *STADYO-FORM* – solving a particular problem of eigenvalues: determining the significant part of the spectrum of eigenfrequencies and vibration modes, critical loads and forms of stability loss;
- *STADYO-SEISM* – quasi-static "normative" spectral calculation for seismic actions specified by the acceleration spectra, with the determination of displacements, accelerations, forces and stresses using alternative methods;
- *STADYO-VIBR* – estimation of parameters of forced steady-state oscillations of systems without damping, with orthogonal and non-orthogonal damping;
- *STADYO-SPEC* – spectral dynamic calculation of linear-elastic systems (and systems with local nonlinearities) for force and kinematic effects with decomposition according to the modes of natural oscillations;
- *STADYO-DYN* – direct integration over time of the equations of motion of linear-elastic systems for given thermo-force and kinematic influences (including «non-platform» excitation schemes) with determination of accelerograms and response spectra;

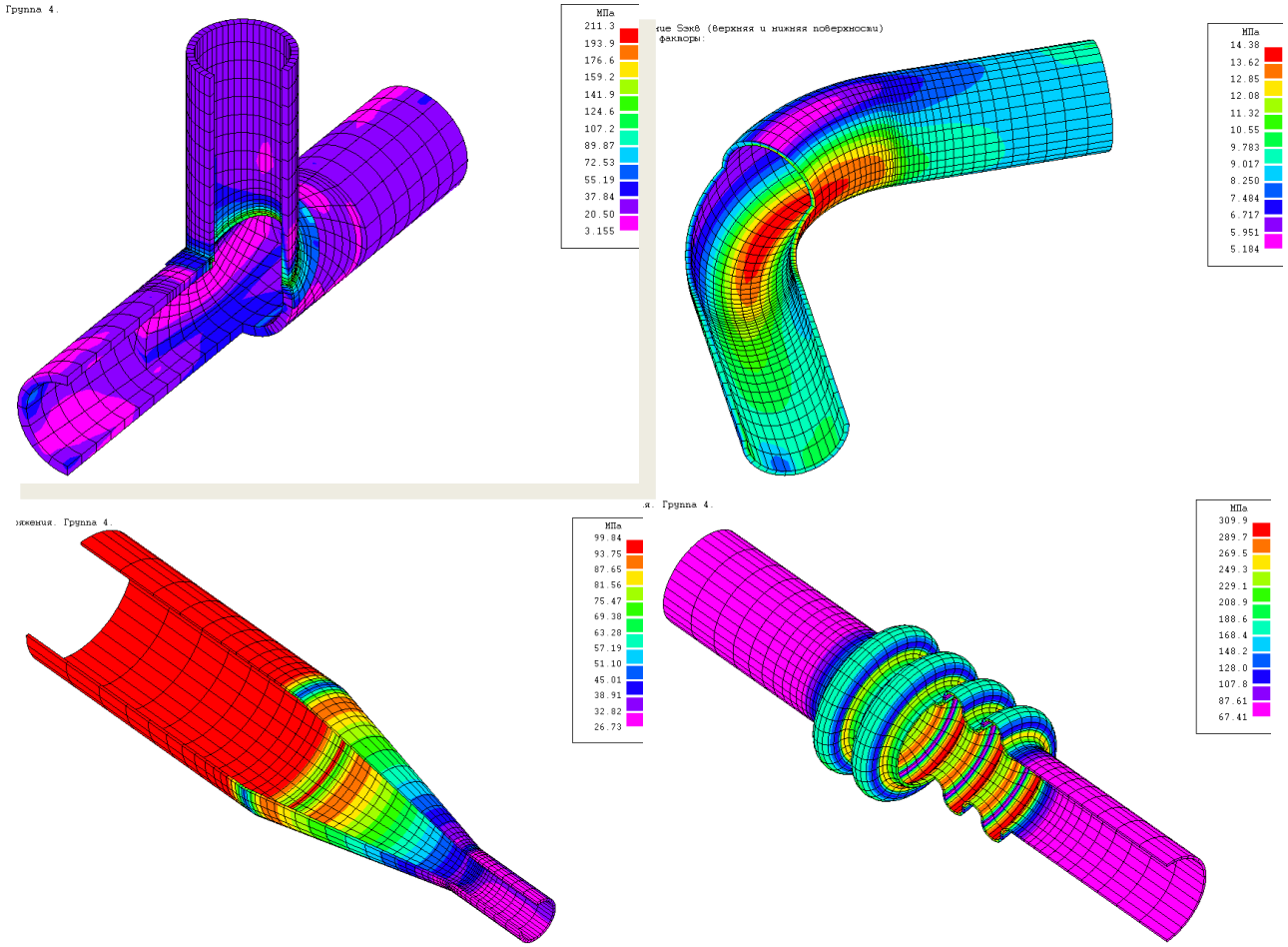


Figure 2. Stress state of pipeline parts (STADYO-ASTRA), 2005.

- *STADYO-NLIN* – solution of nonlinear problems (large displacements, finite deformations, plasticity, viscoplasticity and heredity effects for metals, concretes and soils, unilateral joints, seams and cracks with friction) for given static and dynamic thermal and kinematic influences;
- *STADYO-FRACT* – solving the linear problems of fracture mechanics, including the determination of stress intensity factors and J-integrals in bodies with cracks;
- *STADYO-SNIP* – the estimated evaluation of the strength and longitudinal reinforcement of reinforced concrete structures for the first and second limit states in accordance with the provisions of the current Russian building codes and regulations (SNiPs);
- *STADYO-ASTRA* – an object-oriented subsystem of refined automated calculation of the spatial temperature and stress-strain state, estimation of static, seismic and cyclic strength (in accordance with the requirements of the PNAE standards G-7-002-86) of typical pipeline parts: tees, bends and knees, conical transitions, lens compensators and zones of welded joints;
- *STADYO-CABINET* – an object-oriented subsystem of automated seismic resistance calculation (in accordance with the requirements of nuclear energy norms) of standard instrument cabinets of nuclear power plants;
- *STADYO-PED* – object-oriented subsystem of automated calculation of vibration of submersible electric motors (multi-layer thick-walled orthotropic finned shells in a viscous liquid);

- *STADYO-WEU* – an object-oriented subsystem of automated static and dynamic calculation of typical orthogonal wind power plants.

3. METHODS OF SUBMODULATION AND DYNAMIC SYNTHESIS OF SUBCONTRACTIONS

3.1. Preliminary remarks.

Modern "heavy" finite-element software systems (ANSYS, NASTRAN, SIMULIA Abaqus) contain options for constructing and importing-exporting reduced impact matrices to ensure, in particular, joint development and accurate analysis of complex multiply connected statically and dynamically loaded engineering structures and buildings. Another side of the same process is submodelling, for example, refined three-dimensional nonlinear analysis of complex and / or originally solved structural components of rod systems (column support, connections of chord-diagonal members, parts of pipeline systems). In this paragraph, the main provisions and matrix relations of methods of dynamic synthesis of substructures (MDS) and submodelling implemented in "STADYO" product are given.

3.2. The concept of the method of superelements.

One of the most effective ways to increase the computational efficiency of finite element algorithms is the superelement method (SEM), also known as the sub-structure method. The key procedure of the SEM is static condensation [9, 10] — elimination of internal degrees of freedom of the substructure $\{u_i\}$, — leading the initial block system of equilibrium equations

$$\begin{bmatrix} K_{ii} & K_{ib} \\ K_{bi} & K_{bb} \end{bmatrix} \begin{Bmatrix} u_i \\ u_b \end{Bmatrix} = \begin{Bmatrix} F_i \\ F_b \end{Bmatrix} \qquad (3.1)$$

to the reduced system with respect to the components of the vector of the corresponding boundary unknowns $\{u_b\}$:

$$[\bar{K}]\{u_b\} = \{\bar{F}\}, \qquad (3.2)$$

where

$$[\bar{K}] = [K_{bb}] - [K_{bi}][K_{ii}]^{-1}[K_{ib}]; \qquad (3.3)$$

$$\{\bar{F}\} = \{F_b\} - [K_{bi}][K_{ii}]^{-1}\{F_i\}. \qquad (3.4)$$

Accounting of the possible repeatability of subsystems leads to significant savings both by reducing the number of arithmetic operations, and to a significant reduction in the amount of stored and processed information. The data structure is organized hierarchically, so that making local changes to the calculation scheme, i.e. the correction of a part of the numerical model of the structure can be performed independently for each substructure with minimal computational costs. Representation of the global design model of the system as a set of substructures is also very convenient for its description and creates the prerequisite for the creation (application) of effective pre- and postprocessor software [1].

3.3. Methods of dynamic synthesis of substructures.

The superelement algorithm is also extended to solving a system of linear equations at each step of the implicit scheme of direct integration of the equations of motion and at each iteration in the calculation of natural oscillations [1]. An alternative and more efficient approach is the construction of special superelement algorithms based on the direct condensation of the equations of motion and ideologically close to the method of dynamic synthesis of substructures.

Methods for the dynamic synthesis of substructures can be classified by the method of selecting the basis vectors of the Rayleigh - Ritz method for substructures and by the method of their joining. Most often, as a basis for substructures, its vibration forms are used under certain boundary conditions: R.R. Craig, M.C.C. Bampton [15] and [16] – for the fixed boundary, [20] – for the free boundary, [17] – for the partially fixed boundary of the subconstruction.

The most preferable from the computational and realization points of view among the three considered variants of the method is the first one, which uses the vibration modes of the basic system of the displacement method. In order to simplify the joining of substructures and to correctly take into account their rigid displacements and displacements of boundary points, the basis of the vibration modes is expediently supplemented by a set of static functions of the superelement form, each of which is a vector of elastic displacements of the substructure nodes caused by a single displacement in the direction of the corresponding fictitious bond for the basic system of the displacement method. Such an approach, in particular, is described in [18,19].

In the general case, in a dynamic synthesis any suitable system of linearly independent vectors can be used as a basis for substructures, not necessarily including oscillation modes. Thus, in [21] a certain specific basis is used, for the construction of which a solution of the particular eigenvalue problem for the subconstruction is not required.

The numerical solution of the resulting reduced system of nonlinear integro-differential equations is found by modified implicit difference schemes of the Newmark type with the use of a significant part of the natural frequencies

$$[\Omega] = diag(\omega_1, \omega_2, ..., \omega_n)$$

and form $[\Phi]$ of the partial subsystems-substructures [14]:

$$[\overline{M}]\{\ddot{u}_b\} + [\overline{C}]\{\dot{u}_b\} + [\overline{K}]\{u_b\} + \\ + \sum [G][\Omega] \int_0^t \mathrm{SIN}[\Omega(t-\tau)][G]^{\mathrm{T}} \{u_b(\tau)\} d\tau = \\ = \sum (\{\overline{F}(t)\} - [G][\Omega]^2 \{q(t)\}); \quad (3.5)$$

$$\{u_b(0)\} = \{u_{0b}\}; \quad \{\dot{u}_b(0)\} = \{v_{0b}\}; \quad (3.6)$$

$$[\overline{M}] = [M_b] + \sum [\overline{M}]; \quad [\overline{C}] = [C_b]; \quad (3.7)$$

$$[\overline{K}] = [K_b] + \sum [\overline{K}]; \quad (3.8)$$

$$[\overline{M}] = [M_{bb}] - [M_{bi}][M_{ii}]^{-1}[M_{ib}]; \quad (3.9)$$

$$[\overline{K}] = [K_{bb}] - [K_{bi}][K_{ii}]^{-1}[K_{ib}]; \quad (3.10)$$

$$\{\overline{F}(t)\} = \{F_b(t)\} - [M_{bi}][M_{ii}]^{-1}\{F_i(t)\}; \quad (3.11)$$

$$[G] = [K_{bi}][\Phi][\Omega]^{-2} - [M_{bi}][\Phi]; \quad (3.12)$$

$$\{q\} = \{q(t)\} = \mathrm{COS}[\Omega t][\Phi]^{\mathrm{T}}[M_{ii}]\{\overline{u}_{0i}\} + \\ + [\Omega]^{-1}\,\mathrm{SIN}[\Omega t][\Phi]^{\mathrm{T}}[M_{ii}]\{\overline{v}_{0i}\} + \\ + [\Omega]^{-1}\,\mathrm{SIN}[\Omega t] * [\Phi]^{\mathrm{T}}\{F_i(t)\}; \quad (3.13)$$

$$\{\overline{u}_{0i}\} = \{u_{0i}\} + [K_{ii}]^{-1}[K_{ib}]\{u_{0b}\}; \quad (3.14)$$

$$\{\overline{v}_{0i}\} = \{v_{0i}\} + [K_{ii}]^{-1}[K_{ib}]\{v_{0b}\}; \quad (3.15)$$

$$\mathrm{SIN}[\Omega t] = diag[sin(\omega_1 t), sin(\omega_2 t), ..., sin(\omega_n t)]. \quad (3.16)$$

Craig-Bempton approach [5,7,13,16] realized in universal “commercial” products (NASTRAN, ANSYS, ADAMS, ...), is mentioned most popular, which reduces to the construction of reduced stiffness and mass matrices:

$$[\hat{K}] = [\hat{\Phi}]^{\mathrm{T}} \begin{bmatrix} K_{ii} & K_{ib} \\ K_{bi} & K_{bb} \end{bmatrix}; \quad [\hat{\Phi}] = \begin{bmatrix} \hat{K}_{CC} & 0 \\ 0 & \hat{K}_{NN} \end{bmatrix}; \quad (3.17)$$

$$[\hat{M}] = [\hat{\Phi}]^{\mathrm{T}} \begin{bmatrix} M_{ii} & M_{ib} \\ M_{bi} & M_{bb} \end{bmatrix}; \quad [\hat{\Phi}] = \begin{bmatrix} \hat{M}_{CC} & \hat{M}_{NC} \\ \hat{M}_{CN} & \hat{M}_{NN} \end{bmatrix}, \quad (3.18)$$

where

$$[\hat{\Phi}] = \begin{bmatrix} I & 0 \\ \Phi_{iC} & \Phi_{iN} \end{bmatrix}; \quad (3.19)$$

Φ_{iC} – displacement of internal degrees of freedom for given single displacements of boundary (docking) nodes; Φ_{iN} – displacements of the internal degrees of freedom, corresponding to the retention of its own forms of oscillation, while limiting the degrees of freedom (sealing) of the boundary nodes; $[\hat{K}_{NN}]$ and $[\hat{M}_{NN}]$ – diagonal modal stiffness and mass matrices;

$$[\hat{K}_{CC}] \equiv [\overline{K}]; \quad [\hat{M}_{CC}] \equiv [\overline{M}]; \quad [\hat{M}_{NC}] = [\hat{M}_{CN}]^{\mathrm{T}} \tag{3.20}$$

– filled matrix.

The same algorithm has been implemented since 1999 in the research "STADYO" software product [2]. The software implementation of matrix operations in the formation of $[\hat{K}]$ and $[\hat{M}]$ (and reduced load vectors $\{\hat{F}\}$), as well as possible affine transformations, is basically built on standard procedures contained in software package modules. Fulfilling the canonical finite(-super)-element assembly does not encounter any difficulties and allowance for consideration of $[\hat{K}]$, $[\hat{M}]$ and $\{\hat{F}\}$ in the general super-element model.

4. VERIFICATION AND EXPERIENCE OF USING THE STADYO SOFTWARE SYSTEM

The «STADYO» software system is verified in detail on a representative set of test and practical tasks, certified in Rostekhnadzor (2011, as part of ASTRA-STADYO [4]), documented in detail and implemented in leading design and research organizations "Atomenergoproject" and "Hydroproject", Special Design Bureau "Hydropress", All-Russian Research Institute of Atomic Engineering, All-Russian Research Institute of Electromechanics, Central Research Institute of Construction Structures, Design Bureau "Krasnaya Zvezda", JSC "Melaks", etc.). There is more than 41 years of experience with the complex in calculating studies of the spatial temperature and stress-strain state, strength and reliability of pipelines and their elements, technological, electrical equipment, machines and mechanisms, building structures and "foundation – construction" systems of particularly responsible industrial facilities and civil construction, taking into account the normatively regulated combinations of temperature, static, special dynamic (wind, seismic shock, wave, vibration, etc.) and emergency actions (Figure 3-14), such as:

- protective shells, reactor compartments, computer rooms, special buildings, diesel-generating standby electric power stations, cooling towers and waste storages of nuclear power plants (Armenian, Kursk, Smolensk, Chernobyl, Ignalina, Leningrad, Bilibinskaya, Novovoronezhskaya, Kalininskaya, Rostovskaya, Balakovo, Lovisa (Finland), Kozloduy (Bulgaria), Busher (Iran), Kudankulam (India), nuclear power plants of the new generation, etc.);
- dams, buildings of hydroelectric power plants and underground hydraulic structures, taking into account the stage-by-stage construction, nonlinear effects in seams and macro cracks, soil rheology, hydrodynamic effects of reservoirs (Volga, Kama, Inguri, Khudoni, Kurpsai, Nurek, Rogun, Namakhvani, Katun, Gekhi, Kapanda, Teri, Tang-E-Duk, Zagorskaya hydroelectric pumped storage power plant, etc. [3]);
- wind power plants of various types;
- unique buildings and typical civil engineering constructions (roof slab of the Big sports arena of Luzhniki, the monument to the 300th anniversary of the Russian Navy, the high-rise complex of the Moscow International Currency of Moscow Central Stock Exchange, the underground parking on the Manege Square shopping complex, the Aquadrome and Transvaal Park, the Basmanny Building market, the indoor swimming pool of the "Iskra" sanatorium (Sochi), multistorey panel and prefabricated monolithic block sections and their "assemblies" with an assessment of stability in emergency situations, high-altitude multifunctional complexes, etc. [6]);
- aboveground and underground pipelines of heating systems, main oil and gas pipelines, oil and gas processing and petrochemical industries, oil and gas exploration complexes;
- floating structures, ice-resistant platforms for oil and gas production on the shelf (Chayvo-1 and others);

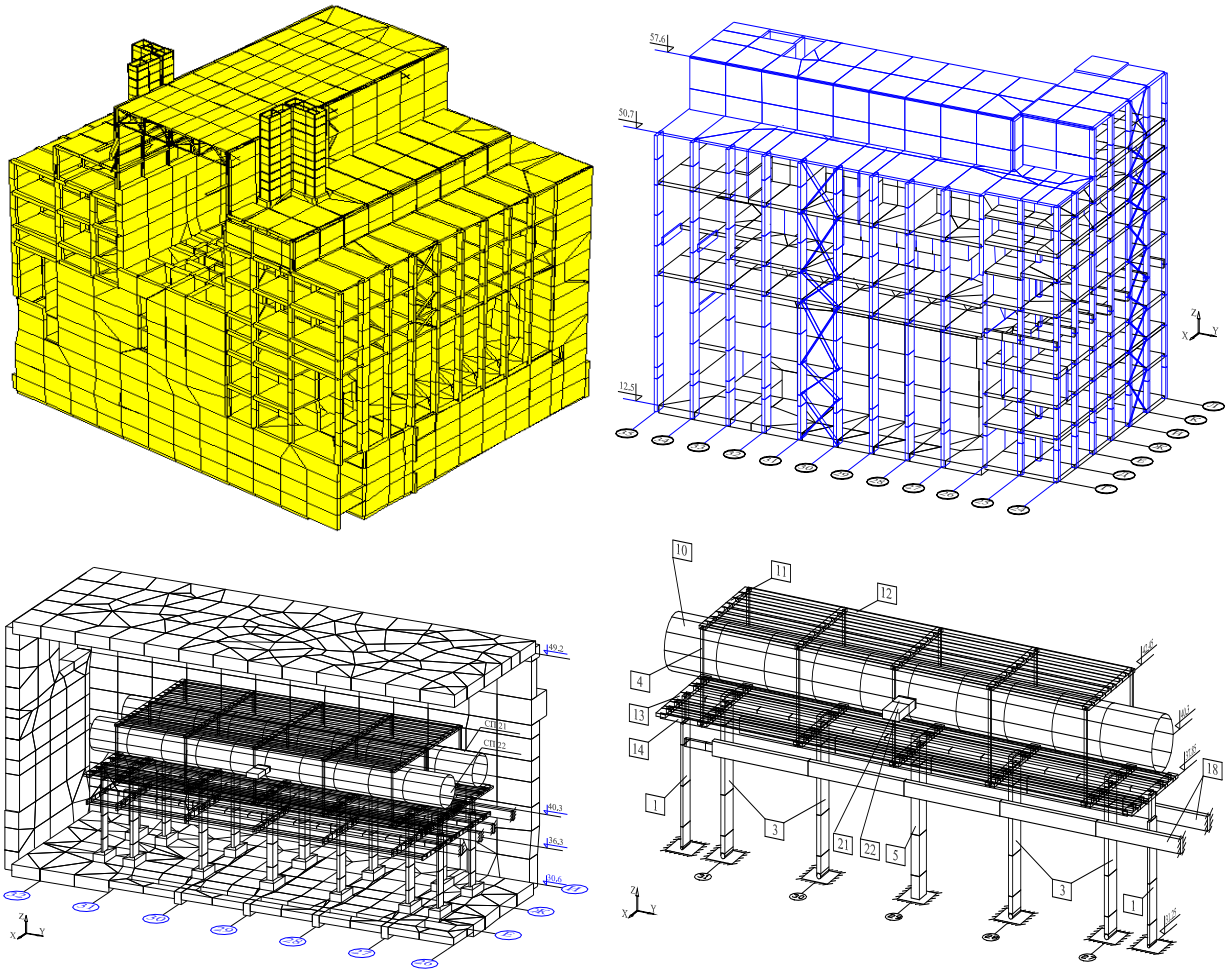


Figure 3. Multilevel superelement dynamic model of the system “Building structures – equipment” of the NPP with LWGR (1989).

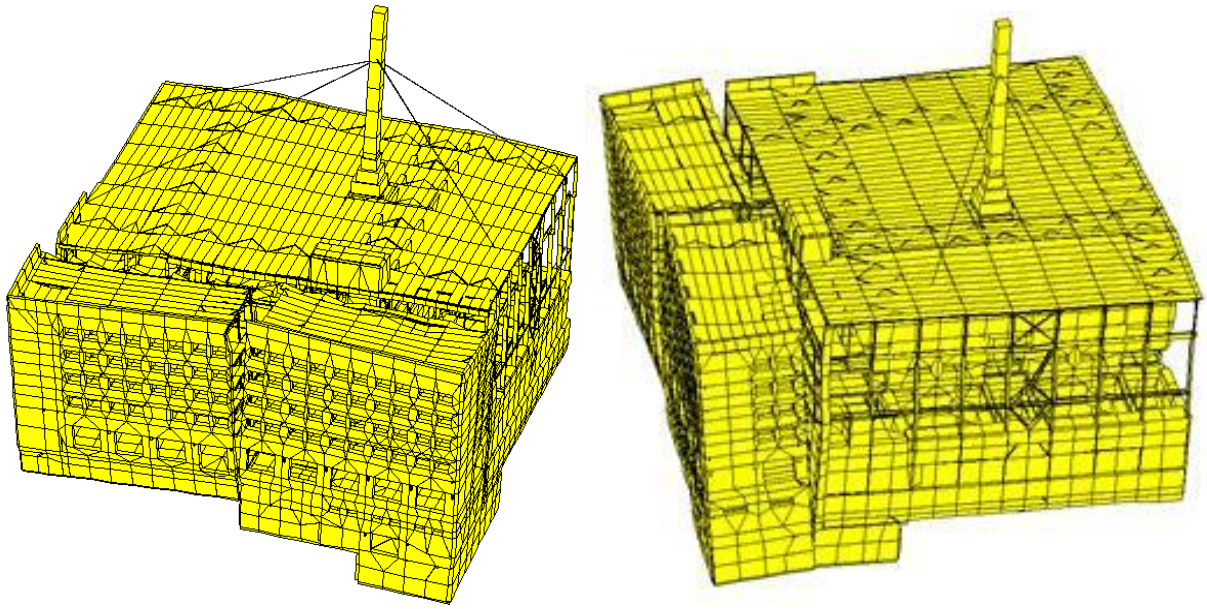


Figure 4. The calculated deformed state of the main building of Bilibino NPP (2001).

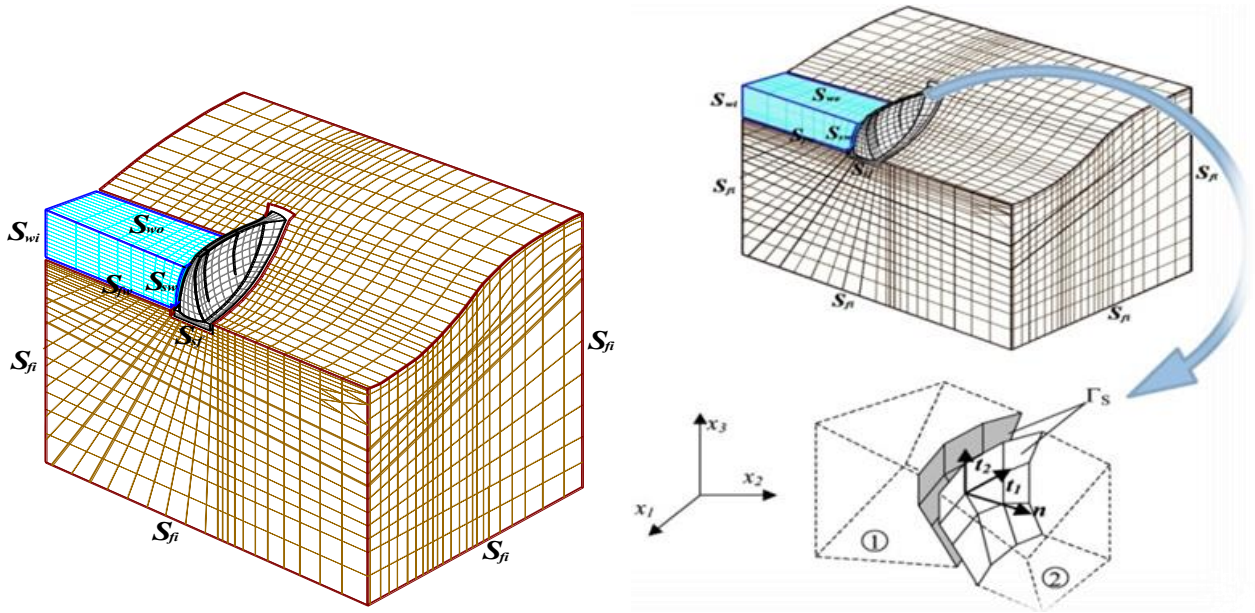


Figure 5. Typical superelement model of the "foundation – dam – reservoir" system.

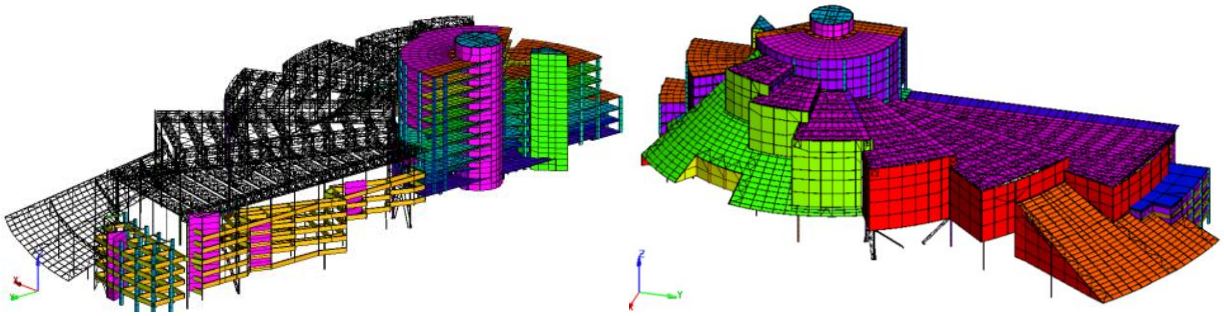


Figure 6. Super-element model of the sports complex "Aquadrom".

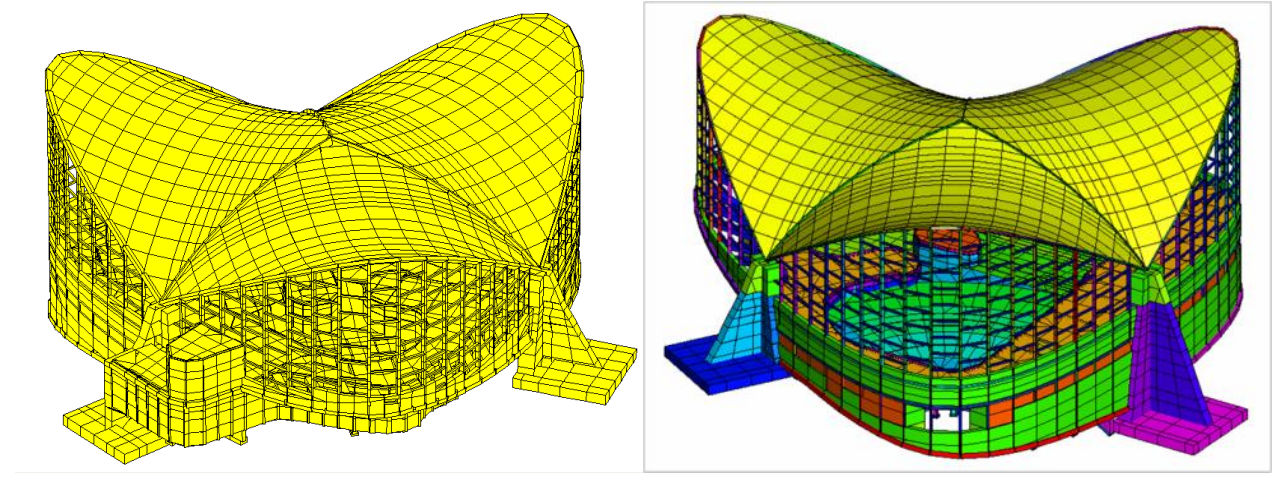


Figure 7. Super-element model of the indoor pool of the "Iskra" sanatorium (Sochi).

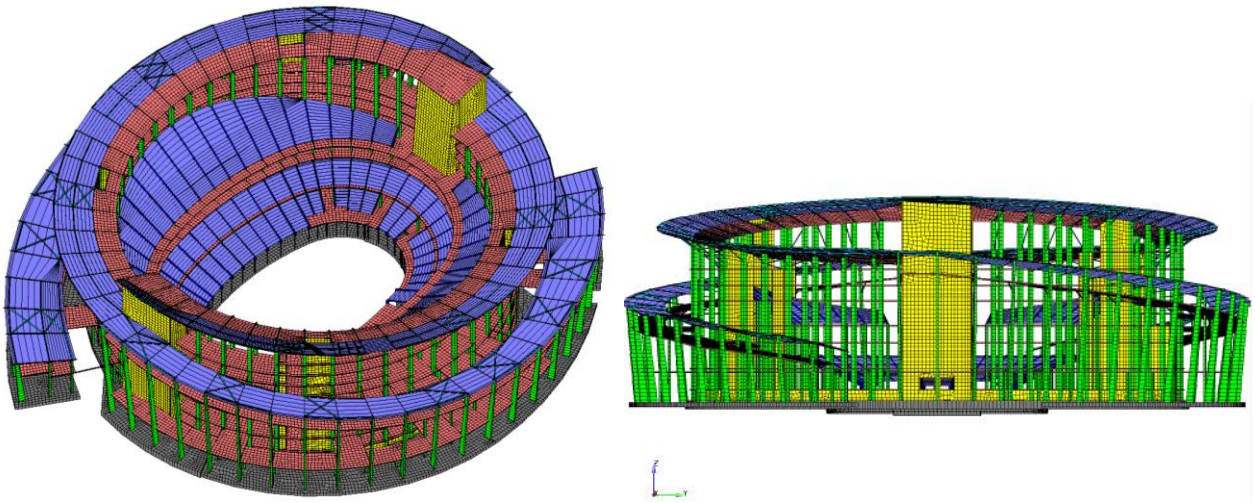


Figure 8. Superelement model of the ice palace of sports on Khodynka.

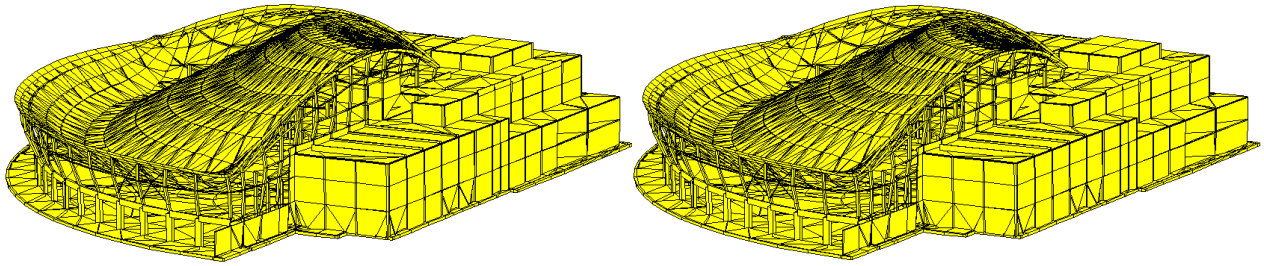


Figure 9. Deformed states of the “construction – foundation” system of the Transvaal-Park sports and fitness center with estimated load combinations (2005).

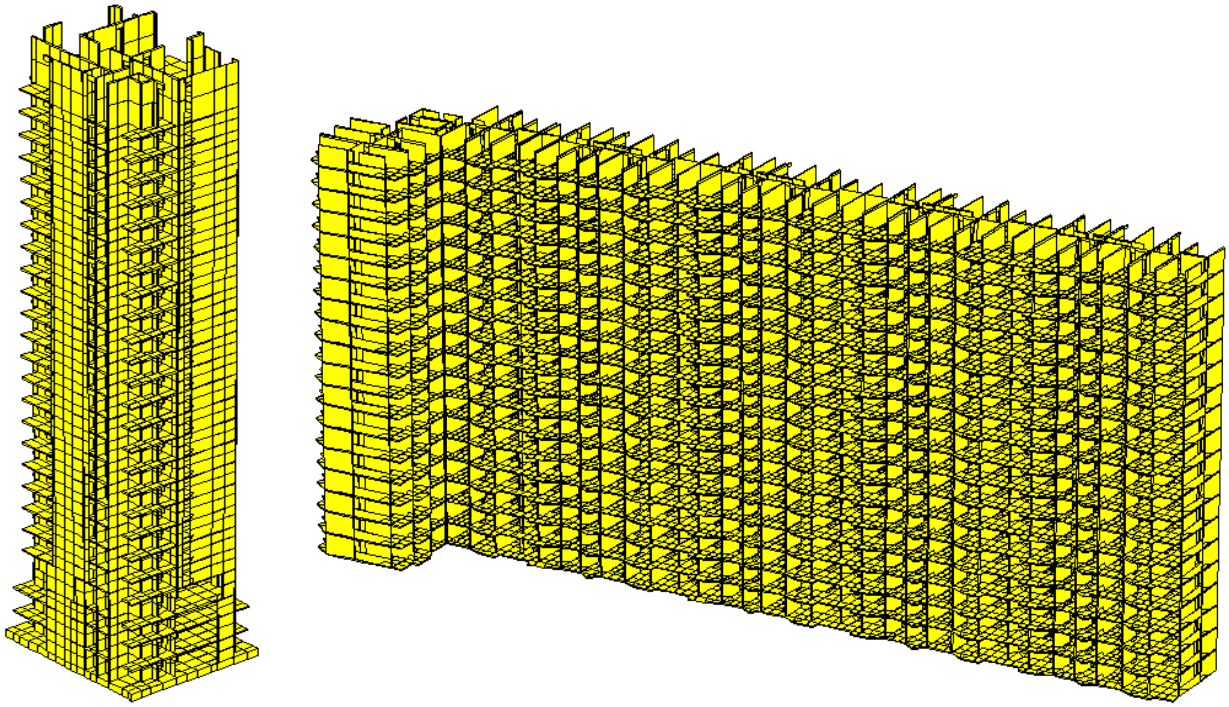


Figure 10. Superelementary models of single- and multisectional houses of typical series.

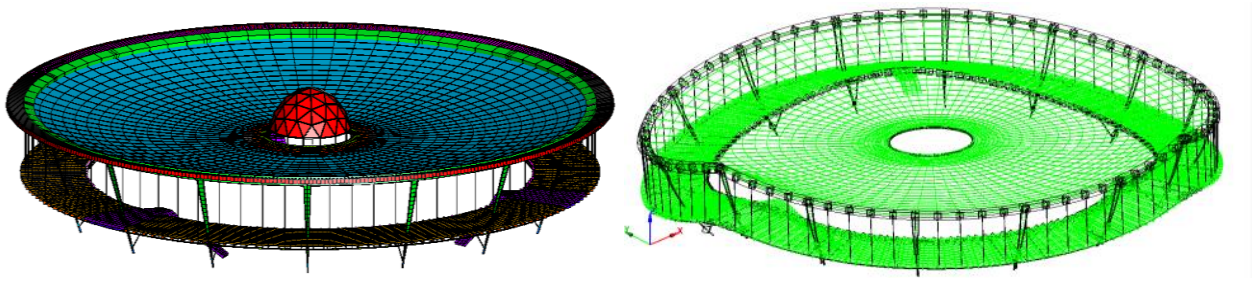


Figure 11. Superelement model and deformed state of the Basmanny market (2007).

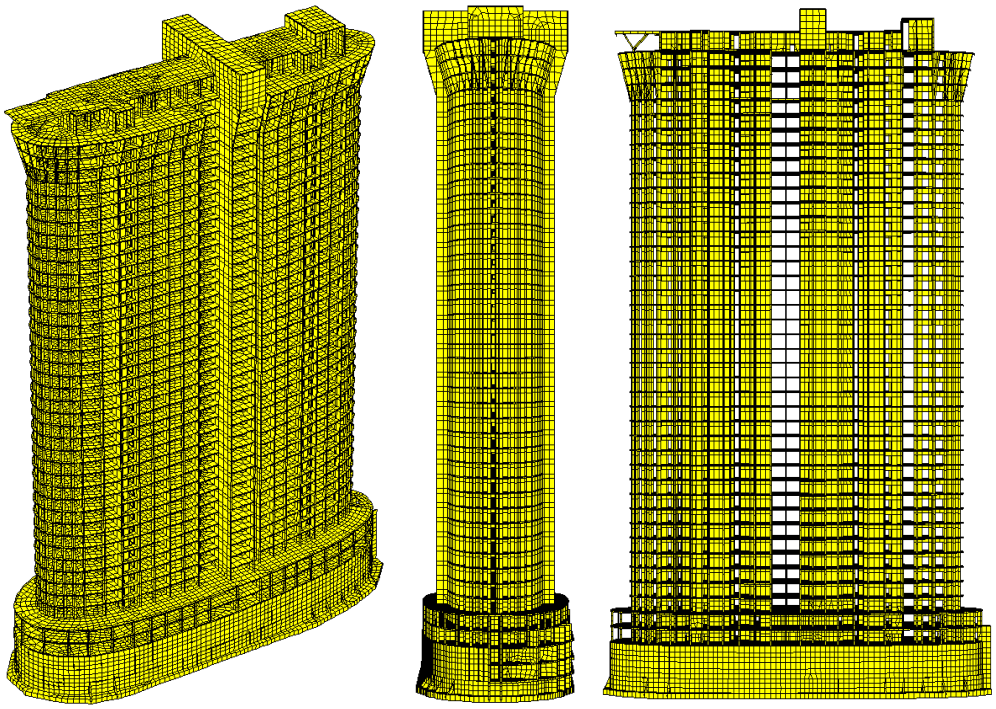


Figure 12. Model of multifunctional high-rise (44 floors) of the complex.

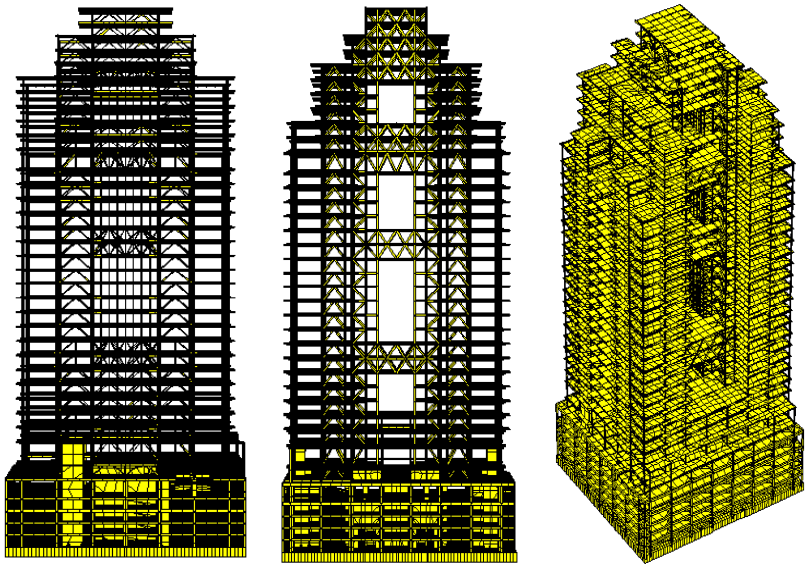


Figure 13. Model of a high-rise building of the Interbank Currency Exchange (5 underground and 31 above-ground floors).

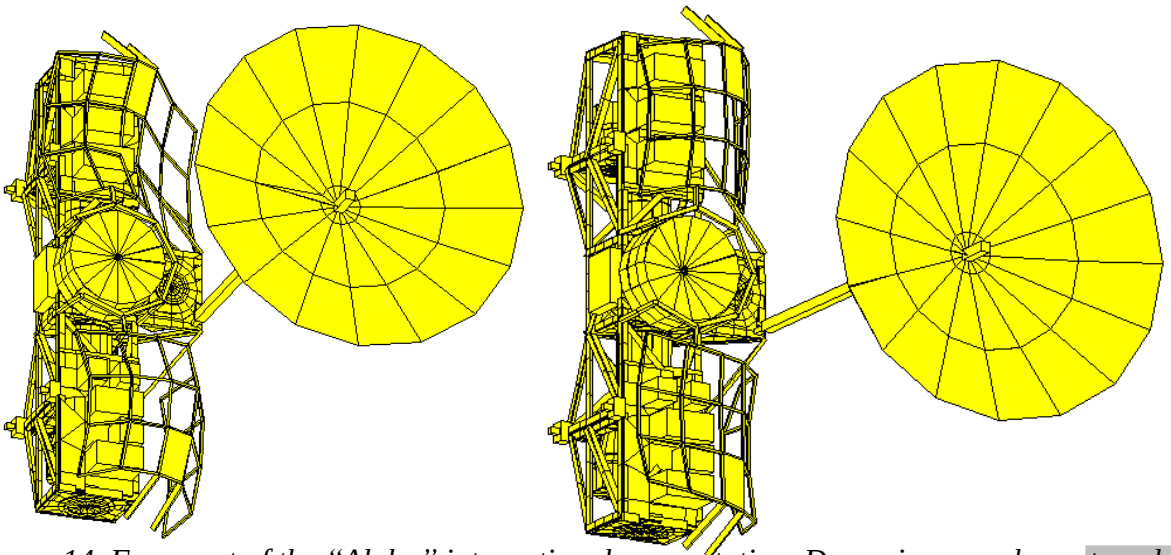


Figure 14. Fragment of the "Alpha" international space station. Dynamic superelement model. Lower own vibration modes (1999).

- complex machine-building structures, parts, machines and mechanisms (aerospace systems, transport, ship and power engineering, ferrous and non-ferrous metallurgy, household appliances, etc.).

Among the solved pioneering tasks is the modelling of the dynamics and strength of the "Russian segment – drive units – solar cells" system of the International Space Station "Alpha" at the stages of transportation, launch and orbital activity.

It should be noted that the outrunning development and use of the method of dynamic synthesis of substructures in the aerospace industry — this is evidenced by the above-mentioned fundamental theoretical works [12, 16, 17-19, 21] – seems historically and substantively substantiated. Indeed, dozens of design firms in different countries independently develop and optimize dynamically linked main subsystems (blocks and nodes), and the «price of the issue» is extremely high.

5. HORIZONS FOR THE DEVELOPMENT OF THE «STADYO» SOFTWARE SYSTEM

Among the planned tasks for the development of "STADYO" software system we can name the following, reinforcing its status of a universal research software system [11]:

- development of an interface with "heavy" CAD systems for import-export models;
- development of a complete verification report reflecting the new capabilities of the software package;
- increase the computational dimension of the solved problems due to the new possibilities for creating geometric and FE models, the implementation of algorithms for parallel computations [12];
- further development of software implementations of alternative algorithms for dynamic synthesis of substructures;
- realization of a discrete-continual version of the finite element method as a competitive alternative and complement to the traditional FEM schemes;
- allowance for plastic deformation of metals (associated flow law with isotropic and kinematic hardening) for an adequate assessment of the static strength of pipeline parts, equipment and metal structures.

REFERENCES

1. **Belostotsky A.M., Akimov P.A.** (Eds.). Aktual`ny`e Problemy` Chislennogo Mode-

lirovaniya Zdanij, Sooruzhenij i Kompleksov [Actual Problems of Numerical Modelling of Structures, Buildings and Facilities]. Vol 2. To the 25th anniversary of the Scientific Research Center "StaDyO". Moscow, ASV, 2016, 596 pages.

2. **Belostotsky A.M., Akimov P.A.** Nauchno-issledovatel`skij Centr STADYO. 25 Let na Fronte Chislennogo Modelirovaniya [25th Anniversary of Scientific Centre StaDyO]. // International Journal for Computational Civil and Structural Engineering, 2016, Volume 12, Issue 1, pp. 8-45.
3. **Belostotsky A.M., Akimov P.A., Dmitriev D.S.** O Sovremenny`x Metodax Reducirovaniya Vy`chislitel`noj Razmernosti Zadach Rascheta Konstrukcij, Zdanij i Sooruzhenij v Ramkax Metoda Konechny`x E`lementov [About Contemporary Approaches to Reduction of Computational Dimension of Problems of Structural Analysis within Finite Element Method]. // International Journal for Computational Civil and Structural Engineering, 2017, Volume 13, Issue 3, 2017, pp. 19-33.
4. **Belostotsky A.M., Voronova G.A., Potapenko A.L.** Razvitie i Integraciya v SAPR "Semejstva" Programmny`x Kompleksov ASTRA-NOVA dlya Normativny`x Raschetov na Prochnost` Truboprovodny`x Sistem Razlichnogo Naznacheniya [Development and integration into CAD of "software family" Astra-NOVA systems for normative calculations on the strength of pipeline systems for various purposes]. // SAPR i grafika, 2003, No. 5, pp. 55-65.
5. **Belostotsky A.M., Dubinsky S.I., Potapenko A.L.** Metody` Dinamicheskogo Sinteza Podkonstrukcij v Zadachax Modelirovaniya Slozhny`x Inzhenerny`x Sistem [Methods of Dynamic Synthesis of Substructures in the Modeling of Complex Engineering Systems]. // Stroitel`naya mexanika i raschet sooruzhenij, 2006, No. 6, pp. 45-52.
6. **Belostotsky A.M., Penkovoj S.B., Scherbina S.V., Kaytukov T.B., Akimov P.A.** Razrabotka i Verifikaciya Metodiki Chislennogo Modelirovaniya NDS, Prochnosti i Ustojchivosti Mnogoe`tazhny`x Panel`ny`x Zdanij [Development and Verification of Methods of Numerical Simulation of Stress-Strain State, Strength and Stability of Multi-storey Panel Buildings]. // Stroitel`naya Mexanika i Raschet Sooruzhenij, 2014, No. 6, pp. 24-30.
7. **Belostotsky A.M., Potapenko A.L.** Realizaciya i Verifikaciya Metodov Submodelirovaniya i Dinamicheskogo Sinteza Podkonstrukcij v Universal`ny`x i Specializirovanny`x Programmny`x Kompleksax [Implementation and Verification of Methods of Submodeling and Dynamic Synthesis of Substructures in Universal and Specialized Software Systems]. // International Journal for Computational Civil and Structural Engineering, 2011, Volume 7, Issue 1, pp. 76-83.
8. **Belostotsky A.M., Potapenko A.L., Klepets O.Yu.** Realizaciya Metodov Dinamicheskogo Sinteza Podkonstrukcij i Submodelirovaniya v Programmny`x Kompleksax STADYO i ASTRA-NOVA [Implementation of Methods of Dynamic Synthesis of Substructures and Submodeling in Software Systems STADIO and ASTRA-NOVA]. // International Journal for Computational Civil and Structural Engineering, 2010, Volume 6, Issue 1&2, pp. 87-91.
9. **Gajan R.** Privedenie Matricz Zhestkosti i Massy` [Reduction of stiffness and mass matrices]. // Raketnaya texnika i kosmonavtika, 1965, Vol. 3, No. 2, pp. 277-278.
10. **Zienkiewicz O.C.** Metod Konechny`x E`lementov v Texnike [Finite Element Method in Engineering]. Moscow, Mir, 1975, 511 pages.
11. **Travush V.I., Akimov P.A., Baenxaev A.V., Bekker A.T., Belostotsky A.M., Kaytukov T.B., Sidorov V.N.** Ob Osnov-

ny`x Itogax Shestogo Mezhdunarodnogo simpoziuma “Aktual`ny`e Problemy` Komp`yuternogo Modelirovaniya Konstrukcij i Sooruzhenij” [About Main Results of the Sixth International Symposium "Actual Problems of Computer Simulations in Civil Engineering”]. // International Journal for Computational Civil and Structural Engineering, 2016, Volume 12, Issue 3, pp. 129-144.

12. **Belostotsky A.M., Akimov P.A., Afanasyeva I.N., Kaytukov T.B.** Contemporary Problems of Numerical Modelling of Unique Structures and Buildings. // International Journal for Computational Civil and Structural Engineering / Международный журнал по расчету гражданских и строительных конструкций, Volume 13, Issue 2, 2017, pp. 9-34.
13. **Belostotsky A.M., Akimov P.A., Potapenko A.L., Vershinin V.V., Scherbina S.V.** Dynamic Substructures Synthesis Methods for NPP Systems “Foundation – Structure – Equipment – Pipelines” Analysis. // International Journal for Computational Civil and Structural Engineering, Volume 9, Issue 4, 2013, pp. 15-22.
14. **Belyi M.V.** Superelement method for transient dynamic analysis of structural systems. // Int. J. Numer. Meth. Eng., 1993, Vol. 36, pp. 2263-2286.
15. **Benfield W.A., Hruda R.F.** Vibration analysis of structures by component mode substitution. // AIAA Journal J., 1976, Vol. 9, pp. 1255-1261.
16. **Craig R.R. Jr., Bampton M.C.C.** Coupling of substructures for dynamic analysis. // AIAA Journal, 1968, Vol. 6, No. 7, pp. 1313-1319.
17. **Hale A.L., Meirovitch L.** A general procedure for improving substructures representation in dynamic synthesis. // Journal of Sound and vibration, 1982, Vol. 84, No. 2, pp. 269-287.
18. **Hurty W.C.** Dynamic analysis of structural systems using component modes. // AIAA Journal, 1984, Vol.4, pp. 733-738.
19. **Leung Y.T.** Dynamic substructure response. // Journal of sound and vibration, 1991, Vol. 149, No. 1, pp. 83-90.
20. **MacNeal R.H.** A hybrid method of component mode synthesis. // Computers and structures, 1971, Vol. 4, pp. 591-601.
21. **Wang J.H., Chen H.R.** Substructure modal synthesis method with high computation efficiency. // Computer methods in applied mechanics and engineering, 1990, Vol. 79, No. 2, pp. 203-217.

СПИСОК ЛИТЕРАТУРЫ

1. **Белостоцкий А.М., Акимов П.А.** (ред.). Актуальные проблемы численного моделирования зданий, сооружений и комплексов. Том 2. К 25-летию Научно-исследовательского центра СтаДиО. – М.: АСВ, 2016. – 596 с.
2. **Белостоцкий А.М., Акимов П.А.** Научно-исследовательский центр СтаДиО. 25 лет на фронте численного моделирования. // International Journal for Computational Civil and Structural Engineering / Международный журнал по расчету гражданских и строительных конструкций, Volume 12, Issue 1, 2016, pp. 8-45.
3. **Белостоцкий А.М., Акимов П.А., Дмитриев Д.С.** О современных методах редуцирования вычислительной размерности задач расчета конструкций, зданий и сооружений в рамках метода конечных элементов. // International Journal for Computational Civil and Structural Engineering / Международный журнал по расчету гражданских и строительных конструкций, Volume 13, Issue 3, 2017, pp. 19-33.
4. **Белостоцкий А.М., Воронова Г.А., Потапенко А.Л.** Развитие и интеграция в САПР «семейства» программных комплексов АСТРА-НОВА для нормативных расчетов на прочность трубопро-

водных систем различного назначения. // САПР и графика, 2003, №5, с. 55-65.

5. **Белостоцкий А.М., Дубинский С.И., Потапенко А.Л.** Методы динамического синтеза подконструкций в задачах моделирования сложных инженерных систем. // Строительная механика и расчет сооружений, №6, 2006, с. 45-52.
6. **Белостоцкий А.М., Пеньковой С.Б., Щербина С.В., Кайтуков Т.Б., Акимов П.А.** Разработка и верификация методики численного моделирования НДС, прочности и устойчивости многоэтажных панельных зданий. // Строительная механика и расчет сооружений, №6, 2014, с. 24-30.
7. **Белостоцкий А.М., Потапенко А.Л.** Реализация и верификация методов субмоделирования и динамического синтеза подконструкций в универсальных и специализированных программных комплексах. // International Journal for Computational Civil and Structural Engineering / Международный журнал по расчету гражданских и строительных конструкций, Volume 7, Issue 1, 2011, pp. 76-83.
8. **Белостоцкий А.М., Потапенко А.Л., Клепец О.Ю.** Реализация методов динамического синтеза подконструкций и субмоделирования в программных комплексах СТАДИО и АСТРА-НОВА. // International Journal for Computational Civil and Structural Engineering / Международный журнал по расчету гражданских и строительных конструкций, Volume 6, Issue 1&2, 2010, pp. 87-91.
9. **Гайан Р.** Приведение матриц жесткости и массы. // Ракетная техника и космонавтика, том 3, №2, 1965, с. 277-278.
10. **Зенкевич О.** Метод конечных элементов в технике. – М.: Мир, 1975. – 511 с.
11. **Травуш В.И., Акимов П.А., Баенхаев А.В., Беккер А.Т., Белостоцкий А.М., Кайтуков Т.Б., Сидоров В.Н.** Об основных итогах Шестого Международного симпозиума «Актуальные проблемы компьютерного моделирования конструкций и сооружений». // International Journal for Computational Civil and Structural Engineering / Международный журнал по расчету гражданских и строительных конструкций, Volume 12, Issue 3, 2016, pp. 129-144.
12. **Belostotsky A.M., Akimov P.A., Afanasyeva I.N., Kaytukov T.B.** Contemporary Problems of Numerical Modelling of Unique Structures and Buildings. // International Journal for Computational Civil and Structural Engineering / Международный журнал по расчету гражданских и строительных конструкций, Volume 13, Issue 2, 2017, pp. 9-34.
13. **Belostotsky A.M., Akimov P.A., Potapenko A.L., Vershinin V.V., Scherbina S.V.** Dynamic Substructures Synthesis Methods for NPP Systems “Foundation – Structure – Equipment – Pipelines” Analysis. // International Journal for Computational Civil and Structural Engineering, Volume 9, Issue 4, 2013, pp. 15-22.
14. **Belyi M.V.** Superelement method for transient dynamic analysis of structural systems. // Int. J. Numer. Meth. Eng., 1993, vol. 36, pp. 2263-2286.
15. **Benfield W.A., Hruda R.F.** Vibration analysis of structures by component mode substitution. // AIAA Journal J., 1976, vol. 9, pp. 1255-1261.
16. **Craig R.R. Jr., Bampton M.C.C.** Coupling of substructures for dynamic analysis. // AIAA Journal, 1968, vol. 6, No. 7, pp. 1313-1319.
17. **Hale A.L., Meirovitch L.** A general procedure for improving substructures representation in dynamic synthesis. // Journal of Sound and vibration, 1982, vol. 84, No. 2, pp. 269-287.
18. **Hurty W.C.** Dynamic analysis of structural systems using component modes. // AIAA Journal., 1984, vol.4, pp. 733-738.
19. **Leung Y.T.** Dynamic substructure response. // Journal of sound and vibration, 1991, vol. 149, # 1, pp. 83-90.

20. **MacNeal R.H.** A hybrid method of component mode synthesis. // Computers and structures, 1971, vol. 4, pp. 591-601.
21. **Wang J.H., Chen H.R.** Substructure modal synthesis method with high computation efficiency. // Computer methods in applied mechanics and engineering, 1990, vol. 79, No. 2, pp. 203-217.

Alexander M. Belostotsky, Corresponding Member of the Russian Academy of Architecture and Construction Sciences, Professor, Dr.Sc.; Director of Scientific Research Center “StaDyO”; Professor of Department of Structures, Buildings and Facilities, Russian University of Transport» (RUT – MIIT); Professor of Department of Architecture and Construction, Peoples’ Friendship University; Professor of Department of Building Structures and Computational Mechanics, Peoples' Friendship University of Russia; office 810, 18, 3ya Ulitsa Yamskogo Polya, Moscow, 125040, Russia; phone +7 (499) 706-88-10;
E-mail: amb@stadyo.ru.

Potapenko Aleksey Leonidovich, chief specialist-programmer of the Program Development and Support Department, CJSC «STADYO» Scientific Research Center; 125040, Russia, Moscow ul. 3rd Yamskogo polja, 18, 8 floor, office 810, phone +7 (495) 706-88-10,
E-mail: stadyo@stadyo.ru.

Pavel A. Akimov, Full Member of the Russian Academy of Architecture and Construction Sciences, PhD, Professor; Executive Scientific Secretary of Russian Academy of Architecture and Construction Sciences; Vice-Director for Science Activities, Scientific Research Center “StaDyO”; Professor of Department of Architecture and Construction, Peoples’ Friendship University of Russia; Professor of Department of Structural Mechanics, Tomsk State University of Architecture and Building; 24, Ul. Bolshaya Dmitrovka, 107031, Moscow, Russia;
phone +7(495) 625-71-63; fax: +7 (495) 650-27-31;
E-mail: akimov@raasn.ru, pavel.akimov@gmail.com.

Белостоцкий Александр Михайлович, член-корреспондент РААСН, профессор, доктор технических наук; генеральный директор ЗАО «Научно-исследовательский центр СтаДиО»; профессор кафедры «Строительные конструкции, здания и сооружения» Российского университета транспорта (МИИТ); профессор Департамента архитектуры и строительства Российского университета дружбы народов; профессор кафедры строительных конструкций и вычислительной механики Пермского национального исследовательского политехнического университета; профессор кафедры строительной механики Томского государственного архитектурно-строительного университета, 125040, Россия, Москва, ул. 3-я Ямского Поля, д.18, офис 810; тел. +7 (499) 706-88-10;
E-mail: amb@stadyo.ru.

Потапенко Алексей Леонидович, главный специалист-программист Отдела разработки и сопровождения программ, ЗАО «Научно-исследовательский центр СтаДиО»; 125040, Россия, г. Москва ул. 3-я Ямского Поля, д.18, 8 этаж, офис 810, тел. +7 (495) 706-88-10, E-mail: stadyo@stadyo.ru.

Акимов Павел Алексеевич, академик РААСН, профессор, доктор технических наук; главный ученый секретарь Российской академии архитектуры и строительных наук; заместитель генерального директора по науке ЗАО «Научно-исследовательский центр СтаДиО»; профессор Департамента архитектуры и строительства Российского университета дружбы народов; профессор кафедры строительной механики Томского государственного архитектурно-строительного университета; 107031, г. Москва, ул. Большая Дмитровка, д. 24, стр. 1; тел. +7(495) 625-71-63;
факс +7 (495) 650-27-31; Email: akimov@raasn.ru, pavel.akimov@gmail.com.

DOI:10.22337/2587-9618-2018-14-3-42-49

MOISTURE REGIME CALCULATION FOR SINGLE-LAYER ENCLOSING STRUCTURES USING DISCRETE-CONTINUAL MATHEMATICAL MODEL

Vladimir G. Gagarin [1, 2], ***Kirill P. Zubarev*** [1]

[1] National Research Moscow State University of Civil Engineering, Moscow, RUSSIA

[2] Research Institute of Building Physics of Russian Academy of Architecture and Construction Sciences, Moscow, RUSSIA

Abstract: The paper describes moisture regime calculation for single-layer enclosing structures using discrete-continual method. A formula for calculation of moisture potential dependence on time in any enclosing structure section, at any time, under continuous control for temperature distribution, has been derived. Moisture regime calculation results under the proposed method have been compared to results obtained by well-known methods by V.G. Gagarin and V.V. Kozlov for aerated concrete single-layer enclosing structure. It has been found out that the proposed method gives quantitative and qualitative results similar to results obtained using Gagarin's unsteady-state method.

Keywords: moisture regime, discrete-continual method, moisture potential, enclosing structure, aerated concrete, moisture exchange coefficient

РАСЧЕТ ВЛАЖНОСТНОГО РЕЖИМА ОДНОСЛОЙНЫХ ОГРАЖДАЮЩИХ КОНСТРУКЦИЙ С ИСПОЛЬЗОВАНИЕМ ДИСКРЕТНО-КОНТИНУАЛЬНОЙ МАТЕМАТИЧЕСКОЙ МОДЕЛИ

В.Г. Гагарин [1, 2], ***К.П. Зубарев*** [1]

[1] Национальный исследовательский Московский государственный строительный университет, г. Москва, РОССИЯ

[2] Научно-исследовательский институт строительной физики Российской академии архитектуры и строительных наук, г. Москва, РОССИЯ

Аннотация: В настоящей статье представлен расчет влажностного режима однослойных ограждающих конструкций зданий с применением дискретно-континуального метода. Выведена формула, позволяющая рассчитывать зависимость потенциала влажности от времени в любом сечении ограждающей конструкции, в любой момент времени, при непрерывном учете температурного поля. Проведено сравнение результатов расчета влажностного режима по предложенному методу режима с известными методами В.Г. Гагарина и В.В. Козлова для однослойной ограждающей конструкции из газобетона. Получено, что предложенный метод дает и количественный и качественный результат с нестационарным методом В.Г. Гагарина.

Ключевые слова: влажностный режим, дискретно-континуальный метод, потенциал влажности, ограждающая конструкция, газобетон, коэффициент влагообмена

1. INTRODUCTION

Moisture regime calculation for enclosing structures is an actual and high-demand area of focus in construction.

Wet construction material can result in higher heat loss [1, 2, 3] and premature failure of load-bearing structures [4, 5, 6, 7]. Construction material moisture influence on human

electromagnetic shielding has also been studied recently [8, 9].

Development of moisture regime calculation methods for enclosing structure is one of the most important research trends [10, 11, 12]. Methods based on moisture potential theory are the most progressive ones [13]. Gagarin's moisture potential [14], which is a function of temperature and moisture, is well-known:

$$F(w,t) = E_t(t) \cdot \varphi(w) + \frac{1}{\mu}\int_0^w \beta(\zeta)\, d\zeta., \qquad (1)$$

where F – moisture potential, Pa; E_t – maximum water vapor tension, Pa; φ – relative air humidity, %; μ – vapor permeability coefficient, *kg/(m · s · Pa);* β – moisture conductivity coefficient, *kg/(m · s · kg/kg)*, which depends on moisture.

Moisture potential F (1) distribution for single-layer enclosing structure is described by moisture transfer differential equation:

$$\frac{\partial F(w,t)}{\partial \tau} = \left(\frac{1}{\mu}\beta(w) + \frac{\partial \varphi(w)}{\partial w} E_t(t)\right)\frac{\mu}{\gamma_0}\frac{\partial^2 F(w,t)}{\partial x^2}. \qquad (2)$$

where γ_0 – enclosing structure dry material density, kg/m^3, τ – time, s; x - coordinate, m.

Within a month a temperature distribution is appears to be constant [14] and has the following form for single-layer enclosing structure:

$$\frac{\partial^2 t}{\partial x^2} = 0. \qquad (3)$$

where t – temperature, ^oC;

Association between temperature and moisture distribution is determined by Clausius-Clapeyron correlation:

$$E_t(t) = 1.84 \cdot 10^{11} \cdot \exp(-5330/(273+t)). \qquad (4)$$

As temperature distribution is assumed to be steady within the model, water vapor tension E_t is constant during a month.

Third-order boundary conditions of moisture exchange are set for the equation (2) at the enclosing structure boundaries.

Boundary condition of moisture exchange between outside air and structure surface can be represented as follows:

$$-\mu \left.\frac{\partial F}{\partial x}\right|_{i=1} = \beta_{ext}\left(F_{ext} - F_1\right), \qquad (5)$$

where F_{ext} – outside air moisture potential equal to partial pressure of outside air water vapor, *Pa*; F_1 – moisture potential of the enclosing structure surface which contacts with outside air, *Pa*; β_{ext} – moisture exchange coefficient of outside air and enclosing structure section, $kg/(m^2 \cdot s \cdot Pa)$.

Boundary condition of moisture exchange between inside air and structure inner surface can be represented as follows:

$$\mu \left.\frac{\partial F}{\partial x}\right|_{i=N} = \beta_{in}\left(F_{in} - F_N\right), \qquad (6)$$

where F_{in} – inside air moisture potential equal to partial pressure of inside air water vapor, *Pa*; F_N – moisture potential of the enclosing structure surface which contacts with inside air, *Pa*; β_{in} – moisture exchange coefficient of inside air and enclosing structure section, $kg/(m^2 \cdot s \cdot Pa)$.

Moisture regime calculation by equations (1) – (6) requires numerical method application using computer, thus, it is difficult to be used in engineering practice. Kozlov's engineering method [15], based on moisture potential steady-state distribution examination is the most applicable method for moisture state assessment of an enclosing structure:

$$\frac{\partial^2 F(w,t)}{\partial x^2} = 0. \qquad (7)$$

Computer modelling methods have been advanced in parallel to moisture regime theory

development. In papers [16, 17] A.B. Zolotov, P.A. Akmov et al. Propose a thermal conductivity formula, which stays steady in time:

$$\bar{U}(\tau) = e^{A\cdot\tau}\cdot\bar{U}_0 - A^{-1}\left(E - e^{A\cdot\tau}\right)\cdot\bar{S}, \qquad (8)$$

where $\bar{U}$ – temperature distribution column vector; $\bar{U}_0$ – initial temperature distribution column vector; A – coefficient matrix; $\bar{S}$ – boundary conditions column vector.

In practice, equation (8) is a solution for unsteady-state thermal conductivity problem under time-constant first-order boundary conditions.

This method has been developed in papers by V.N. Sidorov and S.M. Matskevich [18, 19, 20]. First-order boundary conditions varied with time, and temperature distribution was described by the following expression at any time:

$$\bar{U}(\tau) = e^{A\cdot\tau}\cdot\bar{U}_0 + \int_0^{\tau} e^{A\cdot(\tau-\sigma)}\cdot\bar{S}(\sigma)d\sigma. \qquad (9)$$

Integral in equation (9) has been determined by trapezoidal method.

2. THE PROBLEM

Development of moisture regime engineering calculation method for single-layer enclosing structure in unsteady-state moisture regime using discrete-continual method.

3. MATERIALS AND METHODS

The following expression has been proposed:

$$\varphi_F(w,t) = \varphi(w) + \frac{1}{\mu}\int_0^w \beta(\sigma)d\sigma / E_t(t). \qquad (10)$$

where φ_F – "relative elasticity of moisture potential".

"Relative elasticity of moisture potential" can be represented as a characteristic curve, which is called as "sorption-oversorption isotherms". "Sorption-oversorption isotherms" is of the following form for aerated concrete D400 (Figure 1).

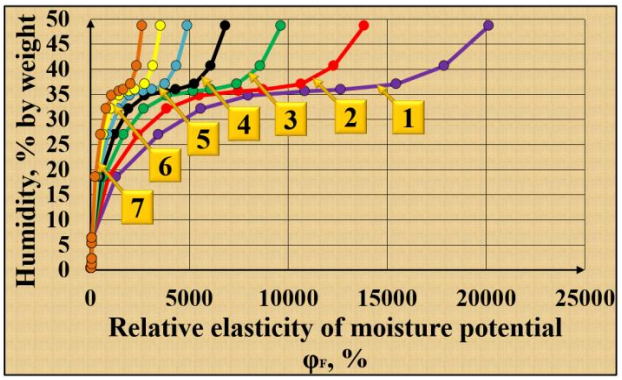


Figure 1. "Sorption-over sorption isotherms" for aerated concrete D400 (1 – temperature -10°C; 2 – temperature -5 °C; 3 – temperature 0 °C; 4 – temperature 5 °C; 5 – temperature 10 °C; 6 – temperature 15 °C; 7 – temperature 20 °C).

"Average coefficient of construction material hygrothermal properties" $\kappa(w,t)$ has been introduced. The coefficient has been taken to be constant within the assessment month:

$$\kappa(w,t) = \frac{\mu}{\gamma_0\cdot(dw/d\varphi_F(w,t))}. \qquad (11)$$

According to expressions (10) and (11) a modified differential moisture transfer equation can be derived:

$$\frac{\partial F(w,t)}{\partial\tau} = \kappa(w,t)\cdot E_t(t)\frac{\partial^2 F(w,t)}{\partial x^2}. \qquad (12)$$

Taking into account boundary conditions (5) and (6), the equation (12) can be represented by a system of simultaneous equations:

$$\begin{cases} \frac{\partial F_1}{\partial \tau} = \frac{\kappa}{h^2} \cdot E_{t1} \cdot (-(1+\frac{\beta_{ext}}{\mu} \cdot h) \cdot F_1 + F_2) + \frac{\kappa}{h^2} \cdot E_{t1} \cdot \frac{\beta_{ext}}{\mu} \cdot h \cdot F_{ext} \\ \frac{\partial F_i}{\partial \tau} = \frac{\kappa}{h^2} \cdot E_{ti} \cdot (F_{i-1} - 2 \cdot F_i + F_{i+1}), i = 2,3,4,\ldots,N-1 \\ \frac{\partial F_N}{\partial \tau} = \frac{\kappa}{h^2} \cdot E_{tN} \cdot (F_{N-1} - (1+\frac{\beta_{in}}{\mu} \cdot h) F_N) + \frac{\kappa}{h^2} \cdot E_{tN} \cdot \frac{\beta_{in}}{\mu} \cdot h \cdot F_{in} \\ F(x,0) = \chi(x), 0 \le x \le l \end{cases}. \quad (13)$$

where h – enclosing structure partition step in coordinate x; – enclosing structure section number; – initial moisture potential distribution, Pa.

Assuming that inside air moisture potential is constant, let's represent moisture potential variation outside construction during the month as a linear function:

$$F_{ext} = m \cdot \tau + n, \quad (14)$$

where m – boundary conditions slope ratio within a month; – boundary conditions graph rise within a month (Figure 1), Pa;

Taking into account boundary condition (14), simultaneous equations (14) represent a Cauchy problem in matrix form.

$$\begin{cases} \bar{F}_\tau^{'} = E_t \cdot A \cdot \bar{F} + p \cdot \tau \cdot \bar{L} + \bar{B} \\ \bar{F}(0) = \bar{\chi}, 0 \le x \le l \end{cases}. \quad (15)$$

where

$$p = \kappa \cdot E_{t1} \cdot \beta_{ext} \cdot h \cdot m / (h^2 \cdot \mu).$$

$$A = \frac{\kappa}{h^2} \cdot \begin{pmatrix} -\left(1+\beta_{ext} \cdot \frac{h}{\mu}\right) & 1 & 0 & 0 & 0 \\ 1 & -2 & 1 & 0 & 0 \\ 0 & \ddots & \ddots & \ddots & 0 \\ 0 & 0 & 1 & -2 & 1 \\ 0 & 0 & 0 & 1 & -\left(1+\beta_{in} \cdot \frac{h}{\mu}\right) \end{pmatrix}$$

$$E_t = \begin{pmatrix} E_{t1} & 0 & 0 & 0 & 0 \\ 0 & E_{t2} & 0 & 0 & 0 \\ \ldots & \ldots & \ldots & \ldots & \ldots \\ 0 & 0 & 0 & E_{t(N-1)} & 0 \\ 0 & 0 & 0 & 0 & E_{tN} \end{pmatrix}. \quad \bar{F} = \begin{pmatrix} F_1 \\ F_2 \\ \ldots \\ F_{N-1} \\ F_N \end{pmatrix}. \quad \bar{L} = \begin{pmatrix} 1 \\ 0 \\ \ldots \\ 0 \\ 0 \end{pmatrix}.$$

$$\bar{B} = \begin{pmatrix} \kappa \cdot E_{t1} \cdot \beta_{ext} \cdot h \cdot n / (h^2 \cdot \mu) \\ 0 \\ \ldots \\ 0 \\ \kappa \cdot E_{tN} \cdot \beta_{in} \cdot h \cdot F_{in} / (h^2 \cdot \mu) \end{pmatrix}. \quad \bar{F}_\tau^{'} = \begin{pmatrix} F_1^{'}(\tau) \\ F_2^{'}(\tau) \\ \ldots \\ F_{N-1}^{'}(\tau) \\ F_N^{'}(\tau) \end{pmatrix}.$$

Problem (15) solution can be written as:

$$\bar{F} = p \cdot \left((E_t \cdot A)^{-2} \cdot e^{E_t \cdot A \cdot \tau} - \tau \cdot (E_t \cdot A)^{-1} - (E_t \cdot A)^{-2} \right) \cdot . \\ \cdot \bar{L} + (E_t \cdot A)^{-1} \left(e^{E_t \cdot A \cdot \tau} - E \right) \cdot \bar{B} + e^{E_t \cdot A \cdot \tau} \cdot \bar{F}_0. \quad (16)$$

Calculation by formula (16) is executed during a month. Moisture distribution value at the end of the current month is taken as initial moisture distribution value at the following month start.

4. RESULTS AND DISCUSSION

Single-layer enclosing structure made of 0.6 m thick aerated concrete D400 has been studied. Construction area: Moscow. Inside air temperature 20 °C and relative air humidity 50% have been maintained constant in the building during a year.

Moisture regime calculation results for the single-layer enclosing structure obtained by different moisture potential theory methods – the proposed discrete-continual method, Gagarin's unsteady-state method, and Kozlov's engineering method – have been compared.

Calculation according to Gagarin's unsteady-state method has been based on equations (1) – (6) by finite difference method using and explicit difference scheme. Calculation according to Kozlov's engineering method has been based on analytical dependence (7). Calculation according to discrete-continual method has been based on expression (16).

Calculation results obtained by different moisture potential methods are given at (Figure 2).

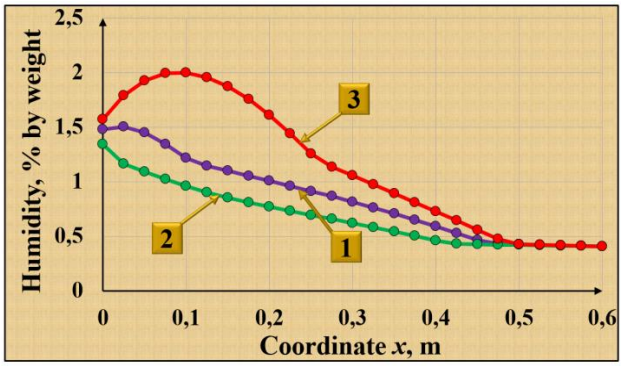


Figure 2. Comparison of moisture potential theory methods for moisture regime calculation of single-layer enclosing structure in January (1 – moisture distribution in enclosing structure according to Gagarin's unsteady-state method, 2 – moisture distribution in enclosing structure according to discrete-continuous method, 3 – moisture distribution in enclosing structure according to Kozlov's engineering method).

5. CONCLUSIONS

Unsteady-state moisture regime determination method using discrete-continual approach has been developed for single-layer enclosing structures. It was shown that the proposed method for moisture regime calculation gives quantitative and qualitative results similar to results of Gagarin's unsteady-state method. Moisture regime is calculated on equation (16) without numerical method, thus, the proposed method can be used by design engineers in practice.

6. ACKNOWLEDGMENTS

Authors express gratitude to V.K. Akhmetov, professor, Doctor of Engineering, for his assistance in moisture transfer discrete-continual model development.

REFERENCES

1. **Beregovoy A.M., Beregovoy V.A.** Temperaturno-Vlazhnostnoye Sostoyaniye Naruzhnykh Ograzhdeniy v Usloviyakh Fazovykh Perekhodov Vlagi i Agressivnykh Vozdeystviy Sredy [Temperature and Moisture State of Cladding Under Conditions of Moisture Transition and Exposure to Aggressive Environment] // Regional Architecture and Engineering (Regionalnaya Arkhitektura i Stroitelstvo), 2017, Volume 32, Issue 3, pp. 99-104.
2. **Hoseini A., Bahrami A.** Effects of Humidity on Thermal Performance of Aerogel Insulation Blankets. // Journal of building engineering, 2017, Vol. 13, pp. 107-115.
3. **Jin H.Q., Yao X.L., Fan L.W., Xu X., Yu Z.T.** Experimental Determination and Fractal Modeling of the Effective Thermal Conductivity of Autoclaved Aerated Concrete: Effects of Moisture Content. // International Journal of Heat and Mass Transfer, 2016, Vol. 92, pp. 589-602.
4. **Wu Z., Wong H.S., Buenfeld N.R.** Transport Properties of Concrete After Drying-Wetting Regimes to Elucidate the Effects of Moisture Content, Hysteresis and Microcracking. // Cement and Concrete Research, 2017, Vol. 98, pp. 136-154.
5. **Zvicevicius E., Raila A., Cipliene A., Cerniauskiene Z., Kadziuliene Z., Tilvikiene V.** Effects of Moisture and Pressure on Densification Process of Raw Material from Artemisia Dubai Wall. // Renewable Energy, 2018, Vol. 119, pp. 185-192.
6. **Georget F., Prevost J.H., Huet B.** Impact of the Microstructure Model on Coupled Simulation of Drying and Accelerated Carbonation. // Cement and Concrete Research, 2018, Vol. 104, pp. 1-12.
7. **Liu Z.C., Hansen W., Wang F.Z.** Pumping Effect to Accelerate Liquid Uptake in Concrete and its Implications on

Salt Frost Durability. // Construction and Building Materials, 2018, Vol. 158, pp. 181-188.

8. **Girault F., Perrier F.** Estimating the Importance of Factors Influencing the Radon-222 Flux from Building Walls. // Science of the Total Environment, 2012, No. 433, pp. 247-263.
9. **Kupriyanov V.N., Shafigullin R.I.** K Voprosu ob Oslablenii Elektromagnitnykh Voln Ograzhdayushchimi Konstruktsiyami Zdaniy [To the Question of the Weakening of Electromagnetic Waves Enclosing Structures of Buildings]. // Proceedings of higher education institutions. Textile industry technology. (Izvestiya vysshikh uchebnykh zavedeniy. Tekhnologiya tekstilnoy promyshlennosti), 2016, Volume 364, Issue 4, pp. 229-234.
10. **Galbraith G.H., Guo G.H., McLean R.C.** The Effect of Temperature on the Moisture Permeability of Building Materials. // Building Research and Information, 2000, Vol. 28, Issue 4, pp. 245-259.
11. **Vavrovic B.** Importance of Envelope Construction Renewal in Panel Apartment Buildings in Terms of Basic Thermal Properties. // Advanced Materials Research, 2014, Vol. 855, pp. 97-101.
12. **Lal S., Lucci F., Defraeye T., Poulikakos LD., Partl MN., Derome D., Carmeliet J.** CFD Modeling of Convective Scalar Transport in a Macroporous Material for Drying Applications. // International journal of thermal sciences, 2018, Vol. 123, pp. 86-98.
13. **Arfvidsson J., Claesson J.** Isothermal Moisture flow in Building Materials: Modelling, Measurements and Calculations Based on Kirchhoff's Potential. // Building and Environment, 2000, Vol. 35, Issue 6, pp. 519-536.
14. **Gagarin V.G.** Teoriya Sostoyaniya i Perenosa Vlagi v Stroitelnykh Materialakh i Teplozashchitnyye Svoystva Ograzhdayushchikh Konstruktsiy Zdaniy [Theory of Moisture State and Transfer in Construction Materials, and Thermal Properties of Enclosing Structures]. PhD Thetis (Diss. dokt. tekhn. Nauk), Moscow, 2000, 324 pages.
15. **Kozlov V.V.** Metod Inzhenernoy Otsenki Vlazhnostnogo Sostoyaniya Sovremennykh Ograzhdayushchikh Konstruktsiy s Povyshennym Urovnem Teplozashchity pri Uchete Paropronitsayemosti, Vlagoprovodnosti i Filtratsii Vozdukha [Engineering Assessment Method for Moisture State of Modern Enclosing Structures with Higher Thermal Protection Level Taking into Account Vapor Permeability, Moisture Conductivity and Air Filtration]. PhD Thetis (Diss. kand. tekhn. Nauk), Moscow, 2004, 155 pages.
16. **Zolotov A.B., Mozgaleva M.L., Akimov P.A., Sidorov V.N.** Ob Odnom Diskretno-Kontinualnom Podkhode k Resheniyu Odnomernoy Zadachi Teploprovodnosti [About One Discrete-Continual Method of Solution of One-Dimensional Heat Conductivity Problem]. // Academia. Architecture and Construction (Academia. Arkhitektura i Stroitelstvo), 2010, Issue 3, pp. 287-291.
17. **Zolotov A.B., Mozgaleva M.L., Akimov P.A., Sidorov V.N.** Diskretno-Kontinualnyy Podkhod k Resheniyu Zadachi Teploprovodnosti [Discrete-Continual Approach for Thermal Conductivity Problem Solution]. // Bulletin of Moscow State University of Civil Engineering (Vestnik MGSU), 2010, Issue 3, pp. 58-62.
18. **Sidorov V.N., Matskevich S.M.** Discrete-Analytical Solution of the Unsteady-State Heat Conduction Transfer Problem Based on the Finite Element Method. // IDT 2016 – Proceedings of the International Conference on Information and Digital Technologies 2016, 2016, pp. 241-244.
19. **Sidorov V.N., Matskevich S.M.** Solving Unsteady Boundary Value Problems Using Discrete-Analytic Method for Non-Iterative Simulation of Temperature Processes in

Time. // Key Engineering Materials, 2016, Vol. 685, pp. 211-216.
20. **Sidorov V.N., Matskevich S.M.** Discrete-Analytic Solution of Unsteady-State Heat Conduction Transfer Problem Based on a Theory of Matrix Function. // Procedia Engineering, 2015, Vol. 111, pp. 726-733.

СПИСОК ЛИТЕРАТУРЫ

1. **Береговой А.М., Береговой В.А.** Температурно-влажностное состояние наружных ограждений в условиях фазовых переходов влаги и агрессивных воздействий среды. // Региональная архитектура и строительство, 2017, №3(32), с. 99-104.
2. **Hoseini A., Bahrami A.** Effects of Humidity on Thermal Performance of Aerogel Insulation Blankets. // Journal of building engineering, 2017, Vol. 13, pp. 107-115.
3. **Jin H.Q., Yao X.L., Fan L.W., Xu X., Yu Z.T.** Experimental Determination and Fractal Modeling of the Effective Thermal Conductivity of Autoclaved Aerated Concrete: Effects of Moisture Content. // International Journal of Heat and Mass Transfer, 2016, Vol. 92, pp. 589-602.
4. **Wu Z., Wong H.S., Buenfeld N.R.** Transport Properties of Concrete After Drying-Wetting Regimes to Elucidate the Effects of Moisture Content, Hysteresis and Microcracking. // Cement and Concrete Research, 2017, Vol. 98, pp. 136-154.
5. **Zvicevicius E., Raila A., Cipliene A., Cerniauskiene Z., Kadziuliene Z., Tilvikiene V.** Effects of Moisture and Pressure on Densification Process of Raw Material from Artemisia Dubai Wall. // Renewable Energy, 2018, Vol. 119, pp. 185-192.
6. **Georget F., Prevost J.H., Huet B.** Impact of the Microstructure Model on Coupled Simulation of Drying and Accelerated Carbonation. // Cement and Concrete Research, 2018, Vol. 104, pp. 1-12.
7. **Liu Z.C., Hansen W., Wang F.Z.** Pumping Effect to Accelerate Liquid Uptake in Concrete and its Implications on Salt Frost Durability. // Construction and Building Materials, 2018, Vol. 158, pp. 181-188.
8. **Girault F., Perrier F.** Estimating the Importance of Factors Influencing the Radon-222 Flux from Building Walls. // Science of the Total Environment, 2012, No. 433, pp. 247-263.
9. **Куприянов В.Н., Шафигуллин Р.И.** К вопросу об ослаблении электромагнитных волн ограждающими конструкциями зданий. // Известия высших учебных заведений. Технология текстильной промышленности, 2016, №4(364), с. 229-234.
10. **Galbraith G.H., Guo G.H., McLean R.C.** The Effect of Temperature on the Moisture Permeability of Building Materials. // Building Research and Information, 2000, Vol. 28, Issue 4, pp. 245-259.
11. **Vavrovic B.** Importance of Envelope Construction Renewal in Panel Apartment Buildings in Terms of Basic Thermal Properties. // Advanced Materials Research, 2014, Vol. 855, pp. 97-101.
12. **Lal S., Lucci F., Defraeye T., Poulikakos LD., Partl MN., Derome D., Carmeliet J.** CFD Modeling of Convective Scalar Transport in a Macroporous Material for Drying Applications. // International journal of thermal sciences, 2018, Vol. 123, pp. 86-98.
13. **Arfvidsson J., Claesson J.** Isothermal Moisture flow in Building Materials: Modelling, Measurements and Calculations Based on Kirchhoff's Potential. // Building and Environment, 2000, Vol. 35, Issue 6, pp. 519-536.
14. **Гагарин, В.Г.** Теория состояния и переноса влаги в строительных материалах и теплозащитные свойства ограждающих конструкций зданий. //

Диссертация на соискание ученой степени доктора технических наук. – М., 2000. – 324 с.
15. **Козлов В.В.** Метод инженерной оценки влажностного состояния современных ограждающих конструкций с повышенным уровнем теплозащиты при учете паропроницаемости, влагопроводности и фильтрации воздуха. Диссертация на соискание ученой степени кандидата технических наук. – М., 2004. – 155 с.
16. **Золотов А.Б., Мозгалева М.Л., Акимов П.А., Сидоров В.Н.** Об одном дискретно-континуальном подходе к решению одномерной задачи теплопроводности. // Academia. Архитектура и строительство, 2010, №3, с. 287-291.
17. **Золотов А.Б. Мозгалева М.Л., Акимов П.А., Сидоров В.Н.** Дискретно-континуальный подход к решению задачи теплопроводности. // Вестник МГСУ, 2010, №3, с. 58-62.
18. **Sidorov V.N., Matskevich S.M.** Discrete-Analytical Solution of the Unsteady-State Heat Conduction Transfer Problem Based on the Finite Element Method. // IDT 2016 – Proceedings of the International Conference on Information and Digital Technologies 2016, 2016, pp. 241-244.
19. **Sidorov V.N., Matskevich S.M.** Solving Unsteady Boundary Value Problems Using Discrete-Analytic Method for Non-Iterative Simulation of Temperature Processes in Time. // Key Engineering Materials, 2016, Vol. 685, pp. 211-21.
20. **Sidorov V.N., Matskevich S.M.** Discrete-Analytic Solution of Unsteady-State Heat Conduction Transfer Problem Based on a Theory of Matrix Function. // Procedia Engineering, 2015, Vol. 111, pp. 726-733.

Vladimir G. Gagarin, Corresponding Member of the Russian Academy of Architecture and Construction Sciences, professor, Doctor of engineering; Research Institute of Building Physics of Russian Academy of Architecture and Construction Science; professor in National Research Moscow State University of Civil Engineering; 129337, Moscow, Yaroslavskoe shosse, 26;
phone +7 (495) 781-80-07; fax. +7 (499) 183-44-38;
E-mail.: gagarinvg@yandex.ru.

Kirill P. Zubarev, post-graduate student of National Research Moscow State University of Civil Engineering; 129337, Moscow, Yaroslavskoe shosse, 26;
phone +7 (495) 781-80-07; fax. +7 (499) 183-44-38;
E-mail.: zubarevkirill93@mail.ru.

Гагарин Владимир Геннадьевич, член-корреспондент Российской академии архитектуры и строительных наук, профессор, доктор технических наук; Научно-исследовательский институт строительной физики Российской академии архитектуры и строительных наук; профессор Национального исследовательского Московского государственного строительного университета; 129337, г. Москва, Ярославское шоссе, 26; тел. +7 (495) 781-80-07; факс. +7 (499) 183-44-38;
E-mail.: gagarinvg@yandex.ru.

Зубарев Кирилл Павлович, аспирант Национального исследовательского Московского государственного строительного университета; 129337, г. Москва, Ярославское шоссе, 26; тел. +7 (495) 781-80-07;
факс. +7 (499) 183-44-38;
E-mail.: zubarevkirill93@mail.ru.

DOI:10.22337/2587-9618-2018-14-3-50-58

THE COMPARATIVE ANALYSIS OF THE RESULTS OF REAL AND NUMERICAL EXPERIMENTS FOR DEFINING THE ULTIMATE BEARING CAPACITY OF LIGHT GAUGE STEEL STUDS "ATLANT"

Galina G. Kashevarova, Pavel A. Kosykh
Perm National Research Polytechnic University, Perm, RUSSIA

Abstract: The article in question describes the results of comparison of numerical and real experiments, presented in the report of the Canadian laboratory "Bodycote" [1]. The paper depicts the test fixture, on witch six samples (two typical sizes) of light gauge steel stud "ATLANT" were tested. As a result, dependencies between bearing capacity and characteristic displacements were received. In order to repeat the experiment, the series of computer models were created with the software ANSYS. The computer models have complex nature: geometrical / physical nonlinearity was used. For accounting steel material nonlinearity, we used a multilinear model with isotropic hardening (MISO). The proper diagram was used for each typical size in accordance with the experiments on the tensile-testing machine. For the purpose of supporting condition and load modeling which are identical to the full-scale experiment, a couple of contact elements were used. The utilization of contact elements allowed us to consider friction between the sample and the supporting structures. One of the disadvantages of the full-scale experiment is the absence of measurements of the initial geometrical imperfections. For their consideration the use of probabilistic approach is suggested. This approach entails calculation of several models with different spread of initial imperfections. The initial geometrical imperfections with stochastic nature were included in the computing model. Parameters of distribution were based on the measurements of eighty-eight C-shaped members [8]. In the result of comparison, fine precision in terms of the ultimate bearing capacity and deformation pattern were established. According to expectation, the results of the full-scale experiments were found inside the fictitious "corridor", created in accordance with the results of computer modeling.

Keywords: light gauge steel members, "ATLANT" studs, ANSYS, initial geometrical imperfections, real experiment

СРАВНИТЕЛЬНЫЙ АНАЛИЗ РЕЗУЛЬТАТОВ НАТУРНОГО И ЧИСЛЕННОГО ЭКСПЕРИМЕНТОВ ПО ОПРЕДЕЛЕНИЮ ПРЕДЕЛЬНОЙ НЕСУЩЕЙ СПОСОБНОСТИ ТОНКОСТЕННЫХ ПРОФИЛЕЙ «АТЛАНТ»

Г.Г. Кашеварова, П.А. Косых
Пермский национальный исследовательский политехнический университет, г. Пермь, РОССИЯ

Аннотация: В статье выполнено сравнение результатов натурных экспериментов, изложенных в отчете Канадской лаборатории Bodycote [1], с результатами компьютерного моделирования. Описан испытательный стенд, на котором было испытано шесть образцов (двух типоразмеров) тонкостенных профилей марки «АТЛАНТ». В результате были получены зависимости между сжимающей силой и характерными перемещениями. С целью повторения эксперимента в расчетном комплексе ANSYS была создана серия компьютерных моделей. Модели содержат как физически, так геометрически нелинейную постановку задачи. Для учета физической нелинейности стали использована полилинейная модель с изотропным упрочнением (MISO). Для каждого типоразмера применялась своя диаграмма, соответствующая испытаниям на разрывной машине. С целью моделирования условий опирания и нагружения, идентичных натурному эксперименту, использована пара контактных элементов. Дополнительно применение контактных элементов позволило учесть трение между образцом и опорами.

Одним из недостатков натурного эксперимента является отсутствие замеров начальных геометрических несовершенств. Для их учета предлагается использовать вероятностный подход. Подход подразумевает под собой расчет нескольких моделей с различными по величине и форме распределениями начальных несовершенств. В расчетные модели вносились начальные геометрические несовершенства (местные и общие), имеющие стохастический характер. Параметры распределения были получены на основе обмера восьмидесяти восьми образцов сплошных С-образных профилей [8]. В результате сравнения установлена хорошая сходимость результатов в плане предельной несущей способности. Часть образцов показала схожие картины деформирования. Как и ожидалось, результаты натурного эксперимента попали внутрь мнимого коридора, созданного результатами компьютерного моделирования.

Ключевые слова: ЛСТК, профили марки «АТЛАНТ», ANSYS, начальные геометрические несовершенства, натурный эксперимент

1. TEST FIXTURE

According to the presented report [1], the tests were conducted on the test fixture, depicted in Figure 1. The test fixture consists of three supporting structures, tightly attached to the reinforced floor, between which the horizontally positioned sample can be found. Both of sample ends wereattached totrackswith self-tapping screws with the diameter of 4.8 mm. One of the tracks (“the lower” one) was attached to the supporting structure along the full length with six bolts M12. Another track (“the upper” one) was fixed in its ends on the two remaining supporting structures, positioned at a distance of $L_{br} = 1219\ mm$ with four bolts M 12. While testing both sample flanges, positioned in the center of the span, were constrained by using bands sized 38.1x1.27 mm.The band length was $L_s = 1219\ mm$. Moreover, vertical mobility measurement at the Y-axis was taken in the center of the span.

Sample adjustment on the test fixture was held by means of a laser pointer, positioned near “the lower” track. The load was transferred over the length (Z-axis) through “the upper” track with the help of servo-hydraulic actuator, equipped with the dynamometer. The mechanical motion transducer was installed in combination with the dynamometer at the Z-axis. The metal plate was assembled between the actuator and the track. The load was transferred continually with continuous traversing speed monitoring 0.76 mm/min.

2. TESTS SAMPLES

Three samples of steel studs “ATLANT” of two typical sizes were tested in the course of the experiment [2]. The first typical size (samples S1–S3): web height $H = 152.4\ mm$, flanges width $B = 41.3\ mm$, steel thickness $Tk = 2.0\ mm$. The second typical size (samples S4–S6): web height $H = 152.4\ mm$, flanges width $B = 41.3\ mm$, steel thickness $Tk = 1.0\ mm$. All six samples were of the length $L = 2438\ мм$. Before the experiment the measurements of the main geometrical parameters were made on each sample in three positions (beginning, middle, end). The results of the measurements are presented in Table 1.

According to [5], microscopic analysis of the metallographic specimen of each sample was conducted. The thickness of zinc covering as well as of base metal were defined. As the result of the experiment, there were graphs, made for each sample which describe the correlation between pressure load and sensor reading of the two motion detecting transducers. These graphs will be presented along with the results of computer modeling.

3. COMPUTER MODELLING

In order to display the results of the full-scale experiment by means of the ANSYS software [6] we created a series of CAE-models (Figure 2).

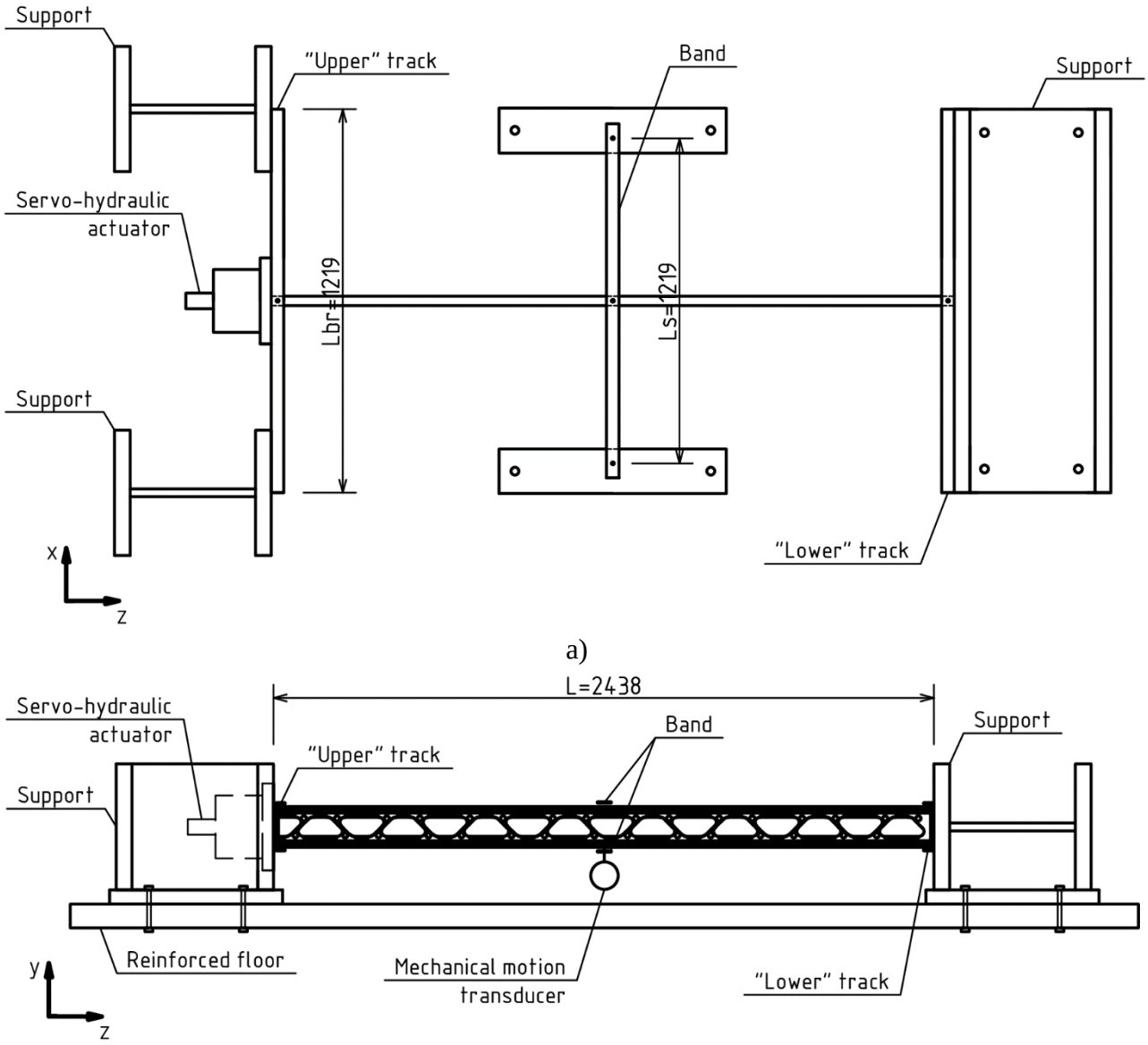


Figure1. Testing bed scheme: a) top view; b) side-view.

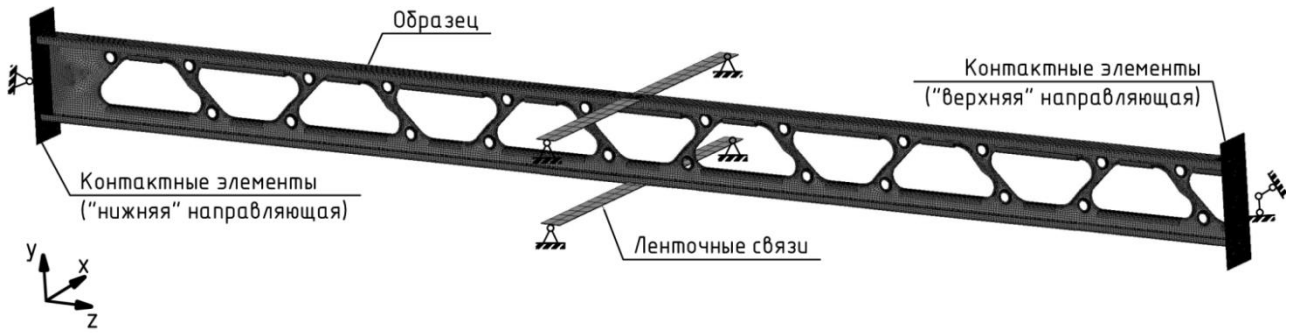


Figure 2. The overview of the calculating model.

Table 1. Geometrical parameters of steel studs.

Parameter	Sample S1			Sample S2		
	Beginning	Middle	End	Beginning	Middle	End
H, mm	152.654	152.883	152.806	153.162	152.806	152.857
B1, mm	41.720	41.605	42.012	41.250	42.520	42.113
B2, mm	41.224	41.948	42.139	41.783	41.694	41.948
C1, mm	12.891	12.751	14.402	12.459	12.586	11.938
C2, mm	12.370	12.802	12.065	13.170	12.192	13.475
Parameter	Sample S3			Sample S4		
	Beginning	Middle	End	Beginning	Middle	End
H, mm	153.886	154.115	153.988	153.695	152.578	152.159
B1,mm	41.123	41.021	41.326	41.554	41.059	42.824
B2, mm	41.250	41.504	41.478	41.720	42.431	41.935
C1,mm	13.284	13.030	14.669	12.852	12.560	13.551
C2, mm	13.551	13.716	13.216	13.145	13.551	12.789
Parameter	Sample S5			Sample S6		
	Beginning	Middle	End	Beginning	Middle	End
H, mm	153.822	152.705	152.171	153.899	152.603	152.438
B1, mm	42.050	41.021	42.901	42.164	41.072	42.824
B2, mm	42.139	42.215	41.745	42.050	41.999	41.707
C1, mm	12.624	12.306	12.687	12.751	12.306	13.360
C2, mm	12.852	13.526	12.751	13.157	13.500	12.954

The model consists of the test sample, bands and rigid supports. Shell members SHELL181 with the average size of 3-5 mm were used for creating the final-element mesh. Beam elements BEAM188 were used for creating bands. For modeling the band attachment in the sample flanges we prepared holes with the diameter of 4.8 mm which is equal to the self-tapping screws diameter. Nodes along the circuit holes joined in the rigid region with "the master" node, positioned in the center of the hole. The attachment of beam elements of bands was done by combination of displacements ((*ux*, *uy*, *uz*) with the correspondent nodes and the "the master" node. For the purpose of supporting condition and load modeling which are identical to the full-scale experiment, we used a pair of contact elements CONTA177 (end of the sample) and TARGE170 (face of support plate). Given that stiffness of rigid supporters transferring the load is considerably greater than the stiffness of the sample, the elements TARGE170 were used in nondeformable formulation and were guided by "the master" nodes.

In addition, the use of contact elements allowed us to consider friction between the sample and the supporting structures (frictional coefficient $\mu = 0.25$). The load modeling was conducted by moving the contact elements TARGE170 of

"the upper" track at the Z-axis toward "the lower" track. The following boundary conditions were put: "the master" node of the contact elements of "the lower" track and the side nodes of the bands were constrained in *ux, uy, uz*; "the master" node of the contact elements of "the upper" track — *ux, uy*. For accounting steel material nonlinearity we used a multilinear model with isotropic hardening (MISO) [7]. The proper diagram was used for each typical size in accordance with the experiments on the tensile-testing machine.

One of the disadvantages of the full-scale experiment isthe absence of measurements of the initial geometrical imperfections. For their consideration the use of probabilistic approach is suggested. This approach entails calculation of several models with different spread of initial imperfections. The value of imperfections was obtained on the basis of normal distribution [8], derived from the measurement of 88m solid C-shaped studs. It is anticipated that distribution of initial imperfections of real samples is in the diapason of computer modeling. Therefore, the results of the full-scale experiments are supposed to be inside the fictitious "corridor", created in accordance with the results of computer modeling.

Implementation of the initial geometrical imperfections with stochastic nature was done in the following order. Firstly, the initial local and general buckling modes were defined on the basis of the linear buckling analyses (Figure 3).

Figure 4a presents *uy* flange displacement in the line 1-2 (Figure 3) in case of local buckling. It is clear that the shape in question is wavy with a variable half-wave length. With the purpose to give this shape stochastic nature it was decided to set up the peak amplitude for each separate section (highlighted by a dashed line) between zero displacement *uy*. The peak amplitude was deduced by normal distribution. The parameters of normal distribution for this type of imperfection are applied to thickness of steel D/Tk and described in paper [8]: mean value$\mu = 0.26$, standard deviation $\sigma = 0.49$.On the basis of this distribution 5 variants of the peak magnitude amplitude were defined for each section. Therefore, we prepared 5 calculating models for each typical size of the stud which are different in their shape and the value of initial geometrical imperfections. The variants ANS1-x relate to the first typical size of the stud with the metal thickness of 2.0 mm; variants ANS2-x relate to the second typical size of the stud with the metal thickness of 1.0 mm. The symbol "x" stands for the variant number of imperfections introduction. The result of amplitude adjustment with the consideration of stochastic nature is presented in Figure 4b.

General initial imperfections were introduced according to the related buckling mode which is a curve along the sinusoidal wave in a plane of lesser stiffness. For each of the 10 variants on the basis of normal distribution [8] ($\mu = 2033$, $\sigma = 3471$) we generated a series of values $(L/2)/\Delta$, where Δ is an imperfection value. In addition to 10 variants described, four models were prepared. Initial imperfections were absolutely absent in variants ANS1-6, ANS2-6. The value of initial imperfections was raised to the level of standard values in variants ANS1-7, ANS2-7. In order to instill the model with stochastic nature, geometrical sizes of the calculating models were also computed on the basis of normal distribution.

4. COMPARATIVE ANALYSIS

According to the results of full-scale experiments and computer modeling, we obtained correlations between the value of pressure load and: a) displacement *uz* of the sample end in the position of "the upper" track; b) displacement *uy* of "the lower" stud flange inthe centre of the span. The correlation of pressure load and displacement *uz* is presented in Figure 5 for pictorial comparison. The value of ultimate compressive force corresponding to full-scale experiments occurred in the interval, obtained by computer modeling.

The diapason of the results of the first type of

the typical size (ANS1-x) was from 67.8 kN to 92.1 kN. The results of full-scale experiments are presented homogeneously inside the interval, which indicates that the value of initial geometrical imperfections in real samples (S1–S3) varied from minimum to maximum-allowable. The diapason of the results of the second type of the typical size (ANS2-x) was from 24.5 kN to 34.6 kN. Furthermore, the results of full-scale experiments (S4–S6) are presented close to the lower limit, which confirms the fact that the value of initial imperfections of the samples was close to the limit value.

According to the results of full-scale experiment u_z and u_y correspond to the ultimate bearing stress and on average 2-4 times exceed similar meanings, derived by computer modeling. Nevertheless, the difference in the absolute values does not exceed 9 mm for the samples of the first typical size, 3.4 mm - for the samples of the second typical size.

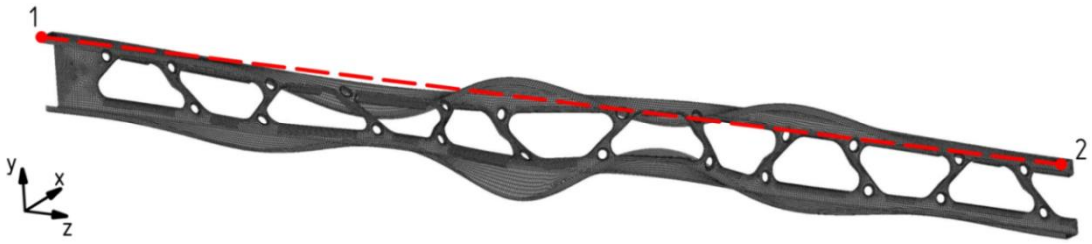
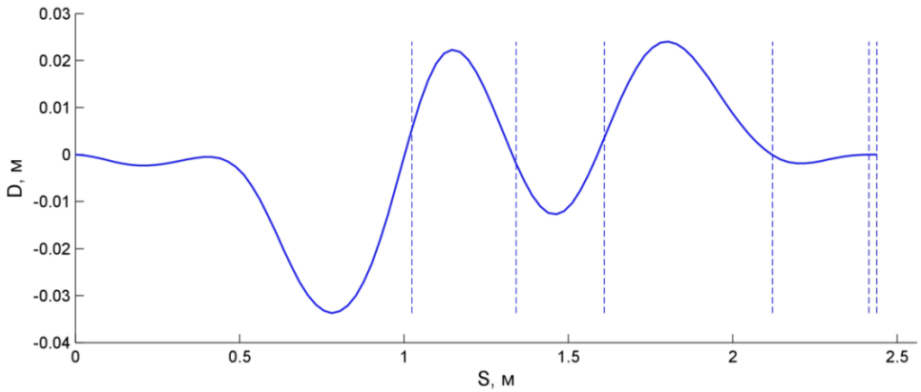
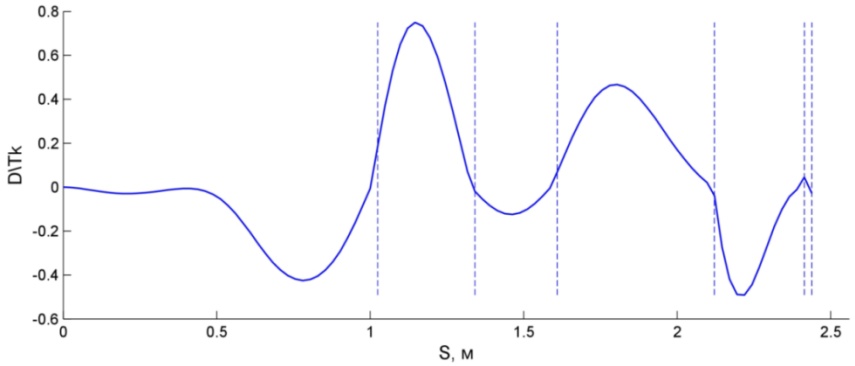


Figure 3. First local buckling mode.



a)



b)

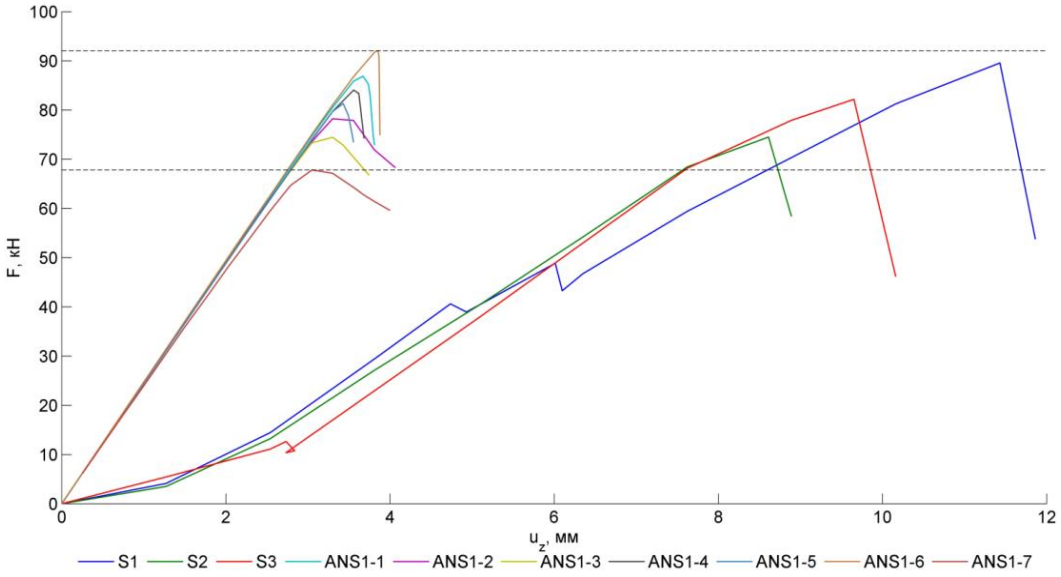
Figure 4. Displacement uy along the line 1–2: a) in original shape; b) in adjusted shape with consideration of stochastic nature.

The results of computer modeling demonstrate patterns of deformation which are similar to full-scale experiments. Sample S1 pattern corresponds to the results of computer modeling of the variant ANS1-4 (Figure 6) — in both cases we can observe a considerable curve of the upper flange in the centre of the second half of the stud. Sample S3 pattern corresponds to the results of computer modeling of the variant ANS1-5— in both cases we can observe a considerable curve of the upper flange in the centre of the first half of the stud.

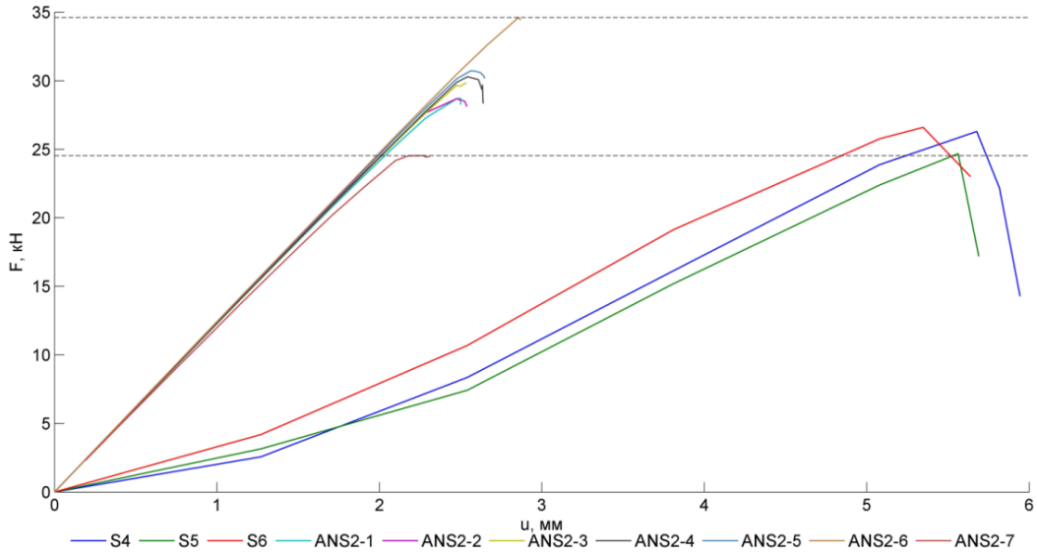
The ultimate bearing stress values were close: the measure of inaccuracy between the results S1 and ANS1-4 — 4.3%, between the results S3 and ANS1-5 — 0.74%.

The identical pattern of deformation is observed in samples S4–S6— a local curve of the upper flange on the first half of the stud.

The similar pattern of deformation is observed in sample ANS2-5.



a)



b)

Figure 5. Correlation between compressive force and displacement uz for samples: a) first typical size; b) second typical size.

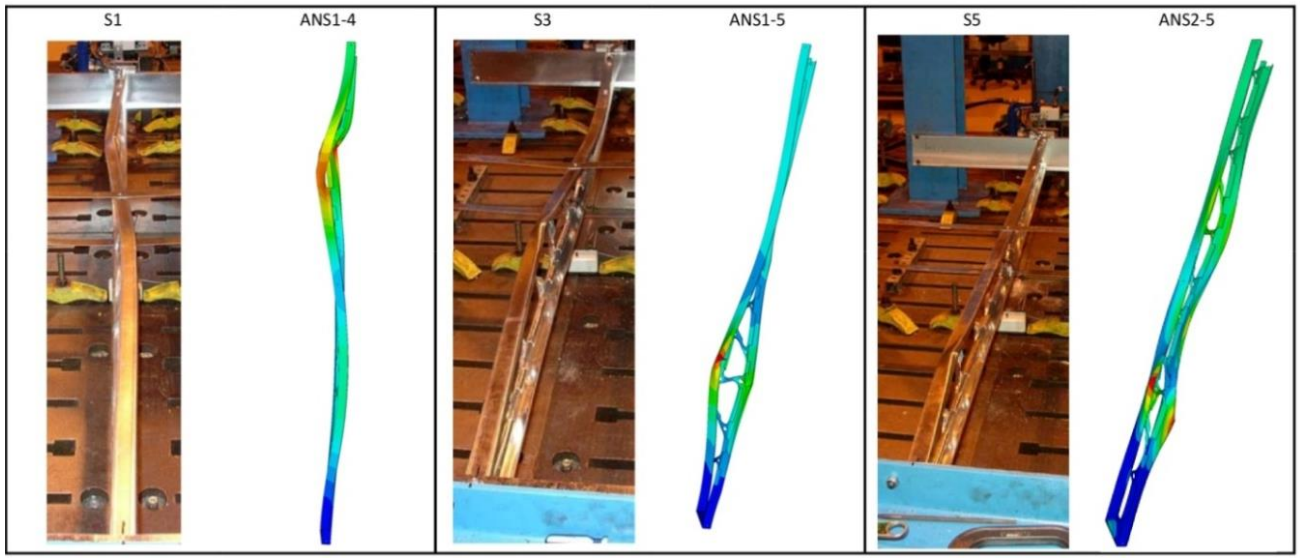


Figure 6. Deformation comparison.

REFERENCE

1. **06-03-C002**. Compression test on single joist sample. Bodycote materials testing Canada, 2006, 5 pages.
2. **TU 1120–001–43048595–2015** Profili holodnognutye “Atlant”, 2015, 25 pages.
3. **ASTM A370—17a.** Standard Test Methods and Definitions for Mechanical Testing of Steel Products. ASTM International, 2017.
4. **Aleksandrov A.V., Potapov V.D., Derzhavin B.P.** Soprotivlenie Materialov [Strength of Materials]. Moscow, Vysshaya Shkola, 2003, 560 pages.
5. **ASTM B487** Standard Test Method for Measurement of Metal and Oxide Coating Thickness by Microscopical Examination of Cross Section. ASTM International, 2013.
6. **Ansys Inc**. ANSYS Mechanical APDL Structural Guide. Edition 15, 2013.
7. **Basov K.A.** ANSYS: Spravochnik Pol'zovatelia [ANSYS: User's guide]. Moscow, DMK Press, 2005, 640 pages.
8. **Vahid Zeinoddini-Meimand.** Geometric imperfections in cold-formed steel members. The Johns Hopkins University, 2011.

СПИСОК ЛИТЕРАТУРЫ

1. **06-03-C002** Compression test on single joist sample. Bodycote materials testing Canada, 2006, 5 pages.
2. **ТУ 1120–001–43048595–2015** Профили холодногнутые «Атлант», 2015. – 25 с.
3. **ASTM A370—17a** Standard Test Methods and Definitions for Mechanical Testing of Steel Products. ASTM International, 2017.
4. **Александров А.В., Потапов В.Д., Державин Б.П.** Сопротивление материалов. – М.: Высшая школа, 2003. – 560 с.
5. **ASTM B487** Standard Test Method for Measurement of Metal and Oxide Coating Thickness by Microscopical Examination of Cross Section. ASTM International, 2013.
6. **Ansys Inc**. ANSYS Mechanical APDL Structural Guide. Edition 15, 2013.
7. **Басов К.А.** ANSYS: Справочник пользователя. – М.: ДМК Пресс, 2005. – 640 с.
8. **Vahid Zeinoddini-Meimand.** Geometric imperfections in cold-formed steel members. The Johns Hopkins University, 2011.

Galina G. Kashevarova, Corresponding Member of Russian Academy of Architecture and Construction Sciences, Professor, Dr.Sc., Head of department "Building constructions and computational mechanics", Perm National Research Polytechnic University; Russia, 614010, Perm, ul. Kuibyshev, 109;
phone +7 (342) 219-83-61, e-mail: ggkash@mail.ru.

Pavel A. Kosykh, Engineer, Perm National Research Polytechnic University; 109, Kujbysheva street, Perm, 614010, Russia; phone +7 (342) 219-83-61,
E-mail: paolo_07@list.ru.

Кашеварова Галина Геннадьевна, член-корреспондент РААСН, доктор технических наук, профессор, заведующая кафедрой «Строительные конструкции и вычислительная механика» Пермского национального исследовательского политехнического университета; 614010, Россия, г. Пермь, ул. Куйбышева, 109;
тел. +7(342) 219-83-61, e-mail: ggkash@mail.ru.

Косых Павел Андреевич, инженер, Пермский национальный исследовательский политехнический университет; 614010, Россия, г. Пермь, ул. Куйбышева, 109; тел. +7 (342) 219-83-61;
E-mail: paolo_07@list.ru.

DOI:10.22337/2587-9618-2018-14-3-59-67

DETERMINATION OF ELASTIC PROPERTIES OF CEMENT-SAND COMPOSITION USING STRUCTURAL SIMULATION MODELING

Yuri E. Kurbatov, Galina G. Kashevarova
Perm National Research Polytechnic University, Perm, RUSSIA

Abstract: The estimation of quantitative influence of fine-grained concrete structural elements on its strength characteristics is a very actual task requiring application of computer technologies. In this article, the authors propose a structural and simulation model of cement-sand composition, which includes pores, cement stone, sand and the contact zone between them. As a result of the numerical calculation of this model, the integrated elastic characteristics of the material (modulus of elasticity and Poisson's ratio) are obtained, which can be assigned as initial data for the model of a higher scale level in order to optimize the composition of concrete.

Keywords: cement-sand composition, fine-grained concrete, structural simulation modeling, mesostructure, Monte Carlo method, boundary problem, contact zone

ОПРЕДЕЛЕНИЕ УПРУГИХ ХАРАКТЕРИСТИК ЦЕМЕНТНО-ПЕСЧАНОЙ КОМПОЗИЦИИ МЕТОДОМ СТРУКТУРНО-ИМИТАЦИОННОГО МОДЕЛИРОВАНИЯ

Ю.Е. Курбатов, Г.Г. Кашеварова
Пермский национальный исследовательский политехнический университет, г. Пермь, РОССИЯ

Аннотация: Оценка количественного влияния структурных элементов мелкозернистого бетона на его прочностные характеристики является весьма актуальной задачей, требующей применения компьютерных технологий. В данной статье авторами предложена структурно-имитационная модель цементно-песчаной композиции, включающая в себя поры, цементный камень, песок и контактную зону между ними. В результате численного расчета данной модели получены интегральные упругие характеристики материала (модуль упругости и коэффициент Пуассона), которые могут быть назначены в качестве исходных данных для модели более высокого масштабного уровня с целью оптимизации состава бетона.

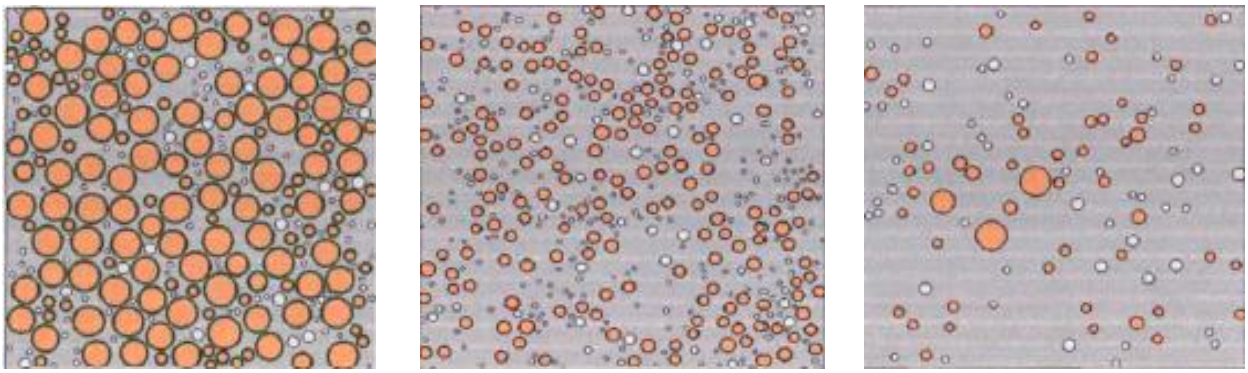
Ключевые слова: цементно-песчаная композиция, мелкозернистый бетон, структурно-имитационное моделирование, мезоструктура, метод Монте-Карло, краевая задача, контактная зона

1. INTRODUCTION

Structural-simulation modeling (SSM) is one of the most effective tools which is suitable for the description of the complex structured systems such as fine-grained concrete. SSM allows to take into account the distribution of structure components in space, their mutual orientation and pairing. In [1] the author presents an analytical review of existing approaches to SSM of a complex composite structures such as fibrobeton, analyzes the main stages of modeling, including the creation of geometry and orientation of structural elements in space, the appointment of effective properties, binding and loading the model.

In the paper [2] Haritonov A.M. offers a generalizing model of fine-grained concrete structure, which can be used to study the heterogeneity of stress distribution in the

material volume. This phenomenon, according to the author, can be explained by a large difference in the values of the elastic modulus of cement stone and fine aggregate. The author created a flat model of cement-sand composite microstructure on three scale levels in order to calculate it. At the same time, the author's program "PoreSolution" [3], implementing the Monte Carlo method, was used to place the structural elements of the model within a given area. An experiment on static compression of a flat concrete model for developed geometrical and finite element models was simulated (see Figure1). Boundary conditions of the experiment are shown in Figure 2. Performed in the work [2] studies have allowed to obtain the strength and deformation regularities in the behavior of cement-sand compositions depending on their composition.



a ***b*** ***c***

Figure 1. The geometric model of cement-sand compositions structure [2]: a) 5x5 mm; b) 20x20 mm; c) 50x50 mm.

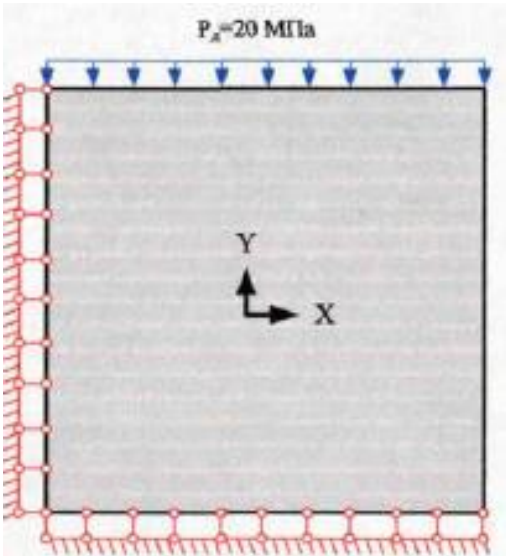


Figure 2. Boundary conditions of the calculation scheme [2].

The authors of this publication have set an aim to conduct an own independent computational experiment on the basis of the study described above to determine additional output parameters and to conduct a comparative analysis of the results with the data presented in [2]. At the same time, to form the geometric scheme of the cement-sand composition, an alternative program in the APDL language was written. Thus, all stages of the computational experiment were implemented in one software environment – ANSYS Mechanical.

2. CONDUCTING OF THE COMPUTATIONAL EXPERIMENT

The formulation of the boundary value problem in this case is traditional for the structural-simulation approach. The basic relations of the elasticity theory are given below:

$$\sigma_{ij,j}(r) + F_i(r) = 0 \quad (1)$$

$$\varepsilon_{ij}(r) = \frac{1}{2}(U_{i,j}(r) + U_{j,i}(r)) \quad (2)$$

$$\sigma_{ij}(r) = C_{ijkl}(r)(I_{ijkl} - \Pi_{ijkl}(r))\varepsilon_{kl}(r) \quad (3)$$

$$\sigma_{ij} \times n_j = F_i \quad (4)$$

$$u|_\Gamma = u* \quad (5)$$

The concept of "probabilistic-geometric concentration" proposed in [4] was used to create a structural-simulation model. A distribution of pores and grains of sand by size, porosity and arrangement of pores and solid phases in model space were considered as a major probability factors that define the geometry model. The design plane of the model is taken in the form of a square with dimensions of 50 x 50 mm. Structural components which considered in the model are as follows:

- the matrix (cement stone);
- grains of sand (0,5-1 mm);
- pores (sizes range from 0.2 mm to 0.8 mm);
- the contact area between the grains of the filler and the matrix (thickness 0.2 mm).

The form of pores and grains of sand is conditionally accepted as circles for simplification of construction of a finite-element grid. The contact area is simulated as an annular shell around each grain of sand.

The modulus of elasticity (E) and Poisson's ratio (μ) of quartz sand are adopted on the basis of literature data and are equal to: E = 72,8 GPa, μ=0,167. The values of the modulus of elasticity and Poisson's ratio of the contact zone are assumed to be equal 10,6 GPa и 0,30 (according to estimates obtained in the work [5]).

The above values were recalculated for use in two-dimensional formulation [6] in order to prepare for the calculation:

$$E_2 = \frac{E_3}{(1-\mu_3^2)}, \quad (6)$$

$$\mu_2 = \frac{\mu_3}{(1-\mu_3)} \quad (7)$$

The values of modulus of elasticity and Poisson's ratio of cement stone for each calculated composition (P1...P10, see Table 2) are taken from the results of experiments carried out at the previous scale level (20x20 mm) in [2]. These values are assigned as initial values for cement stone in model 50x50 mm. Figure 3 shows a typical geometric scheme of the composition for P1, built by the author's macro-program in the language APDL (ANSYS Mechanical). Each time you run the program, it implements a new packaging option that does not repeat the previously built layouts. The conditions of fastening and loading were taken in accordance with Figure 2.

The following two types of finite elements have been selected to build the mesh in the ANSYS library: PLANE 182 and PLANE 183. According to the results of preliminary calculations on two corresponding meshes (with the same partition step, but with different types of finite elements) in one case, the result was noticeably overestimated relative to the experimental value, in the other – slightly understated (see Table 1). After the final selection of the finite element type (PLANE183), a second preliminary calculation was carried out, also on two finite element meshes, but with a different partition step (0.2 mm and 0.4 mm). Based on the results shown in Table 2, it can be concluded that the 0.2 mm mesh pitch gives a slightly more accurate result. The enlarged fragment of this mesh is shown in Figure 4.

.

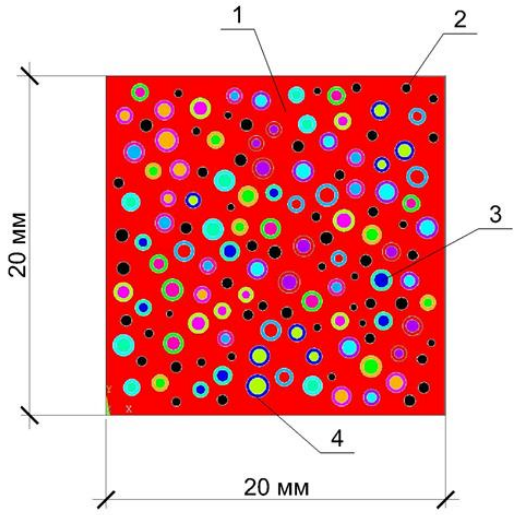


Figure 3. Geometry of composite for structure P1
1 - cement matrix 2 - pore 3 - sand particle 4 - contact area.

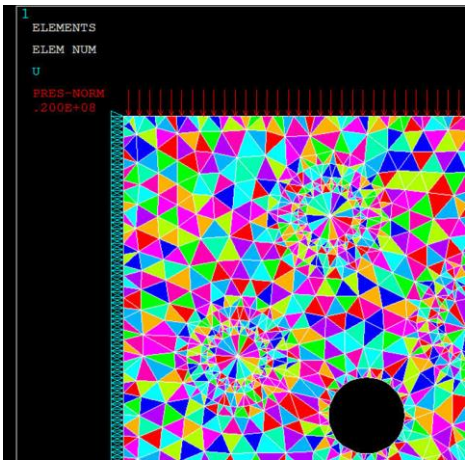


Figure 4. The enlarged fragment of the calculation scheme for the composition P1

Table 1. Parameters of material.

Composition	Sand %	Pores %	Modulus of elasticity, GPa				
			$E_{эксп}$*	$E_{расч}$ (PLANE 182)		$E_{расч}$ (PLANE 183)	
			3D	2D	3D	2D	3D
P1	47,4	19,86	**22,41**	25,262	**23,843**	23,068	**21,772**

Table 2. Parameters of material.

Composition	Sand %	Pores %	Modulus of elasticity, GPa				
			$E_{эксп}$*	$E_{расч}$ (s=0,4 mm)		$E_{расч}$ (s=0,2 mm)	
			3D	2D	3D	2D	3D
P1	47,4	19,86	**22,41**	23,020	**21,727**	23,068	**21,772**

In preparation for the main series of strength calculations for each composition (P1...P10) it was formed on three models with different distribution of structural components in the plane of the model, but with the same percentage, with one type of finite element (PLANE 183), and with one partition step (0.2 mm). The results were averaged for each composition. Then the summary Tables 3 and 4 were made, in which the values of the modulus of elasticity and Poisson's coefficients specified in [2] ($E_{эксп}$*, $E_{теор}$*, $\mu_{теор}$*), and received as a result of the executed calculations ($E_{расч}$, $E_{инт}$, $E_{экв}$, $\mu_{расч}$).

Table 3. Parameters of material.

Composition	Sand %	Pores %	Modulus of elasticity, GPa							
			$E^*_{эксп}$	$E^*_{теор}$		$E_{расч}$		$E_{инт}$	$E_{экв}$	$\frac{E_{экв}}{E_{расч}}$
			3D	2D	3D	2D	3D	2D	2D	
P1	47,4	19,86	**22,41**	25,7	**24,3**	22,884	**21,599**	26,097	42,358	1,85
P2	48,9	19,09	**23,95**	26,8	**24,4**	23,484	**22,165**	26,214	43,241	1,84
P3	52,3	17,68	**32,01**	33,3	**31,5**	28,187	**26,604**	32,015	46,475	1,65
P4	49,1	18,13	**25,34**	27,0	**25,6**	23,560	**22,237**	28,752	43,844	1,86
P5	53,2	20,25	**22,03**	25,1	**23,8**	21,932	**20,762**	27,379	44,834	2,04
P6	55,3	17,65	**27,81**	29,3	**27,8**	24,667	**23,351**	30,037	47,107	1,91
P7	56,1	17,21	**30,56**	32,2	**30,5**	27,701	**26,223**	31,439	47,875	1,73
P8	55,4	19,62	**20,60**	23,4	**22,2**	21,383	**20,242**	28,142	45,921	2,15
P9	58,3	20,05	**22,44**	25,9	**24,6**	21,091	**20,023**	30,808	47,337	2,24
P10	66,1	18,70	**19,02**	22,8	**21,4**	19,492	**18,504**	25,998	50,766	2,60

Table 4. Parameters of material.

Composition	Share of sand, %	Porosity, %	Poisson's ratio			
			$\mu^*_{теор}$		$\mu_{расч}$	
			2D	3D	2D	3D
P1	47,4	19,86	0,31	**0,24**	0,310	**0,237**
P2	48,9	19,09	0,31	**0,24**	0,310	**0,237**
P3	52,3	17,68	0,30	**0,23**	0,310	**0,237**
P4	49,1	18,13	0,30	**0,23**	0,310	**0,237**
P5	53,2	20,25	0,30	**0,23**	0,300	**0,231**
P6	55,3	17,65	0,30	**0,23**	0,300	**0,231**
P7	56,1	17,21	0,30	**0,23**	0,301	**0,231**
P8	55,4	19,62	0,30	**0,23**	0,300	**0,231**
P9	58,3	20,05	0,29	**0,22**	0,291	**0,225**
P10	66,1	18,70	0,29	**0,22**	0,291	**0,225**

3. RESULTS OF CALCULATION

Several approaches were used to obtain the values of the modulus of elasticity and Poisson's ratio based on the results of the computational experiment. According to [7], modulus of elasticity $E_{расч}$ is defined as the ratio of voltage increment from zero to the level of external load equal to 30% from the damage (20 MPa according [2]), to the increment of elastic-instantaneous relative deformation of the sample. The Poisson ratio is calculated as the ratio of the elastic-instantaneous relative transverse strain to the longitudinal strain of the specimen. Thus devices for measurement of

deformations of a concrete sample in the form of a cube shall be established on four free sides. In accordance with the indication (in the transition to the plane problem), the results of strength calculation in ANSYS (values of the elastic deformations) was determined in the nodes located on the free right edge of the model (see Figure 2). According to the obtained data, the average values of longitudinal and transverse strain on the face were calculated (see tables 3 and 4). The calculated values of the elastic modulus $E_{расч}$ and Poisson's ratio $\mu_{расч}$ were determined. Figure 5 shows the distribution fields of elastic longitudinal deformation for the composition P3, which provided the highest value among all the simulated compositions.

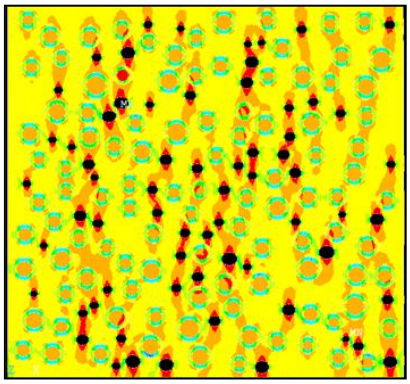


Figure 5. Elastic longitudinal deformation of the composite composition P3.

The second approach to the calculation of the elastic modulus is based on the calculation of the integral value of the obtained data on the stress-strain state in each node of the model. The value of the elastic modulus was defined as the ratio of the normal stress in the node to the elastic longitudinal deformation in the same node:

$$E_{инті} = \frac{\sigma_{yi}}{\varepsilon_{yi}}.$$

Then the integral modulus of elasticity was determined as the average value for all nodes:

$$E_{инт} = \sum` E_{инті}\ .$$

The equivalent modulus of elasticity takes into account the degree of influence of the structure components on the elastic properties of the composite and is calculated by the following expression:

$$\sigma_{экв} = \sum_{m=1}^{N}(k_m E_m) \qquad (8)$$

This value sums the shares of the "contribution" of individual phases to the strength of the model in proportion to the volume occupied by them in the structure of the model. It is obvious that the equivalent modulus of elasticity differs markedly from the actual absolute value of the resulting young modulus. In the paper [2] the following relation is obtained, which according to the author is almost constant:

$$E^*_{экв} = 1{,}61E^*_{теор} \qquad (9)$$

However, according to the results of calculations shown in table 5, the authors of this article found that the ratio is variable and varies in the range of 1.65...2,60. Thus, three alternative values of the elastic modulus for each composition were obtained by different methods, which were compared with the experimental values given in [2] $E^*_{эксп}$ and numerical values $E^*_{теор}$, received on results of calculations. A comparison of the values of all the above values is given in Table 5.

Table 5. Comparison of results.

Composition	Difference (in %) between:			
	$E_{расч}$ и...		$E_{инт}$ и ...	$\frac{E_{экв}}{E_{расч}}$ и...
	$E^*_{эксп}$	$E^*_{теор}$	$E^*_{теор}$	$\frac{E^*_{экв}}{E^*_{теор}}$ **=1,61**
P1	3,62	11,12	1,52	12,97
P2	7,45	9,16	2,19	12,50
P3	16,89	15,54	1,61	2,42
P4	12,25	13,14	6,09	13,44
P5	5,76	12,76	8,32	21,08
P6	16,03	16,00	2,45	15,71
P7	14,19	14,02	2,36	6,94
P8	1,74	8,82	16,85	25,12
P9	10,77	18,61	15,93	28,13
P10	2,71	13,53	12,30	38,08

4. CONCLUSION

The obtained results of the mechanical properties calculations allow us to conclude that a consistent increase in the percentage of sand in the composition to 50-55% leads to an increase in the value of the elastic modulus, but with a further increase in the reinforcement of the cement stone with a small filler, there is a significant decrease in the elastic characteristics of the material.

The obtained values can be used to assign the physical properties of the matrix of a higher scale level (for example, in coarse-grained concrete). Thus, the developed structural simulation model of cement-sand composition allows reproducing the most important mechanical characteristics of the material in order to assess the impact of individual structural components on the strength of the composite.

REFERENCES

1. **Kurbatov Y.E.** Problemy i Vozmozhnye Napravlenija Reshenija Zadachi Strukturno-Imitacionnogo Modelirovanija Fibrobetonnogo Kompozita [Problems and Possible Directions of Solving Problems of Structural-Simulation Modeling of Fiber Composites]. // Vestnik Perm National Research Polytechnic University. Applied ecology. Urbanistics, 2017, No. 1, pp. 126-139.
2. **Haritonov A.M.** Strukturno-Imitacionnoe Modelirovanie v Issledovanijah Svojstv Cementnyh Kompozitov [Structural-simulation Modelling to Study the Properties of Cement Composites]. Dr.Sc. Thesis, Saint Petersburg, 2009, 365 pages.
3. **Haritonov A.M.** Modelirovanie Struktury Cementnogo Kamnja i Processov Usadki "PoreSolution v2.0" [Modeling of Cement Stone Structure and Processes of Shrinkage "Pore Solution v2.0". Certificate of official registration program for computer No. 2008614295 from 08.09.2008.
4. **Bazhenov Y.M., Vorob'ev V.A., Ilyukhin A.V.** Komp'juternoe Materialovedenie i Novyj Algoritm Modelirovanija Struktury Stroitel'nyh Kompozicionnyh Materialov [Computer Science a New Algorithm for Modeling the Structure of Composite Materials. // Design and Execution –

Guarantors of Safety of Life: Proceedings of General Meeting of RAACN (two volumes). Saint-Petersburg State University of Architecture and Civil Engineering, 2006, Volume 1, pp. 142-148.
5. **Haecker, G.-J., Garboczi E.J., Bullard J.W., Bohn R.B., Sun Z., Shah S.P., Voigt T.** Modeling the Linear Elastic Properties of Portland Cement Paste. // Cement and Concrete Research, 2005, Vol. 35, No. 10, pp. 1948-1960.
6. **Meille S., Garboczi E.J.** Linear Elastic Properties of 2-D and 3-D Models of Porous Materials Made from Elongated Objects. // Mod. Sim. Mater. Sci. and Eng., 2001, No. 9(5), pp. 371-390.
7. GOST 24452-80. Betony. Metody Opredelenija Prizmennoj Prochnosti, Modulja Uprugosti i Kojefficienta Puassona [Concretes. Methods of Determination of Prismatic Strength, Modulus of Elasticity and Poisson's Ratio]. Moscow, STANDARTINFORM, 2005, 14 pages.

СПИСОК ЛИТЕРАТУРЫ

1. **Курбатов Ю.Е.** Проблемы и возможные направления решения задачи структурно-имитационного моделирования фибробетонного композита. // Вестник Пермского национального исследовательского политехнического университета. Прикладная экология. Урбанистика, 2017, №1, с. 126-139.
2. **Харитонов А.М.** Структурно-имитационное моделирование в исследованиях свойств цементных композитов. Диссертация на соискание ученой степени доктора технических наук по специальности 05.23.05 – «Строительные материалы и изделия». – СПб., 2009. – 365 с.
3. **Харитонов А.М.** Моделирование структуры цементного камня и процессов усадки «PoreSolution v2.0». Свидетельство об официальной регистрации программы для ЭВМ №2008614295 от 08.09.2008.
4. **Баженов Ю.М., Воробьев В.А., Илюхин А.В.** Компьютерное материаловедение и новый алгоритм моделирования структуры строительных композиционных материалов. // Проект и реализация – гаранты безопасности жизнедеятельности: Труды Общего собрания Российской академии архитектуры и строительных наук (в 2 томах). – СПб.: Санкт-Петербургский государственный архитектурно-строительный университет, 2006, том 1, с. 142-148.
5. **Haecker, G.-J., Garboczi E.J., Bullard J.W., Bohn R.B., Sun Z., Shah S.P., Voigt T.** Modeling the Linear Elastic Properties of Portland Cement Paste. // Cement and Concrete Research, 2005, Vol. 35, No. 10, pp. 1948-1960.
6. **Meille S., Garboczi E.J.** Linear Elastic Properties of 2-D and 3-D Models of Porous Materials Made from Elongated Objects. // Mod. Sim. Mater. Sci. and Eng., 2001, No. 9(5), pp. 371-390.
7. ГОСТ 24452-80. Бетоны. Методы определения призменной прочности, модуля упругости и коэффициента Пуассона. – М.: Стандартинформ, 2005. – 14 с.

Yuri E. Kurbatov, Ph.D. Student, Senior Lecturer, Engineer, Department “Building constructions and computational mechanics”, Perm National Research Polytechnic University, 109, Kujbysheva street, Perm, 614010, Russia; phone +7 (342) 219-83-89,
E-mail: YEK-STF@yandex.ru.

Galina G. Kashevarova, Corresponding Member of Russian Academy of Architecture and Construction Sciences, Professor, Dr.Sc., Head of department “Building constructions and computational mechanics”, Perm National Research Polytechnic University; Russia, 614010, Perm, ul. Kuibyshev, 109;
phone +7 (342) 219-83-61, e-mail: ggkash@mail.ru.

Курбатов Юрий Евгеньевич, аспирант, старший преподаватель кафедры «Строительные конструкции и вычислительная механика» Пермского национального исследовательского политехнического университета; 614010, Россия, г. Пермь, ул. Куйбышева, дом 109, тел. +7(342) 2198389,
E- mail: YEK-STF@yandex.ru.

Кашеварова Галина Геннадьевна, член-корреспондент РААСН, доктор технических наук, профессор, заведующая кафедрой «Строительные конструкции и вычислительная механика» Пермского национального исследовательского политехнического университета; Россия, 614010, г. Пермь, ул. Куйбышева, 109,
тел. +7(342) 2198379, e-mail: ggkash@mail.ru.

DOI:10.22337/2587-9618-2018-14-3-68-82

ARCHITECTURAL MODELLING OF “SOUND” PERGOLA

Valery S. Lesovik, Irina L. Pershina, Dmitry Yu. Popov, Andrey V. Shevchenko

Belgorod State Technological University named after V.G. Shukhov, Belgorod, RUSSIA

Abstract: The article describes architectural solutions of pergolas adapted for the reproduction of synthesized acoustic space. The solution is represented by means of computer modelling and visualizes both processes and objects on the example of construction and calculations. The project design of architectural models is an integral part in the practical reconstruction of the geospatial space studied by the architectural geography.

Keywords: architectural geonics, computer modelling, specific space, acoustic architectural environment, textiles-concrete, reinforcement, composite binder

АРХИТЕКТУРНОЕ МОДЕЛИРОВАНИЕ «ЗВУКОВОЙ» ПЕРГОЛЫ

В.С. Лесовик, И.Л. Першина, Д.Ю. Попов, А.В. Шевченко

Белгородский государственный технологический университет им. В.Г. Шухова, г. Белгород, РОССИЯ

Аннотация: В статье описаны архитектурные решения перголы, приспособленной для воспроизводства сентезированного акустического пространства. Решение представлено средствами компьютерного моделирования и визуализирует как процессы, так и объекты на примере построения и расчетов. Проектная разработка архитектурных моделей является неотъемлемой частью в практическом воссоздании исследуемого архитектурной геоникой геоспецифического пространства.

Ключевые слова: архитектурная геоника, компьютерное моделирование, специфическое пространство, акустическая архитектурная среда, текстиль-бетон, армирование, композиционное вяжущее

1. INTRODUCTION. ABOUT THE PROCESS CONTENT OF THE COMPOSITION

Denoting the problem of creating an architectural environment that exerts a therapeutic intervention on the physical and psychoemotional state of a person, a solution appears to be a fundamentally new way of solving an actual scientific problem. The originality of the formulated approaches allows us to talk about a new paradigm in architecture — architectural geonics [1-3], which formulates the systematic study of the influence of geofactors on humans and has in its deposit tools for creating specificity of space [4-5].

Modern trends of transdisciplinarity in the theory and practice of architectural geology [6], expressed in separate concepts, methods and approaches, are "supported" by the latest knowledge and indicate the development of the vector of geodirectional architecture. Their local manifestations reflect a comprehensive approach to creating a positive architectural and spatial living environment. This confirms the need for the development of architectural geology in the framework of theoretical and project experience in the formation of geo-approaches, as well as the development of principles and models of geosynthetically specific space.

The results presented in this paper are an architectural part of the implementation of the experiment on the practical implementation of the idea of creating an acoustic environment as a form of representation of an architectural space, according to A.G. Rappaport formulation, — one of the types of “perceptual real space, reflected by human perception” [7].

As a model of an architectural specific space, two sketches are implemented, developing ideas for the conceptual shaping of structures for various purposes. The specificity of space in all cases is monosyllabic: one geosynthetized tool of architectural geography using the possibilities of air flows was applied.

The aim is to erect a "sound" surface for practical modelling of a specific medium by means of architectural geography within the framework of scientific research.

At the preparatory stage of the practical solution of this problem, the search and systematization of architectural analogs were carried out; on the basis of this stage, the development of conceptual design proposals for sound architectural structures that form the geospecific nature of space through the application of methods of computer modelling of structures and objects. The possibilities of modern software tools for analyzing and designing the concepts of sound spaces were limited to the ArchiCad, 3-Ds Max, SketchUp programs and the Lumion 3D animation visualization program. As an opportunity to implement it is proposed to use the products of scientific developments of post-graduate students and scientists of BSTU named after V.G. Shukhov. They initiated the research of a non-traditional material for Russian construction — textile-concrete. Textile-concrete is a composite material, consisting, like ordinary reinforced concrete, of concrete and reinforcement, but instead of steel reinforcement, alkali-resistant glass fibers or carbon fibers are used.

2. ARCHITECTURE MODELS

The conceptual proposal is a geological model of the "sound" pergola (Figure 1). The proposed small form is located in Belgorod, on the territory of BSTU named after V.G. Shukhov. The pergola is a lattice black and shade canopy on three visually massive supports (Figure 2 and Figure 3). According to the calculations below, the geometric dimensions of the pergola in the plan are 41.00 × 33.00 m (Figure 4). The shape in the plan is triangular, with radially rounded ends. The lattice structure has a height of 200-600 mm with a cell size of 300 × 300 mm. The conditional plane of the pergola canopy has a complicated concave surface of different heights (within 600 mm).

The expediency of such geometric data is due to the possibility of arbitrary placement of pipes / tubes to create sounds of various required frequencies. The optimal outer diameter of the pipes is 300 mm. In this case, it is possible to place pipes of any larger diameter multiple of 300 mm by cutting a cross-shaped segment of a pergola structure for a diameter of 600 mm or cutting a 900 × 900 mm grating segment to mount a 900 mm diameter pipe.

The concept of sound pergola technology is to form the whole structure with the help of textiles-concrete, described in the section "Applied Materials" of this article.

The estimated height in the span is 4,00 – 5,00 m. The maximum height of the structure is 5,00 – 6,60 m. The sound pipes are metal.

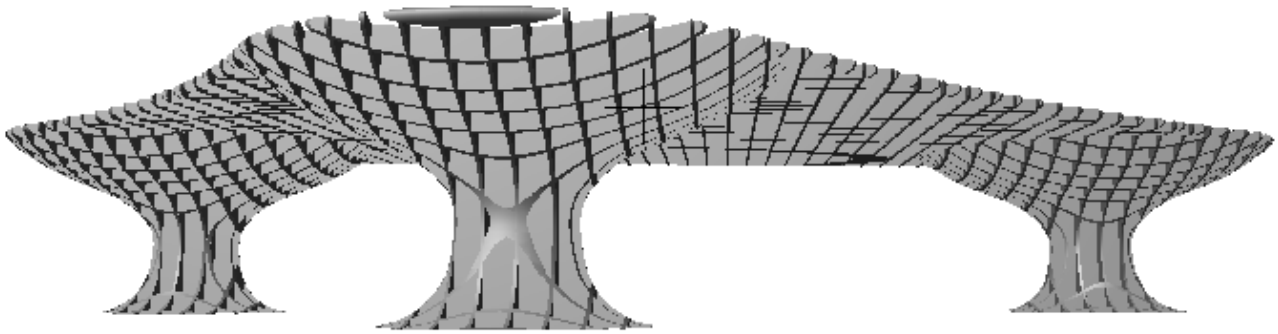


Figure 1. Three-dimensional model of pergola from height of human scale.

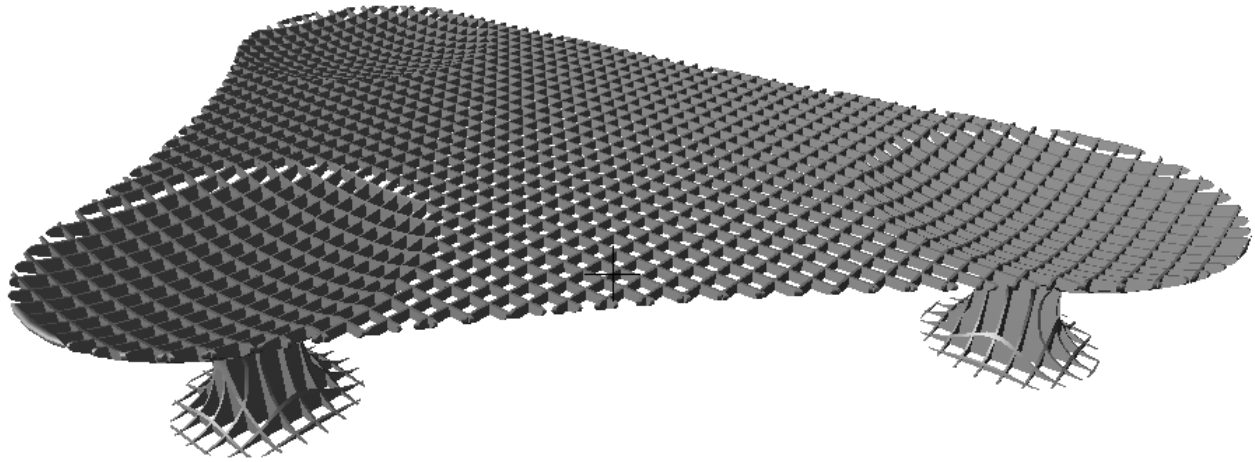


Figure 2. Three-dimensional model of pergola with high chamber height.

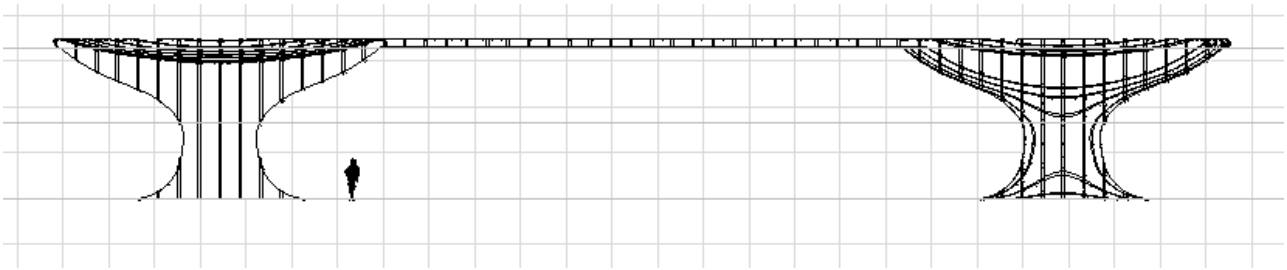


Figure 3. Orthogonal projection of the façade.

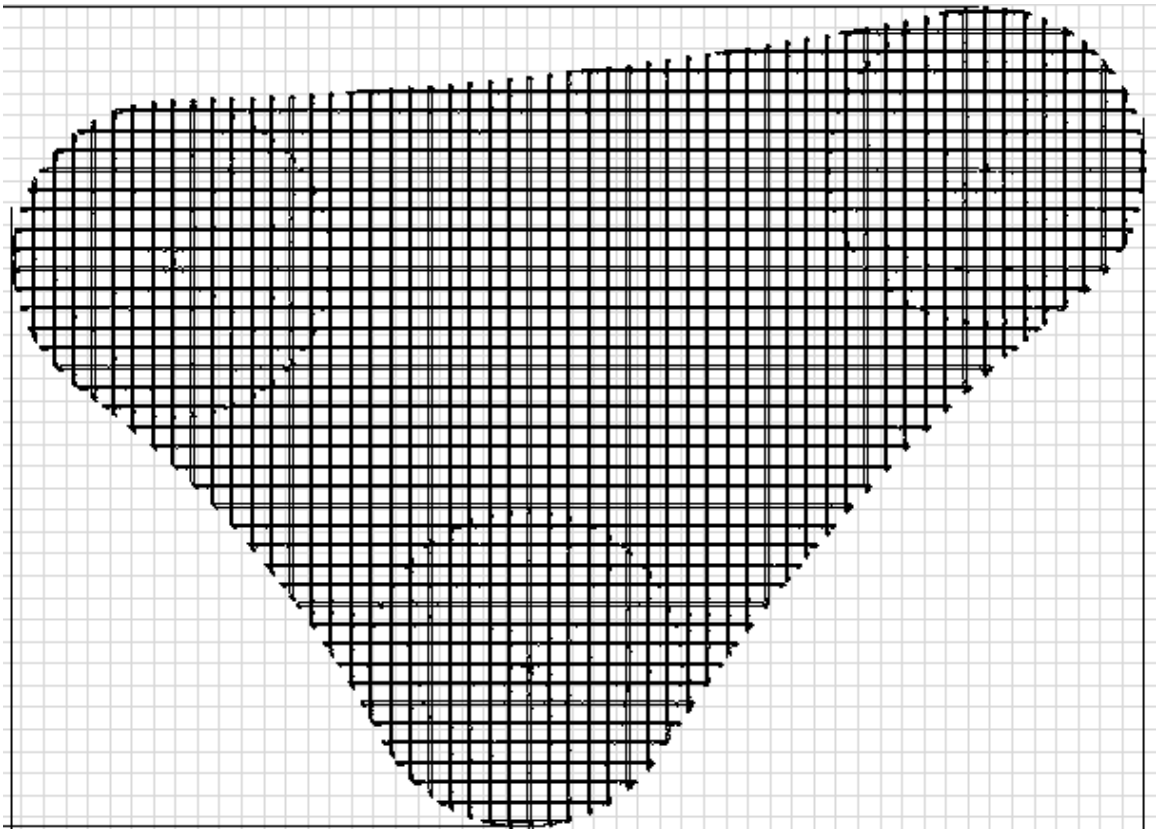


Figure 4. Top view.

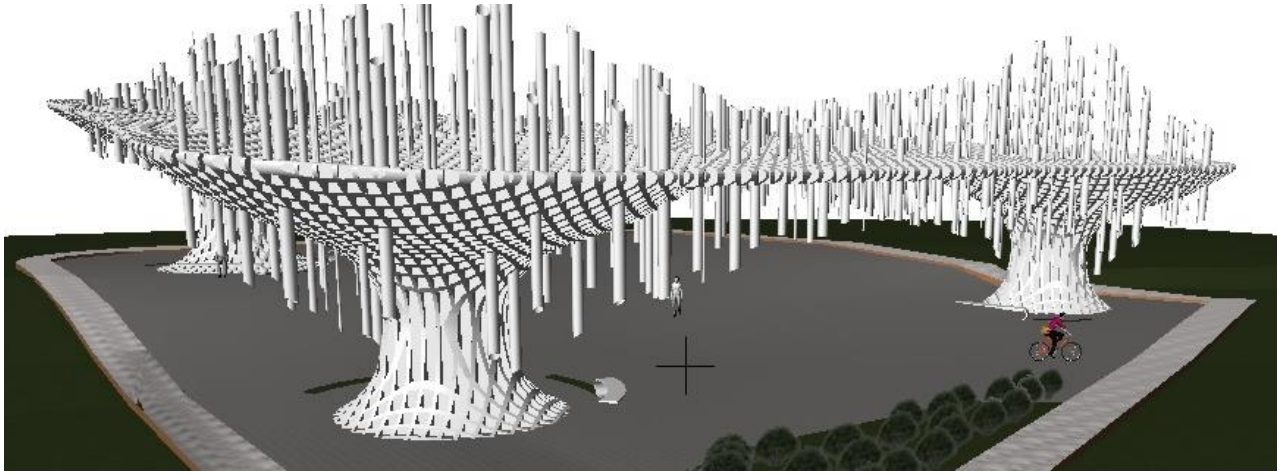


Figure 5. Perspective view of the pergola with the placement of sound tubes.

The initial stage of pergola design involves the search for alternative solutions for support. Acceptable variants in the form of abstract forms are given in Table 1. The shape of each model dictates its own, spatial compatibility of supports, acceptable only for this variant. The optimality of the constructive solution is confirmed by numerical calculations.

Simulation of the lower part of the support (Table 2) assumes design and pragmatism in operation, for example, a reduction in the number of potential places of accumulation of debris and the availability of seats for people.

Theoretical propositions of some design solutions for the creation of sound spaces based on the analysis of the use of the experience of extraction of sounds in wind instruments, set forth in the report and in a published article [8] in the section "Architectural Geonics" of the International Online Congress "Fundamentals of Building Materials Science" (BSTU named after V.G. Shukhov, 2017), allow us to compile the theme of a sound specific environment through the analogy of sound extraction from musical instruments, such as wind and string.

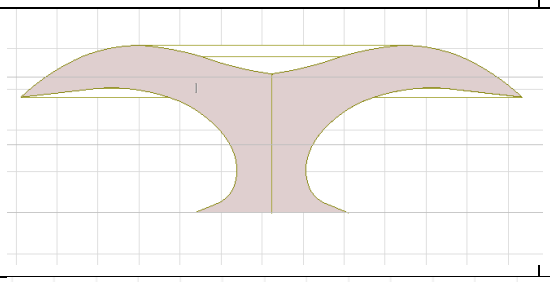
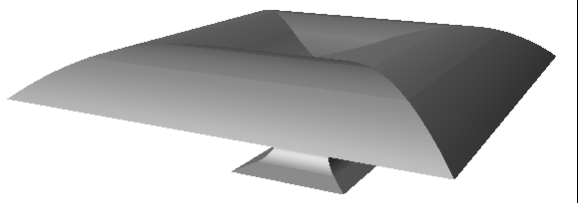
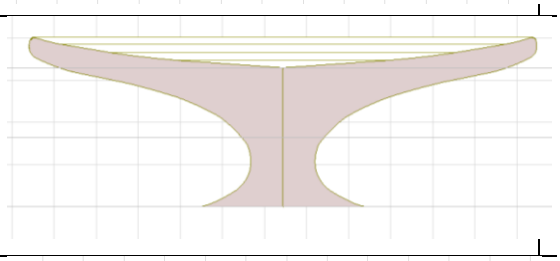
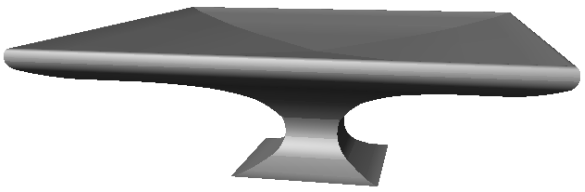
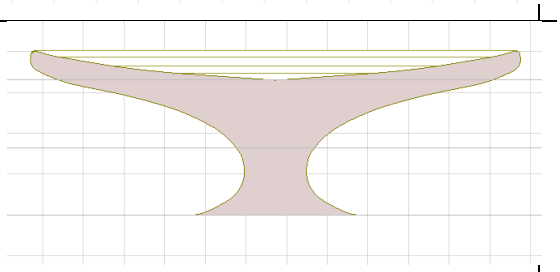
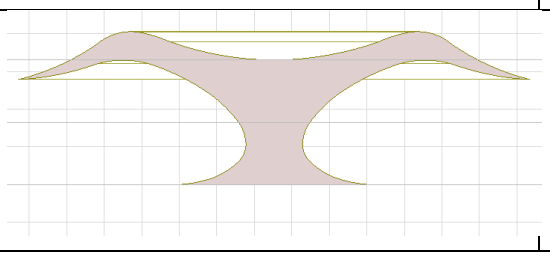
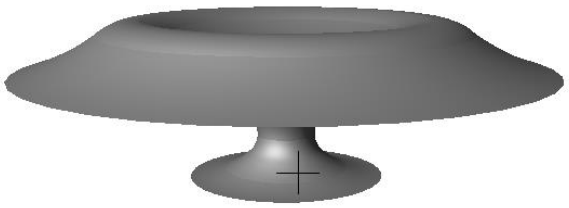
The use of methods for creating musical tones on such instruments will make it possible to repeat the features of sound formation in geological installations, thereby creating the possibility of studying the emotional responses of a person caused by the sound specificity of an architectural space. And this can be considered a modelling of the form of a specific medium by means of architectural geonics.

The analysis of the medical factors of the sound effect on the endogenous rhythms of the organism [9-10] confirms the influence of a specific architectural environment on the creation of a psychological climate [11], the generation of positive emotions, creative mood, and mental activity. And gives a scientific justification of the therapeutic properties of the ecological-physiological method of impact by an acoustic method by quantitative and qualitative assessment of the factors of their optimizing effect.

3. MATERIALS EMPLOYED

To create a new architectural environment, conceptually new efficient building materials are needed, which allow creating complex filigree forms that ensure ease of operation and safety during operation. Attractive from this point of view is a textile-reinforced composite material — textiles-concrete [12, 13]. At present, the composite is widely used in a number of European countries and has established itself as a universal high-quality material [14-16]. To create a "sound" pergola, it is proposed to use textile-concrete of increased efficiency, the composition of which is specially selected taking into account the peculiarities of the local raw materials used, the method of preparation and optimization of the processes of structure

Table 1. Modelling of the abstract form of pergola support.

Model option	Orthogonal projection of the model	Axonometric representation of the model
1		
2		
3		
4		

formation due to application of composite binder properties [17, 18]. The characteristics of the materials used are presented in Table 3. The use of composite binders allows to obtain a new generation of material with high physical-mechanical and operational characteristics that are unattainable with the use of traditional raw materials and will ensure a qualitative structure formation of the material.

The composite binder is prepared by the joint grinding of cement and waste of wet magnetic separation (WMSW) to a specific surface of 550 m^2/kg and optimized by the optimum amount of superplasticizer.

Optimization of the processes of structure formation of composite binders is due to the successive growth of neoplasms during the hardening of the system "clinker minerals – quartz of different origins of WMSW – water-superplasticizer waste", due to the different intensity and time of interaction of polygenetic quartz with the products of hydration of clinker minerals.

Selection of the rational composition of the filler mixture is carried out by the method of calculation of high-density packages [19]. The characteristic of the proposed composition of fine-grained concrete is presented in Table 4.

Table 2. Simulation of the lower part of the pergola.

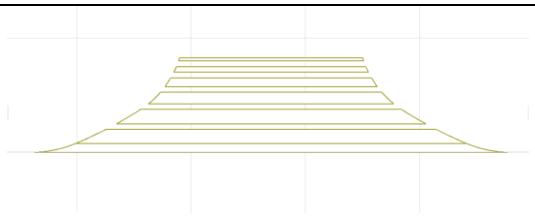
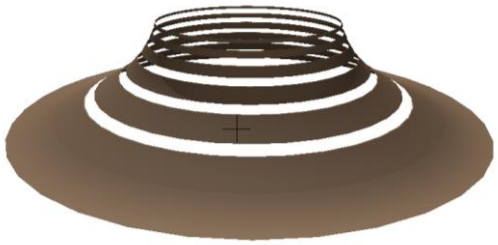
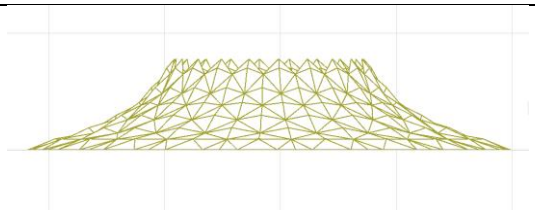
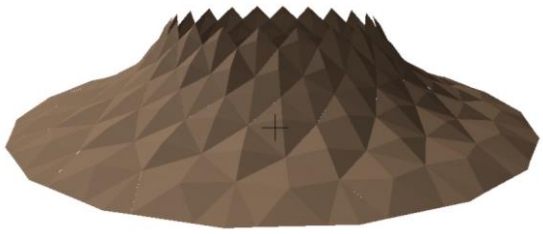
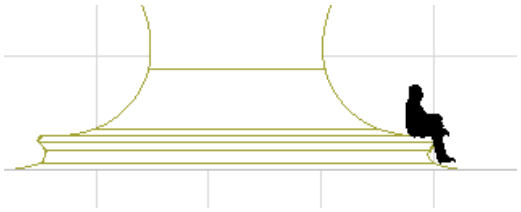
Model option	Orthogonal projection of the lower part of the model	Axonometric view of the bottom part of the model
1		
2		
3		

Table 3. Characteristics of the materials used.

Denomination	Deposit	Dispersability	True specific gravity, kg/m^3
Sand	"Klinovec" quarry, Senevskoe deposit, Korochansky district	0,16–0,63 mm	2630
Cement	ZAO “Belgorodsky Cement”	330 m^2/kg	3100
Wet Magnetic Separation Waste (WMSW)	Lebedinsky GOK, Gubkin	85 m^2/kg	2800
Crushed sand	"Klinovec" quarry, Senevskoe deposit, Korochansky district	200 m^2/kg	2630
Glenium-51		Liquid	1,13–1,15 kg/dm^3

4. NUMERICAL IMPLEMENTATION OF THE CONSTRUCTION

As a design scheme, we take a spatial core system with a span of 22 m. The cell step is 300 × 300 mm. The physical nonlinearity of the materials is first taken as an exponential dependence. Concrete is heavy, fine-grained, class B20 (E_b = 27500 MPa, $R_{b,\,ser}$ = 15 MPa). AR-glass (120 g/m², 2D, Bewehrung Typ 11, E_f = 72,000 MPa, $Rf_{,\,n}$ = 1450 MPa, A_f = 7.07 mm^2) was used as the reinforcing material. The bending moment in the section (for the III snow region) M = 0.83 kNm.

Table 4. Characteristics of the cement matrix of textile-concrete.

Denomination	Condition	Unit	Value
Fresh mortar stiffness		kg/m^3	2400
Elapsed time	at +20 °C	min	≈ 60
Spread in accordance with DIN EN 1015-3	5 min 30 min	cm cm	≥ 17 ≥ 14
Compressive strength in accordance with GOST 10180, prisms 4 × 4 × 16 cm	24 h 7 full days 28 full days	MPa MPa	≥ 15 ≥ 40 ≥ 80
Bending strength in accordance with GOST 10180, prisms 4 × 4 × 16 cm	24 h 7 full days 28 full days	MPa	≥ 3 ≥ 6 ≥ 8
Modulus of elasticity	28 full days	MPa	>25000

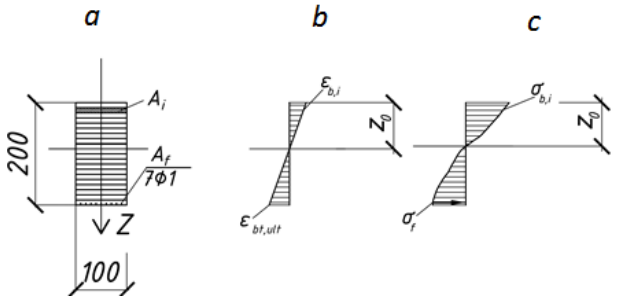


Figure 6. For example of crack resistance calculation: a — the design scheme of the section; b — diagram of relative deformations; c — stress diagram.

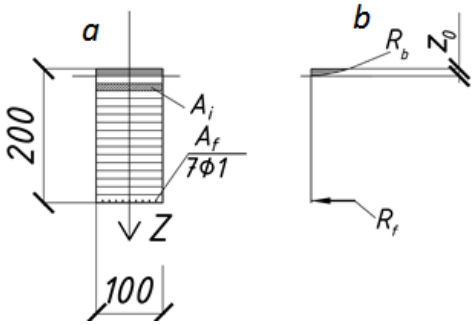


Figure 7. For example of strength calculating: a – the design scheme of the section; b – stress diagram.

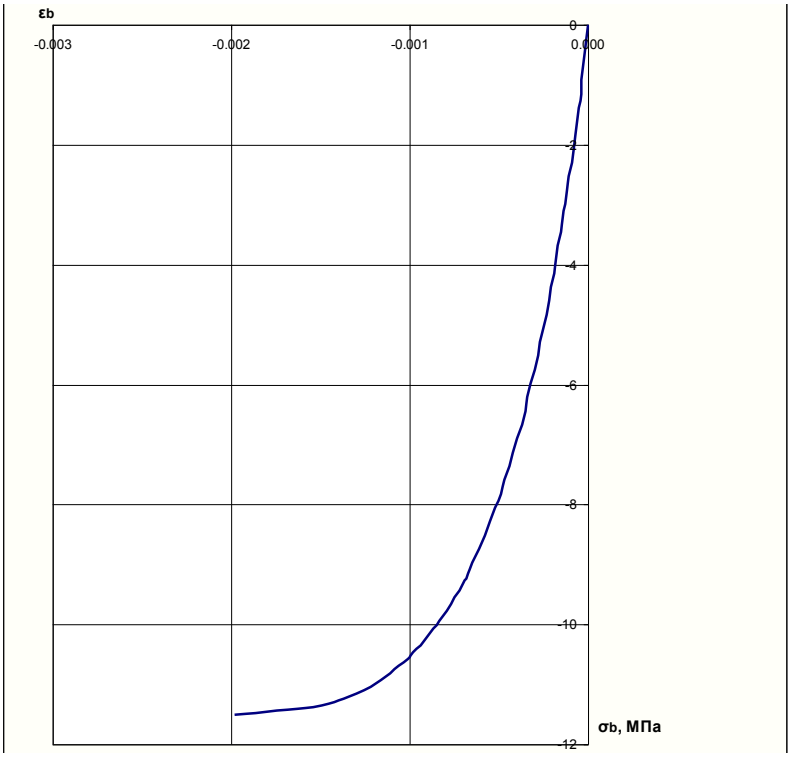


Figure 8. Concrete deformation diagram for strength calculation.

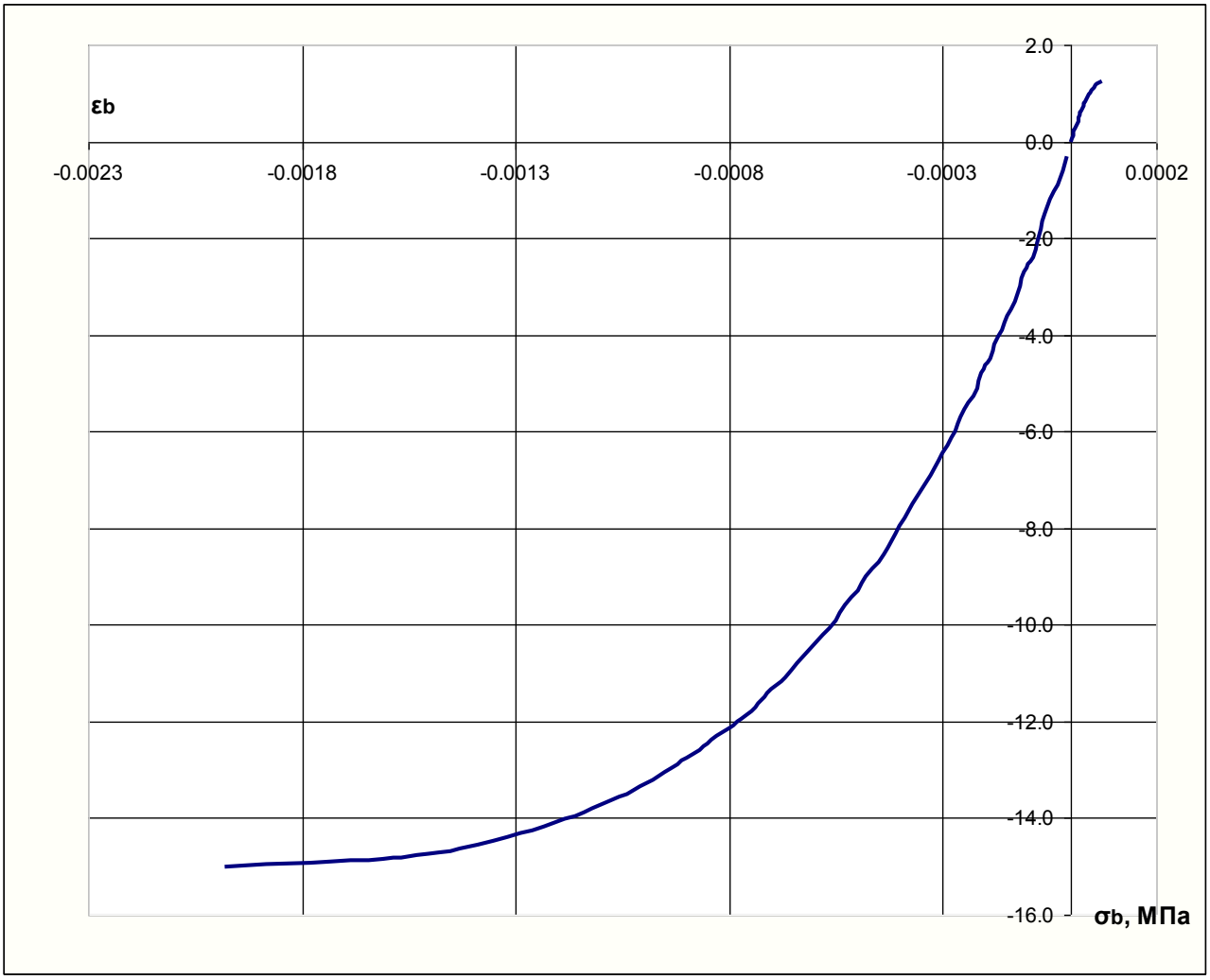


Figure 9. The diagram of the deformation of concrete for the calculation of the second group of limit states.

The results of calculating the strength and fracture toughness are given in Tables 5 and 6.

The minimum cross-section of the structure was previously taken at 100 × 200 (h) mm. In the calculation, we consider the work of only the fly-through part of the pergola. The calculation is carried out according to the procedure [20] on the basis of the nonlinear deformation model of concrete (Figures 6-9), and also taking the proportional dependence of the deformation of the reinforcing material.

The limiting moment, perceived by the cross section, is M_{ult} = 1,41 · 10^6 Nmm = 1,41 kNm. The relative error in the calculations was 7%. The crack resistance moment M_{crc} = 1.08 · 10^6 Nmm = 1.08 kNm (calculated with a relative error of 2%). The limiting load, perceived by the cross section M_{crc} = 1.08 kNm> M = 0.83 kNm. Tables 5 and 6 show the results of calculating the strength and crack resistance of the normal section: strength and crack resistance are provided.

Based on the results of calculating the structural strength of one element of a triangular shaped canopy of “sonic” pergola, the following textile-concrete construction is proposed to provide the required strength (Table 7).

Table 5. Results of calculating the strength of a normal section.

Section number	Plottage, mm^2	Coordinate Z_b, мм	Coordinate Z_f, мм	ε_i	$E_{b,i}$, МПа	σ_{bi}, МПа	$E_{f,i}$, МПа	σ_{fi}, МПа	$1/\rho$, $мм^{-1}$	$\varepsilon_{b,ult}$	Z0, мм	$\sigma_{i \cdot Ai}$	$\sigma_{i \cdot Ai} \cdot Z_i$
1	2	3	4	5	6	7	8	9	10	11	12	13	14
1	275	-9.625		-0.00198	5808.1	-11.500						-3163	30439
2	275	-6.875		-0.00057	14929.8	-8.510						-2340	16089
3	275	-4.125		-0.00034	18264.7	-6.210						-1708	7044
4	275	-1.375		-0.00011	23000	-2.530						-696	957
5	1100	5..5		0.00046	0	0.000						0	0
6	1100	16.5		0.00137	0	0.000						0	0
7	1100	27.5		0.00228	0	0.000						0	0
8	1200	39.5		0.00328	0	0.000						0	0
9	1200	51.5		0.00428	0	0.000			8.30E-05	0.00198	11.0	0	0
10	1200	63.5		0.00527	0	0.000						0	0
11	1200	75.5		0.00627	0	0.000						0	0
12	1200	87.5		0.00727	0	0.000						0	0
13	1200	99.5		0.00826	0	0.000						0	0
14	1200	111.5		0.00926	0	0.000						0	0
15	1200	123.5		0.01026	0	0.000						0	0
16	1200	135.5		0.01125	0	0.000						0	0
17	1200	147.5		0.01225	0	0.000						0	0
18	1200	159.5		0.01325	0	0.000						0	0
19	1200	171.5		0.01424	0	0.000						0	0
20	1200	183.5		0.01524	0	0.000						0	0
21	7.07		185.5	0.01438			72000.000	1035.71				7323	1358324
											Σ=	-584	1412853

Table 6. Results of calculation of fracture toughness of normal section.

Section number	Plot-tage, mm^2	Coordinate Z_b, мм	Coordinate Z_f, мм	ε_i	$E_{b,i}$, МПа	σ_{bi}, МПа	$E_{f,i}$, МПа	σ_{fi}, МПа	$1/\rho$, $мм^{-1}$	$\varepsilon_{bt,ult}$	Z0, мм	$\sigma_{i \cdot Ai}$	$\sigma_{i \cdot Ai \cdot Zi}$
1	1000	-90.5		-0.00006	26217	-1.573						-1573	142357
2	1000	-80.5		-0.00006	26217	-1.573						-1573	126627
3	1000	-70.5		-0.00005	26480	-1.324						-1324	93342
4	1000	-60.5		-0.00004	26775	-1.071						-1071	64796
5	1000	-50.5		-0.00003	27067	-0.812						-812	41006
6	1000	-40.5		-0.00003	27067	-0.812						-812	32886
7	1000	-30.5		-0.00002	27350	-0.547						-547	16684
8	1000	-20.5		-0.00001	27500	-0.276						-276	5658
9	1000	-10.5		-0.00001	27500	-0.276			6,89E-07	0,000007		-276	2898
10	100	-0.5		0	-	0.000						0	0
11	1900	9.5		0.00001	26900	0.269						511	4855
12	1000	19.5		0.00001	26900	0.269						269	5246
13	1000	29.5		0.00002	26000	0.520						520	15340
14	1000	39.5		0.00003	24867	0.746						746	29467
15	1000	49.5		0.00003	24867	0.746						746	36927
16	1000	59.5		0.00004	23575	0.943						943	56109
17	1000	69.5		0.00005	22080	1.104						1104	76728
18	1000	79.5		0.00005	22080	1.104						1104	87768
19	1000	89.5		0.00006	20383	1.223						1223	109459
20	1000	99.5		0.00007	18486	1.294						1294	128753
21	7.07		101.5	0.00007			72000.000	5.04				36	3617
											Σ=	232	1080523

The minimum cross-section of the structure was previously taken at 100 × 200 (h) mm. In the calculation, we consider the work of only the fly-through part of the pergola. The calculation is carried out according to the procedure [20] on the basis of the nonlinear deformation

model of concrete (Figures 6 - 9), and also taking the proportional dependence of the deformation of the reinforcing material.
The limiting moment, perceived by the cross section, is M_{ult} = 1,41 · 10^6 Nmm = 1,41 kNm. The relative error in the calculations was 7%. The crack resistance moment M_{crc} = 1.08 · 10^6 Nmm = 1.08 kNm (calculated with a relative error of 2%). The limiting load, perceived by the cross section M_{crc} = 1.08 kNm> M = 0.83 kNm. Tables 5 and 6 show the results of calculating the strength and crack resistance of the normal section: strength and crack resistance are provided.
Based on the results of calculating the structural strength of one element of a triangular shaped canopy of "sonic" pergola, the following textile-concrete construction is proposed to provide the required strength (Table 7).

Table 7. Textile-concrete construction.

Denomination	Parameter	Number of layers	Thickness of layer, mm
Fine grained concrete	Table 2	7	40
Textile matrix	AR-glass, 120 g/m², 2D	6	1

CONCLUSIONS

The proposed composition of high-performance textile-concrete and its construction can provide the necessary strength of the entire canopy of "sound" pergola and safety of operation. Composite materials with a set of different properties have become the main building materials of the 21st century, which allows to expand the possibilities of modern architecture and open new boundaries of excellence. In this connection, the use of textiles-concrete in modern architecture as the main material for creating complex spatial forms is seen as particularly interesting.
The presented architectural concepts are the result of the first stage of the systemic study of the influence of one of the geofactors on a human within the framework of an architectural geonics, assuming the transdisciplinarity of the study. This stage formulates the problem of the need for mathematical calculations of geometric characteristics of the main sound translators – tubes. The formulation of this problem is reduced to the definition of the following:

- the length of the tube;
- diameter of the internal cavity;
- the size of the end of the tube;
- selection of pipe material with different sound reflectance;
- the effect of the wall thickness of the tube in the case of using the methods of creating wind musical instruments to extract sound harmonic oscillations in conditions of spontaneity of wind force and direction.

At the decision of this task the sound background will be controlled and therefore – directed. Calculations of “correcting” natural spontaneity will help create an alternative that mimics the sound frequencies of music, in the range of which a positive effect on a person occurs.

REFERENCES

1. **Lesovik V.S.** Arkhitekturnaya Geonika [Architectural Geonics]. // Zhilishchnoe stroitel'stvo, 2013, No. 1, pp. 9-12.
2. **Lesovik V.S.** Arkhitekturnaya Geonika. Vzglyad v budushchee [Architectural Geonics. Prospection]. // Vestnik VGASU. Seriya: Stroitel'stvo i arkhitektura, 2013, No. 31-1(50), pp. 131-136.
3. **Pershina I.L.** Arkhitekturnaya Geonika i Sreda Obitaniya Cheloveka [Architectural Geonics and Human Habitat]. // Inno-

vatsiyni tekhnologiï v arkhitekturi i dizayni. Kharkivs'kiy natsional'niy universitet budivnitstva ta arkhitekturi, 2017, pp. pp.150-156.

4. **Lesovik V.S., Pershina I.L.** Opredelenie Spetsifichnosti Prostranstva v Arkhitekturnoy Geonike [Defining the Specificity of Space in Architectural Geonics]. // Aktual'nye voprosy arkhitektury i stroitel'stva: materialy Pyatnadtsatoy Mezhdunar. nauch.-tekhn. konf., Saransk 26-28 December 2016, Saransk: Izd-vo Mordov. un-ta, 2017, pp. 196-201.
5. **Pershina I.L.** Spetsificheskaya Sreda Geoniki – Vid Sredovogo Proektirovaniya v Arkhitekture [Specific Environment of Geonics – Type of Environmental Design in Architecture]. // Mezhdunarodnye akademicheskie chteniya RAACS “Bezopasnost' stroitel'nogo fonda Rossii. Problemy i resheniya”, 29-30 November 2017, Kursk, KGU, pp. 220-225.
6. **Lesovik V.S., Pershina I.L.** Transdistsiplinarnost' Arkhitekturnoy Geoniki kak Opredelyayushchiy Faktor ee Sushchestvovaniya [Transdisciplinarity of Architectural Geonics as a Determining Factor of its Existence]. // Academia. Arkhitektura i stroitel'stvo, 2017, No. 4, pp. 107-110.
7. **Rappaport A.G.** Kontseptsii Arkhitekturnogo Prostranstva [Concepts of Architectural Space]. Moscow, TSNTI, 1988.
8. **Pershina I.L., Panchenko E.I.** Proektnye Predlozheniya Sozdaniya Zvukovogo Prostranstva kak Kompilyatora Spetsificheskoy Sredy [Project Proposals for Creating a Sound Space as a Compiler of a Specific Environment]. // Mezhdunarodnyy onlayn kongress “Fundamental'nye osnovy stroitel'nogo materialovedeniya”, Belgorod, BGTU im.V.G. Shukhova, 2017.
9. **Lesovik V.S. Pershina I.L.** Meditsinskiy Aaspekt Arkhitekturnoy Geoniki – Vliyanie Zvukov na Cheloveka [The Medical Aspect of Architectural Geonics as the Influence of Sounds on People]. // Vestnik fizioterapii i kurortologii, 2017, Vol. 23, No. 4, pp. 58-63.
10. **Pershina I.L.** O Transdistsiplinarnom Tandeme Meditsiny i Arkhitekturnoy Geoniki [About Transdisciplinary Tandem of Medicine and Architectural Geonics] // III Vserossiyskaya nauchnaya konferentsiya molodykh spetsialistov, aspirantov, ordinatorov “Innovatsionnye tekhnologii v meditsine: vzglyad molodogo spetsialista”. Sektsiya: Mediko-profilakticheskie nauki, FGBOU VO RyazGMU Minzdrava Rossii, Ryazan', OOP UITT i OP, 2017, pp. 68-70.
11. **Pershina I.L.** Ob Ispol'zovanii dostizheniy Sredovoy Psikhologii v Arkhitekturnoy Geonike [On the use of the Achievements of Environmental Psychology in Architectural Geonics]. // IX Mezhdunarodnyy forum “Obrazovanie. Nauka. Proizvodstvo”, 6-13 October 2017, Belgorod.
12. **Lesovik V.S., Popov D.Yu., Glagolev E.S.** Tekstil'-beton – Effektivnyy Armirovannyy Kompozit Budushchego [Textile-Concrete is Effective Reinforced Composite of the Future], // Stroitel'nye materialy, 2017, No. 3, pp. 81-84.
13. **Scherer S., Michler H., Curbach M.** Brücken aus Textilbeton. Handbuch Brücken: Entwerfen, Konstruieren, Berechnen, Bauen und Erhalten, 2014, pp. 118-129.
14. **Curbach M., Graf W., Jesse D., Sickert J. U., Weiland S.** Segmentbrücke aus Textil-Bewehrtem Beton – Konstruktion, Fertigung, Numerische Berechnung. // Beton- und Stahlbetonbau, 2007, No. 6(102), pp. 342-352.
15. **Hegger J., Goralksi C., Kulas C.** Schlanke Fußgängerbrücke aus Textilbeton – Sechs-feldrige Fußgängerbrücke mit einer Gesamtlänge von 97 m. // Beton- und Stahlbetonbau, 2011, No. 106, Heft 2, pp. 64-71.
16. **Scholzen A., Chudoba R., Hegger J.** Dünnwandiges Schalentragwerk aus textilbe-wehrtem Beton. Entwurf, Bemessung und baupraktische Umsetzung. // Beton-

und Stahlbetonbau, 2012, Heft 11, pp. 767-776.
17. **Zagorodnyuk L.Kh., Lesovik V.S., Glagolev E.S., Elistratkin M.Yu., Lashina I.V., Masanin O.O.** Ob"ektivnye Predposylki Perekhoda k Kompozitsionnym Vyazhushchim [Objective Prerequisites for the Transition to Composite Binders]. // "Naukoemkie tekhnologii i innovatsii", Sbornik dokladov Mezhdunarodnoy nauchno-prakticheskoy konferentsii, 2016, pp. 110-116.
18. **Lesovik V.S., Strokova V.V., Krivenkova A.N., Khodykin E.I.** Kompozitsionnoe Vyazhushchee s Ispol'zovaniem Kremnistykh Porod [Composite Binders with the Use of Siliceous Rocks]. // Vestnik Belgorodskogo gosudarstvennogo tekhnologicheskogo universiteta im. V.G. Shukhova, 2009, No. 1, pp. 25-27.
19. **Kharkhardin A.N.** Strukturnaya Topologiya Dispersnykh Naterialov [Structural Topology of Dispersed Materials]. Belgorod, Izd-vo BGTU, 2011.
20. SP 63.13330.2012 Betonnyye i zhelezobetonnyye konstruktsii. Osnovnyye polozheniya. Aktualizirovannaya redaktsiya SNiP 52-01-2003 [Concrete and reinforced concrete structures. Fundamentals. Updated version of SNiP 52-01-2003]. Moscow, Minregion Rossii, 2012.

REFERENCES

1. **Лесовик В.С.** Архитектурная геоника. // Жилищное строительство, 2013, №1, с. 9-12.
2. **Лесовик В.С.** Архитектурная геоника. Взгляд в будущее. // Вестник ВГАСУ. Серия: Строительство и архитектура, 2013, №31-1(50), с. 131-136.
3. **Першина И.Л.** Архитектурная геоника и среда обитания человека. // Інноваційні технології в архітектурі і дизайні. Харківський національний університет будівництва та архітектури, 2017, с. 150-156.
4. **Лесовик В.С., Першина И.Л.** Определение специфичности пространства в архитектурной геонике. // Актуальные вопросы архитектуры и строительства: материалы Пятнадцатой Междунар. науч.-техн. конф., г. Саранск, 26-28 дек. 2016 г. – Саранск: Изд-во Мордов. ун-та, 2017, с. 196-201.
5. **Першина И.Л.** Специфическая среда геоники – вид средового проектирования в архитектуре. // Международные академические чтения РААСН «Безопасность строительного фонда России. Проблемы и решения», 29-30 ноября 2017 г. – Курск, КГУ г. Курск, 2017, с. 220-225.
6. **Лесовик В.С., Першина И.Л.** Трансдисциплинарность архитектурной геоники как определяющий фактор её существования. // Academia. Архитектура и строительство, 2017, №4, с. 107-110.
7. **Раппапорт А.Г.** Концепции архитектурного пространства. – М.: ЦНТИ, 1988.
8. **Першина И.Л., Панченко Е.И.** Проектные предложения создания звукового пространства как компилятора специфической среды. // Международный онлайн-конгресс «Фундаментальные основы строительного материаловедения», БГТУ им. В.Г. Шухова, Белгород, 2017.
9. **Лесовик В.С. Першина И.Л.** Медицинский аспект архитектурной геоники – влияние звуков на человека. // Вестник физиотерапии и курортологии, 2017, том 23, №4, с. 58-63.
10. **Першина И.Л.** О трансдисциплинарном тандеме медицины и архитектурной геоники. // III Всероссийская научная конференция молодых специалистов, аспирантов, ординаторов «Инновационные технологии в медицине: взгляд молодого специалиста». Секция: Медико-профилактические науки, ФГБОУ ВО

РязГМУ Минздрава России. – Рязань: ООП УИТТ и ОП, 2017, с. 68-70.
11. **Першина И.Л.** Об использовании достижений средовой психологии в архитектурной геонике. // IX Международный форум «Образование. Наука. Производство», 6-13 октября 2017 г. Белгород.
12. **Лесовик В.С., Попов Д.Ю., Глаголев Е.С.** Текстиль-бетон – эффективный армированный композит будущего. // Строительные материалы, 2017, №3, с. 81-84.
13. **Scherer S., Michler H., Curbach M.** Brücken aus Textilbeton. Handbuch Brücken: Entwerfen, Konstruieren, Berechnen, Bauen und Erhalten, 2014, pp. 118-129.
14. **Curbach M., Graf W., Jesse D., Sickert J. U., Weiland S.** Segmentbrücke aus Textil-Bewehrtem Beton – Konstruktion, Fertigung, Numerische Berechnung. // Beton- und Stahlbetonbau, 2007, No. 6(102), pp. 342-352.
15. **Hegger J., Goralksi C., Kulas C.** Schlanke Fußgängerbrücke aus Textilbeton – Sechs-feldrige Fußgängerbrücke mit einer Gesamtlänge von 97 m. // Beton- und Stahlbetonbau, 2011, No. 106, Heft 2, pp. 64-71.
16. **Scholzen A., Chudoba R., Hegger J.** Dünnwandiges Schalentragwerk aus textilbe-wehrtem Beton. Entwurf, Bemessung und baupraktische Umsetzung. // Beton- und Stahlbetonbau, 2012, Heft 11, pp. 767-776.
17. **Загороднюк Л.Х., Лесовик В.С., Глаголев Е.С., Елистраткин М.Ю., Лашина И.В., Масанин О.О.** Объективные предпосылки перехода к композиционным вяжущим. // «Наукоемкие технологии и инновации». Сборник докладов Международной научно-практической конференции, 2016, с. 110-116.
18. **Лесовик В.С., Строкова В.В., Кривенкова А.Н., Ходыкин Е.И.** Композиционное вяжущее с использованием кремнистых пород. // Вестник Белгородского государственного технологического университета им. В.Г. Шухова, 2009, №1, с. 25-27.
19. **Хархардин А.Н.** Структурная топология дисперсных материалов. – Белгород: Изд-во БГТУ, 2011.
20. **СП 63.13330.2012** Бетонные и железобетонные конструкции. Основные положения. Актуализированная редакция СНиП 52-01-2003. – М.: Минрегион России, 2012.

Lesovik Valery Stanislavovich, Corresponding Member of the Russian Academy of Architecture and Construction Sciences, Full Professor, Dr of Sci. (Engineering)l; Head of the Department of Building Materials, Products and Structures; Belgorod Shukhov State Technological University; 308012, Russian Federation; Belgorod, Kostyukova Street, 46; phone: +7 (4722) 55-13-66,
E-mail: naukavs@mail.ru.

Pershina Irina Leonidovna, architect, postgraduate student; Department of Architecture and City Construction; Belgorod Shukhov State Technological University; 308012, Russian Federation; Belgorod, Kostyukova Street, 46; phone: +7 (915) 568-31-27,
E-mail: Irina.Pershina@mail.ru.

Popov Dmitry Yur'evich, engineer, postgraduate student; Department of Building Materials Science, Products and Structures, Belgorod Shukhov State Technological University; 308012, Russian Federation; Belgorod, Kostyukova Street, 46; phone: +7 (4722) 55-82-01,
E-mail: popov.dmitry412@yandex.ru.

Shevchenko Andrey Viktorovich, associate Professor, Ph.D (Engineering); Department of Urban Construction and economy, Belgorod Shukhov State Technological University; 308012, Russian Federation; Belgorod, Kostyukova Street, 46; phone: +7 (910) 225-35-85,
E-mail: andsheff@rambler.ru.

Лесовик Валерий Станиславович, член-корреспондент РААСН, профессор, доктор технических наук; заведующий кафедрой Строительного материаловедения, изделий и конструкций, Белгородский государственный технологический университет им. В.Г. Шухова; 308012, Российская Федерация, г. Белгород, ул. Костюкова, 46; тел. +7 (4722) 55-13-66, E-mail: naukavs@mail.ru.

Першина Ирина Леонидовна, архитектор, аспирант; кафедра Архитектуры и градостроительства, Белгородский государственный технологический университет им. В.Г. Шухова; 308012, Российская Федерация, г. Белгород, ул. Костюкова, 46; тел. +7 (915) 568-31-27, e-mail: rina.Pershina@mail.ru.

Попов Дмитрий Юрьевич, инженер, аспирант; кафедра Строительного материаловедения, изделий и конструкций, Белгородский государственный технологический университет им. В.Г. Шухова; 308012, Российская Федерация, г. Белгород, ул. Костюкова, 46; тел. +7 (4722) 55-82-01,
E-mail: popov.dmitry412@yandex.ru.

Шевченко Андрей Викторович, доцент, кандидат технических наук; кафедра Строительства и городского хозяйства, Белгородский государственный технологический университет им. В.Г. Шухова; 308012, Российская Федерация, г. Белгород, ул. Костюкова, 46; тел. +7 (910) 225-35-85,
E-mail: andsheff@rambler.ru.

DOI:10.22337/2587-9618-2018-14-3-83-102

ABOUT WAVELET-BASED MULTIGRID NUMERICAL METHOD OF STRUCTURAL ANALYSIS WITH THE USE OF DISCRETE HAAR BASIS

Marina L. Mozgaleva [1], Pavel A. Akimov [2, 3, 4, 5], Taymuraz B. Kaytukov [2, 6]

[1] National Research Moscow State University of Civil Engineering, Moscow, RUSSIA
[2] Russian Academy of Architecture and Construction Sciences, Moscow, RUSSIA
[3] Scientific Research Center "StaDyO", Moscow, RUSSIA
[4] Tomsk State University of Architecture and Building, Tomsk, RUSSIA
[5] Peoples' Friendship University of Russia, Moscow, RUSSIA
[6] Central Institute for Research and Design of the Ministry of Construction and Housing and Communal Services of the Russian Federation, Moscow, RUSSIA

Abstract: The distinctive paper is devoted to so-called multigrid (particularly two-grid) method of structural analysis based on discrete Haar basis (one-dimensional, two-dimensional and three-dimensional problems are under consideration). Approximations of the mesh functions in discrete Haar bases of zero and first levels are described (the mesh function is represented as the sum in which one term is its approximation of the first level, and the second term is so-called complement (up to the initial state) on the grid of the first level). Special projectors are constructed for the spaces of vector functions of the original grid to the space of their approximation on the first-level grid and its complement (the refinement component) to the initial state. Basic scheme of the two-grid method is presented. This method allows solution of boundary problems of structural mechanics with the use of matrix operators of significantly smaller dimension. It should be noted that discrete analogue of the initial operator equation is a system of linear algebraic equations which is constructed with the use of finite element method or finite difference method. Block Gauss method can be used for direct solution.

Keywords: structural analysis, wavelet analysis, numerical methods, multigrid methods, two-grid method, discrete Haar basis, reduction, local structural analysis, approximation, boundary problem

О ВЕЙВЛЕТ-РЕАЛИЗАЦИИ МНОГОСЕТОЧНОГО ЧИСЛЕННОГО МЕТОДА РАСЧЕТА КОНСТРУКЦИЙ НА ОСНОВЕ ДИСКРЕТНОГО БАЗИСА ХААРА

М.Л. Мозгалева [1], П.А. Акимов [2, 3, 4, 5], Т.Б. Кайтуков [2, 6]

[1] Национальный исследовательский Московский государственный строительный университет, г. Москва, РОССИЯ
[2] Российская академия архитектуры и строительных наук, г. Москва, РОССИЯ
[3] Научно-исследовательский центр СтаДиО, г. Москва, РОССИЯ
[4] Томский государственный архитектурно-строительный университет, г. Томск, РОССИЯ
[5] Российский университет дружбы народов, г. Москва, РОССИЯ
[6] Центральный научно-исследовательский и проектный институт Министерства строительства и жилищно-коммунального хозяйства, г. Москва, РОССИЯ

Аннотация: Настоящая статья посвящена так называемому многосеточному (в частности, двухсеточному) методу расчета строительных конструкций, основанному на использовании дискретного базиса Хаара (рассматриваются одномерные, двумерные и трехмерные задачи). Описана аппроксимации сеточных функций на нулевом и первом уровнях дискретного базиса Хаара (сеточная функция представляется в виде суммы, в которой первое слагаемое соответствует аппроксимации на первом уровне, а второе слагаемое представляет собой так называемую детализацию (дополнение до исходного состояния) на сетке первого уровня. Строятся специальные проекторы пространства векторных функций на исходной стеке на пространство их аппроксимаций на сетке первого уровня и детализацию (дополнение до исходного состояния). Изложена общая схема двухсеточного метода. Данный метод позволяет решать краевые за-

дачи строительной механики с использованием соответствующих матричных операторов существенно меньшей размерности. Следует отметить, что дискретным аналогом исходного операторного уравнения является система линейных алгебраических уравнений, формируемая с использованием техники метода конечных элементов или метода конечных разностей. Для прямого решения указанной системы может использоваться блочный метод Ланцоша.

Ключевые слова: расчеты строительных конструкций, вейвлет-анализ, численные методы, многосеточные методы, двухсеточный метод, дискретный базис Хаара, редукция, локальный расчет конструкций, аппроксимация, краевая задача

1. ONE-DIMENSIONAL PROBLEMS

1.1. About alternative discrete basis.

Let us consider the following functions:
– father wavelet (Figure 1),

$$\Phi(x)=\begin{cases}1, & 0\le x<1\\ 0, & x<0\vee x\ge 1;\end{cases} \qquad (1.1)$$

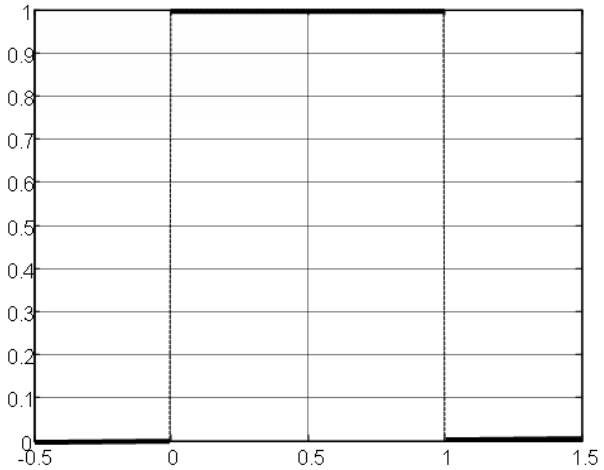


Figure 1. Father wavelet.

– the first mother wavelet (Figure 2),

$$\Psi_1(x)=\begin{cases}1, & 0\le x<1/3\\ -1, & 2/3\le x<1\\ 0, & x<0\vee 1/3\le x<2/3\vee x\ge 1;\end{cases} \qquad (1.2)$$

– the second mother wavelet (Figure 3) i.e. variant of French Hat,

$$\Psi_1(x)=\begin{cases}-1, & 0\le x<1/3\vee 2/3\le x<1\\ 2, & 1/3\le x<2/3\\ 0, & x<0\vee x\ge 1;\end{cases} \qquad (1.3)$$

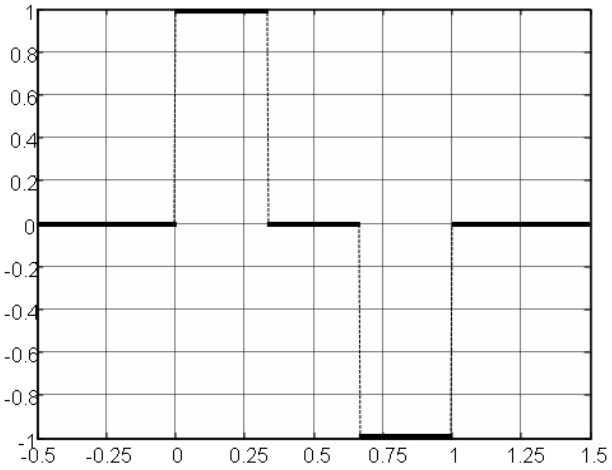


Figure 2. The first Mother wavelet.

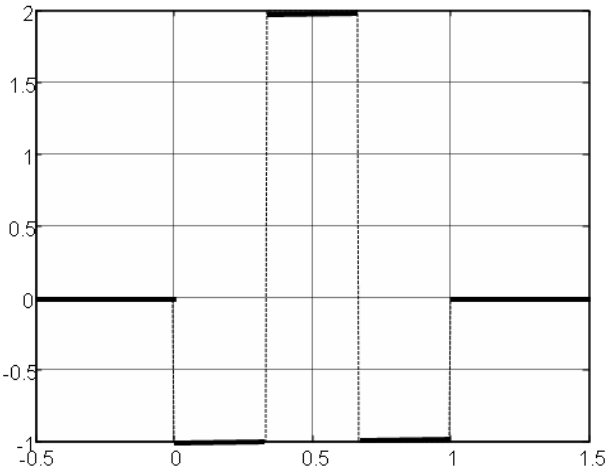


Figure 3. The second Mother wavelet.

Matrix of transition from one level to the next level has the same structure as in the Haar basis [1-25]

$$\begin{bmatrix} Q & & \\ & \ddots & \\ & & Q \end{bmatrix},$$

where for the Haar basis we have

$$Q = \frac{1}{\sqrt{2}}\begin{vmatrix} 1 & 1 \\ 1 & -1 \end{vmatrix}$$

and for considering basis we have

$$Q = \begin{bmatrix} 1 & 1 & -1 \\ 1 & 0 & 2 \\ 1 & -1 & -1 \end{bmatrix} \begin{bmatrix} 1/\sqrt{3} & & \\ & 1/\sqrt{2} & \\ & & 1/\sqrt{6} \end{bmatrix}. \quad (1.4)$$

Let us denote a family of discrete functions:

$$\{\overline{\psi}_j^p\},\ j = 1,2,\ldots,N_p,\quad p = 1,\ldots,M,$$

where M is the number of levels; $N = 3^M$ is space dimension,

$$\underline{1 \le p < M}:\quad \overline{\psi}_j^p = [\overline{\psi}_{1,j}^p \quad \overline{\psi}_{2,j}^p], \quad (1.5)$$

$$\psi_{1,j}^p(i) = \alpha_{1,p}\Psi_1\left(\frac{i-0.5}{3^p} - (j-1)\right); \quad (1.6)$$

$$\psi_{2,j}^p(i) = \alpha_{2,p}\Psi_2\left(\frac{i-0.5}{3^p} - (j-1)\right); \quad (1.7)$$

$$\underline{p = M}:\quad \overline{\psi}_1^M = [\overline{\psi}_{1,1}^M \quad \overline{\psi}_{2,1}^M \quad \overline{\phi}_{2,1}^M]; \quad (1.8)$$

$$\phi_1^M(i) = \alpha_M\Phi\left(\frac{i-0.5}{3^M}\right); \quad (1.9)$$

$N_p = N/3^p$ is the number of $\psi_{1,j}^p$ and $\psi_{2,j}^p$ at level number p;

$$\alpha_p = \frac{1}{\sqrt{3^p}};\quad \alpha_{1,p} = \frac{1}{\sqrt{2^p}};\quad \alpha_{2,p} = \frac{1}{\sqrt{6^p}} \quad (1.10)$$

are normalizing factors.
Because $1/3$ has no finite exact value, the expression

$$\frac{i-0.5}{3^p}$$

is used to evaluate correctly instead of

$$\frac{i-1}{3^p}.$$

The set $\{\overline{\psi}_j^p\}$ presented in this way is a basis in the N-dimensional vector space. Moreover, this basis will be orthonormal.
Let's consider a given vector

$$\bar{u} \in R^N,\quad \bar{u} = \{u_i\}_{1\le i\le N}.$$

We present its decomposition in the Haar basis

$$\bar{u} = \sum_{p=1}^{M}\left(\sum_{j=1}^{N_p}(v_j^p\overline{\psi 1}_j^p + w_j^p\overline{\psi 2}_j^p\right) + u_1^M\bar{\phi}_1^M, \quad (1.11)$$

where we have

$$v_j^p = (\overline{\psi}_{1,j}^p,\ \bar{u});\quad w_j^p = (\overline{\psi}_{2,j}^p,\ \bar{u});$$
$$u_1^M = (\bar{\phi}_1^M,\ \bar{u}),\quad j = 1,2,\ldots,N_p,\quad p = 1,\ldots,M. \quad (1.12)$$

1.2. Determination of averaging coefficients.
Let us consider an example of a grid partition for $N = 9 = 3^2$, i.e. $M = 2$. Then the location of nodes by levels can be represented as shown in Figure 4. The formation of the decomposition coefficients at the first level is carried out according to the following formulas:

$$k = 1,2,3$$

$$u_k^1 = \frac{1}{\sqrt{3}}(u_{3k-2}^0 + u_{3k-1}^0 + u_{3k}^0) = \sqrt{3}\tilde{u}_k^0; \quad (1.13)$$

$$\tilde{u}_k^0 = \frac{1}{3}(u_{3k-2}^0 + u_{3k-1}^0 + u_{3k}^0); \quad (1.14)$$

$$v_k^1 = \frac{1}{\sqrt{2}}(u_{3k-2}^0 - u_{3k}^0) = -\frac{1}{\sqrt{2}}2h\frac{u_{3k}^0 - u_{3k-2}^0}{2h} = -\sqrt{2}h(D_0u^0)_{3k-1}; \quad (1.15)$$

$$w_k^1 = \frac{1}{\sqrt{6}}(-u_{3k-2}^0 + 2u_{3k-1}^0 - u_{3k}^0) = -\frac{1}{\sqrt{6}}h^2\frac{u_{3k-2}^0 - 2u_{3k-1}^0 + u_{3k}^0}{h^2}) = -\frac{h^2}{\sqrt{6}}(D^2u^0)_{3k-1}. \quad (1.16)$$

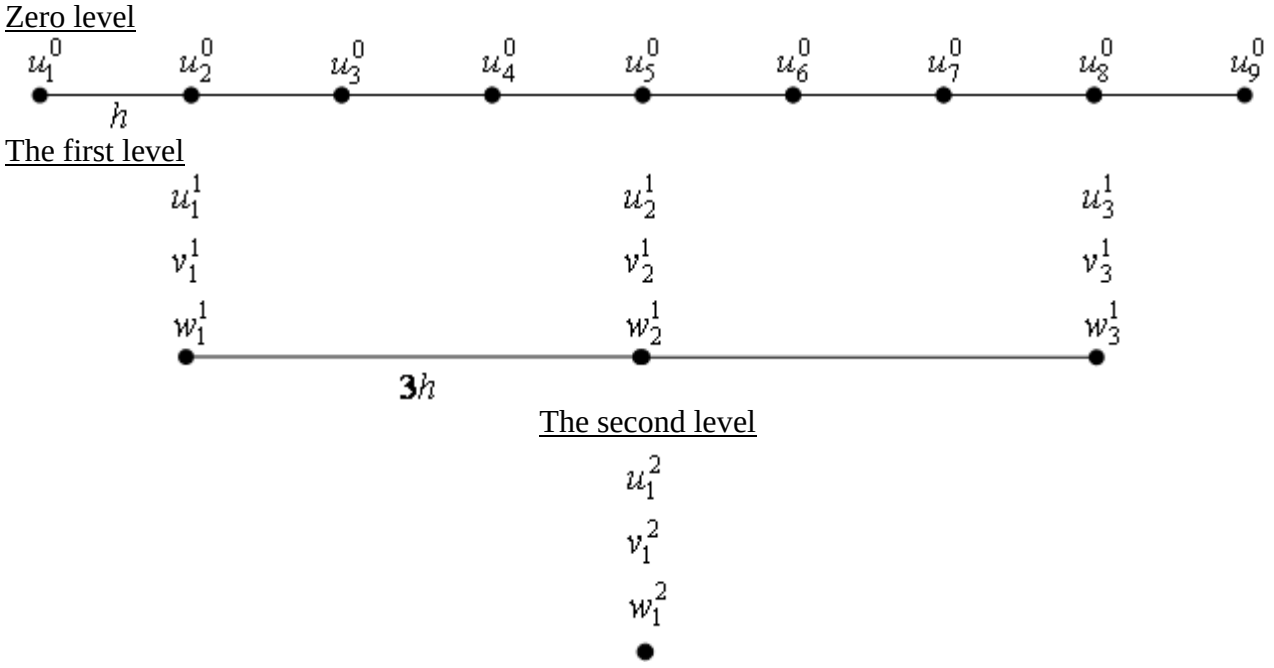


Figure 4. About determination of averaging coefficients.

The formation of the decomposition coefficients at the second level is carried out according to the following formulas:

$$u_k^2 = \frac{1}{\sqrt{3}}(u_1^1 + u_2^1 + u_3^1); \qquad (1.17)$$

$$\begin{aligned} v_1^2 &= \frac{1}{\sqrt{2}}(u_1^1 - u_3^1) = -\frac{1}{\sqrt{2}} 6h \frac{u_3^1 - u_1^1}{6h} = \\ &= -\frac{\sqrt{3}}{\sqrt{2}} 6h \frac{\tilde{u}_3^0 - \tilde{u}_1^0}{6h} = -\frac{\sqrt{3}}{\sqrt{2}} 6h (D_0 \tilde{u}^0)_2; \end{aligned} \qquad (1.18)$$

$$\begin{aligned} w_1^1 &= \frac{1}{\sqrt{6}}(-u_1^1 + 2u_2^1 - u_3^1) = \\ &= -\frac{1}{\sqrt{6}}(3h)^2 \frac{u_1^1 - 2u_2^1 + u_3^1}{(3h)^2}) = \\ &= -\frac{\sqrt{3}}{\sqrt{6}}(3h)^2 \frac{\tilde{u}_1^0 - 2\tilde{u}_2^0 + \tilde{u}_3^0}{(3h)^2}) = \\ &= -\frac{(3h)^2}{\sqrt{2}}(D^2 \tilde{u}^0)_2. \end{aligned} \qquad (1.19)$$

For averaging (reduction) we assume

$$\begin{aligned} (D_0 u^0)_{3k-1} &= (D_0 \tilde{u}^0)_2, \\ (D^2 u^0)_{3k-1} &= (D^2 \tilde{u}^0)_2, \quad k = 1,2,3. \end{aligned} \qquad (1.20)$$

The following dependencies can be noted

$$\begin{cases} (D_0 u^0)_{3k-1} = -\dfrac{1}{\sqrt{2}h} v_k^1 \\ (D^2 u^0)_{3k-1} = -\dfrac{\sqrt{6}}{h^2} w_k^1; \end{cases} \qquad (1.21)$$

$$\begin{cases} (D_0 \tilde{u}^0)_2 = -\dfrac{\sqrt{2}}{\sqrt{3} \cdot 6h} v_1^2 \\ (D^2 \tilde{u}^0)_2 = -\dfrac{\sqrt{2}}{(3h)^2} w_1^2; \end{cases} \qquad (1.22)$$

and then we have

$$\begin{cases} v_k^1 = \dfrac{1}{3\sqrt{3}} v_1^2 \\ w_k^1 = \dfrac{1}{3^2\sqrt{3}} w_1^2, \end{cases} \quad k = 1,2,3. \qquad (1.23)$$

1.3. The final formulas.

Let the initial one-dimensional domain be given as interval with length L. We can use simple mesh (grid) for approximation of domain and divide interval (the initial domain) into $(N-1)$ equal parts. We can represent the mesh vector function $\bar{u} = [u_1 \ \ldots \ u_N]^T$ in the form

$$\bar{u} = \sum_{j=1}^{N_0} u_j^0 \bar{\Phi}_j^0 , \qquad (1.24)$$

where we have

$$N_0 = N = 3^M ; \qquad (1.25)$$

$$u_j^0 = u_j , \quad 1 \le j \le N ; \qquad (1.26)$$

$$\bar{\Phi}_j^0(i) = \begin{cases} 1, & i = j \\ 0, & i \ne j \end{cases} \qquad (1.27)$$

– j-th vector of unit basis of level 0,

$$1 \le j \le N_0 = N , \quad 1 \le i \le N .$$

At the same time, this grid function can be represented in the basis of the first level as

$$\bar{u} = \sum_{j=1}^{N_1} u_j^1 \bar{\Phi}_j^1 + \sum_{j=1}^{N_1} v_j^1 \bar{\Psi}_{1,j}^1 + \sum_{j=1}^{N_1} w_j^1 \bar{\Psi}_{2,j}^1 , \quad (1.28)$$

where we have

$$N_1 = N / 3 ;$$

$$u_j^1 = (\bar{u}, \bar{\Phi}_j^1) ; \quad v_j^1 = (\bar{u}, \overline{\Psi 1}_j^1) ;$$

$$w_j^1 = (\bar{u}, \bar{\Psi}_{2,j}^1) , \quad 1 \le j \le N_1 , \quad (1.29)$$

$$\bar{u}^1 = [u_1^1 \dots u_{N_1}^1]^{\mathrm{T}} , \quad \bar{v}^1 = [v_1^1 \dots v_{N_1}^1]^{\mathrm{T}} ,$$

$$\bar{w}^1 = [w_1^1 \dots w_{N_1}^1]^{\mathrm{T}} . \quad (1.30)$$

$$\bar{\Phi}_j^1 = \alpha(\bar{\Phi}_{3j-2}^0 + \bar{\Phi}_{3j-1}^0 + \bar{\Phi}_{3j}^0) \qquad (1.31)$$

is the j-th approximation vector of discrete wavelet basis of the first level, $1 \le j \le N_1$;

$$\bar{\Psi}_{1,j}^1 = \alpha_1(\bar{\Phi}_{3j-2}^0 - \bar{\Phi}_{3j}^0) \qquad (1.32)$$

is the j-th refinement vector of discrete wavelet basis of the first level, $1 \le j \le N_1$;

$$\bar{\Psi}_{2,j}^1 = \alpha_2(-\bar{\Phi}_{3j-2}^0 + 2\bar{\Phi}_{3j-1}^0 - \bar{\Phi}_{3j}^0) \quad (1.33)$$

is the j-th refinement vector of discrete wavelet basis of the first level, $1 \le j \le N_1$;

$$\begin{cases} \alpha = 1/\sqrt{3} \\ \alpha_1 = 1/\sqrt{2} \\ \alpha_2 = 1/\sqrt{6} \end{cases} \qquad (1.34)$$

are normalizing factors.

Based on the representation of (1.28), the mesh function is represented as a sum, where the first term is its approximation on the mesh (grid) of the first level, consisting of N_1 nodes, and the second and third terms are called refinement (addition to the initial state) on the mesh (grid) of the first level.

The representation (1.28) can be written as

$$\bar{u} = \bar{u}_1^0 + \bar{v}_1^0 + \bar{w}_1^0 ; \qquad (1.35)$$

$$\bar{u}_1^0 = \sum_{j=1}^{N_1} u_j^1 \bar{\Phi}_j^1 = \Phi_1 \Phi_1^T \bar{u} = \Phi_1 \bar{u}^1 ; \qquad (1.36)$$

$$\bar{v}_1^0 = \sum_{j=1}^{N_1} v_j^1 \bar{\Psi}_{1,j}^1 = \Psi_{1,1} \Psi_{1,1}^T \bar{u} = \Psi_{1,1} \bar{v}^1 ; \quad (1.37)$$

$$\bar{w}_1^0 = \sum_{j=1}^{N_1} w_j^1 \bar{\Psi}_{2,j}^1 = \Psi_{2,1} \Psi_{2,1}^T \bar{u} = \Psi_{2,1} \bar{w}^1 , \quad (1.38)$$

where we have

$$\Phi_1 = [\, \bar{\Phi}_1^1 \ \dots \ \bar{\Phi}_{N_1}^1 \,] ; \qquad (1.39)$$

$$\Psi_{1,1} = [\bar{\Psi}_{1,1}^1 \ \dots \ \bar{\Psi}_{1,N_1}^1] ; \qquad (1.40)$$

$$\Psi_{2,1} = [\bar{\Psi}_{2,1}^1 \ \dots \ \bar{\Psi}_{2,N_1}^1] \qquad (1.41)$$

matrices of size $N \times N_1$, the columns of which are respectively approximation and refinement vectors of the discrete basis of the first level.

Due to the orthonormality of the Haar basis [1-7,9-25], the operators

$$P_\Phi = \Phi_1 \Phi_1^T , \quad P_{\Psi,1} = \Psi_{1,1} \Psi_{1,1}^T , \quad P_{\Psi,2} = \Psi_{2,1} \Psi_{2,1}^T \qquad (1.42)$$

are projectors of the space of vector functions of the original mesh (grid) to the space of their approximation on the first-level grid and its complement (the refining component) to the initial state, respectively.
spectively.

1.4. Basic scheme of the two-grid method.
Let systems of linear algebraic equations

$$A\bar{u} = \bar{f} \tag{1.43}$$

are discrete analogs of some operator equation defined on a given interval of order N.
We can substitute in (1.43) the expression for $\bar{u}$ in the form (1.35). Then we can multiply, in turn, both sides of the equality on the left by the matrices Φ_1^T and $\Psi_{1,1}^T, \Psi_{2,1}^T$. Thus we have

$$\begin{aligned}
&\Phi_1^T A\Phi_1\bar{u}^1 + \Phi_1^T A\Psi_{1,1}\bar{v}^1 + \\
&\qquad + \Phi_1^T A\Psi_{2,1}\bar{w}^1 = \Phi_1^T\bar{f} \\
&\Psi_{1,1}^T A\Phi_1\bar{u}^1 + \Psi_{1,1}^T A\Psi_{1,1}\bar{v}^1 + \\
&\qquad + \Psi_{1,1}^T A\Psi_{2,1}\bar{w}^1 = \Psi_{1,1}^T\bar{f} \\
&\Psi_{2,1}^T A\Phi_1\bar{u}^1 + \Psi_{2,1}^T A\Psi_{1,1}\bar{v}^1 + \\
&\qquad + \Psi_{2,1}^T A\Psi_{2,1}\bar{w}^1 = \Psi_{2,1}^T\bar{f};
\end{aligned} \tag{1.44}$$

or

$$\begin{aligned}
&A_{1,1}\bar{u}^1 + A_{1,2}\bar{v}^1 + A_{1,3}\bar{w}^1 = \bar{f}_u \\
&A_{2,1}\bar{u}^1 + A_{2,2}\bar{v}^1 + A_{2,3}\bar{w}^1 = \bar{f}_v \\
&A_{3,1}\bar{u}^1 + A_{3,2}\bar{v}^1 + A_{3,3}\bar{w}^1 = \bar{f}_w,
\end{aligned} \tag{1.45}$$

where we have

$$A_{1,1} = \Phi_1^T A\Phi_1; \quad A_{1,2} = \Phi_1^T A\Psi_{1,1}; \tag{1.46}$$

$$A_{1,3} = \Phi_1^T A\Psi_{2,1}; \quad A_{2,1} = \Psi_{1,1}^T A\Phi_1; \tag{1.47}$$

$$A_{2,2} = \Psi_{1,1}^T A\Psi_{1,1}; \quad A_{2,3} = \Psi_{1,1}^T A\Psi_{2,1}; \tag{1.48}$$

$$A_{3,1} = \Psi_{2,1}^T A\Phi_1; \quad A_{3,2} = \Psi_{2,1}^T A\Psi_{1,1}; \tag{1.49}$$

$$A_{3,3} = \Psi_{2,1}^T A\Psi_{2,1} \tag{1.50}$$

are block matrices of size $N_1 \times N_1$.

$$\bar{f}_u = \Phi_1^T\bar{f}; \quad \bar{f}_v = \Psi_{1,1}^T\bar{f}; \quad \bar{f}_w = \Psi_{2,1}^T\bar{f} \tag{1.51}$$

are right-side vectors of length N_1.
We can find the solution of the system (1.45) using the block Gaussian method.
The expanded block matrix has the form:

$$\left[\begin{array}{ccc|c} A_{1,1} & A_{1,2} & A_{1,3} & \bar{f}_u \\ A_{2,1} & A_{2,2} & A_{2,3} & \bar{f}_v \\ A_{3,1} & A_{3,2} & A_{3,3} & \bar{f}_w \end{array}\right]. \tag{1.52}$$

We have the following result of forward algorithm:
– the first step

$$\left[\begin{array}{ccc|c} A_{11} & A_{12} & A_{13} & \bar{f}_u \\ 0 & A_{22}^1 & A_{23}^1 & \bar{f}_v^1 \\ 0 & A_{32}^1 & A_{33}^1 & \bar{f}_w^1 \end{array}\right], \tag{1.53}$$

where we have

$$A_{2,2}^1 = A_{2,2} - C_{2,1}A_{1,2}; \quad A_{2,3}^1 = A_{2,3} - C_{2,1}A_{1,3}; \tag{1.54}$$

$$\bar{f}_v^1 = \bar{f}_v - C_{2,1}\bar{f}_u; \quad C_{2,1} = A_{2,1}A_{1,1}^{-1}; \tag{1.55}$$

$$A_{3,2}^1 = A_{3,2} - C_{3,1}A_{1,2}; \quad A_{3,3}^1 = A_{3,3} - C_{3,1}A_{1,3}; \tag{1.56}$$

$$\bar{f}_w^1 = \bar{f}_w - C_{3,1}\bar{f}_u, \quad C_{3,1} = A_{3,1}A_{1,1}^{-1}. \tag{1.57}$$

– the second step

$$\left[\begin{array}{ccc|c} A_{1,1} & A_{1,2} & A_{1,3} & \bar{f}_u \\ 0 & A_{2,2}^1 & A_{2,3}^1 & \bar{f}_v^1 \\ 0 & 0 & A_{3,3}^2 & \bar{f}_w^2 \end{array}\right], \tag{1.58}$$

where we have

$$A_{3,3}^2 = A_{3,3}^1 - C_{3,2}A_{2,3}^2; \tag{1.59}$$

$$\bar{f}_w^2 = \bar{f}_w^1 - C_{3,2}\bar{f}_v^1, \quad C_{3,2} = A_{3,2}^1(A_{2,2}^1)^{-1}. \tag{1.60}$$

We have the following result of backward algorithm

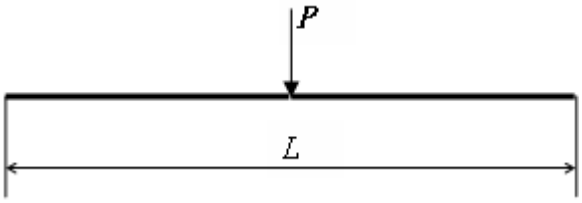


Figure 5. To the formulation of the boundary problem.

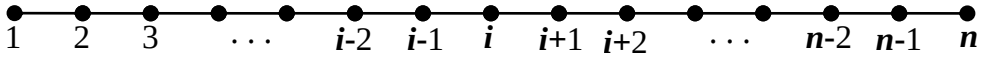


Figure 6. Discrete approximation of the domain.

$$\begin{aligned}\bar{w}^1 &= (A^2_{3,3})^{-1}\,\bar{f}^2_w \\ \bar{v}^1 &= (A^1_{2,2})^{-1}(\bar{f}^1_v - A^1_{2,3}\bar{v}^1) \\ \bar{u}^1 &= A^{-1}_{1,1}(\bar{f}_u - A_{1,2}\bar{v}^1 - A_{1,3}\bar{w}^1).\end{aligned} \qquad (1.61)$$

In accordance with formulas (1.35)-(1.38) solution of the considering problem (1.43) has the form

$$\bar{u} = \Phi_1\bar{u}^1 + \Psi_{1,1}\bar{v}^1 + \Psi_{2,1}\bar{w}^1. \qquad (1.62)$$

It should be noted that the proposed method makes it possible to obtain a solution with the use of matrices of size $N_1 = N/3$ and vectors of size $N_1 = N/3$.

1.5. Numerical sample.

Let us consider (as a model example) the numerical solution of the boundary problem of the bending of a beam on an elastic foundation with the following parameters: L=8 m is the length of the beam; h=1.3 m is the height of the cross section of the beam; b=1 m is the width of the cross section of the beam; $E = 2560\cdot10^4$ kN/m^2 is the modulus of elasticity; $P = 100$ kN is the load set at the middle point, $P_h = 100/h_b$; $k = 75\cdot10^3$ kN/m^3 is the coefficient characterizing the resistance of the foundation in the model of Winkler; $\bar{k} = k\cdot b$, $J = bh^3/12$ (Figure 5).

The definition of the deflection of the Bernoulli beam is reduced to the solution of the following boundary problem:

$$y^{(4)}(x) + 4\alpha^4 y(x) = F(x), \quad 0 < x < L; \qquad (1.63)$$

$$\begin{cases} y(0) = y''(0) = 0 \\ y(L) = y''(L) = 0, \end{cases} \qquad (1.64)$$

where we have

$$4\alpha^4 = \frac{\bar{k}}{EJ}; \quad F = \frac{P}{EJ}\delta(x - \frac{L}{2}). \qquad (1.65)$$

Let us divide the interval $(0,\ L)$ into equal parts with step (Figure 6).

If n is the total number of points, it is obvious that

$$h_b = L/(n-1). \qquad (1.66)$$

Next, we move from the solution of the boundary problem (1.63)-(1.64) to the solution of the following system of difference equations:

$$\begin{aligned}
&i = 1: \quad y_1 = f_1 \\
&i = 2: \quad -2y_1 + (5 + 4h_b^4\alpha^4)y_2 - 4y_3 + y_4 = f_2 \\
&2 < i < n-1: \quad y_{i-2} - 4y_{i-1} + (6 + 4h_b^4\alpha^4)y_i - \\
&\qquad\qquad - 4y_{i+1} + y_{i+2} = f_i \\
&i = n-1: \quad y_{n-3} - 4y_{n-2} + (5 + 4h_b^4\alpha^4)y_{n-1} - \\
&\qquad\qquad - 2y_n = f_{n-1} \\
&i = n: \quad y_n = f_n,
\end{aligned} \qquad (1.67)$$

where we have

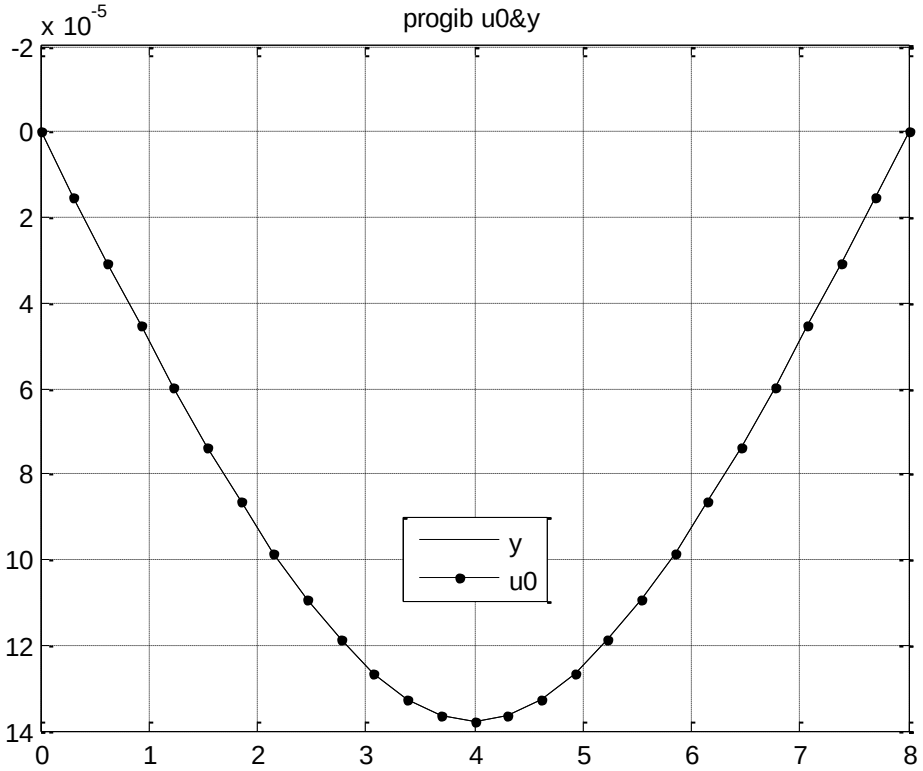


Figure 7. Comparison of results.

$$x_i = h_b(i-1); \quad y_i = y(x_i); \tag{1.68}$$

$$f_i = \begin{cases} 0, & i = 1 \\ h_b^4[F(x_i)/h_b], & 2 \le i \le n-1 \\ 0, & i = n. \end{cases} \tag{1.69}$$

In accordance with the results of analysis comparative graphs of deflections were obtained. Direct solution of the system (1.67) and solution defined by the formula (1.62) are presented at Figure 7. It should be noted that full match results obtained.

2. TWO-DIMENSIONAL PROBLEMS

2.1. General information.

Let the initial two-dimensional domain be given as a rectangle [8]. Let L_1 and L_2 be lengths of sides of this rectangle in directions corresponding to Cartesian coordinates x_1 and x_2. We can use simple rectangular mesh (grid) for approximation of domain and divide each side of the rectangle (the initial domain) into $(N-1)$ equal parts. The corresponding mesh (grid) width are defined by formulas

$$h_1 = L_1/(N-1); \quad h_2 = L_2/(N-1). \tag{2.1}$$

Thus, the resulting mesh contains N^2 nodes. Let us introduce the mesh function

$$\bar{u} = [u_{1,1} \ldots u_{1,N} \ldots u_{N,1} \ldots u_{N,N}]^T. \tag{2.2}$$

We can represent the mesh function (1.2) in the form

$$\bar{u} = \sum_{j_2=1}^{N_0} \sum_{j_1=1}^{N_0} u^0_{j_2,j_1} \bar{\Phi}^0_{j_2,j_1}, \tag{2.3}$$

where we have

$$N_0 = N; \tag{2.4}$$

$$u^0_{j_2,j_1} = u_{j_2,j_1}, \quad 1 \le j_1, j_2 \le N; \tag{2.5}$$

$$\overline{\Phi}^0_{j_2,j_1}(i_2,i_1)=\begin{cases}1, & i_1=j_1\wedge i_2=j_2\\ 0, & \neg(i_1=j_1\wedge i_2=j_2)\end{cases}$$
$$1\le j_2,j_1\le N_0=N,\ 1\le i_2,i_1\le N, \quad (2.6)$$

where $\overline{\Phi}^0_{j_2,j_1}$ is (j_2,j_1)-th vector of a unit basis or a discrete zero-level Haar basis

The mesh function (2) can also be represented in the form of an expansion in the Haar basis of the first level:

$$\bar{u}=\sum_{j_2=1}^{N_1}\sum_{j_1=1}^{N_1}u^1_{j_2,j_1}\overline{\Phi}^1_{j_2,j_1}+\sum_{j_2=1}^{N_1}\sum_{j_1=1}^{N_1}v^1_{1,j_2,j_1}\overline{\Psi}^1_{1,j_2,j_1}+ \\ +\sum_{j_2=1}^{N_1}\sum_{j_1=1}^{N_1}v^1_{2,j_2,j_1}\overline{\Psi}^1_{2,j_2,j_1}+\sum_{j_2=1}^{N_1}\sum_{j_1=1}^{N_1}v^1_{3,j_2,j_1}\overline{\Psi}^1_{3,j_2,j_1}, \quad (2.7)$$

where we have

$$N_1=N/2; \quad (2.8)$$
$$u^1_{j_2,j_1}=(\bar{u},\overline{\Phi}^1_{j_2,j_1}); \quad v^1_{1,j_2,j_1}=(\bar{u},\overline{\Psi}^1_{1,j_2,j_1}), \quad (2.9)$$
$$v^1_{2,j_2,j_1}=(\bar{u},\overline{\Psi}^1_{2,j_2,j_1}); \quad v^1_{3,j_2,j_1}=(\bar{u},\overline{\Psi}^1_{3,j_2,j_1}); \quad (2.10)$$
$$\bar{u}^1=[u^1_{1,1}\dots u^1_{1,N_1}\dots u^1_{N_1,1}\dots u^1_{N_1,N_1}]^T; \quad (2.11)$$
$$\bar{v}^1_k=[v^1_{k,1,1}\dots v^1_{k,1,N_1},\dots v^1_{k,N_1,1}\dots {}^1_{k,N_1,N_1}]^T,\ k=1,2,3; \quad (2.12)$$
$$\overline{\Phi}^1_{j_2,j_1}=\alpha(\overline{\Phi}^0_{2j_2-1,2j_1-1}+\overline{\Phi}^0_{2j_2-1,2j_1}+ \\ +\overline{\Phi}^0_{2j_2,2j_1-1}+\overline{\Phi}^0_{2j_2,2j_1}) \quad (2.13)$$

– (j_2,j_1)- th approximating vector of the discrete Haar basis of the first level, $1\le j_2,j_1\le N_1$;

$$\overline{\Psi}^1_{1,j_2,j_1}=\alpha(\overline{\Phi}^0_{2j_2-1,2j_1-1}-\overline{\Phi}^0_{2j_2-1,2j_1}+ \\ +\overline{\Phi}^0_{2j_2,2j_1-1}-\overline{\Phi}^0_{2j_2,2j_1}) \quad (2.14)$$

– $(1,j_2,j_1)$- th refining vector of the discrete Haar basis of the first level,

$$\overline{\Psi}^1_{2,j_2,j_1}=\alpha(\overline{\Phi}^0_{2j_2-1,2j_1-1}+\overline{\Phi}^0_{2j_2-1,2j_1}- \\ -\overline{\Phi}^0_{2j_2,2j_1-1}-\overline{\Phi}^0_{2j_2,2j_1}); \quad (2.15)$$

– $(2,j_2,j_1)$-th refining vector of the discrete Haar basis of the first level,

$$\overline{\Psi}^1_{3,j_2,j_1}=\alpha(\overline{\Phi}^0_{2j_2-1,2j_1-1}-\overline{\Phi}^0_{2j_2-1,2j_1}- \\ -\overline{\Phi}^0_{2j_2,2j_1-1}+\overline{\Phi}^0_{2j_2,2j_1}) \quad (2.16)$$

– $(3,j_2,j_1)$- th refining vector of the discrete Haar basis of the first level,

$$1\le j_2,j_1\le N_1; \quad (2.17)$$

$\alpha=1/2$ is normalizing factor.

In accordance with (2.7), the mesh function $\bar{u}$ is represented as a sum in which the first summand (the first sum) is its approximation on the grid of the first level including N_1^2 nodes, and other three terms are called the refinement (the complement to the initial state) on the grid the first level. The representation (2.7) can be written in the form

$$\bar{u}=\bar{u}^0_1+\bar{v}^0_{1,1}+\bar{v}^0_{2,1}+\bar{v}^0_{3,1}; \quad (2.18)$$
$$\bar{u}^0_1=\sum_{j_2=1}^{N_1}\sum_{j_1=1}^{N_1}u^1_{j_2,j_1}\overline{\Phi}^1_{j_2,j_1}=\Phi_1\Phi_1^T\bar{u}=\Phi_1\bar{u}^1; \quad (2.19)$$
$$\bar{v}^0_{k,1}=\sum_{j_2=1}^{N_1}\sum_{j_1=1}^{N_1}v^1_{k,j_2,j_1}\overline{\Psi}^1_{k,j_2,j_1}=\Psi_{k,1}\Psi^T_{k,1}\bar{u}=\Psi_{k,1}\bar{v}^1_k,\ k=1,2,3, \quad (2.20)$$

where we have

$$\Phi_1=[\overline{\Phi}^1_{1,1}\dots\overline{\Phi}^1_{1,N_1},..\overline{\Phi}^1_{N_1,1}\dots\overline{\Phi}^1_{N_1,N_1}]; \quad (2.21)$$
$$\Psi_{k,1}=[\overline{\Psi}^1_{k,1,1}\dots\overline{\Psi}^1_{k,1,N_1}\dots\overline{\Psi}^1_{k,N_1,1}\dots\overline{\Psi}^1_{k,N_1,N_1}],\ k=1,2,3 \quad (2.22)$$

are matrices of size $N^2\times N_1^2$, whose columns are, respectively, approximating and detailing vectors of the discrete Haar basis of the first level.

Due to the orthonormality of the Haar basis [1-7,9-25], the operators

$$P_\Phi=\Phi_1\Phi_1^T,\ P_{\Psi,k}=\Psi_{k,1}\Psi^T_{k,1},\ k=1,2,3 \quad (2.23)$$

are projectors of the space of vector functions of the original grid to the space of their approxima-

tion on the first-level grid and its complement (the refining component) to the initial state, respectively.

2.2. Basic scheme of the two-grid method.
Let systems of linear algebraic equations

$$A\bar{u} = \bar{f} \tag{2.24}$$

are discrete analogs of some operator equation defined on a given rectangular prism of order N^2.
We can substitute in (2.24) the expression for $\bar{u}$ in the form (2.18). Then we can multiply, in turn, both sides of the equality on the left by the matrices Φ_1^T and $\Psi_{k,1}^T$, $k=1,2,3$. Thus we have

$$\begin{aligned}
&\Phi_1^T A\Phi_1\bar{u}^1 + \sum_{k=1}^{3}\Phi_1^T A\Psi_{k1}\bar{v}_k^1 = \Phi_1^T\bar{f}\\
&\Psi_{1,1}^T A\Phi_1\bar{u}^1 + \sum_{k=1}^{3}\Psi_{1,1}^T A\Psi_{k,1}\bar{v}_k^1 = \Psi_{1,1}^T\bar{f}\\
&\Psi_{2,1}^T A\Phi_1\bar{u}^1 + \sum_{k=1}^{3}\Psi_{2,1}^T A\Psi_{k,1}\bar{v}_k^1 = \Psi_{2,1}^T\bar{f}\\
&\Psi_{3,1}^T A\Phi_1\bar{u}^1 + \sum_{k=1}^{3}\Psi_{3,1}^T A\Psi_{k,1}\bar{v}_k^1 = \Psi_{3,1}^T\bar{f}
\end{aligned} \tag{2.25}$$

Equations (2.25) can be rewritten in the form

$$\sum_{i=1}^{4} A_{i,j}\bar{w}_j = \bar{f}_i,\quad i=1,...,4. \tag{2.26}$$

where $A_{i,j}$ are block matrices of size $N_1^2\times N_1^2$; $\bar{f}_i$ and $\bar{w}_j$ are block vectors of size N_1^2,

$$A_{1,1} = \Phi_1^T A\Phi_1;\quad A_{1,k+1} = \Phi_1^T A\Psi_{k,1},$$

$$A_{k+1,1} = \Psi_{k,1}^T A\Phi_1,\quad k=1,2,3; \tag{2.27}$$

$$A_{k+1,p+1} = \Psi_{k,1}^T A\Psi_{p+1},\quad k,p=1,2,3; \tag{2.28}$$

$$\bar{f}_1 = \Phi_1^T\bar{f},\quad \bar{f}_{k+1} = \Psi_{k,1}^T\bar{f},\quad k=1,...,7; \tag{2.29}$$

$$\bar{w}_1 = \bar{u}^1,\quad \bar{w}_{k+1} = v_k^1,\quad k=1,...,7. \tag{2.30}$$

We can find the solution of the system (2.26) using the block Gaussian method.
The expanded block matrix has the form:

$$\left[\begin{array}{cccc|c}
A_{1,1} & A_{1,2} & A_{1,3} & A_{1,4} & \bar{f}_1\\
A_{2,1} & A_{2,2} & A_{2,3} & A_{2,4} & \bar{f}_2\\
A_{3,1} & A_{3,2} & A_{3,3} & A_{3,4} & \bar{f}_3\\
A_{4,1} & A_{4,2} & A_{4,3} & A_{4,4} & \bar{f}_4
\end{array}\right]. \tag{2.31}$$

We have the following result of forward algorithm:

$$\left[\begin{array}{cccc|c}
A_{1,1} & A_{1,2} & A_{1,3} & A_{1,4} & \bar{f}_1\\
0 & A_{2,2}^1 & A_{2,3}^1 & A_{2,4}^1 & \bar{f}_2^1\\
0 & 0 & A_{3,3}^2 & A_{3,4}^2 & \bar{f}_3^2\\
0 & 0 & 0 & A_{4,4}^3 & \bar{f}_4^3
\end{array}\right], \tag{2.32}$$

where we have

$$A_{i,j}^k = A_{i,j}^{k-1} - C_{i,k}A_{k,j}^{k-1},\quad k=1,...,4,$$
$$i=k+1,...,4,\quad j=k+1,...,4; \tag{2.33}$$

$$\bar{f}_i^{\,k} = \bar{f}_i^{\,k-1} - C_{i,k}\bar{f}_k^{\,k-1},\quad k=1,...,4,$$
$$i=k+1,...,4; \tag{2.34}$$

$$C_{i,k} = A_{i,k}^{k-1}(A_{k,k}^{k-1})^{-1},\quad k=1,...,3,$$
$$i=k+1,...,4. \tag{2.35}$$

We have the following result of backward algorithm

$$\bar{w}_8 = (A_{4,4}^3)^{-1}\bar{f}_4^{\,3}; \tag{2.36}$$

$$\bar{w}_i = (A_{i,i}^{i-1})^{-1}\left(\bar{f}_i^{\,i-1} - \sum_{j=i+1}^{4}A_{i,i}^{i-1}\bar{w}_j\right),\ i=3,2,1. \tag{2.37}$$

In accordance with formulas (2.18)-(2.20) solution of the considering problem (2.24) has the form

$$\begin{aligned}
\bar{u} &= \bar{u}_1^0 + \sum_{k=1}^{7}\bar{v}_{k,1}^0 =\\
&= \Phi_1\bar{u}^1 + \sum_{k=1}^{7}\Psi_{k,1}\bar{v}_k^1 = \Phi_1\bar{w}_1 + \sum_{k=1}^{7}\Psi_{k,1}\bar{w}_{k+1}.
\end{aligned} \tag{2.38}$$

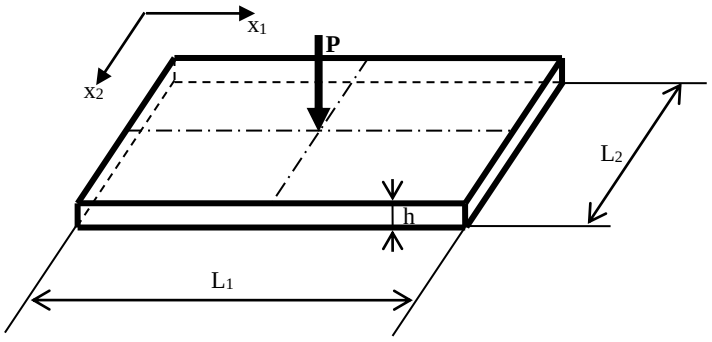
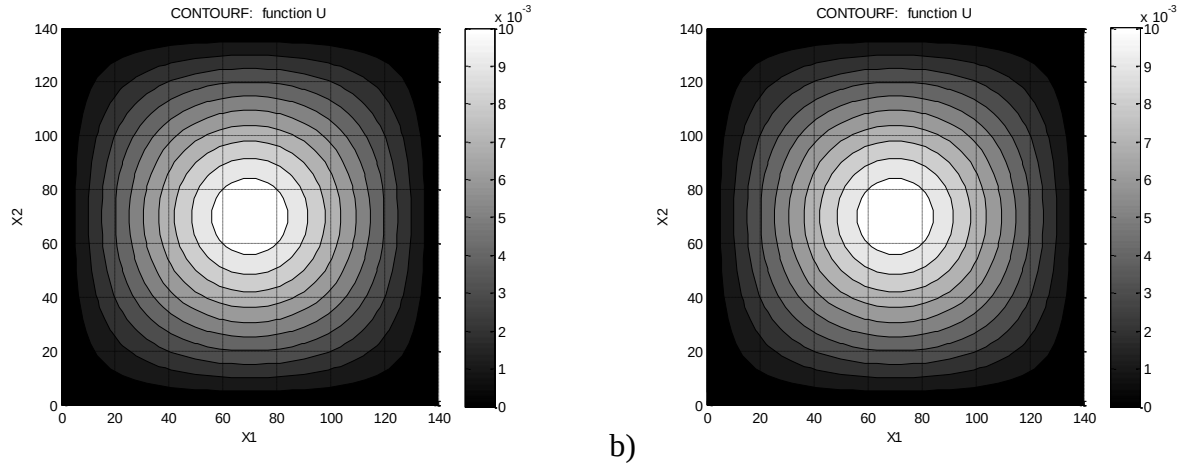


Figure 8. To the formulation of the boundary problem.



a) b)

Figure 9. Solution of the boundary problem: a) solution of problem in initial formulation; b) solution with the use of two-grid method.

It should be noted that the proposed method makes it possible to obtain a solution with the use of matrices of size $N_1^2 \times N_1^2$ and vectors of size N_1^2 ($N_1^2 = (N/2)^2$).

3.3. Numerical samples.

Let us consider (as an example) the definition of bending a rectangular plate, hinged on the edges, loaded in the center by the concentrated force (Figure 8).

Design scheme of a rectangular plate is shown on Figure 8: $L_1 = L_2 = 140$ mm are dimensions of plate; $h = 20$ cm is thickness of plate; $E = 3 \cdot 10^3$ kN/cm^2 is modulus of elasticity of the material of plate; $\nu = 0.16$ is Poisson's ratio of the material of plate; $P = 100$ kN is parameter of concentrated load.

We can use finite difference method for numerical solution of the considering problem. Thus, we can get resultant system of equations with respect to the nodal deflections,

$$A\bar{U} = \bar{f}\,, \qquad (2.39)$$

where A is matrix of coefficients; $\bar{f}$ is load vector; $\bar{U}$ is vector of unknown nodal deflections having the following structure

$$\bar{U} = [U_{1,1} \ldots U_{1,N} \ldots U_{N,1} \ldots U_{N,N}]^T; \qquad (2.40)$$

$U_{i,j} = u(x_{1,j}, x_{2,i})$ is the deflection in the node (i, j), $i, j = 1, \ldots, N$.

In accordance with the results of analysis graphs of deflections were obtained. Direct solution of the system (2.39) and solution defined by the formula (2.38) are presented at Figure 9.

Let us consider (as an example) the static analysis of a trapezoidal beam-wall (Figure 10).

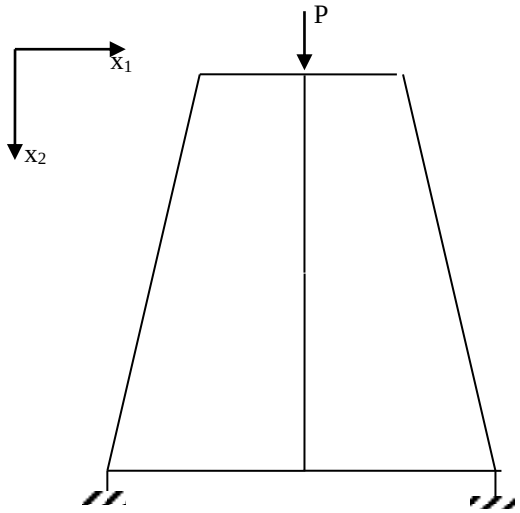


Figure 10. Design scheme.

Design scheme of a trapezoidal beams-wall is shown on Figure 10: height is equal to 140 cm; width at base is equal to 140 cm and at the top of the structure is equal to 70 cm; $E = 3 \cdot 10^3$ kN/cm^2 is the modulus of elasticity of the material of structure; $\nu = 0.16$ is Poisson's ratio of elasticity of the material of structure; $P = 100$ kN is parameter of concentrated load. Besides, we have fastening at the bottom corner points in both directions.

We can use finite element method for numerical solution of the considering problem. Thus, we can get resultant system of equations with respect to the nodal displacements (u_1 and u_2),

$$K\overline{U} = \overline{R}, \qquad (2.41)$$

where K is global stiffness matrix; $\overline{R}$ is global load vector; $\overline{U}$ is vector of unknown nodal displacements having the following structure,

$$\overline{U} = [\overline{u}_{1,1}^T \dots u_{1,N}^T \dots u_{N,1}^T \dots u_{N,N}^T]^T; \qquad (2.42)$$

$$\overline{u}_{i,j} = \begin{vmatrix} u_1(x_{1,j}, x_{2,i}) \\ u_2(x_{1,j}, x_{2,i}) \end{vmatrix} \qquad (2.43)$$

are displacements u_1 and u_2 in the node (i, j), $i, j = 1, \dots, N$.

Let us denote P_{12} as the matrix operator of such a permutation, i.e.

$$\overline{V} = P_{12}\overline{U} \quad \text{or} \quad \overline{U} = P_{12}^T\overline{V}. \qquad (2.44)$$

As a result, the resolving system (13) is converted to the form

$$K_v\overline{V} = \overline{R}_v, \qquad (2.45)$$

where we have

$$K_v = P_{12}KP_{12}^T; \quad \overline{R}_v = P_{12}\overline{R}. \qquad (2.46)$$

Besides, we use the following block matrices in formulas (2.26)-(2.38):

$$\Phi_1^b = \begin{vmatrix} \Phi_1 & 0 \\ 0 & \Phi_1 \end{vmatrix}; \qquad (2.47)$$

$$\Psi_{k,1}^b = \begin{vmatrix} \Psi_{k,1} & 0 \\ 0 & \Psi_{k,1} \end{vmatrix}, \quad k = 1, 2, 3. \qquad (2.48)$$

In accordance with the second equation of the formula (2.44), the solution of the initial problem (2.41) has the form:

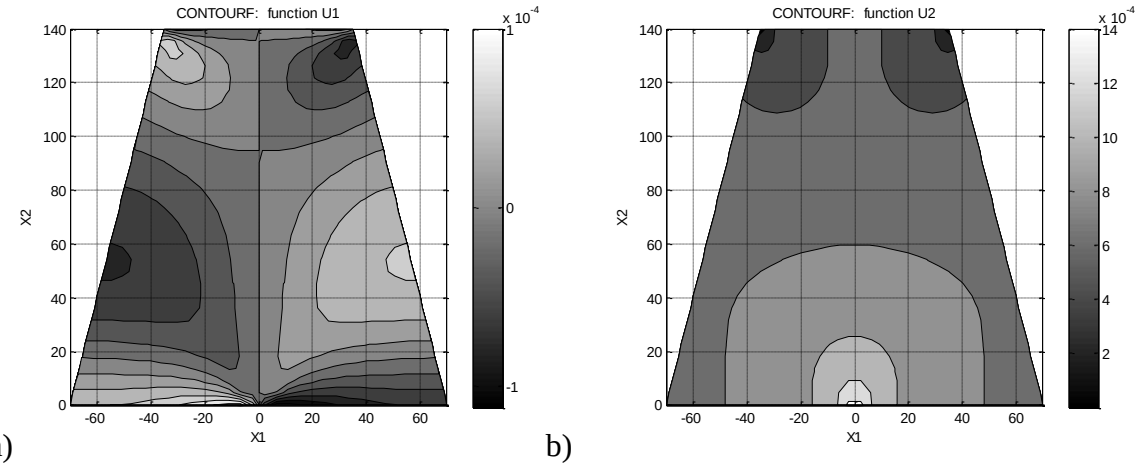
$$\overline{U} = P_{12}^T(\Phi_1^b\overline{w}_1 + \sum_{k=1}^{3}\Psi_{k1}^b\overline{w}_{k+1}). \qquad (2.49)$$

In accordance with the results of analysis graphs of displacements were obtained. Direct solution of the system (2.41) and solution defined by the formula (2.49) are presented at Figures 11-12.

3. THREE-DIMENSIONAL PROBLEMS

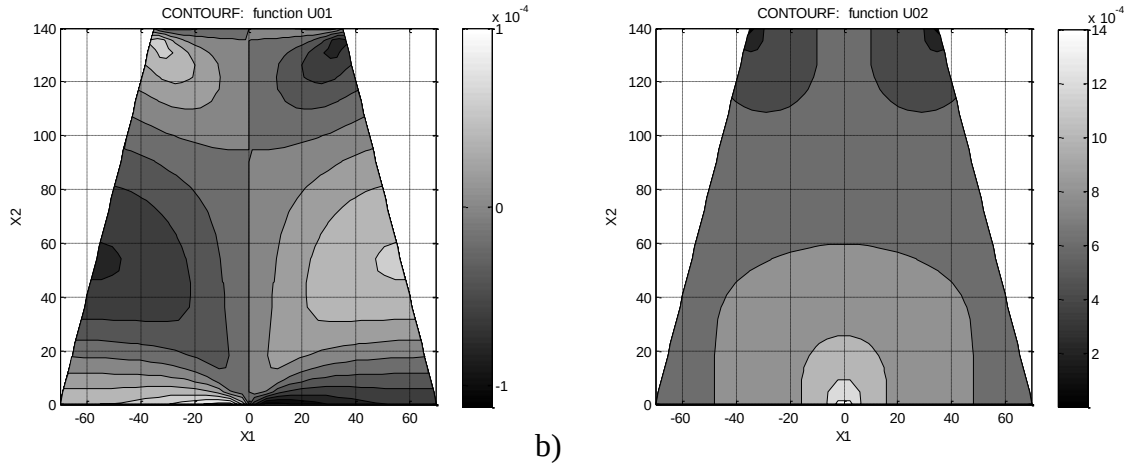
3.1. General information.

Let the initial three-dimensional domain be given as a rectangular prism [1]. Let L_1, L_2 and L_3 be lengths of sides of this prism in directions corresponding to Cartesian coordinates x_1, x_2 and x_3.



a) b)

Figure 11. Solution of the boundary problem (displacements u_1 (a) and u_2 (b)) in initial formulation.



a) b)

Figure 12. Solution of the boundary problem (displacements u_1 (a) and u_2 (b)) with the use of two-grid method.

We can use simple rectangular mesh (grid) for approximation of domain and divide each side of the rectangular prism (the initial domain) into $(N-1)$ equal parts. The corresponding mesh (grid) width are defined by formulas

$$h_1 = L_1/(N-1); \quad h_2 = L_2/(N-1); \quad h_3 = L_3/(N-1). \quad (3.1)$$

Thus, the resulting mesh contains N^3 nodes. Let us introduce the mesh function

$$\bar{u} = [\, u_{1,1,1} \;\; \ldots \;\; u_{1,N,1} \;\; \ldots \;\; u_{N,N,1} \;\; \ldots \;\; u_{N,N,N} \,]^T. \quad (3.2)$$

We can represent the mesh function (1.2) in the form

$$\bar{u} = \sum_{j_3=1}^{N_0} \sum_{j_2=1}^{N_0} \sum_{j_1=1}^{N_0} u^0_{j_2,j_1,j_3} \bar{\Phi}^0_{j_2,j_1,j_3}, \quad (3.3)$$

where $\bar{\Phi}^0_{j_2,j_1,j_3}(i_2,i_1,i_3)$ is the (j_2, j_1, j_3)-th vector of a unit basis or a discrete zero-level Haar basis

$$\overline{\Phi}^0_{j_2,j_1,j_3}(i_2,i_1,i_3) = \begin{cases} 1, \ (i_1 = j_1)\bigcap(i_2 = j_2)\bigcap(i_3 = j_3) \\ 0, \ (i_1 \neq j_1)\bigcup(i_2 \neq j_2)\bigcup(i_3 \neq j_3), \end{cases}$$

$$1 \le j_2, j_1, j_3 \le N_0 = N; \quad 1 \le i_2, i_1, i_3 \le N_0 = N; \tag{3.4}$$

$$u^0_{j_2,j_1,j_3} = u_{j_2,j_1,j_3}, \quad 1 \le j_1, j_2, j_3 \le N; \tag{3.5}$$

$$N_0 = N. \tag{3.6}$$

The mesh function (3.2) can also be represented in the form of an expansion in the Haar basis [1-7,9-25] of the first level:

$$\bar{u} = \sum_{j_3=1}^{N_1}\sum_{j_2=1}^{N_1}\sum_{j_1=1}^{N_1} u^1_{j_2,j_1,j_3}\overline{\Phi}^1_{j_2,j_1,j_3} + \sum_{k=1}^{7}\sum_{j_3=1}^{N_1}\sum_{j_2=1}^{N_1}\sum_{j_1=1}^{N_1} v^1_{k,j_2,j_1,j_3}\overline{\Psi}^1_{k,j_2,j_1,j_3}, \tag{3.7}$$

where $\overline{\Phi}^1_{j_2,j_1,j_3}$ is (j_2,j_1,j_3)-th approximating vector of the discrete Haar basis of the first level,

$$\begin{aligned}\overline{\Phi}^1_{j_2,j_1,j_3} = \alpha(&\overline{\Phi}^0_{2j_2-1,2j_1-1,2j_3-1} + \overline{\Phi}^0_{2j_2-1,2j_1,2j_3-1} + \\ &+ \overline{\Phi}^0_{2j_2,2j_1-1,2j_3-1} + \overline{\Phi}^0_{2j_2,2j_1,2j_3-1} + \\ &+ \overline{\Phi}^0_{2j_2-1,2j_1-1,2j_3} + \overline{\Phi}^0_{2j_2-1,2j_1,2j_3} + \\ &+ \overline{\Phi}^0_{2j_2,2j_1-1,2j_3} + \overline{\Phi}^0_{2j_2,2j_1,2j_3});\end{aligned} \tag{3.8}$$

$\overline{\Psi}^1_{k,j_2,j_1,j_3}$ – (k,j_2,j_1,j_3)-th refining vector of the discrete Haar basis of the first level,

$$\begin{aligned}\overline{\Psi}^1_{1,j_2,j_1,j_3} = \alpha(&\overline{\Phi}^0_{2j_2-1,2j_1-1,2j_3-1} - \overline{\Phi}^0_{2j_2-1,2j_1,2j_3-1} + \\ &+ \overline{\Phi}^0_{2j_2,2j_1-1,2j_3-1} - \overline{\Phi}^0_{2j_2,2j_1,2j_3-1} + \\ &+ \overline{\Phi}^0_{2j_2-1,2j_1-1,2j_3} - \overline{\Phi}^0_{2j_2-1,2j_1,2j_3} + \\ &+ \overline{\Phi}^0_{2j_2,2j_1-1,2j_3} - \overline{\Phi}^0_{2j_2,2j_1,2j_3});\end{aligned} \tag{3.9}$$

$$\begin{aligned}\overline{\Psi}^1_{2,j_2,j_1,j_3} = \alpha(&\overline{\Phi}^0_{2j_2-1,2j_1-1,2j_3-1} + \overline{\Phi}^0_{2j_2-1,2j_1,2j_3-1} - \\ &- \overline{\Phi}^0_{2j_2,2j_1-1,2j_3-1} - \overline{\Phi}^0_{2j_2,2j_1,2j_3-1} + \\ &+ \overline{\Phi}^0_{2j_2-1,2j_1-1,2j_3} + \overline{\Phi}^0_{2j_2-1,2j_1,2j_3} - \\ &- \overline{\Phi}^0_{2j_2,2j_1-1,2j_3} - \overline{\Phi}^0_{2j_2,2j_1,2j_3});\end{aligned} \tag{3.10}$$

$$\begin{aligned}\overline{\Psi}^1_{3,j_2,j_1,j_3} = \alpha(&\overline{\Phi}^0_{2j_2-1,2j_1-1,2j_3-1} - \overline{\Phi}^0_{2j_2-1,2j_1,2j_3-1} - \\ &- \overline{\Phi}^0_{2j_2,2j_1-1,2j_3-1} + \overline{\Phi}^0_{2j_2,2j_1,2j_3-1} + \\ &+ \overline{\Phi}^0_{2j_2-1,2j_1-1,2j_3} - \overline{\Phi}^0_{2j_2-1,2j_1,2j_3} - \\ &- \overline{\Phi}^0_{2j_2,2j_1-1,2j_3} + \overline{\Phi}^0_{2j_2,2j_1,2j_3});\end{aligned} \tag{3.11}$$

$$\begin{aligned}\overline{\Psi}^1_{4,j_2,j_1,j_3} = \alpha(&\overline{\Phi}^0_{2j_2-1,2j_1-1,2j_3-1} + \overline{\Phi}^0_{2j_2-1,2j_1,2j_3-1} + \\ &+ \overline{\Phi}^0_{2j_2,2j_1-1,2j_3-1} + \overline{\Phi}^0_{2j_2,2j_1,2j_3-1} - \\ &- \overline{\Phi}^0_{2j_2-1,2j_1-1,2j_3} - \overline{\Phi}^0_{2j_2-1,2j_1,2j_3} - \\ &- \overline{\Phi}^0_{2j_2,2j_1-1,2j_3} - \overline{\Phi}^0_{2j_2,2j_1,2j_3});\end{aligned} \tag{3.12}$$

$$\begin{aligned}\overline{\Psi}^1_{5,j_2,j_1,j_3} = \alpha(&\overline{\Phi}^0_{2j_2-1,2j_1-1,2j_3-1} - \overline{\Phi}^0_{2j_2-1,2j_1,2j_3-1} + \\ &+ \overline{\Phi}^0_{2j_2,2j_1-1,2j_3-1} - \overline{\Phi}^0_{2j_2,2j_1,2j_3-1} - \\ &- \overline{\Phi}^0_{2j_2-1,2j_1-1,2j_3} + \overline{\Phi}^0_{2j_2-1,2j_1,2j_3} - \\ &- \overline{\Phi}^0_{2j_2,2j_1-1,2j_3} + \overline{\Phi}^0_{2j_2,2j_1,2j_3});\end{aligned} \tag{3.13}$$

$$\begin{aligned}\overline{\Psi}^1_{6,j_2,j_1,j_3} = \alpha(&\overline{\Phi}^0_{2j_2-1,2j_1-1,2j_3-1} + \overline{\Phi}^0_{2j_2-1,2j_1,2j_3-1} - \\ &- \overline{\Phi}^0_{2j_2,2j_1-1,2j_3-1} - \overline{\Phi}^0_{2j_2,2j_1,2j_3-1} - \\ &- \overline{\Phi}^0_{2j_2-1,2j_1-1,2j_3} - \overline{\Phi}^0_{2j_2-1,2j_1,2j_3} + \\ &+ \overline{\Phi}^0_{2j_2,2j_1-1,2j_3} + \overline{\Phi}^0_{2j_2,2j_1,2j_3});\end{aligned} \tag{3.14}$$

$$\begin{aligned}\overline{\Psi}^1_{7,j_2,j_1,j_3} = \alpha(&\overline{\Phi}^0_{2j_2-1,2j_1-1,2j_3-1} - \overline{\Phi}^0_{2j_2-1,2j_1,2j_3-1} \\ &- \overline{\Phi}^0_{2j_2,2j_1-1,2j_3-1} + \overline{\Phi}^0_{2j_2,2j_1,2j_3-1} - \\ &- \overline{\Phi}^0_{2j_2-1,2j_1-1,2j_3} + \overline{\Phi}^0_{2j_2-1,2j_1,2j_3} + \\ &+ \overline{\Phi}^0_{2j_2,2j_1-1,2j_3} - \overline{\Phi}^0_{2j_2,2j_1,2j_3});\end{aligned} \tag{3.15}$$

$$u^1_{j_2,j_1,j_3} = (\bar{u}, \overline{\Phi}^1_{j_2,j_1,j_3});$$

$$v^1_{k,j_2,j_1,j_3} = (\bar{u}, \overline{\Psi}^1_{k,j_2,j_1,j_3}), \ k = 1,...,7; \tag{3.16}$$

$$\alpha = 1/(2\sqrt{2}); \quad N_1 = N/2 \tag{3.17}$$

α is normalizing factor.

In accordance with (3.7), the mesh function $\bar{u}$ is represented as a sum in which the first summand (the first sum) is its approximation on the grid of the first level including N_1^3 nodes, and the second term (the second sum) is called the refinement (the complement to the initial state) on the grid the first level. The representation (3.6) can be written in the form

$$\bar{u} = \bar{u}_1^0 + \sum_{k=1}^{7} \bar{v}_{k,1}^0 , \qquad (3.18)$$

$$\bar{u}_1^0 = \sum_{j_3=1}^{N_1}\sum_{j_2=1}^{N_1}\sum_{j_1=1}^{N_1} u_{j_2,j_1,j_3}^1 \overline{\Phi}_{j_2,j_1,j_3}^1 = \\ = \Phi_1(\Phi_1, \bar{u}) = \Phi_1 \Phi_1^T \bar{u}; \qquad (3.19)$$

$$\bar{v}_{k,1}^0 = \sum_{j_3=1}^{N_1}\sum_{j_2=1}^{N_1}\sum_{j_1=1}^{N_1} v_{k,j_2,j_1,j_3}^1 \overline{\Psi}_{k,j_2,j_1,j_3}^1 = \\ = \Psi_{k,1}(\Psi_{k,1}, \bar{u}) = \Psi_{k,1}\Psi_{k,1}^T \bar{u}, \ k = 1,...,7; \qquad (3.20)$$

$$\Phi_1 = \\ = [\overline{\Phi}_{1,1,1}^1 \ ... \ \overline{\Phi}_{1,N_1,1}^1 \ ... \ \overline{\Phi}_{N_1,N_1,1}^1 \ ... \ \overline{\Phi}_{N_1,N_1,N_1}^1]; \qquad (3.21)$$

$$\Psi_{k,1} = \\ = [\overline{\Psi}_{k,1,1,1}^1 \ ... \ \overline{\Psi}_{k,1,N_1,1}^1 \ ... \ \overline{\Psi}_{k,N_1,N_1,1}^1 \ ... \ \overline{\Psi}_{k,N_1,N_1,N_1}^1], \\ k = 1,...,7. \qquad (3.22)$$

Due to the orthonormality of the Haar basis [2,3,5,6], the operators

$$P_\Phi = \Phi_1 \Phi_1^T, \ \ P_{\Psi,k} = \Psi_{k,1}\Psi_{k,1}^T, \ \ k = 1,...,7 \qquad (3.23)$$

are projectors of the space of vector functions of the original grid to the space of their approximation on the first-level grid and its complement (the refining component) to the initial state, respectively.

3.2. Basic scheme of the two-grid method.

Let systems of linear algebraic equations

$$A\bar{u} = \bar{f} \qquad (3.24)$$

are discrete analogs of some operator equation defined on a given rectangular prism of order N^3.

We can substitute in (3.22) the expression for $\bar{u}$ in the form (3.16). Then we can multiply, in turn, both sides of the equality on the left by the matrices Φ_1^T and $\Psi_{k,1}^T$, $k = 1,2,3,4,5,6,7$. Thus we have

$$\Phi_1^T A\bar{u}_1^0 + \sum_{k=1}^{7} \Phi_1^T A \Psi_{k,1} \bar{v}_k^1 = \Phi_1^T \bar{f} , \qquad (3.25)$$

$$\Psi_{k,1}^T A\bar{u}_1^0 + \sum_{k=1}^{7} \Psi_{k,1}^T A \Psi_{k,1} \bar{v}_k^1 = \Psi_{k,1}^T \bar{f}, \ \ k = 1,...,7. \qquad (3.26)$$

Equations (3.25) and (3.26) can be combined in the system

$$\sum_{i=1}^{4} A_{i,j} \overline{w}_j = \bar{f}_i, \ \ i = 1,...,8. \qquad (3.27)$$

where $A_{i,j}$ are block matrices of size $N_1^3 \times N_1^3$; $\bar{f}_i$ and $\overline{w}_j$ are block vectors of size N_1^3,

$$A_{1,1} = \Phi_1^T A \Phi_1; \quad A_{1,k+1} = \Phi_1^T A \Psi_{k,1}, \\ A_{k+1,1} = \Psi_{k,1}^T A \Phi_1, \quad k = 1,...,7; \qquad (3.28)$$

$$A_{k+1,p+1} = \Psi_{k,1}^T A \Psi_{p+1}, \quad k, p = 1,2,3,4,5,6,7; \qquad (3.29)$$

$$\bar{f}_1 = \Phi_1^T \bar{f}, \quad \bar{f}_{k+1} = \Psi_{k,1}^T \bar{f}, \quad k = 1,...,7; \qquad (3.30)$$

$$\overline{w}_1 = \bar{u}^1, \quad \overline{w}_{k+1} = v_k^1, \quad k = 1,...,7. \qquad (3.31)$$

We can find the solution of the system (3.27) using the block Gaussian method.

The expanded block matrix has the form:

$$\left[\begin{array}{cccccccc|c} A_{1,1} & A_{1,2} & A_{1,3} & A_{1,4} & A_{1,5} & A_{1,6} & A_{1,7} & A_{1,8} & \bar{f}_1 \\ A_{2,1} & A_{2,2} & A_{2,3} & A_{2,4} & A_{2,5} & A_{2,6} & A_{2,7} & A_{2,8} & \bar{f}_2 \\ A_{3,1} & A_{3,2} & A_{3,3} & A_{3,4} & A_{3,5} & A_{3,6} & A_{3,7} & A_{3,8} & \bar{f}_3 \\ A_{4,1} & A_{4,2} & A_{4,3} & A_{4,4} & A_{4,5} & A_{4,6} & A_{4,7} & A_{4,8} & \bar{f}_4 \\ A_{5,1} & A_{5,2} & A_{5,3} & A_{5,4} & A_{5,5} & A_{5,6} & A_{5,7} & A_{5,8} & \bar{f}_5 \\ A_{6,1} & A_{6,2} & A_{6,3} & A_{6,4} & A_{6,5} & A_{6,6} & A_{6,7} & A_{6,8} & \bar{f}_6 \\ A_{7,1} & A_{7,2} & A_{7,3} & A_{7,4} & A_{7,5} & A_{7,6} & A_{7,7} & A_{7,8} & \bar{f}_7 \\ A_{8,1} & A_{8,2} & A_{8,3} & A_{8,4} & A_{8,5} & A_{8,6} & A_{8,7} & A_{8,8} & \bar{f}_8 \end{array}\right]. \qquad (3.32)$$

We have the following result of forward algorithm:

$$\left[\begin{array}{cccccccc|c} A^0_{1,1} & A^0_{1,2} & A^0_{1,3} & A^0_{1,4} & A^0_{1,5} & A^0_{1,6} & A^0_{1,7} & A^0_{1,8} & \bar{f}^0_1 \\ 0 & A^1_{2,2} & A^1_{2,3} & A^1_{2,4} & A^1_{2,5} & A^1_{2,6} & A^1_{2,7} & A^1_{2,8} & \bar{f}^1_2 \\ 0 & 0 & A^2_{3,3} & A^2_{3,4} & A^2_{3,5} & A^2_{3,6} & A^2_{3,7} & A^2_{3,8} & \bar{f}^2_3 \\ 0 & 0 & 0 & A^3_{4,4} & A^3_{4,5} & A^3_{4,6} & A^3_{4,7} & A^3_{4,8} & \bar{f}^3_4 \\ 0 & 0 & 0 & 0 & A^4_{5,5} & A^4_{5,6} & A^4_{5,7} & A^4_{5,8} & \bar{f}^4_5 \\ 0 & 0 & 0 & 0 & 0 & A^5_{6,6} & A^5_{6,7} & A^5_{6,8} & \bar{f}^5_6 \\ 0 & 0 & 0 & 0 & 0 & 0 & A^6_{7,7} & A^6_{7,8} & \bar{f}^6_7 \\ 0 & 0 & 0 & 0 & 0 & 0 & 0 & A^7_{8,8} & \bar{f}^7_8 \end{array}\right], \quad (3.33)$$

where

$$A^k_{i,j} = A^{k-1}_{i,j} - C_{i,k} A^{k-1}_{k,j}, \quad k = 1,...,7, \quad i = k+1,...,8, \quad j = k+1,...,8; \quad (3.34)$$

$$\bar{f}^k_i = \bar{f}^{k-1}_i - C_{i,k} \bar{f}^{k-1}_k, \quad k = 1,...,7, \quad i = k+1,...,8; \quad (3.35)$$

$$C_{i,k} = A^{k-1}_{i,k} (A^{k-1}_{k,k})^{-1}, \quad k = 1,...,7, \quad i = k+1,...,8. \quad (3.36)$$

We have the following result of backward algorithm

$$\overline{w}_8 = (A^7_{8,8})^{-1} \bar{f}^7_8; \quad (3.37)$$

$$\overline{w}_i = (A^{i-1}_{i,i})^{-1} \left(\bar{f}^{i-1}_i - \sum_{j=i+1}^{4} A^{i-1}_{i,i} \overline{w}_j \right), \quad i = 7,...,1. \quad (3.38)$$

In accordance with formulas (3.18)-(3.20) solution of the considering problem (3.24) has the form

$$\bar{u} = \bar{u}^0_1 + \sum_{k=1}^{7} \bar{v}^0_{k,1} = \\ = \Phi_1 \bar{u}^1 + \sum_{k=1}^{7} \Psi_{k,1} \bar{v}^1_k = \Phi_1 \overline{w}_1 + \sum_{k=1}^{7} \Psi_{k,1} \overline{w}_{k+1}. \quad (3.39)$$

It should be noted that the proposed method makes it possible to obtain a solution with the use of matrices of size $N^3_1 \times N^3_1$ and vectors of size N^3_1.

REFERENCES

1. **Mozgaleva M.L., Akimov P.A.** Dvuhsetochnyj Metod Rascheta Stroitel'nyh Konstrukcij na Osnove Ispol'zovaniya Diskretnogo Bazisa Haara. CHast' 1: Odnomernye Problemy [Two-Grid method of Structural Analysis Based on Discrete Haar Basis. Part 1: One-Dimensional Problems]. // International Journal for Computational Civil and Structural Engineering, Volume 13, Issue 4, 2017, pp. 128-139.
2. **Mozgaleva M.L., Akimov P.A.** K Voprosu ob Otscenke Vliyaniya Spryamleniya Approksimiruyushchej Setki na Chislennoe Reshenie Kraevoj Zadachi [About the Problem of the Assessment of the Impact of the Flatness of the Approximating Mesh on the Numerical Solution of the Boundary Problem]. // International Journal for Computational Civil and Structural Engineering, Volume 11, Issue 1, 2015, pp. 115-120.
3. **Mozgaleva M.L., Akimov P.A.** Ob Issledovanii Diskretnyh Metodov Polucheniya Lokal'nyh Reshenij Odnomernyh Zadach Rascheta Konstrukcij [About the Study of Discrete Methods for Obtaining Local Solutions to One-Dimensional Problems of Structural Analysis]. // International Journal for Computational Civil and Structural Engineering, Volume 11, Issue 1, 2015, pp. 121-134.
4. **Mozgaleva M.L., Akimov P.A., Semin D.F.** Lokal'noe Chislennoe Reshenie Kraevyh Zadach Stroitel'noj Mekhaniki s Ispol'zovaniem Gibridnogo Diskretnogo Vejvet-Bazisa [Local Numerical Solution of Boundary Problems of Structural Mechanics With the Use of Hybrid Discrete Wavelet Basis]. // International Journal for Computational Civil and Structural Engineering, Volume 14, Issue 1, 2018, pp. 113-125.
5. **Akimov P.A., Mojtaba Aslami.** Theoretical Foundations of Correct Wavelet-Based Approach to Local Static Analysis of Bernoulli Beam. // Applied Mechanics and Ma-

terials, 2014, Vols. 580-583, pp. 2924-2927.
6. **Akimov P.A., Mozgaleva M.L.** Correct Wavelet-based Multilevel Discrete-Continual Methods for Local Solution of Boundary Problems of Structural Analysis. // Applied Mechanics and Materials, 2013, Vols. 353-356, pp. 3224-3227.
7. **Akimov P.A., Mozgaleva M.L.** Correct Wavelet-based Multilevel Numerical Method of Local Solution of Boundary Problems of Structural Analysis. // Applied Mechanics and Materials, 2012, Vols. 166-169, pp. 3155-3158.
8. **Akimov P.A., Mozgaleva M.L.** Method of Extended Domain and General Principles of Mesh Approximation for Boundary Problems of Structural Analysis. // Applied Mechanics and Materials, 2014, Vols. 580-583, pp. 2898-2902.
9. **Arbabi S., Nazari A., Darvishi M.T.** A Two-Dimensional Haar Wavelets Method for Solving Systems of PDEs. // Applied Mathematics and Computation, 2017, Volume 292, pp. 33-46.
10. **Aziz I., Amin R.** Numerical Solution of a Class of Delay Differential and Delay Partial Differential Equations via Haar Wavelet. // Applied Mathematical Modelling, 2016, Volume 40, Issues 23-24, pp. 10286-10299.
11. **Aziz I., Siraj-ul-Islam, Asif M.** Haar Wavelet Collocation Method for Three-Dimensional Elliptic Partial Differential Equations. // Computers & Mathematics with Applications, 2017, Volume 73, Issue 9, pp. 2023-2034.
12. **Babaaghaie A., Maleknejad K.** Numerical Solution of Integro-Differential Equations of High Order by Wavelet Basis, its Algorithm and Convergence Analysis. // Journal of Computational and Applied Mathematics, 2017, Volume 325, pp. 125-133.
13. **Babaaghaie A., Maleknejad K.** Numerical Solutions of Nonlinear Two-Dimensional Partial Volterra Integro-Differential Equations by Haar Wavelet. // Journal of Computational and Applied Mathematics, 2017, Volume 317, pp. 643-651.
14. **Dai Q., Cao Q., Chen Y.** Frequency Analysis of Rotating Truncated Conical Shells Using the Haar Wavelet Method. // Applied Mathematical Modelling, 2018, Volume 57, pp. 603-613.
15. **Ezzati R., Sadatrasoul S.M.** On Numerical Solution of Two-Dimensional Nonlinear Urysohn Fuzzy Integral Equations Based on Fuzzy Haar Wavelets. // Fuzzy Sets and Systems, 2017, Volume 309, pp. 145-164.
16. **Hsiao C.-H.** A Haar Wavelets Method of Solving Differential Equations Characterizing the Dynamics of a Current Collection System for an Electric Locomotive. // Applied Mathematics and Computation, 2015, Volume 265, pp. 928-935.
17. **Kaur H., Mittal R.C., Mishra V.** Haar Wavelet Solutions of Nonlinear Oscillator Equations. // Applied Mathematical Modelling, 2014, Volume 38, Issues 21-22, pp. 4958-4971.
18. **Mojtaba Aslami, Akimov P.A.** Wavelet-based finite element method for multilevel local plate analysis. // Thin-Walled Structures, Volume 98, Part B (2015-2016), pp. 392-402.
19. **Mozgaleva M.L., Akimov P.A.** Multilevel wavelet-based numerical method of local structural analysis for three-dimensional problem. // Procedia Engineering, 2015, Vol. 111, pp. 569-574.
20. **Prakash B., Setia A., Alapatt D.** Numerical Solution of Nonlinear Fractional SEIR Epidemic Model by Using Haar Wavelets. // Journal of Computational Science, 2017, Volume 22, pp. 109-118.
21. **Shiralashetti S.C., Deshi A.B., Mutalik Desai P.B.** Haar Wavelet Collocation Method for the Numerical Solution of Singular Initial Value Problems. // Ain Shams Engineering Journal, 2016, Volume 7, Issue 2, pp. 663-670.
22. **Shiralashetti S.C., Kantli M.H., Deshi A.B.** A New Wavelet Multigrid Method for the Numerical Solution of Elliptic Type

Differential Equations. // Alexandria Engineering Journal, 2018, Volume 57, Issue 1, pp. 203-209.
23. **Wang L., Ma Y., Meng Z.** Haar Wavelet Method for Solving Fractional Partial Differential Equations Numerically. // Applied Mathematics and Computation, 2014, Volume 227, pp. 66-76.
24. **Xie X., Jin G., Yan Y., Shi S.X., Liu Z.** Free Vibration Analysis of Composite Laminated Cylindrical Shells Using the Haar Wavelet Method. // Composite Structures, 2014, Volume 109, pp. 169-177.

СПИСОК ЛИТЕРАТУРЫ

1. **Мозгалева М.Л., Акимов П.А.** Двухсеточный метод расчета строительных конструкций на основе использования дискретного базиса Хаара. Часть 1: Одномерные проблемы. // International Journal for Computational Civil and Structural Engineering / Международный журнал по расчету гражданских и строительных конструкций, Volume 13, Issue 4, 2017, pp. 128-139.
2. **Мозгалева М.Л., Акимов П.А.** К вопросу об оценке влияния спрямления аппроксимирующей сетки на численное решение краевой задачи. // International Journal for Computational Civil and Structural Engineering / Международный журнал по расчету гражданских и строительных конструкций, Volume 11, Issue 1, 2015, pp. 115-120.
3. **Мозгалева М.Л., Акимов П.А.** Об исследовании дискретных методов получения локальных решений одномерных задач расчета конструкций. // International Journal for Computational Civil and Structural Engineering / Международный журнал по расчету гражданских и строительных конструкций, Volume 11, Issue 1, 2015, pp. 121-134.
4. **Мозгалева М.Л., Акимов П.А., Семин Д.Ф.** Локальное численное решение краевых задач строительной механики с использованием гибридного дискретного вейвет-базиса. // International Journal for Computational Civil and Structural Engineering / Международный журнал по расчету гражданских и строительных конструкций, Volume 14, Issue 1, 2018, pp. 113-125.
5. **Akimov P.A., Mojtaba Aslami.** Theoretical Foundations of Correct Wavelet-Based Approach to Local Static Analysis of Bernoulli Beam. // Applied Mechanics and Materials, 2014, Vols. 580-583, pp. 2924-2927.
6. **Akimov P.A., Mozgaleva M.L.** Correct Wavelet-based Multilevel Discrete-Continual Methods for Local Solution of Boundary Problems of Structural Analysis. // Applied Mechanics and Materials, 2013, Vols. 353-356, pp. 3224-3227.
7. **Akimov P.A., Mozgaleva M.L.** Correct Wavelet-based Multilevel Numerical Method of Local Solution of Boundary Problems of Structural Analysis. // Applied Mechanics and Materials, 2012, Vols. 166-169, pp. 3155-3158.
8. **Akimov P.A., Mozgaleva M.L.** Method of Extended Domain and General Principles of Mesh Approximation for Boundary Problems of Structural Analysis. // Applied Mechanics and Materials, 2014, Vols. 580-583, pp. 2898-2902.
9. **Arbabi S., Nazari A., Darvishi M.T.** A Two-Dimensional Haar Wavelets Method for Solving Systems of PDEs. // Applied Mathematics and Computation, 2017, Volume 292, pp. 33-46.
10. **Aziz I., Amin R.** Numerical Solution of a Class of Delay Differential and Delay Partial Differential Equations via Haar Wavelet. // Applied Mathematical Modelling, 2016, Volume 40, Issues 23-24, pp. 10286-10299.
11. **Aziz I., Siraj-ul-Islam, Asif M.** Haar Wavelet Collocation Method for Three-Dimensional Elliptic Partial Differential Equations. // Computers & Mathematics

with Applications, 2017, Volume 73, Issue 9, pp. 2023-2034.
12. **Babaaghaie A., Maleknejad K.** Numerical Solution of Integro-Differential Equations of High Order by Wavelet Basis, its Algorithm and Convergence Analysis. // Journal of Computational and Applied Mathematics, 2017, Volume 325, pp. 125-133.
13. **Babaaghaie A., Maleknejad K.** Numerical Solutions of Nonlinear Two-Dimensional Partial Volterra Integro-Differential Equations by Haar Wavelet. // Journal of Computational and Applied Mathematics, 2017, Volume 317, pp. 643-651.
14. **Dai Q., Cao Q., Chen Y.** Frequency Analysis of Rotating Truncated Conical Shells Using the Haar Wavelet Method. // Applied Mathematical Modelling, 2018, Volume 57, pp. 603-613.
15. **Ezzati R., Sadatrasoul S.M.** On Numerical Solution of Two-Dimensional Nonlinear Urysohn Fuzzy Integral Equations Based on Fuzzy Haar Wavelets. // Fuzzy Sets and Systems, 2017, Volume 309, pp. 145-164.
16. **Hsiao C.-H.** A Haar Wavelets Method of Solving Differential Equations Characterizing the Dynamics of a Current Collection System for an Electric Locomotive. // Applied Mathematics and Computation, 2015, Volume 265, pp. 928-935.
17. **Kaur H., Mittal R.C., Mishra V.** Haar Wavelet Solutions of Nonlinear Oscillator Equations. // Applied Mathematical Modelling, 2014, Volume 38, Issues 21-22, pp. 4958-4971.
18. **Mojtaba Aslami, Akimov P.A.** Wavelet-based finite element method for multilevel local plate analysis. // Thin-Walled Structures, Volume 98, Part B (2015-2016), pp. 392-402.
19. **Mozgaleva M.L., Akimov P.A.** Multilevel wavelet-based numerical method of local structural analysis for three-dimensional problem. // Procedia Engineering, 2015, Vol. 111, pp. 569-574.
20. **Prakash B., Setia A., Alapatt D.** Numerical Solution of Nonlinear Fractional SEIR Epidemic Model by Using Haar Wavelets. // Journal of Computational Science, 2017, Volume 22, pp. 109-118.
21. **Shiralashetti S.C., Deshi A.B., Mutalik Desai P.B.** Haar Wavelet Collocation Method for the Numerical Solution of Singular Initial Value Problems. // Ain Shams Engineering Journal, 2016, Volume 7, Issue 2, pp. 663-670.
22. **Shiralashetti S.C., Kantli M.H., Deshi A.B.** A New Wavelet Multigrid Method for the Numerical Solution of Elliptic Type Differential Equations. // Alexandria Engineering Journal, 2018, Volume 57, Issue 1, pp. 203-209.
23. **Wang L., Ma Y., Meng Z.** Haar Wavelet Method for Solving Fractional Partial Differential Equations Numerically. // Applied Mathematics and Computation, 2014, Volume 227, pp. 66-76.
24. **Xie X., Jin G., Yan Y., Shi S.X., Liu Z.** Free Vibration Analysis of Composite Laminated Cylindrical Shells Using the Haar Wavelet Method. // Composite Structures, 2014, Volume 109, pp. 169-177.

Marina L. Mozgaleva, PhD, Professor, Department of Applied Mathematics, National Research Moscow State University of Civil Engineering, 26, Yaroslavskoe Shosse, Moscow, 129337, Russia;
phone/fax: +7(499) 183-59-94;
E-mail: marina.mozgaleva@gmail.com.

Pavel A. Akimov, Full Member of the Russian Academy of Architecture and Construction Sciences, PhD, Professor; Executive Scientific Secretary of Russian Academy of Architecture and Construction Sciences; Vice-Director for Science Activities, Scientific Research Center "StaDyO"; Professor of Department of Architecture and Construction, Peoples' Friendship University of Russia; Professor of Department of Structural Mechanics, Tomsk State University of Architecture and Building; 24, Ul. Bolshaya Dmitrovka, 107031, Moscow, Russia;
phone +7(495) 625-71-63; fax: +7 (495) 650-27-31;
E-mail: akimov@raasn.ru, pavel.akimov@gmail.com.

Taymuraz B. Kaytukov, Advisor of the Russian Academy of Architecture and Construction Sciences, Associated Professor, Ph.D.; Deputy Executive Scientific Secretary of Russian Academy of Architecture and Construction Sciences; Central Institute for Research and Design of the

Ministry of Construction and Housing and Communal Services of the Russian Federation; 24, Ul. Bolshaya Dmitrovka, 107031, Moscow, Russia;
phone +7(495) 625-81-53; fax: +7 (495) 650-27-31;
Email: kaytukov@raasn.ru, tkaytukov@gmail.com.

Мозгалева Марина Леонидовна, доцент, доктор технических наук, профессор кафедры прикладной математики, Национальный исследовательский Московский государственный строительный университет (НИУ МГСУ), Россия, 129337, Москва, Ярославское шоссе, д.26, тел./факс: +7(499) 183-59-94,
E-mail: marina.mozgaleva@gmail.com.

Акимов Павел Алексеевич, академик РААСН, профессор, доктор технических наук; главный ученый секретарь Российской академии архитектуры и строительных наук; заместитель генерального директора по науке ЗАО «Научно-исследовательский центр СтаДиО»; профессор Департамента архитектуры и строительства Российского университета дружбы народов; профессор кафедры строительной механики Томского государственного архитектурно-строительного университета; 107031, г. Москва, ул. Большая Дмитровка, д. 24, стр. 1; тел. +7(495) 625-71-63;
факс +7 (495) 650-27-31; e-mail: akimov@raasn.ru, pavel.akimov@gmail.com.

Кайтуков Таймураз Батразович, советник РААСН, доцент, кандидат технических наук, заместитель главного ученого секретаря Российской академии архитектуры и строительных наук; Центральный научно-исследовательский и проектный институт Министерства строительства и жилищно-коммунального хозяйства Российской Федерации; 107031, г. Москва, ул. Большая Дмитровка, д. 24, стр. 1;
тел. +7(495) 625-81-53; факс +7 (495) 650-27-31;
E-mail: kaytukov@raasn.ru, tkaytukov@gmail.com.

DOI:10.22337/2587-9618-2018-14-3-103-113

ABOUT THE PROBLEM OF ANALYSIS RESISTANCE BEARING SYSTEMS IN FAILURE OF A STRUCTURAL ELEMENT

Anatoly V. Perelmuter [1], Oleg V. Kabantsev [2]
[1] SCAD Soft Ltd, Kyiv, UKRAINE
[2] National Research Moscow State University of Civil Engineering, Moscow, RUSSIA

Abstract: This paper focuses on the methods of calculating load-bearing systems in the case of a failure of a structural element. This kind of failure makes it necessary to assess further behavior of the structure with a possibility of the progressive collapse development. The stress-strain state analysis of a load-bearing system in the case of a failure of a structure is carried out by two main methods – static and dynamic calculation. It is shown that the static calculation (quasi-static analysis using the dynamic amplification factor) is not a universal method. This paper justifies the application of the direct dynamic calculation in the mode of direct integration of motion for the design analysis of load-bearing systems with high rigidity stories (protection structures for a load-bearing system). It also gives recommendations for selecting parameters of the direct dynamic calculation in the case of a failure analysis of a bearing structure.

Keywords: modeling, numerical methods, calculation model, strain-stress state, progressive collapse

ОБ АНАЛИЗЕ СОПРОТИВЛЕНИЯ НЕСУЩИХ СИСТЕМ ПРИ ОТКАЗЕ КОНСТРУКТИВНОГО ЭЛЕМЕНТА

А.В. Перельмутер [1], О.В. Кабанцев [2]
[1] НПО СКАД Софт, г. Киев, УКРАИНА
[2] Национальный исследовательский Московский государственный строительный университет, г. Москва, РОССИЯ

Аннотация: Рассматриваются вопросы методики расчета несущих систем при отказе конструктивного элемента. Отказ такого рода приводит к необходимости оценить дальнейшее поведение конструкции с возможностью развития прогрессирующего разрушения. Анализ напряженно-деформированного состояния (НДС) несущей системы в условиях отказа конструкции выполняется по двум основным методикам – статический и динамический расчет. Показано, что статический расчет (квазистатический анализ с использованием коэффициента динамичности) не является универсальным методом. Приведены обоснования того, что для расчетного анализа несущих систем с этажами повышенной жесткости (конструкции защиты несущей системы) целесообразно применять прямой динамический расчет в режиме прямого интегрирования движения. Приведены рекомендации по выбору параметров прямого динамического расчета при анализе отказа несущей конструкции.

Ключевые слова: моделирование, численные методы, расчетная модель, напряженно-деформированное состояние, прогрессирующее обрушение

1. INTRODUCTION AND TASK STATEMENT

Stability evaluation of the load-bearing system in the event of individual load-bearing structure failure or when a local defect is created in the structural system is one of the most important tasks when assessing the safety level of the building bearing system in its entirety. In some cases, this task is formulated as an estimate of the structure survivability [1,2,3] which seems to be one of the justified approaches. The legislative document in force [4] outlines requirements to ensure mechanical safety of buildings and structures in the event of an emergency design situation:

'when designing a facility of an increased criticality rating, an emergency design situation must also be taken into account, which has a low chance of appearance and short-term duration, but ... which is crucial from the point of view of the consequences of reaching the limit states that may be generated in this situation (including the limit states arising in connection with explosion, collision, emergency situation, fire, and also right after the failure of one of the supporting structures)'.

Following further description of the requirements [4], the state standard [5] outlines the requirements with regard to the stress-strain forecast of the bearing systems: 'When performing structural design, the following design situations should be taken into account: 'emergency' being a situation which implies exceptional conditions of the building operation and which can lead to significant social, environmental and economic losses'. The state standard [5] introduces a new kind of limit state: 'special limit states, namely the states arising from particular impacts and situations exceeding of which leads to the failure of structures with disastrous consequences'. It should be mentioned that previously the regulatory documents did not cover 'special limit states'.

The definition of special effect sis thoroughly studied in the regulatory document [6], where in the definition is follow sis given: 'Special loads are those loads and impacts (e.g., explosion, collision with vehicles, equipment failure, fire, earthquake, certain climate-relevant impact, failure of a structural element) which result in emergency situations with eventual catastrophic consequences'. Code of Practice [6] defines that' the impact caused by particular emergency effects needs to be taken into account in modeling to determine the structures progressive collapse. Along with the wording of the aforementioned state standard [5], the following is defined: 'Calculation model for the structures progressive collapse may be considered not compulsory if special measures are ensured and which exclude progressive collapse of the structure or part thereof'.

The standard [5] requires as follows: 'For every limit state there should be taken into account the design models of the structure, its structural elements and bases which can characterize their behavior under the most unfavorable conditions at the time of their construction and operation.

As a matter of fact, evaluation of the bearing system resistance in the event of failure of the structural element can be reduced to an analysis of the development of fracture processes in the bearing system due to a local cause (failure of an individual structural unit). This approach corresponds to the modern interpretation of the well-known and frequently used concept of a' progressive collapse' which is considered to be a' disproportional' destruction owing to a local failure. It seems that the term 'disproportional' in view of destruction more closely corresponds to a phenomenon that the norms require to prevent, namely: it is deemed compulsory to avoid advancement (development) of destructions in the bearing system due to occurrence of the initial failure of an individual structural unit.

To evaluate the bearing system resistance against a local structural failure, various methods are proposed. For instance, in [7] it is proposed to employ the survivability index I_{RC}:

$$I_{RC} = \frac{R_{\max} - R}{R_{\max}} \tag{1}$$

where R_{max} is the maximum possible failure; R is the failure caused.

The source [8] thus defines the quantitative index of survivability K:

$$K = \frac{\sum_{i=1}^{m} k_i (N_i - n_i)}{\sum_{i=1}^{m} N_i} \tag{2}$$

where N_i is the total of the structural elements in this group; m is the total of the groups of elements; k_i is the weight factor for i-th of the group of elements; n_i is the total of the damaged elements of the i-th group.

It should be noted that the proposed methods of resistance of the bearing system (evaluation of 'survivability' as the terminology proposed by the authors) imply the information on the extent of destruction. In order to estimate the survivability of the designed buildings using the methods as above, a forecast of the extent of damage needs to be carried out and which can be supported by the outcome of the design analysis.

Information on the extent of destruction that occurred and was caused by the initial local failure is also needed to assess the correspondence of such an extent to the maximum admissible values of the destruction in the building (structure) which are outlined by the norms [6] (Item 5.7):

'Under the action of design and emergency specific circumstances, the maximum allowable area of local destruction of the load-bearing structures is determined as follows:

- for buildings with height of less than 75 m it is up to 40 m^2;
- for buildings with height of 75 to 200 m it is up to 80 m^2;
- for buildings with height of more than 200 m it is up to 100 m^2;
- for other facilities it is determined by the design brief and depends on the structure type (large-span shells, bridges, cooling towers, air-discharge pipes, etc.).

Thus, the task of the calculation model of the bearing system in the absence of a local structural element to provide a consistent result (namely the process of development or neutralization of the development of destructions and the scope of destroyed elements) is by all means important from the point of view of implementation of the requirements of the existing laws and regulations.

It should be emphasized that the contemporary best practice of designing the load-bearing systems provides an approach which proves to be not entirely justifiable to allow the formation of such significant 'allowable' degrees of structural damage (re. Item 5.7 [6]). In order to block the development of the destruction caused by the initial local event, various types of 'special measures excluding the progressive collapse of the structure or part thereof ([5]) or '… measures limiting the destruction area ([6])' are proposed. For instance, the source [9] suggests one method of protection against progressive collapse based on the arrangement of floors of increased stiffness (outrigger floors) and which ensure certain modification in the operation pattern of the vertical load-bearing structure in the event of failure of a lower-lying element; such structural unit is suspended to an outrigger floor. The principle of operation of the outrigger floor as a structure providing for the 'suspension' of vertical bearing structures is quite consistent with the definition of 'a special measure excluding progressive collapse of the structure or part thereof' which causes its extensive practical use when designing high-rise reinforced concrete buildings.

As the above mentioned concise analysis of the issues of estimating the resistance of a load-bearing building system in event of failure of the individual load-bearing structural units shows that the most important element ensuring the possibility to forecast the behavior of the bearing system, as well as assessing the compliance of the system with the regulatory requirements, represents the method of calculating of the bearing system under the special design situation. This method of calculation should ensure that the particularities of the processes occurring in the bearing system are taken into account when the bearing element locally fails and this requires the implementation of a number of special numerical methods.

2. ANALYSIS OF METHODS TO CALCULATE BEARING SYSTEMS IN THE EVENT OF LOCAL STRUCTURAL FAILURE

In line with the established practice of design analysis of load-bearing systems in the special design situation, two cases of failure of local design can be considered:

a) the structural element is not included into the operation of the bearing system due to external causes: failure to complete the design solution of the node (absence of bracing elements, unacceptable plays and clearances,

etc.); structural material not envisioned by the design brief (when mixing concrete mortar low-quality or defective cement is used); non-fulfillment of the design solution for the structural element (underestimated longitudinal / transverse reinforcement, low-quality rolled products profile is used);

b) the structural element is included into the operation of the bearing system structure; still owing to some external impact it gets destroyed and loses its bearing capacity.

Case (a) corresponds to a design model which features no defective structure, and this leads to the formation of an adequate stress-strain state for this kind of a bearing system in its entirety.

Case b) illustrates a more complicated situation; therein should be considered several stages of existence of a calculation model of the bearing system:

1. A calculation model corresponding to the design state with a full set of structural elements and formed stress-strain state;
2. A calculation model corresponding to the changed state of the bearing system (without a failure of a structural element), which leads to alteration of the original stress-strain state and, consequently, may lead to subsequent (secondary) destructions of the bearing system elements;
3. A calculation model corresponding to the modified state of the bearing system with consideration for secondary destructions which also lead to alteration of the original stress-strain state formed at stage 2, and, consequently, may lead to further subsequent destructions of the bearing system elements.

Thus, the failure of the load-bearing structure in case (b) predetermines the need for a multi-stage design analysis accounting for the inherited stress-strain state from stage to stage. Calculation techniques for a multi-stage design analysis should provide an accurate solution to the problem under the conditions of stiffness degradation in individual elements of the design model; similar questions of multi-stage calculations are considered in the source [10].

The most important provision in the event of failure of the bearing structure in view of the design analysis in case (b) is the possibility to correctly consider the mechanism of 'removal' of the stressed-strained element out of the design model composition, which leads to the formation of a certain dynamic effect. It is certain that problems of this sort can be successfully solved within the process of a direct dynamic calculation (when it comes to the field construction, the modules of direct dynamic calculation are included in all the main computational software). Nonetheless, the direct dynamic calculation technique is quite comprehensive, and requires generation of a variety of special raw data inclusive of the structural materials performance characteristics under dynamic influences, etc.

For the purposes of impact mitigation in the direct dynamical modeling problems it is proposed to employ the quasi-static calculation method using the k_d dynamic factor (see, for instance, sources [11, 12]). By virtue of its simplicity, the calculation based on the dynamic factor usage has gained popularity. It is due in no small part to the fact that for a system with one degree of freedom which is acted upon by a short-time loading the values of the dynamic coefficient [13] and its ceiling limit (k_d=2) are known.

It is known that making a quasi-static calculation with the account for the dynamic coefficient is justified only for systems with one degree of freedom when this coefficient is defined as a ratio of displacements triggered by the same load at its dynamic and static actions (Figure 1).

When it comes to multi-element systems, quite good results can be obtained in those cases when the system motion mode is close to the form of its static equilibrium without a remote element. Only then one can discuss the ratio of displacements common to all nodes of the system.

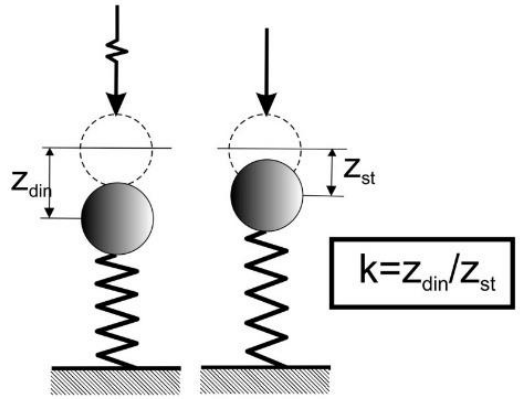


Figure 1. Determination of dynamic coefficient.

In critical cases it is natural to check the dynamic behavior of the system. This can be achieved and illustrated by means of a simplified model of a truss (Figure 2) which is studied in the sources [14, 15].

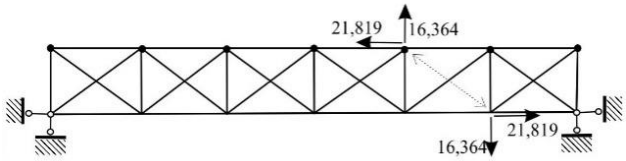


Figure 2. Design model to illustrate the example.

The truss elements are made of square pipes: belts 160x5, braces 140x5, racks 80x5. The main weight is assumed to be concentrated in the upper nodes of the truss; the weights are shown in Figure 2.

Based on the static loading of the truss with all elements in the diagonal rod of 6-12, the force value equals to N = 27,274 t.

If the truss is studied with no consideration of the diagonal rod of 6-12, in order to restore the static equilibrium for the nodes of 6 and 12 of the finite element model, it is compulsory to apply the load equal to the force acting in this diagonal rod. In Fig. 3 such a load is represented by means of components directed along coordinate axes. In this case (units of measurement are tons) the following is valid:

$$N = 27,274 = \sqrt{16,362^2 + 21,819^2} \qquad (3)$$

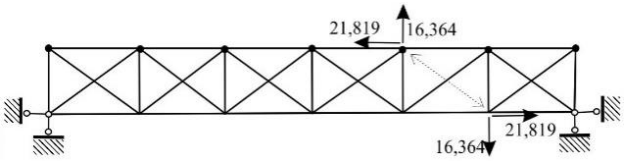


Figure 3. Elements replaced by reactions.

The physical withdrawal of the diagonal rod 6-12 is associated with a sudden (very rapid) dump of the loads shown in Figure 3 which in the calculation model is implemented by generation of a new load with the forces directed in opposite directions (Figure 4) and which increase in time from zero (at the beginning of the loading process) to their full value.

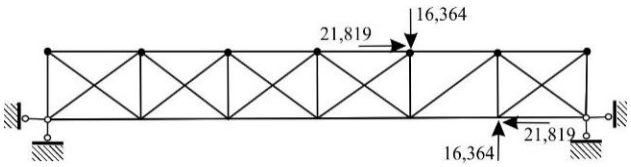


Figure 4. Impact from the element withdrawal.

In theory, the pattern of time variation of this conditional loading should be established by trial and error, and can be different for different forces; still taking into account the high failure rate, the connection can be assumed as a piecewise linear one and remaining identical for all forces.

Hence, it is essential to make a dynamic calculation to assess the forces arising from a sudden removal of the element. In this case, the dynamic effect can be described by the bilinear time-dependent forces (Figure 5) where t_d is the failure time during which the structure once received a 'negative impulse' at first 'gets stuck' in its initial position due to the inertia forces and then starts to move yet in a defective state.

The solution to the problem is found using the SCAD software complex [16] performing in the *Direct motion integration* mode. At that, the required procedural modeling is carried out in accordance with the requirements of the design mode: a special static load is gained, a file describing the law on variation of forces arising from the sudden removal of an element is generated, a value of the modal damping action is specified, integration spacing (0.01 sec.) is recorded a well as the action period (2 sec.).

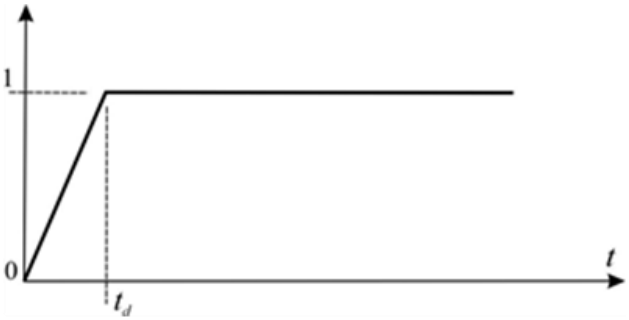


Figure 5. Time-depended load increase (force P is given on the vertical axis).

In order to analyze the state of the elements of the structural design, it is prerequisite to consider the graphs illustrating the change in forces in the elements. SCAD features this function in the query mode to obtain data on an element (Figure 6 can be referred to as an example).

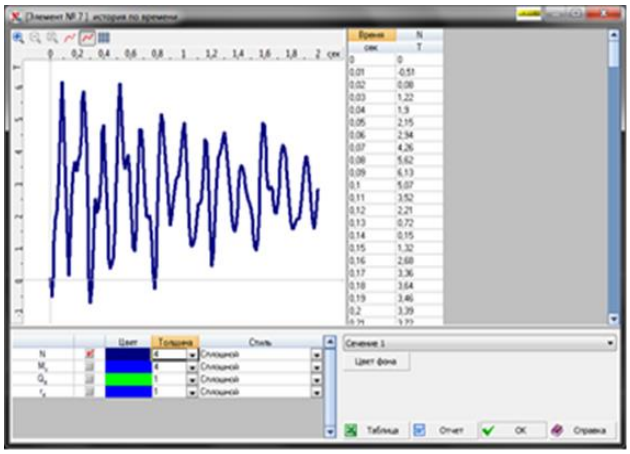


Figure 6. Track record on time-dependent change in force in the design model elements.

The stress-strain analysis of the elements of the model in time shows that the utmost force values generated in the elements of the system (as well as the movements of the nodes) are not achieved simultaneously (for reference see an example of the change in forces in individual elements in Figure 7). Thus, in element 8 the extremum is reached at time t = 0.21 sec., in element 11 at t = 0.17 sec., and in elements 20 and 31 at t = 0.16 sec.

Likewise, it should be taken into account that all motions of the system occur around the displaced equilibrium which was gained by the structure at the moment preceding the element destruction. Therefore, the results of the dynamic calculation obtained at direct integration of the equations of motion should be added up with the results of a static calculation of an intact structure.

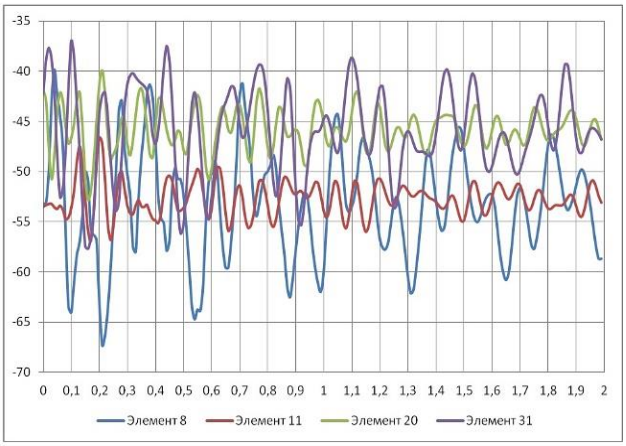


Figure 7. Time-dependent change in forces for some elements of the design model.

The research problem to study the stress-strain state of the design model elements as shown in Figure is also solved in quasi-static mode employing the dynamic factor k_d = 2.0 (at the utmost theoretical value). Correlated values of the solution results obtained through various methods are given in Table 1.

Juxtaposition of the obtained results with the numerical method in [15] proves good agreement of results. When it comes to the quasi-static solution obtained employing the dynamic factor k_d = 2.0, strong divergence gets to the surface. Such fundamental difference in results can be explained through the incongruity of the static equilibrium model form without a removed element and the first form of self-induced oscillations (Figure 8). Thus, the very concept of dynamic factor as a multiplier to the static deformation bears no significance. It should be noted that the idea of a quasi-static calculation employing the dynamic factor and based on the energy approach (ref. [11]), is widely used by various authors in view of the structures made of materials in which the stress-strain state is not linear. At that, the researchers of the stress-strain state for the bearing system in the mode of failure of its individual elements highlight that if there is inelastic deformation detected in the construction material (and

Table 1. Correlated values of the solution results obtained through various methods.

# of element	Forces in element				Divergence of results through SCAD (%)	
	Intact system	Dynamics [15]	Dynamics [SCAD]	Quasi-statics k_d =2,0	vs. the results of [15]	vs. the results ofquasi-statics k_d =2,0
1-2	-28,778	-36,21	-36,404	-20,116	0,54	44,74
2-3	4,862	18,18	18,539	13,717	1,97	26,01
3-4	23,916	34,86	34,676	31,932	-0,53	7,91
4-5	23,916	35,03	35,597	39,712	1,62	-11,56
5-6	4,862	-20,29	-19,869	-52,084	-2,07	-162,14
6-7	-28,778	-30,66	-30,203	-13,16	-1,49	56,43
8-9	-11,822	-18,81	-17,202	-13,094	-8,55	23,88
9-10	-52,847	-66,68	-67,555	-53,93	1,31	20,17
10-11	-71,127	-87,93	-87,725	-73,05	-0,23	16,73
11-12	-71,127	-80,11	-80,171	-65,271	0,08	18,59
12-13	-52,847	-94,54	-94,811	-119,731	0,29	-26,28
13-14	-11,822	-13,74	-13,983	-6,134	1,77	56,13
1-8	-15,866	-22,18	-22,445	-16,82	1,19	25,06
2-9	7,498	12,00	12,257	5,733	2,14	53,23
3-10	5,019	7,39	7,514	2,767	1,68	63,18
4-11	5,309	9,20	9,712	8,264	5,57	14,91
5-12	5,019	-19,29	-18,779	-40,75	-2,65	-116,99
6-13	7,498	-10,22	-10,32	-38,4	0,98	-272,09
7-14	-15,866	-17,14	-17,244	-11,6	0,61	32,73
1-9	-43,556	-59,77	-59,558	-41,968	-0,35	29,53
2-8	14,777	23,06	22,293	16,367	-3,33	26,58
2-10	-27,274	-56,63	-54,172	-25,923	-4,34	52,15
3-9	7,726	14,49	14,477	9,079	-0,09	37,29
3-11	-16,091	-19,99	-20,04	-13,692	0,25	31,68
4-10	-4,424	-8,88	-8,616	-2,023	-2,97	76,52
4-12	-4,424	-13,38	-14,217	-11,751	6,26	17,35
5-11	-16,091	-24,5	-25,052	-23,415	2,25	6,53
5-13	7,726	48,32	47,918	91,332	-0,83	-90,60
6-12	-27,274	—	—	—	—	-
6-14	14,777	17,03	17,203	7,667	1,02	55,43
7-13	-43,556	-58,02	-57,717	-50,664	-0,52	12,22

with due regard to their consideration while performing the analysis), the dynamic factor decreases substantially and reaches the value of 1 (for reference see the studies by V.A. Almazov and his students).

The grounds of choosing the quasi-static methods are preconditioned by constant total energy for the element under consideration. Still it must be borne in mind that the total potential energy is a constant for the system in its entirety, and for the multi-element system it is very much likely to observe the shift of this value from one element to another in the process of deformation. In other words, it is not only a system with one degree of freedom, for which the concept of a dynamic factor appears worthwhile but also, on top

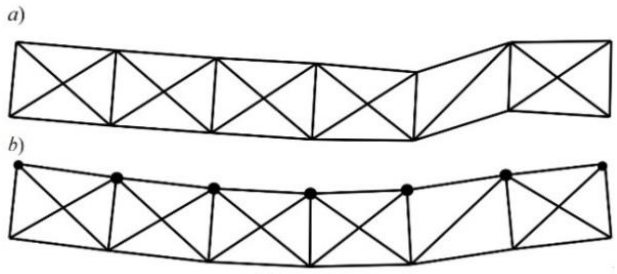


Figure 8. Juxtaposition of the deformation forms: a) static equilibrium form of the model without a removed element; b) the first form of self-induced oscillations of the model.

of everything, it is also a system with one deformable element.

The use of quasi-static methods for the system analysis which include 'special measures to prevent progressive collapse of the structure or part thereof' [5], e.g., outrigger floors (the overall view is shown in Figure 9), does not in principle enable us to obtain a correct result to be proved by the reasons given above.

Some aspects influencing the selection of time-dependent load increase.

First of all, this concerns the choice of the failure time t_d value. Owing to the ambiguity of this parameter, for structures of the increased criticality rating it is recommended to perform a series of calculations spotting a variation of t_d from 0.001 to 0.01 sec.

In the American regulatory document [17] it is indicated that $t_d \leq 0,1 T_{1,\text{failure}}$. Here $T_{1,\text{failure}}$ is the timeline of the initial stage of the self-induced oscillations detected in the failure-impacted design model, namely the design model from which the failed element under consideration has already been removed.

Some foreign sources [18, 19, 20] recommend considering the general integration time as no less than $0,5 \times T_{1,\text{failure}}$. This recommendation arises from the fact that the utmost values of internal forces upon the failure in the majority of cases act till the moment in time calculated as $0,5 \times T_{i,\text{failure}}$, where $T_{i,\text{failure}}$ is the oscillations cycle at i-th frequency of design model affected by failure in that way of oscillations which is the most proximate to the type of deformation upon the element failure (as per the type shown in Figure 8a).

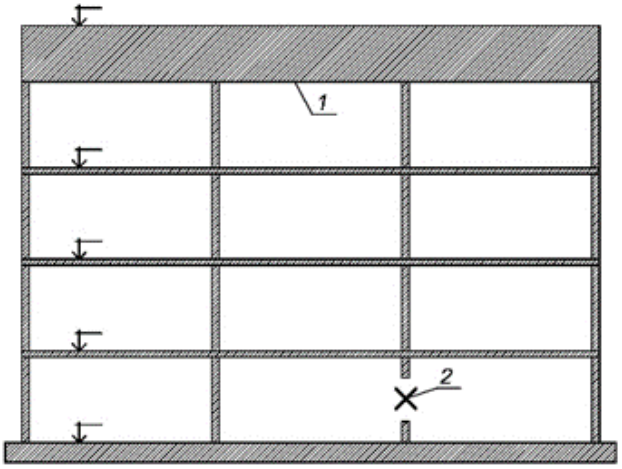


Figure 9. Overall view of the bearing system with outrigger floor: 1 – outrigger floor; 2 – local failure of a structural element.

3. CONCLUSIONS

Methods of design analysis of the bearing systems operation in the event of failure of an individual element should accurately account for the processes occurring in actual design. The failure of the local element leads to a realignment of not only the design analysis and the associated forces redistribution, but also results in rather complex dynamic phenomena. The application of simplified methods of the design analysis, i.e. a quasi-static method employing the dynamic factor does not ensure the conditions for modeling accuracy and, thus, the reliability of the design analysis outcome.

REFERENCES

1. **Kolchunov V.I., Klyueva N.V., Androsova N.B., Buchtiyarova A.S.** Zhivuchest' zdanii i Sooruzhenii pri Zaproektnykh Vozdeistviiakh [Survivability of Buildings and Structures Under the Impacts Beyond the Design]. Moscow, ASB, 2014, 208 pages.

2. **Klyueva N.V., Korenkov P.A.** Metodika Eksperimental'nogo Opredeleniia Parametrov Zhivuchesti Zhelezobetonnykh Ramno-Sterzhnevykh Konstruktivnykh Sistem [Experimental Determination Methods to Define Survivability Criteria for Reinforced Concrete Frame – Rod Structural Systems]. // Nonresidential Industrial and Civil Engineering, 2016, No. 2, pp. 44-48.
3. **Bondarenko B.M., Kolchunov V.I.** Kontseptsiia i Napravleniia Razvitiia Teorii Konstruktivnoi Bezopasnosti Zdanii i Sooruzhenii pri Silovykh i Sredovykh Vozdeistviiakh [Concepts and Development Trends in the Structural Safety Theory for Buildings and Structures Under the Impact of Stress and Environmental Effects]. // Nonresidential industrial and civil engineering, 2013. No. 2, pp. 28-31.
4. Federal'nyi Zakon "Tekhnicheskii Reglament o Bezopasnosti Zdanii i Sooruzhenii", 30.12.2009, No. 384-FZ [Federal Law No. 384 on Technical Regulations on the Safety of Buildings and Structures].
5. GOST 27751-2014 Nadezhnost' Stroitel'nykh Konstruktsii i Osnovanii. Osnovnye Polozheniia [State Standard GOST 27751-2014 on Reliability of Building Structures and Foundations. Main Provisions].
6. SP 296.1325800.2017 Zdaniia i Sooruzheniia. Osobye Vozdeistviia [Code of Practice SP 296.1325800.2017. Buildings and Structures. Special effects]. Ministry of construction of Russia. Moscow, 2017, 27 pages.
7. **Kudishin Yu.I., Drobot D.Yu.** Zhivuchest' Stroitel'nykh Konstruktsii – Vazhnyi Faktor Snizheniia Poter' v Usloviiakh Avariinykh Situatsii [Survivability of Structures as a Crucial Factor in Reducing Losses in Emergency Situations]. // Steel structures, 2009, Vol. 15, No. 1, pp. 59-71.
8. **Berzhinsky Yu.A., Berzhinskaya L.P.** Rezervy Zhivuchesti Bezrigel'nogo Karkasa pri Zaproektnykh Vozdeistviiakh [Survivability Margin of Girdles Frame Work Beyond the Design Impacts]. // Construction in Seismic-Prone Areas. Buildings Safety. 2013, No. 3, pp. 31-35.
9. **Kabantsev O.V.** Nekotorye Voprosy Metodiki Normirovanija Raschetov Zhelezobetonnyh Konstrukcij Vysotnyh Zdanij [Some Issues Related to Normalization of Calculations of the Reinforced Concrete Structures of High-Rise Buildings]. // Transregional Public Organization Assistance in Development and Application of Spatial Structures in Construction. Proc. of the scientific session reports, Moscow, 2009, pp. 36-39.
10. **Perelmuter A.V., Kabantsev O.V.** Uchet Izmeneniia Zhestkostei Elementov v Protsesse Montazha i Ekspluatatsii [Account of Changes in Stiffness of the Elements in the Course of Assembling and Operation]. // Journal on engineering and construction, 2015, No. 5, pp. 6-14.
11. **Geniev G.A.** Ob Ocenke Dinamicheskih Jeffektov v Sterzhnevyh Sistemah iz Hrupkih Materialov [On Evaluation of the Dynamic Effect in Rod Systems of Brittle Materials]. // Concrete and reinforced concrete, 1992, No. 9, pp. 25-27.
12. **Geniev G.A., Kolchunov V.I., Kluyeva N.V., Nikulin A.I., Pyatikrestovsky K.P.** Prochnost' i Deformativnost' Zhelezobetonnyh Konstrukcij pri Zaproektnyh Vozdejstvijah [Strength and Deformation Properties of Reinforced Concrete Structures Beyond the Design Impacts]. Moscow, ASV, 2004, 216 pages.
13. **Korenev B.G., Rabinovich I.M.** Dinamicheskij Raschet Zdanij i Sooruzhenij (Spravochnik Proektirovshhika) [Dynamic Calculation of Buildings and Structures (Designer manual)]. Moscow, Stroyizdat, 1984, 303 pages.
14. **Bondarev Yu.V., Nguen Thankh Suan.** Raschet Sterzhnevyh Sistem pri Vnezapnom Udalenii Otdel'nyh Jelementov [Calculation of Rod Systems at Sudden Removal of Individual Elements]. // Construction mechanics and calculation of structures, 2010, No. 4, pp. 43-48.

15. **Potapov A.N., Solomin V.I., Gerbensky A.V., Lemberg E.V.** Dinamicheskij Analiz Konstrukcij s Razrushajushhimi Svjazjami [Dynamic Analysis of Structures with Destructive Ties]. // Bulletin of the South Ural State University. Series: Construction and Architecture, 2012, No. 17 (276), pp. 8-12.
16. **Karpilovsky V.S., Kriksunov E.Z., Malyarenko A.A., Perelmuter A.V., Perelmuter M.A., Fialko S.U.** SCAD Office. Versija 21. Vychislitel'nyj Kompleks SCAD++ [SCAD Office. Version 21. Computational Software SCAD++]. Moscow, SCAD SOFT Publishing House, 2018, 948 pages.
17. **GSA** Alternate Path Analysis and Design Guidelines for Progressive Collapse Resistance. Washington, DC, General Services Administration, 2013, 127 pages.
18. **Fahnestock L., Hoffman S.T.** Behavior of Multi-Story Steel Buildings under Dynamic Column Loss Scenarios. // Steel and Composite Structures, 2011, Volume 11, No. 2, pp. 149-168.
19. **Gerasimidis S., Baniotopoulos C.C.** Disproportionate Collapse Analysis of Cable-Stayed Steel Roofs for Cable Loss. // International Journal of Steel Structures, 2011, Vol. 11, Issue 1, pp. 91-98.
20. **Zoli T, Woodward R.** Design of Long Span Bridges for Cable Loss. // IABSE Symposium: Structures and Extreme Events. Lisbon, Portugal, September 14-16, 2005, pp. 17-25.

СПИСОК ЛИТЕРАТУРЫ

1. **Колчунов В.И., Клюева Н.В., Андросова Н.Б., Бухтиярова А.С.** Живучесть зданий и сооружений при запроектных воздействиях. – М.: АСВ, 2014. – 208 с.
2. **Клюева Н.В., Кореньков П.А.** Методика экспериментального определения параметров живучести железобетонных рамно-стержневых конструктивных систем. // Промышленное и гражданское строительство, 2016, №2, с. 44-48.
3. **Бондаренко В.М., Колчунов В.И.** Концепция и направления развития теории конструктивной безопасности зданий и сооружений при силовых и средовых воздействиях. // Промышленное и гражданское строительство, 2013, №2, с. 28-31.
4. **Федеральный закон** «Технический регламент о безопасности зданий и сооружений» от 30.12.2009 №384-ФЗ.
5. **ГОСТ 27751-2014** Надежность строительных конструкций и оснований. Основные положения.
6. **СП 296.1325800.2017** Здания и сооружения. Особые воздействия. – М.: Министерство строительства и жилищно-коммунального хозяйства Российской Федерации, 2017. – 27 с.
7. **Кудишин Ю.И., Дробот Д.Ю.** Живучесть строительных конструкций – важный фактор снижения потерь в условиях аварийных ситуаций. // Металлические конструкции, 2009, том 15, №1, с. 59-71.
8. **Бержинский Ю.А., Бержинская Л.П.** Резервы живучести безригельного каркаса при запроектных воздействиях. // Сейсмостойкое строительство. Безопасность сооружений, 2013, №3, с. 31-35.
9. **Кабанцев О.В.** Некоторые вопросы методики нормирования расчетов железобетонных конструкций высотных зданий. // Межрегиональная общественная организация «Содействие развитию и применению пространственных конструкций в строительстве»: Тезисы доклада научной сессии. – М., 2009, с. 36-39.
10. **Перельмутер А.В., Кабанцев О.В.** Учет изменения жесткостей элементов в процессе монтажа и эксплуатации. // Инженерно-строительный журнал, 2015, №1(53), с. 6-14.
11. **Гениев Г.А.** Об оценке динамических эффектов в стержневых системах из хрупких материалов. // Бетон и железобетон, 1992, №9, с. 25-27.

12. **Гениев Г.А., Колчунов В.И., Клюева Н.В., Никулин А.И., Пятикрестовский К.П.** Прочность и деформативность железобетонных конструкций при запроектных воздействиях. – М.: АСВ, 2004. – 218 с.
13. **Коренев Б.Г., Рабинович И.М.** Динамический расчет зданий и сооружений (Справочник проектировщика). – М.: Стройиздат, 1984. – 303 с.
14. **Бондарев Ю.В., Нгуиен Тханх Суан.** Расчет стержневых систем при внезапном удалении отдельных элементов. // Строительная механика и расчет сооружений, 2010, №4(231), с. 43-48.
15. **Потапов А.Н., Соломин В.И., Гербенский А.В., Лемберг Е.В.** Динамический анализ конструкций с разрушающими связями. // Вестник Южно-Уральского государственного университета. Серия: Строительство и архитектура, 2012, №17(276), с. 8-12.
16. **Карпиловский В.С., Криксунов Э.З., Маляренко А.А., Перельмутер А.В., Перельмутер М.А., Фиалко С.Ю.** SCAD Office. Версия 21. Вычислительный комплекс SCAD++. – М.: SCAD Софт, 2018. – 948 с.
17. **GSA** Alternate Path Analysis and Design Guidelines for Progressive Collapse Resistance. Washington, DC: General Services Administration, 2013, 127 pages.
18. **Fahnestock L., Hoffman S.T.** Behavior of Multi-Story Steel Buildings under Dynamic Column Loss Scenarios. // Steel and Composite Structures, 2011, Volume 11, No. 2, pp. 149-168.
19. **Gerasimidis S., Baniotopoulos C.C.** Disproportionate collapse analysis of cable-stayed steel roofs for cable loss. // International Journal of Steel Structures, 2011, Vol. 11, Issue 1, pp. 91-98.
20. **Zoli T, Woodward R.** Design of Long Span Bridges for Cable Loss. // IABSE Symposium: Structures and Extreme Events. Lisbon, Portugal, September 14-16, 2005, pp. 17-25.

Anatoly V. Perelmuter, Foreign member of the Russian Academy of Architecture and Construction Sciences (RAACS), Doctor of Science, Professor; SCAD Soft Ltd; office 1,2, 3a Osvity street, Kiev, 03037, Ukraine;
phone: +38 044 249 71 93 (91), +38 044 248 71 00,
+38 044 248 80 60; e-mail: avp@scadsoft.com.

Oleg V. Kabantsev, Professor, Dr.Sc., Professor of Department of Reinforced Concrete and Masonry Structures; National Research Moscow State University of Civil Engineering; 26, Yaroslavskoe Shosse, Moscow, 129337, Russia; phone +7 (495) 287-49-14 add 3036, 3084;
E-mail: ovk531@gmail.com.

Перельмутер Анатолий Викторович, иностранный член Российской академии архитектуры и строительных наук (РААСН), профессор, доктор технических наук; НПО СКАД Софт; 03037, Украина, г. Киев, ул. Просвещения (Освиты), 3а, к. 1,2;
тел.: +38 044 249 71 93 (91), +38 044 248 71 00,
+38 044 248 80 60; e-mail: avp@scadsoft.com.

Кабанцев Олег Васильевич, доктор технических наук, профессор кафедры железобетонных и каменных конструкций, Национальный исследовательский Московский государственный строительный университет; 129337, Россия, г. Москва, Ярославское ш., 26, (SPIN-код: 2114-1185); тел. +7 (495) 287-49-14 add 3036, 3084;
E-mail: ovk531@gmail.com.

DOI:10.22337/2587-9618-2018-14-3-114-125

ABOUT THE FREE-VIBRATION MODE SHAPES OF ELASTOPLASTIC DISSIPATIVE SYSTEMS

Aleksander N. Potapov
South Ural State University (National Research University), Chelyabinsk, RUSSIA

Abstract: The author presents the conditions of the generalized orthogonality of the free-vibration mode shapes of an elastic dissipative system, for which traditional classical orthogonality conditions are a private case. As opposed to these conditions, the above ratios contain the mass matrix, the damping matrix, and the diagonal form of the spectral characteristics (damping coefficients and mode-shape frequencies). Within the theory of time analysis, free-vibration mode shapes of an elastoplastic system are built on the basis of using a schematized diagram of strain with hardening. The author proposes a design scheme that reduces the process of nonlinear vibrations to a sequence of processes flowing according to a linear scenario within the time intervals called quasilinear. In these intervals, the parameters of the dynamic model (elements of the stiffness matrix and the damping matrix) remain unchanged, all the changes occur only when passing through the critical points. As a result, the author formulated the condition for the nondegenerate state of an elastoplastic dissipative system. According to the condition, local plastic zones characterized by the size, the number and location of the zones on the design scheme of the structure correspond to each quasilinear interval. Since within the intervals, the parameters of the plastic zones are unchanged, the conditions of the generalized orthogonality of the mode shapes of the elastoplastic system are satisfied by analogy with the vibration mode shapes of an elastic dissipative system. The free-vibration motion of a hinged beam with three degrees of freedom are analyzed taking into account local plastic zones with different lengths and the location of zones in different nodes. It is shown that the configuration of the forms of elastoplastic oscillations differs qualitatively from the configuration of the corresponding forms of elastic vibrations.

Keywords: elastoplastic system, dissipative system, free-vibration mode shapes, plastic zone, orthogonality, stiffness matrix, damping matrix

О ФОРМАХ СОБСТВЕННЫХ КОЛЕБАНИЙ УПРУГОПЛАСТИЧЕСКИХ ДИССИПАТИВНЫХ СИСТЕМ

А.Н. Потапов
Южно-Уральский государственный университет (национальный исследовательский университет), г. Челябинск, РОССИЯ

Аннотация: Приведены условия обобщённой ортогональности форм собственных колебаний упругой диссипативной системы, для которых традиционные классические условия ортогональности являются частным случаем. В отличие от этих условий приведённые соотношения содержат связанные между собой матрицы масс, демпфирования и диагональную форму спектральных характеристик (коэффициентов демпфирования и частот собственных колебаний). В рамках теории временного анализа осуществлено построение форм собственных колебаний упругопластической системы на основе использования схематизированной диаграммы деформирования с упрочнением. Предложена расчётная схема, сводящая процесс нелинейных колебаний к последовательности процессов, протекающих по линейному сценарию на интервалах времени, называемых квазилинейными. На данных интервалах параметры расчетной динамической модели (элементы матриц жесткости и демпфирования) остаются неизменными, все изменения происходят только при переходе через критические точки. В результате сформулировано условие невырожденного состояния упругопластической диссипативной системы. Согласно условию, каждому квазилинейному интервалу соответствуют локальные пластические зоны, характеризуемые размерами, количеством и расположением зон на расчётной схеме сооружения. Так как внутри интервалов параметры пластических зон – неизменны, то условия обобщённой ортогональности собственных форм колебаний упругопластической системы выполняются по аналогии с формами колебаний упругой диссипативной системы. Проведён анализ собственных колебаний шарнирной балки с тремя степенями свободы с учётом локальных пластиче-

ских зон с различной длиной и различным расположением зон в узлах. Показано, что конфигурация собственных форм упругопластических колебаний качественно отличается от конфигурации соответствующих форм упругих колебаний.

Ключевые слова: упругопластическая система, диссипативная система, форма собственных колебаний, пластическая зона, ортогональность, матрица жёсткости, матрица демпфирования

1. INTRODUCTION

Modern structures operate in the conditions of complex dynamic influences, when maximum stresses in the main bearing elements often exceed the value of the elastic limit. Off the scale stresses must be considered, for example, in the design of seismic buildings and structures [1, 2]. In this case, the appearance of nonlinear strains in frame buildings is not only considered admissible, but also justified by special calculations for the organization of so-called "plasticity zones" generally located in horizontal bearing elements (crossbars). These zones are created in order to absorb the seismic action energy and its subsequent diversion (dissipation) into the environment, which ensures the integrity of the system in general. The developments in this field are reflected in national regulatory documents [3, 4] and in advanced foreign studies and regulations [5-7].

The presence of plastic zones in the bearing elements of structures naturally influences the system stiffness parameters, and, consequently, its internal dynamic characteristics. [8, 9] studied the behavior of the beams made of an elastoplastic material under impulse actions. [8] obtained an approximate solution of the problem of residual deflections of an impulse loaded rigidly fixed beam at its nonlinear vibrations, taking into account the sensitivity of the material to the strain rate in the plastic zone.[9]gives an original solution of the problem of free vibrations of a hinged beam beyond the elastic limit under the influence of a distributed impulse simulating an explosion, based on the analytical approach. The article presents algorithm of formation of mode frequencies for an ideal elastoplastic material and demonstrates a decrease of their values with an increasing length of the plastic zones.

Using computer simulation of frame buildings within of the elastoplastic analysis, frequency-damped characteristics and free-vibration mode shapes were determined on the basis of Prandtl diagram [10, 11]. A frame building was presented in the form of a discrete dissipative system (DDS), for which it was also shown that an increase in the yield in the frame floors leads to a decrease in the frequency spectrum.

The present work deals with the issues relating to the free-vibration motion in the DDS taking into account elastoplastic strains. We obtained the conditions, under which the fundamental properties of the orthogonality of free-vibration mode shapes are satisfied in a dissipative system in the yield state associated with the appearance of local plastic zones. The qualitative nature of the influence of a nonlinear process on the configurations of mode shapes is exemplified by a hinged beam.

2. BASIC RATIOS

Free-vibration mode shapes of any system (linear or nonlinear) are determined by its strained state caused by the action of inertial and dissipative forces. Free mode shapes are unchanged in the process of vibrations in a linearly strained system, so their configuration does not depend on time. It is manifested in a known property: the ratio of any two ordinates of the *k*-th mode shape is a constant value: $p_{jk} / p_{ik} = \text{const}$.

In the elastoplastic system, the appearance of yield in structural elements is accompanied by a decrease in its stiffness parameters. The presence of plastic strain zones in the structure leads to a redistribution of internal forces and stresses and, as a consequence, to a change in the configuration of mode shapes. Therefore, the ratio of the ordinates p_{jk} and p_{ik} of an arbitrary *k*-th mode shape of an elastoplastic system taken at different

instants of time will no longer be a constant value: $p_{jk} / p_{ik} \neq \text{const}$.

Let us denote the free-vibration mode shapes of a discrete system through P_k ($k = 1, \ldots, n$). These mode shapes have some properties known as orthogonality conditions. For an elastic conservative system, the mode shapes are orthogonal in relation to the mass matrix

$$M = \text{diag}\,(m_1, \ldots, m_n)$$

and to the stiffness matrix $K = K^{\mathrm{T}}$ [12, 13]:

$$P_j^{\mathrm{T}} M P_k = 0, \quad P_j^{\mathrm{T}} K P_k = 0 \qquad (k, j = 1, \ldots, n;\ k \neq j). \tag{1}$$

In case of the DDS vibrations, the damping matrix C is generally chosen so that the equations of motion could be reduced to a diagonal form. In this case, the matrix C corresponds to a proportional damping model [14], and one more orthogonality condition, including the damping matrix C, is added to the orthogonality conditions, which take the same form as for the conservative system:

$$P_l^{\mathrm{T}} C P_k = 0 \ (k \neq l). \tag{2}$$

The presence of conditions (1), (2) is a consequence of the separation of all the three forces: inertia, elasticity, and damping in the normal coordinates.

The equations of motion are not reduced to normal coordinates or dissipative structures with an arbitrary damping matrix. In this case, building of orthogonality ratios faces considerable difficulties [15-17], in particular, in [16, 17] the orthogonality conditions of the free-vibration mode shapes are obtained in convolutions.

The time analysis theory [11] introduces matrix conditions for the generalized orthogonality of free elastic vibration mode shapes of the DDS with an arbitrary symmetric damping matrix C. These ratios have a rather simple mathematical form (represented by equations (10), (12)) due to the developed apparatus associated with the analysis of the characteristic matrix quadratic equation (the equation of motion of mode shapes):

$$MS^2 + CS + K = 0. \tag{3}$$

Equation (3) in the basis consisting of the mode-shape vectors of the matrix

$$S = P \Lambda P^{-1}$$

has the form:

$$MP\Lambda^2 + CP\Lambda + KP = 0, \tag{4}$$

where S – matrix of internal dynamic characteristics of the system;

$$P = [P_1, \ldots, P_n]$$

– matrix of the mode-shape vectors (vibration mode shapes);

$$\Lambda = \text{diag}\,(\lambda_1, \ldots, \lambda_n)$$

– diagonal matrix of spectral characteristics.

Each vector P_k determining the k-th mode shape of damped vibrations corresponds to the characteristic complex number $\lambda_k = -\varepsilon_k + i\omega_k$, which contains the damping factor $\varepsilon_k$in the real part and the mode frequency ω_k in the imaginary part.

The solution of equation (3) is presented in the form of the root pair

$$S_{1,2} = M^{-1}(-C + V \pm U)/2, \tag{5}$$

where the matrices V and U have the properties of oblique and direct symmetry:

$$V = -V^{\mathrm{T}}, \ U = U^{\mathrm{T}},$$

and Vieta's formulas are valid for the root pair S_1, S_2

$$S_l^{\mathrm{T}} M + M S_m = -C, \quad S_l^{\mathrm{T}} M S_m = K \qquad (m, l = 1, 2;\ m \neq l). \tag{6}$$

Under the condition of a small dissipation, the elements of the matrices V and iU (i is the imaginary unit) belong to the real number field [11], therefore, the matrix roots (5) are complex conjugate $S_1 = S$, $S_2 = \bar{S}$. Then, ratios (6) are converted into the form:

$$S^*M + MS = -C, \quad S^*MS = K, \tag{7}$$

where $S^* = \bar{S}^{\mathrm{T}}$.
If the mode-shape matrix P is normalized, the symmetrical matrix U is determined by the formula

$$U = (PP^{\mathrm{T}})^{-1}.$$

3. GENERALIZED ORTHOGONALITY OF THE FREEVIBRATION MODE SHAPES OF AN ELASTIC DDS

Equation (3) is reduced to a system of equivalent equations [11]:

$$S^{\mathrm{T}}M + MS + C = U, \quad S^{\mathrm{T}}MS - K = US,$$

which after the transformation in the new basis are converted into the form:

$$\Lambda P^{\mathrm{T}}MP + P^{\mathrm{T}}MP\Lambda + P^{\mathrm{T}}CP = E, \tag{8}$$
$$\Lambda P^{\mathrm{T}}MP\Lambda - P^{\mathrm{T}}KP = \Lambda. \tag{9}$$

Matrix equation (8) is the ratio of the generalized orthogonality of the matrix P. Unlike traditional orthogonality conditions (1), (2), this equation contains the matrices M, C and the diagonal form Λ. Equation (9) is a diagonal form of writing the equation of motion of the free mode shapes (3). The left-hand side of this equation is an algebraic sum total of two terms, each of which is not a diagonal matrix in the general case.
Passing from equation (8) to the system of n^2 scalar equations, we obtain respectively $n(n–1)$ conditions of the generalized orthogonality of the mode shapes P_k, P_j (at $k \neq j$) and n conditions of their normalization (at $k = j$):

$$P_j^{\mathrm{T}}[M(\lambda_j + \lambda_k) + C]P_k = 0 (k \neq j), \tag{10}$$
$$P_k^{\mathrm{T}}[2M\lambda_k + C]P_k = 1 (k = j) \tag{11}$$
$$(k, j = 1, \ldots, n).$$

n^2 scalar rational so follow from the diagonal form equation (9), wherein $n(n–1)$ conditions analogous to the orthogonality ratios result at $k \neq j$ and n conditions at $k = j$:

$$P_j^{\mathrm{T}}[M\lambda_j\lambda_k - K]P_k = 0 (k \neq j), \tag{12}$$
$$P_k^{\mathrm{T}}[M\lambda_k^2 - K]P_k = \lambda_k (k = j) \tag{13}$$
$$(k, j = 1, \ldots, n).$$

In the private case of the conservative system ($C = 0$, $\varepsilon_j = \varepsilon_k = 0$), formulas (10), (12), due to $(\lambda_j + \lambda_k) = i(\omega_k + \omega_j) \neq 0$ and $\lambda_j \cdot \lambda_k = -\omega_k \cdot \omega_j \neq 0$, are reduced to ratios (1).
The conditions, under which the ratios of the generalized orthogonality (10), (12) become applicable to an elastoplastic system, are shown below.

4. NONDEGENERATE STATE OF THE ELASTOPLASTIC DDS

Let us consider a fragment of the design scheme (to be specific–a beam model) shown in Figure 1. Suppose that plastic strains develop near the j-th node forming a local zone with the sizes a_j and b_j (respectively, left and right of the node). In relative quantities, the length of this zone is determined by the parameters

$$\alpha_j = a_j/d, \quad \beta_j = b_j / d,$$

where d represents the distance between the adjacent nodes. At the boundaries of the plastic zone, the stress value corresponds to the yield limit σ_{yl}. According to the schematic diagram of strain with hardening (Figure 2), the maximum stress $\sigma_{\max}$ in the j-th node should not exceed the strength limit σ_u.
[11, 18] analyze elastoplastic systems using Prandtl diagram and the bilinear diagram.

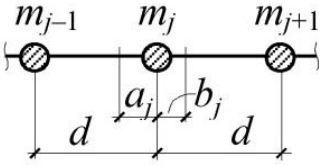


Figure 1. Fragment of the CMD with a plastic zone (a_i, b_i) near the j-th node.

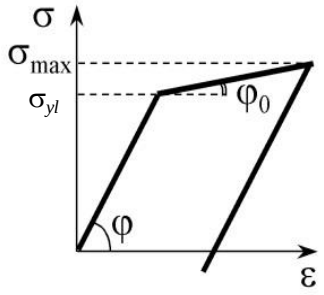


Figure 2. "σ-ε" bilinear diagram.

The process of calculating the inelastic response according to the mathematical vibration models was divided into a series of successive (quasilinear) intervals $t\in [t_i, t_{i+1}]$ (i = 0, 1, 2, …), within which the parameters of the design scheme (elements of the stiffness and damping matrices) remained unchanged. The elements of the mass matrix were taken constant during the entire elastoplastic strain process.

According to the proposed scheme of analysis, a certain local plastic zone (one or several) with fixed parameters, characterized by the sizes, number and location of the zones in the design scheme of the structure corresponds to the i-th quasilinear interval $t\in [t_i, t_{i+1}]$. Any non-linear events occurring in the structural elements of the system, including the beginning or the end of non-linear strains (yield and unloading), as well as changes in the parameters of the local plastic zones, are considered to occur only at the boundaries of these intervals–at the critical points t_i, t_{i+1}, ... As a result of this simulation, the inelastic analysis is reduced to a successive series of discretely varying systems that are implemented in these intervals according to the elastic design scheme.

The value of the determinant of the matrix $K(t_i) > 0$, where t_i is the time at the beginning of the i-th interval, is used to evaluate the nondegenerate state of a quasilinear system. The condition of the nondegenerate state is formulated as the following statement [11].

The stiffness matrix $K(t_i)$ of a quasilinear system is *nondegenerate if and only if both matrices of internal dynamical characteristics S_1, S_2* in (5) *are nondegenerate:*

$$\det K(t_i) > 0 \Leftrightarrow \det S_m \neq 0 \quad (m = 1, 2). \qquad (14)$$

The fact of non-degeneracy of both matrix roots S_m follows from the second Vieta's formula in (6). Let us demonstrate the need for the condition. Suppose that the matrix $K(t_i)$ is nondegenerate in the quasilinear interval $t\in[t_i, t_{i+1}]$, then

$$\det K(t_i) = \det (S_l^{\mathrm{T}} M S_m) =$$
$$= \det (S_l)\cdot\det (S_m)\cdot\det (M) > 0 \ (m\neq l).$$

Hence, $\det S_m \neq 0$ (m = 1, 2) follows for both matrices. The need is demonstrated. The sufficiency of the statement is also obvious.

It follows from the above result, under the condition of a small dissipation, that matrices (5) in the considered interval, as well as for the elastic solution, are presented in a complex conjugate form. Therefore, conditions (6) take the form analogous to (7):

$$S^* M + M S = -C(t_i),\ S^* M S = K(t_i). \qquad (15)$$

The following inequality results from the second ratio in (15) for the lower boundary of the matrix S:

$$\|S\| \geq \sqrt{\| M \|^{-1} \cdot \| K(t_i) \|},$$

where $\|\cdot\|$ – norm of the corresponding matrix. A decrease in the stiffness parameters with a growing yield leads to a decrease in the norm $\|K(t_i)\|$, and, consequently, $\|S\|$. At the same time, the weaker the norm of the matrix S, the smaller the modules of its characteristic numbers

$$\lambda_k = -\varepsilon_k + i\omega_k (k = 1, \ldots, n).$$

Since under the usual conditions of the elastic system vibrations, the damping coefficients $_k(t_0)$are

much less than the corresponding mode frequencies $\omega_k(t_0)$,these are the frequencies that are most sensitive to the change in the elements of the matrix K. Therefore, a decrease in the modules $\lambda_k$is initially due to a decrease in the frequency spectrum $\omega_k(t)$ ($k = 1, \dots, n$) (Figure 3).

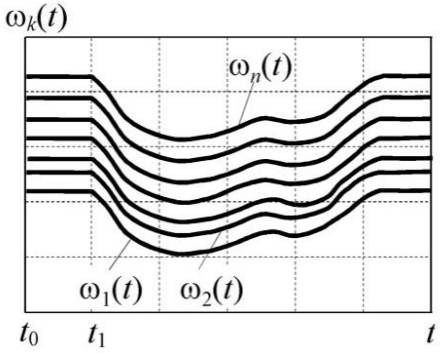


Figure 3. Frequency spectrum of a nondegenerate elastoplastic system in the course of vibrations.

Consequently, when condition (14) is met, the frequency spectrum is strictly positive and below the elastic one $0<\omega_k(t)\le\omega_k(t_0)$, where $\omega_k(t_0)$ is the mode frequency in the elastic state of the calculation model at $t\in[t_0, t_1]$.
Hence, it follows that all the mode shapes have a harmonic law of motion

$$\varphi_k(t) = (A_k \cos \omega_k t + B_k \sin \omega_k t)\, e^{-\varepsilon_j t},$$

where A_k, B_k represents arbitrary constants. For a conservative system ($C = 0$), there is no damping term in the equations of mode shapes.

5. GENERALIZED ORTHOGONALITY OF THE MODE SHAPES OF ANELASTOPLASTIC DDS

An important consequence of the above result is that, under the condition of a nondegenerate state of the elastoplastic system (14), equalities (8) – (13) will be satisfied together with ratios (15). In particular, the orthogonality conditions in the matrix (8) and scalar (10), (11) form, respectively, take the form:

$$\Lambda P^{\mathrm{T}} M P + P^{\mathrm{T}} M P \Lambda + P^{\mathrm{T}} C(t_i) P = E, \quad (16)$$

$$P_j^{\mathrm{T}}[M(\lambda_j + \lambda_k) + C(t_i)]P_k = 0 \ \ (k \neq j), \quad (17)$$

$$P_k^{\mathrm{T}}[2M\lambda_k + C(t_i)]P_k = 1 \ (k = j) \quad (18)$$

$$(k, j = 1, \dots, n).$$

These conditions will be valid only if two arbitrary mode shapes P_k, P_j ($k\neq j$) belong to the same quasilinear interval $t\in[t_i, t_{i+1}]$ or, which is the same, *correspond to the plastic zone (or zones) with the same parameters.*

6. EXAMPLE

Let us consider an example of elastoplastic vibrations of a hinged beam with three degrees of freedom ($n = 3$) under a dynamic action. The parameters of the design scheme of the beam are: I-beam No. 70, A516 steel, $E = 2{,}1\cdot10^5$ MPa, stiffness of the beam $EJ = 2{,}83\cdot10^9$ kN·cm^2, $d = 300$ cm (Figure 4a). The characteristics of the strength and deformability of the beam material: $\sigma_{yl} = 305$ MPa, $\sigma_u = 440$ MPa, $\delta_{yl} = \sigma_{yl}/E = 0{,}00145$, $\delta_u = 0{,}21$.
The mass matrix and stiffness matrix of the elastic system were:

$$M = \mathrm{diag}\,(0{,}5 \ \ 0{,}6 \ \ 0{,}5)\cdot10^{-2}\,\mathrm{kN\cdot s^2/cm},$$

$$K = \begin{bmatrix} 1{,}0319 & -0{,}9871 & 0{,}4038 \\ -0{,}9871 & 1{,}4357 & -0{,}9871 \\ 0{,}4038 & -0{,}9871 & 1{,}0319 \end{bmatrix}\cdot10^3 \ (\mathrm{kN/cm}).$$

A nonproportional damping model was used to build the damping matrix [11]:

$$C(t_i) = [K(t_i)T + TK(t_i)]/2,$$

where: $T = \gamma W_0^{-1}$, $W_0 = \mathrm{diag}(w_{01}, \dots, w_{0n})$, $w_{0i} = \sqrt{r_{jj} / m_j}$ (r_{jj},m_j– diagonal elements of the matrices $K(t_i)$ and M), $\gamma = \delta/\pi$, $\delta = 0{,}07$.
In the elastoplastic vibration mod shape, the stiffness matrix was formed using the flexibility matrix $L(t_i) = K(t_i)^{-1}$. The displacements$\delta_{kj}(t_i)$– elements of the flexibility matrix were determined by the known methods of structural mechanics, taking into account the presence of the plastic

zones in the nodal sections of the beam: $\delta_{kj}(t_i) = \delta_{kj} \cdot f_{kj}(t_i)$.Here,$\delta_{kj}$– elements of the flexibility matrix L of the elastic system; $f_{kj}(t_i)$–correction functions that take into account non-linear strains, depend on the size and location of the plasticity zones, on the value $\xi = E_0/E$, where$E$= tgφ, E_0= tgφ$_0$(ξ = 0,003). The functions $f_{kj}(t_i)$ (k, j= 1, 2, 3) for the plastic zones near nodes 2 (Figure 4*b*) and 3 (Figure 4*c*) are shown below.

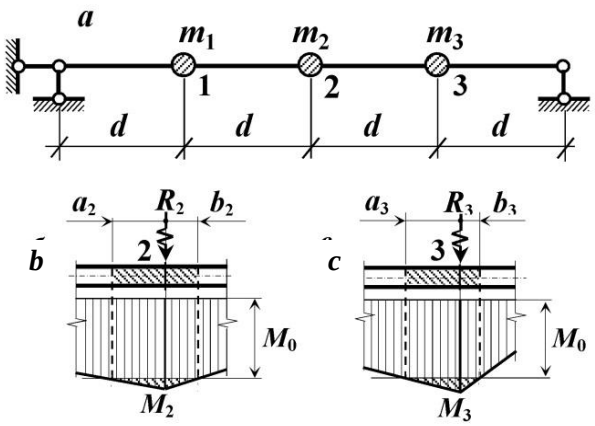


Figure 4. Design scheme of the beam (a); fragments of bending-moment curves for the plastic zones near: (b) – node 2; (c) – node 3.

Node 2 ($\alpha = a_2 / d$, $\beta = b_2 / d$):

$$f_{11} = 1 + \nu\cdot[\psi_1(\alpha) + \psi_2(\beta)]/36;$$
$$f_{22} = 1 + \nu\cdot[\psi_2(\alpha) + \psi_2(\beta)]/16;$$
$$f_{12} = f_{21} = 1 + \nu\cdot[\psi_3(\alpha) + \psi_2(\beta)]/22;$$
$$f_{33} = 1 + \nu\cdot[\psi_2(\alpha) + \psi_1(\beta)]/36;$$
$$f_{13} = f_{31} = 1 + \nu\cdot[\psi_3(\alpha) + \psi_3(\beta)]/28;$$
$$f_{23} = f_{32} = 1 + \nu\cdot[\psi_2(\alpha) + \psi_3(\beta)]/22,$$

where $\psi_1(\gamma) = 12\gamma + 6\gamma^2 + \gamma^3$, $\psi_2(\gamma) = 12\gamma - 6\gamma^2 + \gamma^3$, $\psi_3(\gamma) = 12\gamma - \gamma^3$($\gamma$= α, β),ν= (1/ ξ – 1).

Node 3 ($\alpha = a_3 / d$, $\beta = b_3 / d$):

$$f_{11} = 1 + \nu\cdot[\eta_1(\alpha) + \eta_3(\beta)]/36;$$
$$f_{22} = 1 + \nu\cdot[\eta_1(\alpha) + \eta_3(\beta)]/16;$$
$$f_{12} = f_{21} = 1 + \nu\cdot[\eta_1(\alpha) + \eta_3(\beta)]/22;$$
$$f_{33} = 1 + \nu\cdot[(27\alpha - 9\alpha^2 + \alpha^3) + 9\eta_3(\beta)]/36;$$
$$f_{13} = f_{31} = 1 + \nu\cdot[\eta_2(\alpha) + 3\eta_3(\beta)]/28;$$
$$f_{23} = f_{32} = 1 + \nu\cdot[\eta_2(\alpha) + 3\eta_3(\beta)]/22,$$

where: $\eta_1(\alpha) = 3\alpha + 3\alpha^2 + \alpha^3$,
$\eta_2(\alpha) = 9\alpha + 3\alpha^2 - \alpha^3$, $\eta_3(\beta) = 3\beta - 3\beta^2 + \beta^3$.

In Figure 4: M_0 – value of the limit moment corresponding to the yield limit; R_j– restoring force at the j-th node.

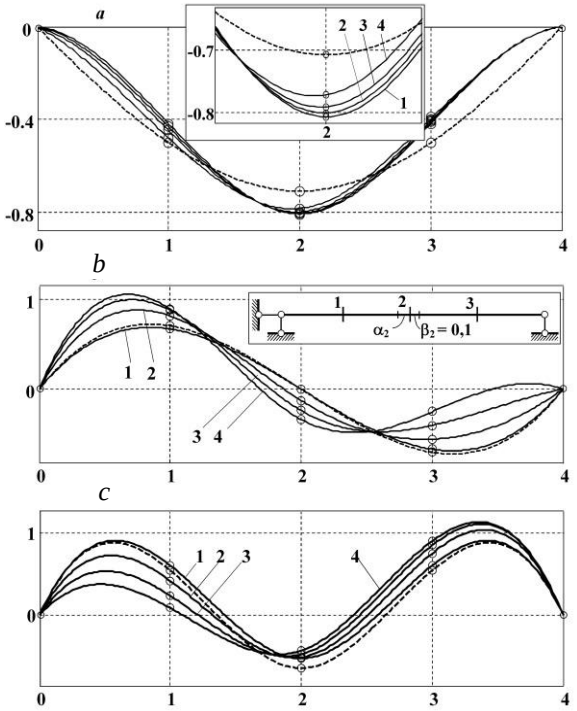


Figure 5. First (a), second (b) and third (c) free mode shapes for the yield zones in node 2 at α_2: 1 – 0,1; 2 – 0,2; 3 – 0,3; 4 – 0,5 (β_2 = 0,1).

We considered various vibration modes of the calculation beam model beyond the elastic limit. Figure 5 shows the free-vibration mode shapes P_k (k = 1, 2, 3) for local plastic zones of different lengths near node 2. Figures 6 and 7 show, respectively, the first and the second elastoplastic mode shapes of the beam for the plastic strains zones near nodes 2 and 3.

It follows from the analysis of Figures 5 – 7 that the configuration of the elastoplastic mode shapes differs sharply from the corresponding mode shapes of elastic vibrations, which are shown by a dotted line in all the figures. The configuration of the elasticoplastic modes depends on many factors: on the intensity of the yield strains development, which influences the sizes (length) of the plastic zones in the dangerous section (Figure 5); on the number of sections with the nonlinear work of the material; on the location of the zones in the design scheme (Figures 6, 7).

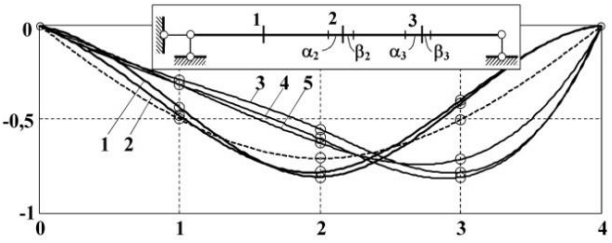


Figure 6. First free mode shape for the yield zones: 1 – $\alpha_2 = \beta_2 = 0{,}1$; 2 (5) – α_2 (α_3)=0,5; β_2 (β_3) = 0,1; 3 – $\alpha_3 = 0{,}05$; $\beta_3 = 0{,}005$; 4 – $\alpha_3 = 0{,}1$; $\beta_3 = 0{,}002$.

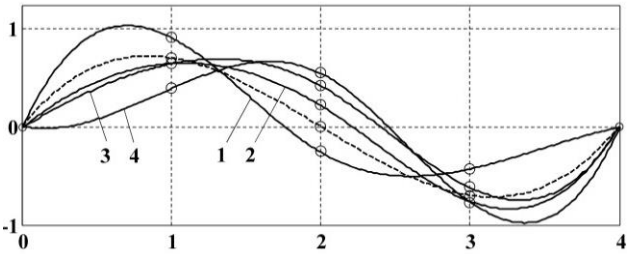


Figure 7. Second free mode shape for the yield zones: 1 – $\alpha_2 = 0{,}3$; $\beta_2 = 0{,}1$; 2 – $\alpha_3 = 0{,}002$; $\beta_3 = 0{,}002$; 3 – $\alpha_3 = 0{,}01$; $\beta_3 = 0{,}001$; 4 – $\alpha_3 = 0{,}5$; $\beta_3 = 0{,}002$.

The curvature of the rod axis sharply increases in the yield zones in comparison with the elastic sections of the design scheme; therefore, even in case of small sizes of the plastic zones, the free mode shapes can differ significantly from the corresponding elastic mode shapes. An example is the second mode shape in Figure 7 (position 2) built at the yield in the 3rd node for a local zone with the total length of 0,004*d*. In percentage terms, this length is (0,004*d*/4*d*)100% = 0,1% of the beam span $l = 4d$, i.e. 1/1000 part of the span, where the beam material works beyond the elastic limit. A comparison of this mode shape with its "double" –a mode shape obtained at the yield in the second node (Figure 7, position 1) with the length of the plastic zone 0,4*d* (10% of the beam span) shows that these mode shapes differ significantly by the configuration not only from the mode shape of elastic vibrations, but also from each other.

As it has already been noted, the critical zones in the elastoplastic process can change in size, disappear and appear again (due to multiple unloadings and loadings), change their location on the structure, etc. Since all this is connected with the appearance of the zones with a concentration of infinitely large curvatures, it will lead to a significant "distortion" of their mode shapes with respect to their elastic analogs and, eventually, to the modification of these mode shapes that cease to be similar to themselves in the process of nonlinear vibrations.

It should be noted that during a nonlinear analysis of structures using numerical methods of the stepwise integration, the dynamic response is generally built using the original (i.e., elastic) mode shapes of undamped vibrations. It is considered to be permissible, "if inelastic strains do not lead to major changes in the nature of their deflections ..." [12]. However, in practice, such estimates are difficult to implement, and their implementation provides for the creation of more sophisticated mathematical models that ensure building of free-vibration mode shape staking into account inelastic strains.

Resorting to the previous example, we will give a comparative analysis of the movements of the third node at elastoplastic beam vibrations caused by the action of the force R_3 (Figure 4c). For a plastic zone with the following parameters: $\alpha_3 = 0{,}002$; $\beta_3 = 0{,}001$,the node movements are 1,73 times larger than the corresponding elastic movements, i.e., the local zone with the total length of 0,003*d* = 0,9 cm leads to a change in the node movements by almost 2 times. If the zone sizes are doubled: $\alpha_3 = 0{,}004$; $\beta_3 = 0{,}002$, the ratio of the movements increases already in 2,45 times.

Thus, the proposed algorithm allows us to obtain not only qualitative but also quantitative estimates of the influence of the inelastic strains on the characteristics of the strain-stress state in the structure. Since even small plastic zones (less than 1 cm) can significantly alter the strained state of structural elements, it suggests the need to create new approaches that allow us to consider nonlinear strains when formation of mode shapes. In this connection, there arises a question

on the correctness of the methods based on the use of elastic vibration mode shapes in a nonlinear analysis, and an estimate of the error degree of such an analysis.

The final part of the paper gives an example of meeting the orthogonality conditions (16) for the free-vibration mode shapes of a beam with a local plastic zone in the second node (Figure 5). The correction functions $f_{kj}(t_i)$ are built for the parameters: $\alpha_2 = 0{,}2$; $\beta_2 = 0{,}1$. As a result, the values of the stiffness matrix and damping matrix were:

$$K(t_i) = \begin{bmatrix} 407{,}96 & -261{,}45 & 83{,}56 \\ -261{,}45 & 319{,}26 & -347{,}94 \\ 83{,}56 & -347{,}94 & 592{,}77 \end{bmatrix} \text{(kN/cm)},$$

$$C(t_i) = \begin{bmatrix} 0.0318 & -0.0228 & 0.00596 \\ -0.0228 & 0.0308 & -0.0281 \\ 0.00596 & -0.0281 & 0.0384 \end{bmatrix} \text{(kN·s/cm)}.$$

From the solution of (3) we obtained matrix roots (5) $S_1 = S$, $S_2 = \bar{S}$, which allows us to calculate the spectral characteristics – the mode-shape matrix P and the diagonal form Λ (the values of the matrices P and Λ correspond to the matrix S_1):

$$S_{1,2} = \begin{bmatrix} -3{,}18 \pm i258{,}77 & 2{,}02 \mp i132{,}44 & -0{,}59 \mp i0{,}62 \\ +2{,}12 \mp i110{,}37 & -2{,}57 \pm i136{,}67 & 2{,}75 \mp i128{,}78 \\ -0{,}60 \mp i0{,}62 & 2{,}31 \mp i154{,}53 & -3{,}84 \pm i314{,}05 \end{bmatrix} (c^{-1}),$$

$$P = \begin{bmatrix} 0.431 & 0.819 & 0.420 + i0{,}39 * 10^{-2} \\ 0.803 & -0.127 + i0{,}12 * 10^{-2} & -.509 - i0{,}46 * 10^{-2} \\ 0.411 & -0.560 - i0{,}25 * 10^{-2} & 0.752 \end{bmatrix},$$

$$\Lambda = \begin{bmatrix} \lambda_1 & 0 & 0 \\ 0 & \lambda_2 & 0 \\ 0 & 0 & \lambda_3 \end{bmatrix},$$

where: $\lambda_1 = -0{,}01 + i11{,}5$; $\lambda_2 = -2{,}91 + i279{,}8$; $\lambda_3 = -6{,}68 + i418{,}19$ (c^{-1}).

For comparison, λ_k corresponding to the elastic solution are shown: $\lambda_1 = -0{,}17 + i85{,}07$; $\lambda_2 = -3{,}08 + i354{,}43$; $\lambda_3 = -12{,}32 + i720{,}45$ (c^{-1}).

The above values of the matrices satisfy ratios (15), (16). Thus, the calculation of the left-side of ratio (16) leads to the identity matrix:

$$\Lambda P^{\mathrm{T}} M P + P^{\mathrm{T}} M P \Lambda + P^{\mathrm{T}} C P = \begin{bmatrix} 1 & 0 & 0 \\ 0 & 1 & 0 \\ 0 & 0 & 1 \end{bmatrix}.$$

The generalized orthogonality conditions presented by the scalar form of the ratios (17) are realized for off-diagonal elements of this matrix. The diagonal elements of the matrix are obtained by normalizing the mode-shape matrix P using the diagonal matrix D:

$$D = \begin{bmatrix} 1.962 - i1.963 & 0 & 0 \\ 0 & 0.422 - i0.423 & 0 \\ 0 & 0 & 0.336 - i0.339 \end{bmatrix},$$

which ensures the fulfillment of the conditions (18).

7. CONCLUSION

1. It is shown that:
- traditional (classical) ratios of the orthogonality for the free-vibration mode shapes are a private case of more general conditions of the generalized orthogonality of the mode shapes valid for an elastic dissipative system;
- the free mode shapes of an elastoplastic system in a quasilinear interval corresponding to the same parameters of the plastic zones have the property of the generalized orthogonality, which is determined by the equations analogous to the equations of an elastic dissipative system.

2. For the free-vibrations motion of a hinged beam with three degrees of freedom, taking into account the internal friction, it is shown that:
- elastoplastic mode shapes are qualitatively different from the corresponding mode shapes

of elastic vibrations in their configuration;

- arbitrary *k*-th free-vibration mode shapes formed for the plastic zones located in different nodes of the calculation model, also differ from each other in their configuration.

3. The proposed algorithm allows us to obtain not only qualitative but also quantitative estimates of the influence of the inelastic strains on the strain-stress state characteristics of the structure. The development of this approach to formating of mode shapes, taking into account the elastoplastic strains, opens the possibility of creating more sophisticated structural analysis methods at nonlinear vibrations.

REFERENCES

1. **Kilimnik L.Sh**. K Razrabotke Metodiki Otsenki Predel'nykh Sostoianii Mnogoetazhnykh Karkasnykh Zdanii pri Seismicheskikh Vozdeistviiakh [To the Development of a Procedure for Estimating the Limiting States of Multi-Story Frame Buildings under Seismic Influence]. // Proceedings of the Central Research Institute of Building Constructions named after V.A. Kucherenko, 1975, Issue 44, pp. 66-82.
2. **Newmark N., Rosenblueth E.** Osnovy Seismostoikogo Stroitel'stva **[**Fundamentals of Earthquake Engineering]. Moscow, Stroyizdat, 1980, 344 pages.
3. Svod pravil SP 14.13330.2014 Stroitel'stvo v Seismicheskikh Raionakh SNiP II-7-81* [Rules and Regulations SP 14.13330.2014 / Construction in Seismic Regions SNiP II-7-81*]. Moscow, 126 pages.
4. **Sosnin A.V.** Ob Osobennostiakh Metodologii Nelineinogo Staticheskogo Analiza i Ego Soglasovannosti s Bazovoi Normativnoi Metodikoi Rascheta Zdanii i Sooruzhenii na Deistvie Seismicheskikh Sil [On the Features of the Methodology of the Non-Linear Static Analysis and its Consistency with the Basic Normative Methodology for Structural Engineering for the Action of Seismic Forces]. // Bulletin of the SUSU. Series "Construction and Architecture", 2016, Vol. 16, No. 1, pp. 12-19.
5. **Paulay T., Priestley M.J.N.** Seismic Design of Reinforced Concrete and Masonry Buildings. New York: John Wiley&Sons, Inc., 1992. – 744 p.
6. **Inel M., Ozmen H.B.** Effects of Plastic Hinge Properties in Nonlinear Analysis of Reinforced Concrete Buildings // Engineering Structures. No. 28. 2006. PP. 1494-1502.
7. **Gorji M.S., Moghaddam M.Z.** Analysis of the Resistance of Joints in Reinforced Concrete Strengthened by FRP Sheets against Released Forces of Earthquake. // Journal of American Science, 2011, No. 7(9), pp. 995-999.
8. **Naida A.A.** Ostatochnye Deformatsii Impul'sno Nagruzhennykh Balok, Dopuskaiushchikh Bol'shie Progiby v Predelakh Uprugostil [Residual Strains of Impulse Loaded Beams Allowing Large Bends Within the Elasticity Range]. // Scientific notes of the Central Aerohydrodynamic Institute, 1987, V. XVIII, No. 5, pp. 106-112.
9. **Vitvitskiy N.K.** Vychislenie Chastot Sobstvennykh Izgibnykh Kolebanii Balok za Predelom Uprugosti pri Nalichii Plasticheskikh Zon [Calculation of the Frequencies of Free Bending Vibrations of Beams Beyond the Elastic Limit in the Presence of Plastic Zones]. // News of S.M. Kirov's Tomsk Polytechnic Institute of the Order of the Red Banner of Labor, 1967, Vol. 154, pp. 28-34.
10. **Potapov A.N.** Analiz Vnutrennikh Dinamicheskikh Parametrov Konstruktsii pri Neuprugikh Kolebaniiakh [Analysis of Internal Dynamic Parameters of Structures at Inelastic Vibrations]. // News of higher educational institutions. Construction, 2000, No. 6, pp. 31-37.
11. **Potapov A.N.** Dinamicheskii Analiz Diskretnykh Dissipativnykh Sistem pri Nestatsionarnykh Vozdeistviiakh [Dynamic Analysis of Discrete Dissipative Systems

under Nonstationary Influences: monograph]. Chelyabinsk, Publishing House of the SUSU, 2003, 167 pages.
12. **Clough R., Penzien D.J.** Dinamika Sooruzhenii [Dynamics of Structures]. Moscow, Stroyizdat, 1979, 320 pages.
13. **Kiselev V.A.** Stroitel'naia Mekhanika [Structural Mechanics]. // Special course: Dynamics and Stability of Structures. Moscow, Stroyizdat, 1980, 616 pages.
14. **Sorokin E.S.** O Pogreshnostiakh Obshcheizvestnogo Metoda Teorii Kolebanii Dissipativnykh Sistem v Primenenii k Neodnorodnomu Dempfirovaniiu [On the Errors of the Well-Known Method of the Theory of Vibrations in Dissipative Systems as Applied to Inhomogeneous Damping]. Structural Mechanics and Analysis of Constructions, 1984, pp. 29-34.
15. **Harris S.M., Krid C.I.** Spravochnik po Udarnym Nagruzkam [Handbook on Shock Loads]. London, Shipbuilding, 1980, 360 pages.
16. **Pashkov I.A.** Ob Ortogonal'nosti Sobstvennykh Form Kolebanii Viazkouprugogo Tela [On the Orthogonality of Free-Vibration Mode Shapes of a Viscoelastic Body]. // News of the Academy of Sciences of the USSR. Solid Mechanics. 1989, No. 4, pp. 104-111.
17. **Pashkov I.A., Troyanovsky I.E.** Metod Razlozhenii po Sobstvennym Formam Kolebanii Uprugogo Tela s Vnutrennim i Vneshnim Treniem [Method of Splitting by the Free-Vibration Mode Shapes of an Elastic Body with Internal and External Friction]. // Applied Mathematics and Mechanics, 1991, Vol. 55, Issue 6, pp. 972-981.
18. **Potapov A.N., Zyambaev N.A.** Postroenie Matematicheskoi Modeli Fizicheski Nelineinykh Kolebanii Mnogoetazhnogo Karkasa [Building of a Mathematical Model of Physically Nonlinear Vibrations of a Multistoried Frame]. // Bulletin of the SUSU. Series “Construction and Architecture”, 2017, Vol. 17, No. 3, pp. 12-17.

СПИСОК ЛИТЕРАТУРЫ

1. **Килимник Л.Ш.** К разработке методики оценки предельных состояний многоэтажных каркасных зданий при сейсмических воздействиях. // Труды Центрального научно-исследовательского институт строительных конструкций им. В.А. Кучеренко, 1975, Вып. 44, с. 66-82.
2. **Ньюмарк Н., Розенблюэт Э.** Основы сейсмостойкого строительства. – М.: Стройиздат, 1980. – 344 с.
3. **Свод правил** СП 14.13330.2014 / Строительство в сейсмических районах СНиП II-7-81*. – М., 126 с.
4. **Соснин А.В.** Об особенностях методологии нелинейного статического анализа и его согласованности с базовой нормативной методикой расчета зданий и сооружений на действие сейсмических сил. // Вестник ЮУрГУ. Серия «Строительство и архитектура», 2016, Том 16, №1, с. 12-19.
5. **Paulay T. Priestley M.J.N.** Seismic Design of Reinforced Concrete and Masonry Buildings. New York, John Wiley&Sons Inc., 1992, 744 pages.
6. **Inel M., Ozmen H.B.** Effects of Plastic Hinge Properties in Nonlinear Analysis of Reinforced Concrete Buildings. // Engineering Structures, 2006, No. 28, pp. 1494-1502.
7. **Gorji M.S., Moghaddam M.Z.** Analysis of the Resistance of Joints in Reinforced Concrete Strengthened by FRP Sheets against Released Forces of Earthquake. // Journal of American Science, 2011, No. 7(9), pp. 995-999.
8. **Найда А.А.** Остаточные деформации импульсно нагруженных балок, допускающих большие прогибы в пределах упругости. // Ученые записки ЦАГИ, 1987, Том XVIII, №5, с. 106-112.
9. **Витвицкий Н.К.** Вычисление частот собственных изгибных колебаний балок за пределом упругости при наличии пластических зон. // Известия Томского ор-

дена трудового красного знамени политехнического института им. С.М. Кирова, 1967, Том 154, с. 28-34.
10. **Потапов А.Н.** Анализ внутренних динамических параметров конструкций при неупругих колебаниях. // Известия вузов. Строительство, 2000, №6, с. 31-37.
11. **Потапов А.Н.** Динамический анализ дискретных диссипативных систем при нестационарных воздействиях. – Челябинск: Издательство ЮУрГУ, 2003. – 167 с.
12. **Клаф Р., Пензиен Д.Ж.** Динамика сооружений. – М.: Стройиздат, 1979. – 320 с.
13. **Киселев В.А.** Строительная механика. Специальный курс: Динамика и устойчивость сооружений. – М.: Стройиздат, 1980. – 616 с.
14. **Сорокин Е.С.** О погрешностях общеизвестного метода теории колебаний диссипативных систем в применении к неоднородному демпфированию. // Строительная механика и расчёт сооружений, 1984, с. 29-34.
15. **Харрис С.М., Крид Ч.И.** Справочник по ударным нагрузкам. – Л.: Судостроение, 1980. – 360 с.
16. **Пашков И.А.** Об ортогональности собственных форм колебаний вязкоупругого тела. // Известия АН СССР. Механика твердого тела, 1989, №4, с. 104-111.
17. **Пашков И.А., Трояновский И.Е.** Метод разложений по собственным формам колебаний упругого тела с внутренним и внешним трением. // Прикладная математика и механика, 1991, Том 55, Вып. 6, с. 972-981.
18. **Потапов А.Н., Зямбаев Н.А.** Построение математической модели физически нелинейных колебаний многоэтажного каркаса. // Вестник ЮУрГУ. Серия «Строительство и архитектура», 2017, Том 17, №3, с. 12-17.

Alexander N. Potapov, Professor, Dr.Sc., Department “Construction production and theory of structures”, South-Ural State University (National Research University); 76, Lenina Avenue, Chelyabinsk, 454080, Russia;
phone: +7(351)267-91-83, +7(919)343-71-29;
E-mail: potapov.alni@gmail.com.

Потапов Александр Николаевич, профессор, доктор технических наук, кафедра «Строительное производство и теория сооружений», Южно-Уральский государственный университет (национальный исследовательский университет); 454080, Россия, г. Челябинск, проспект Ленина, дом 76;
тел.: +7(351) 267-91-83, +7(919)343-71-29
E-mail: potapov.alni@gmail.com.

DOI:10.22337/2587-9618-2018-14-3-126-135

COMPUTER MODELLING OF THE STRESS-STRAIN STATE OF PLUG-IN CONNECTIONS OF REINFORCED CONCRETE COLUMNS WITH THE COVERAGE PLATES UNDER THE OUT-OF-SQUARE ECCENTRIC COMPRESSION

Boris S. Sokolov [1]***, Evgeniy O. Troshkov*** [2]
[1] Joint Stock Company "Kazan Giproniiaviaprom", Kazan, RUSSIA
[2] Povolzhsky State Technological University, Yoshkar-Ola, RUSSIA

Abstract: The technique and results of computer simulation of the stress-strain state of plug joints of reinforced concrete columns with overlap plates under the effect of out-of-square eccentric compression are described. An analysis of the results obtained is provided to optimize the experimental research plan and to develop a technique for calculating the strength of the joints used in the UICSS bearing system.

Keywords: numerical methods, finite element method, reinforced concrete structures, plug-in joint, stress-strain state

КОМПЬЮТЕРНОЕ МОДЕЛИРОВАНИЕ НАПРЯЖЕННО-ДЕФОРМИРОВАННОГО СОСТОЯНИЯ ШТЕПСЕЛЬНЫХ СТЫКОВ ЖЕЛЕЗОБЕТОННЫХ КОЛОНН С ПЛИТАМИ ПЕРЕКРЫТИЯ ПРИ КОСОМ ВНЕЦЕНТРЕННОМ СЖАТИИ

Б.С. Соколов [1]***, Е.О. Трошков*** [2]
[1] Акционерное общество «Казанский Гипрониавиапром», г. Казань, РОССИЯ
[2] Поволжский государственный технологический университет, г. Йошкар-Ола, РОССИЯ

Аннотация: В статье описывается методика и результаты выполненного компьютерного моделирования напряженно-деформированного состояния штепсельных стыков железобетонных колонн с плитами перекрытия при действии косового внецентренного сжатия. Приводится анализ полученных результатов, необходимый для оптимизации плана экспериментальных исследований и разработки методики расчета прочности изучаемых стыков, применяемых в несущей системе «УИКСС».

Ключевые слова: численные методы, метод конечных элементов, железобетонные конструкции, штепсельный стык, напряженно-деформированное состояние

1. INTRODUCTION

The construction of buildings using prefabricated reinforced concrete frame systems is widely used in the territory of the Russian Federation, since it minimizes the labor and financial costs of their erection, and also shortens construction time. The development of technologies promotes the use of new variants of constructive framing solutions, one of which is the precast reinforced concrete bearing system with beamless floor "UIKSS" ("Universal Industrial Frame Construction System") (Figure 1) [1]. A feature of such a frame is the use of plug-in joints for connecting floor slabs to columns.

The proposed joint (Figure 2) is a structure in which the lower column (1) has the outlets (2), in the plate (5) are located the holes (6) for placing these rods, and the upper column (3) is equipped

with boreholes (4), which, when mounted through special holes (7), are injected with a grouting compound. Prior to installation, steel or synthetic (polymeric) centering gaskets (8) are installed on the bottom column and plate.

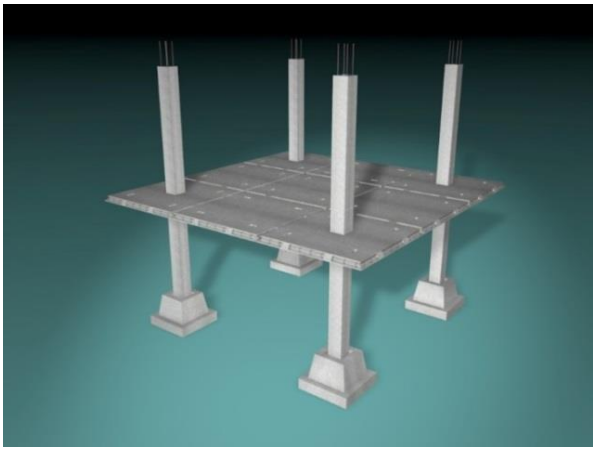


Figure 1. General view of the base cell of the frame system "UIKSS".

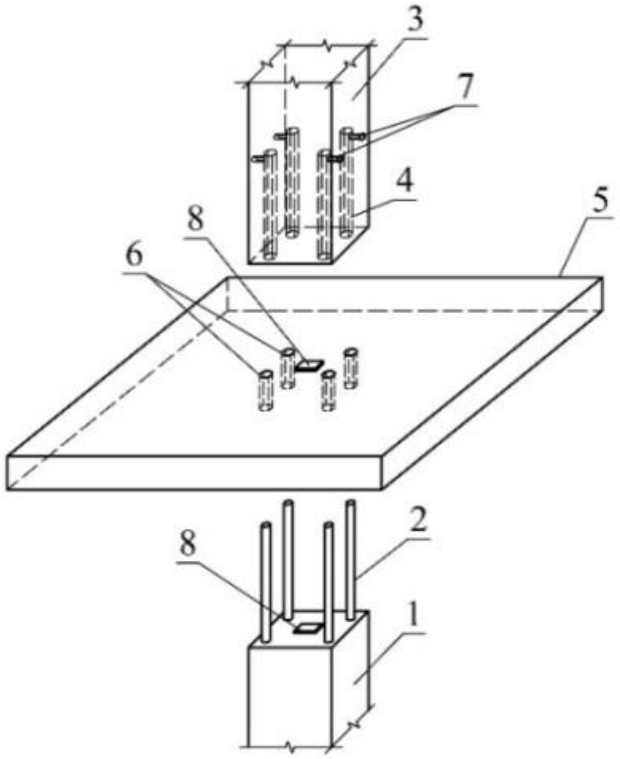


Figure 2. General view of the column joint with a slab.

The "UIKSS" system is applicable for the design and construction of low-rise private, residential multi-apartment and public buildings, school and preschool institutions, as well as for the reconstruction of buildings and structures [2,3, etc.].

The introduction of the proposed frame system is hampered by the absence in the scientific and technical literature on methods for calculating the strength and deformation of the plug joints located in the zone of action of longitudinal and transverse forces and bending moments, therefore for the development of such techniques it is necessary to conduct stress-strain analysis (SSA) of the joints. The study of SSA data of joints includes theoretical, numerical and experimental studies.

2. FORMULATION OF RESEARCH PROBLEMS

The analysis of available scientific, technical and normative literature allowed the authors to divide the joints studied into three types depending on their location in the overlap and on the resulting combinations of forces:

- medium, located in the middle part of the overlap, where the compressive forces with random eccentricity mainly act;
- extreme, connecting the overlapping plates with columns of the extreme row and perceiving longitudinal and transverse forces and bending moments;
- angular, perceiving longitudinal forces, as well as transverse forces, bending and twisting moments in two directions.

In [4,5, etc.] the results of the study of medium and extreme joints are published. This article is devoted to the study of the SSA of corner joints with oblique eccentric compression with the use of computer modeling. The most relevant studies in this area are the work of T.S. Evdokimova, dedicated to the SSA of skew-collapsible fiber-reinforced concrete elements and made under the supervision of the Doctor of Technical Sciences, Professor V.I. Morozov [6,7]. The difference between the author's studies is the study of the SSA of the contact zone of reinforced concrete joint elements under the action of oblique eccentric compression.

Numerical studies were carried out in the PC LIRA-SAPR 2013 R3 implementing the finite element method (FEM) and possessing the necessary functionality for solving the set tasks, including:

- obtaining data on destruction schemes, distribution of stresses in concrete and strength of the joint, as well as its individual elements;
- determination of geometric characteristics of the calculated zones of concrete structures and stresses arising in the reinforcement;
- identify the features of the SSA elements of the joint, taking into account the effect of a combination of loads on the column and slab;
- optimization of the program for conducting physical experiments and reducing the costs of their implementation.

3. METHODOLOGY OF RESEARCH

Numerical studies were carried out taking into account the physical nonlinearity of materials. In the modelling, we used volume isoparametric finite elements (FE) of type 236 and 234 and universal spatial rod FE – type 410.

The physical and mechanical characteristics of concrete were modeled according to the law of deformation of GA. Geniev [8]. The design resistance of the material to compression and stretching, as well as ultimate deformations, were taken according to the current norms [9]. The stiffness characteristics of reinforcing steel were described by two-line diagrams [9].

One of the important issues in the simulation of the SSA of reinforced concrete structures is the issue of the coupling of reinforcing bars to concrete [10 - 12], and in the study of the work of plug joints – the coupling of reinforcing elements with the injection of wells. Analysis of the literature showed that this problem can be solved using various computational models of FEM [13 ± 15]. In the numerical studies carried out, the adhesion of the reinforcement to the concrete and the injection solution is realized by simulating common nodes of elements, without assigning additional boundary conditions.

The simulation was carried out with a step-by-step increase in the load, allowing the structures to be brought to virtual destruction, which is necessary to evaluate the SSA of the joint elements at each loading stage. Criteria for failure were the attainment of limiting stress values along the main areas in the group of bulk FEs, the yield stress in reinforcing bars, and the transition of the system to a geometrically variable one.

To model and study SSA of the joint it was necessary to determine the possible values of eccentricities under the action of external loads. To solve this problem, static calculations of 2-, 3-, 4-, 5-, and 6-storey double-span building schemes loaded with vertical loads were performed earlier. The performed calculations showed that for angular joints the greatest values of the eccentricities of the longitudinal force arise in the coating level,

$$\frac{e_{0x}}{h} = 1{,}68;\ \frac{e_{0y}}{h} = 1.$$

Eccentricities in joints of other floors are within

$$\frac{e_{0x}}{h} = 0{,}09 \ldots 0{,}44;\ \frac{e_{0y}}{h} = 0{,}06 \ldots 0{,}25.$$

The obtained data allow carrying out numerical studies of SSA.

Samples in the numerical studies carried out had the parameters shown in Figure 3. A general view of the FEM of the joint is shown in Figure 4. The maximum geometric dimensions of volumetric FE columns are taken as 25 × 25 × 20 mm. Wells were modeled by volumetric FE with six nodes converging at the central point and simulating the cylindrical shape (see Fig. 4, *b*).

In the framework of numerical studies of the SSA with out-of-square eccentric compression, calculations of the ES-II-5 and ES-II-5.1 series samples were performed. Variable parameters and research tasks are shown in Table 1.

The models of the ES-II-5 series were calculated under the action of constant values of the uniformly distributed vertical load on the overlap (q = 4 kN/m^2) and horizontal loads applied to the slab in two directions ($Q_x = Q_y$ = 40 kN).

Table 1. Variable parameters and research problems.

Model family	Real load	Variable feature	Research objectives
ES-II-5	q = 4 kN/m^2; $Q_x = Q_y$ = 40 kN; N – step-up	*a*) $e_{0X}/h = e_{0Y}/h$ = 0.125; *b*) $e_{0X}/h = e_{0Y}/h$ = 0.25; *c*) $e_{0X}/h = e_{0Y}/h$ = 0.375	Definition of: • destruction schemes; • geometric characteristics of the calculated zones of the contact zone according to the theory of the resistance of anisotropic materials to compression; • stresses in armature, straps made of steel strip, indirect reinforcement mesh
ES-II-5.1	q = 0 kN/m^2; $Q_x = Q_y$ = 0 kN; N – step-up		

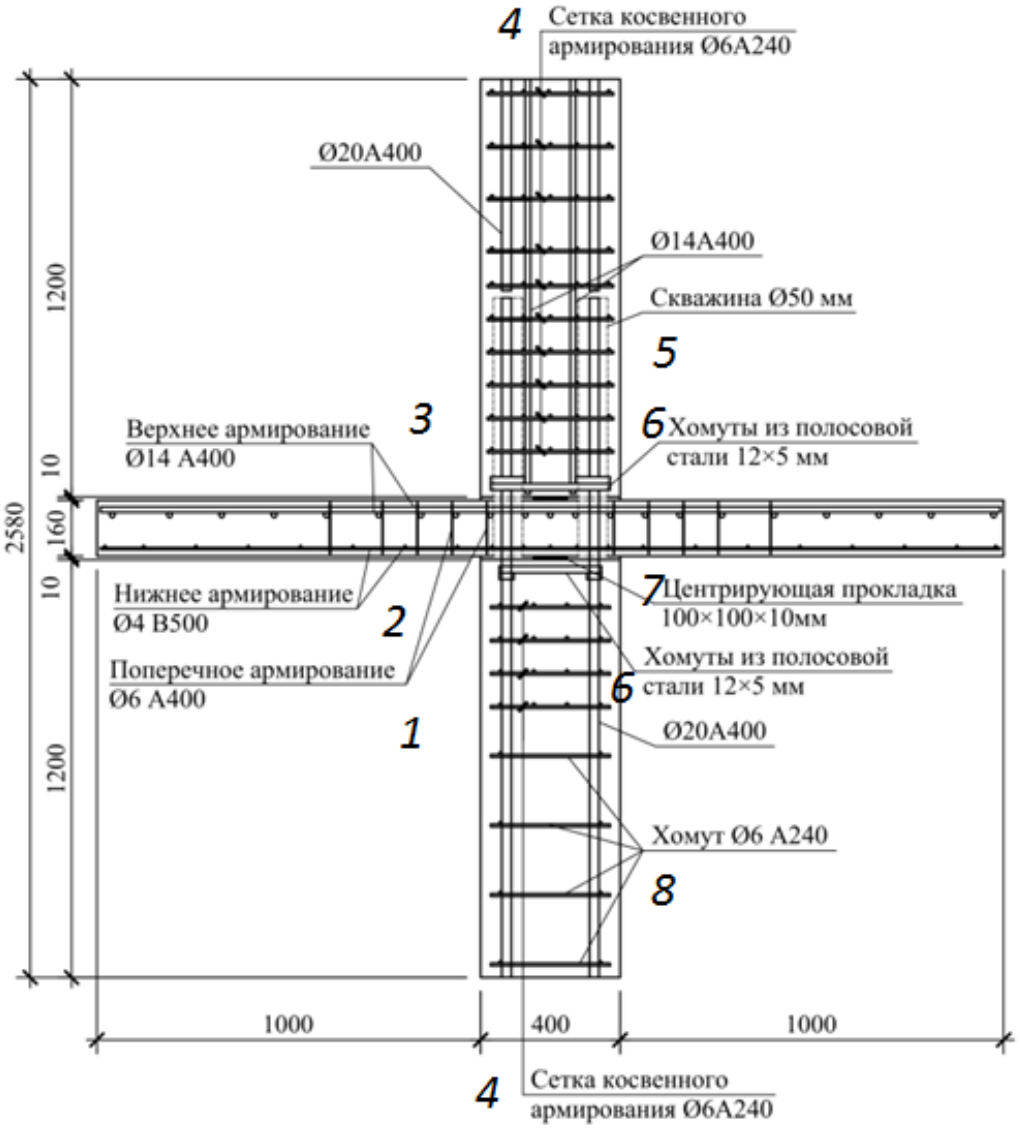
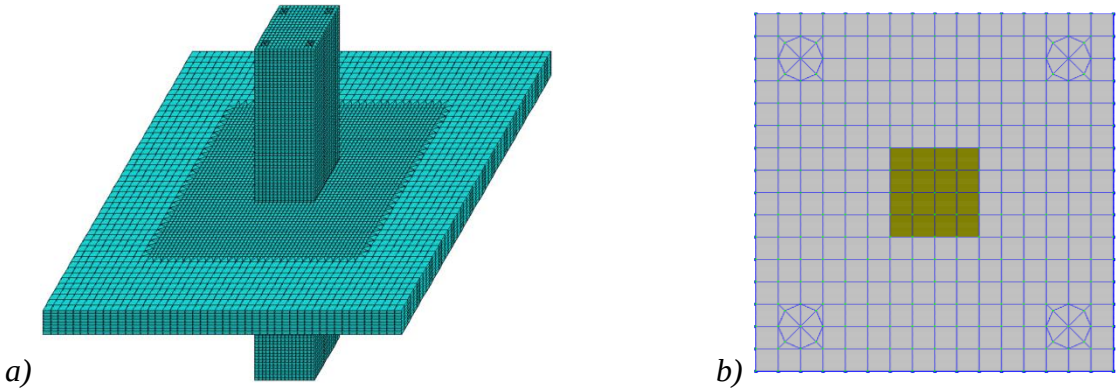


Figure 3. Geometric dimensions and reinforcement scheme for simulated samples: 1 — lateral reinforcement; 2 — bottom reinforcement; 3 — top reinforcement; 4 — grid of confinement reinforcement; 5 — cored hole; 6 — yokes from strap iron; 7 — aligning gasket; 8 — yoke.



a) *b)*

Figure 4. Finite-element design model of the joint: a — general view; b — column with centering gasket (top view).

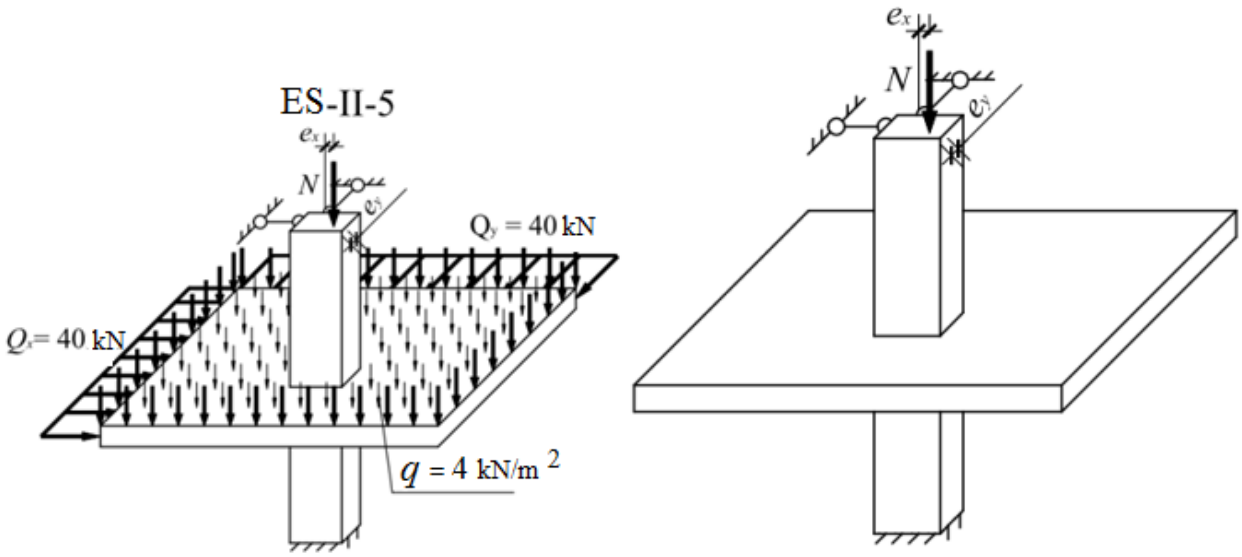


Figure 5. Loading scheme for models ES-II-5 and ES-II-5.1.

In this case, a step-by-step increase in the vertical load on the column with different values of eccentricity and bringing the model to destruction was performed (Figure 5).

4. ANALYSIS OF THE RESULTS OF THE RESEARCH

The destruction pattern of ES-II-5 and ES-II-5.1 series samples should be characterized as the achievement of the endurance strength of the end sections of the columns in the contact zone. The analysis of the principal stresses and the failure scheme showed that their SSA corresponds to the theory of the strength resistance of anisotropic materials to compression [16], while the triaxle compression zone is displaced along the *x* and *y* axes by equal distances with respect to the center of the section, and the slope angles of the wedge α correspond to the theoretical ones [16].

The results of modeling of the ES-II-5 series made it possible to reveal a feature that the geometric characteristics of the calculated zones of the end sections of the upper and lower columns (the wedge height h_k and the width of the L_{loc} load transfer zone) are different. The values of these parameters in the upper column coincide with those obtained in the simulation of eccentric compression with eccentricity of one direction, and in the lower column have large values (Figure 6).

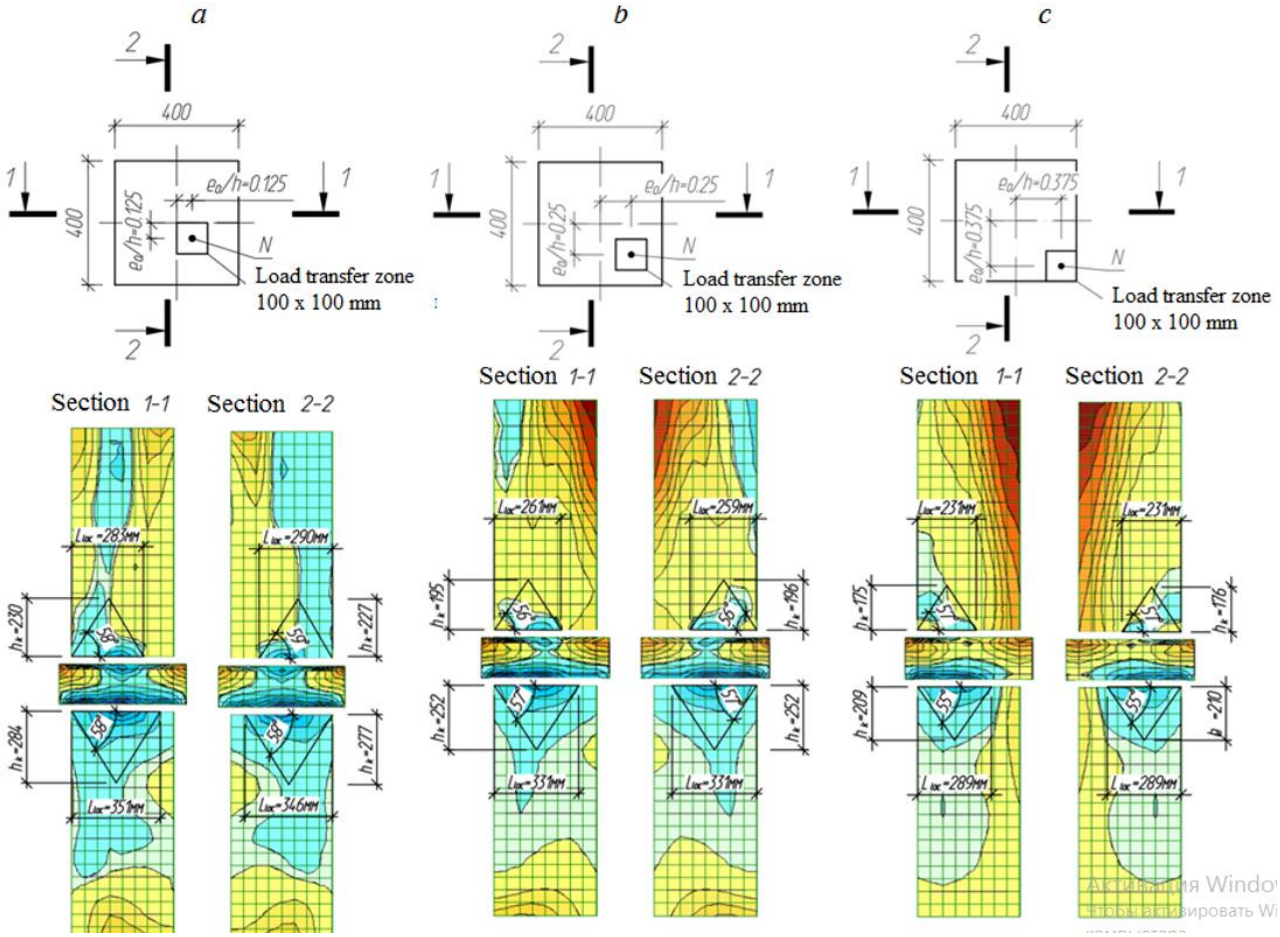


Figure 6. Isofields of principal stresses σ1 in sections 1-1 and 2-2 of samples ES-II-5: a — e0X / h = e0Y / h = 0.125; b — e0X / h = e0Y / h = 0.25; c — e0X / h = e0Y / h = 0.375.

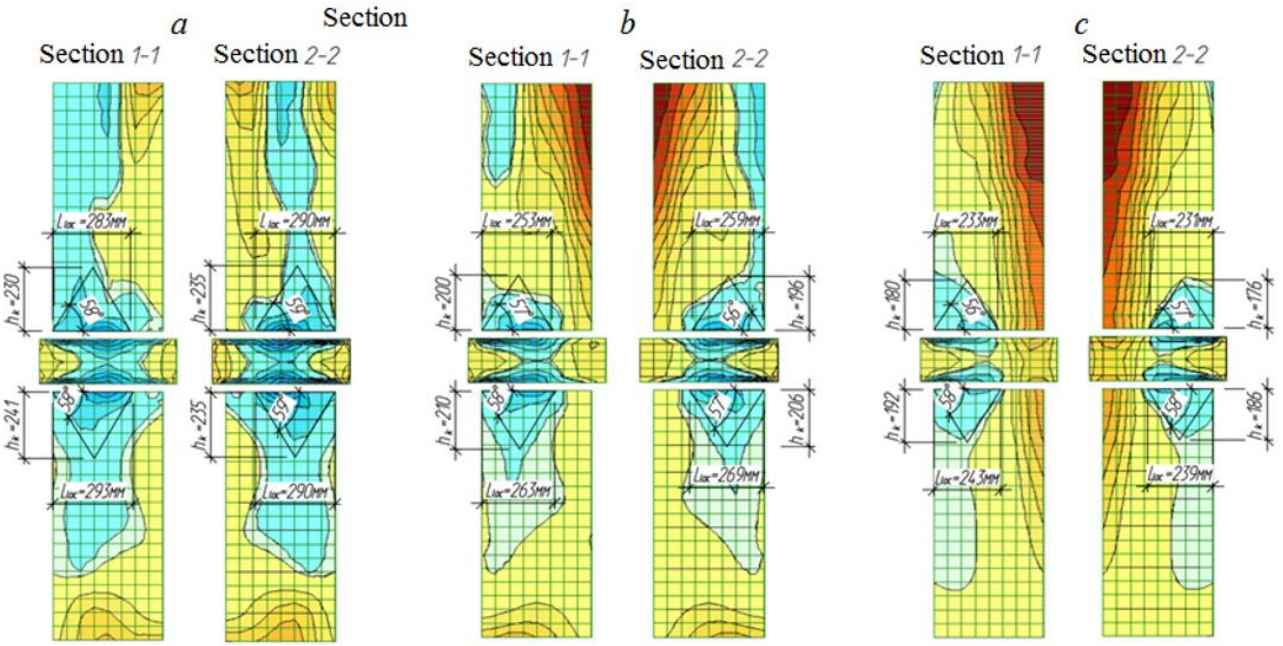


Figure 7. Isofields of principal stresses σ1 in sections 1-1 and 2-2 of ES-II-5.1 samples: a — e0X / h = e0Y / h = 0.125; b — e0X / h = e0Y / h = 0.25; c — e0X / h = e0Y / h = 0.375.

The calculated concrete areas of the end sections of the columns have different geometric dimensions, because a vertical evenly distributed load applied to the overlap plate causes the element to bend, thereby further "squeezing" the upper end of the lower column, causing an increase in the triaxle compression zone.

This conclusion is confirmed by the isofields of the principal stresses obtained by calculation of the ES-II-5.1 series models, according to which the geometric sizes of the calculated zones of the upper and lower columns have low divergences of absolute values (Figure 7).

Analysis of stresses in the reinforcing bars of the ES-II-5 and ES-II-5.1 series models showed that in the corner rod of the longitudinal reinforcement of the columns closest to the load application area, stresses at breakdown reach a yield point. The values of compressive stresses in the remaining rods are lower, and at eccentricities of 0.25 and 0.375 in the opposite angular rods tension was observed. It is determined that the steel strips yokes crossing the area of concrete shear experience tensile forces and should be taken into account in the calculation expressions. Tensile forces are also fixed in the grids of the indirect columns crossing the plane of detachment of concrete [16].

Thus, the obtained data on SSA of the joint allow us to develop the necessary methodology for calculating the strength with oblique eccentric compression.

5. CONCLUSIONS

The computer simulation of the SSA of the plug joints of the slabs with columns of the precast reinforced-concrete frame system "UIKSS" under the action of out-of-square eccentric compression made it possible to formulate the following conclusions.

1. The destruction schemes and the tensioning isofield confirm the possibility of applying the theories of the force resistance of anisotropic materials to compression for the development of a technique for calculating the strength of the joint with out-of-square eccentric compression based on the evaluation of the strength of the end sections of the columns.
2. The characteristics of the calculated zones of concrete (L_{loc}, h_p, α) and stresses arising in the reinforcement elements necessary for the development of the strength calculation procedure are determined.3. It was found that with out-of-square eccentric compression taking into account vertical loads acting on the slab, the zone of triaxle compression of the end portion of the lower column increases due to bending of the plate, increasing the strength of the element.4. Taking into account the obtained results, it is possible to optimize the plan of experimental studies of joint SSA in the operational stage with out-of-square eccentric compression.

REFERENCES

1. Universal'naja Industrial'naja Karkasnaja Sistema Stroitel'stva – Tatarstan (UIKSS-Tatarstan) [Universal industrial frame construction system] – Tatarstan (UIKSS-Tatarstan): pat. 141473 Rossijskaja Federacija: MPK E04V1/20 / Sokolov B.S.; zajavitel' i patentoobladatel' Sokolov B.S. – №2013128714/03; zajavl. 24.06.2013; opubl. 10.06.2014.
2. **Sokolov B.S., Fabrichnaya K.A.** K Sstroitel'stvu Ekoshkol s Ispol'zovaniyem Universal'noy Industrial'noy Karkasnoy Sistemy Stroitel'stva UIKSS-Tatarstan [The Construction of Eco-Schools Using a Universal Industrial Frame Construction System UIFCS-Tatarstan]. // Zhilishchnoye stroitel'stvo, 2015, No. 2, pp. 9-13.
3. **Sokolov B.S., Fabrichnaya K.A.** Primeneniye Karkasnoy Sistemy UIKSS pri Rekonstruktsii Zdaniy [The Use of the UIKSS Framework System at Reconstruction of Buildings]. // Vestnik grazhdanskikh inzhenerov, 2015, No. 6(53), pp. 45-51.
4. **Sokolov B.S., Troshkov E.O.** Deformativnost' Shtepsel'nykh Stykov Sbornykh

Zhelezobetonnykh Plit Perekrytiy s Kolonnami v Nesushchey Sisteme UIKSS [The Ddeformability of Plug-In Joints of Prefabricated Reinforced Concrete Slabs and Columns in the UIKSS Structural Floor System]. // Vestnik grazhdanskikh inzhenerov, 2017, No. 3(62), pp. 32-39.

5. **Sokolov B.S., Troshkov E.O.** Sravneniye Rezul'tatov Komp'yuternogo Modelirovaniya i Eksperimental'nykh Issledovaniy Shtepsel'nykh Stykov Sbornykh Zhelezobetonnykh Kolonn s Plitami Perekrytiy [Comparison of Computer Simulation and Experimental Studies of Socket Joints of Precast Reinforced Concrete Columns with Floor Slabs]. // Zhilishchnoye stroitel'stvo, 2017, No. 7, pp. 41-46.
6. **Evdokimova T.S., Morozov V.I.** Eksperimental'nyye Issledovaniya Kososzhimayemykh Zhelezobetonnykh i Fibrozhelezobetonnykh Elementov [Experimental investigations of reinforced concrete and fiber reinforced concrete members under biaxial] // Vestnik grazhdanskikh inzhenerov, 2015, No. 6 (53), pp. 37-41.
7. **Evdokimova T.S.** Prakticheskiy Metod rascheta Kososzhimayemykh Fibrozhelezobetonnykh Elementov [Practical Method of Calculating Fiber Reinforced Concrete Members Under Biaxial Compression] // Vestnik grazhdanskikh inzhenerov, 2015, No. 3 (50), pp. 68-74.
8. **Geniyev G.A., Kissyuk V.N., Tyupin G.A.** Teoriya Plastichnosti Betona i Zhelezobetona [Theory of Plasticity of Concrete and Reinforced Concrete]. Moscow, Stroyizdat, 1974.
9. SP 63.13330-2012. Betonnyye i Zzhelezobetonnyye Konstruktsii. Osnovnyye Polozheniya. Aktualizirovannaya Redaktsiya SNiP 52-01-2003 [Concrete and reinforced concrete structures. Basic provisions. Updated version of SNiP 52-01-2003]. Moscow, NIIZHB, 2012.
10. **Kholmyanskiy M.M.** Beton i Zhelezobeton: Deformativnost' i Prochnost' [Concrete and Reinforced Concrete: Deformability and Strength]. M.: Stroyizdat, 1997.
11. **Rzhanitsyn A.R.** Sostavnyye Sterzhni i Plastinki [Composite rods and plates]. Moscow, Stroyizdat. 1986.
12. **Matkov N.G.** Bessvarnyye Sstyki Vnetsentrenno Szhatykh Kolonn s Obzhatiyem i Aankerovkoy Armatury Rastvorami [Uncreated Joints of Eccentrically Compressed Columns with Compression and Anchoring of Reinforcement by Solutions]. // Beton i zhelezobeton, 1998, No. 1.
13. **Benin A.V., Semenov A.S., Semenov S.G., Mel'nikov B.E.** Matematicheskoye Modelirovaniye Protsessa Razrusheniya Stsepleniya Armatury s Betonom. Chast' 1. Modeli s Uchetom Nesploshnosti Soyedineniya [Simulation of Degradation of Bond Between Reinforcing Bar and Concrete. Part 1. Models with account of the discontinuity] // Inzhenerno-stroitel'nyy zhurnal, 2013, No. 5, pp. 86-99.
14. **Benin A.V. Semenov A.S., Semenov S.G., Mel'nikov B.E.** Matematicheskoye Modelirovaniye Protsessa Razrusheniya Stsepleniya Armatury s Betonom. Chast' 2. Modeli bez Ucheta Nesploshnosti Soyedineniya [The Simulation of Bond Fracture between Reinforcing Bars and concrete. Part 2. Models Without Taking the Bond Discontinuity into Account] // Inzhenerno-stroitel'nyy zhurnal, 2014, No. 1, pp. 23-40.
15. **Tikhomirov V.M., Astakhov Y.V., Samoshkin A.S.** Modelirovaniye Uprugoplasticheskogo Stsepleniya Armatury s Betonom [Modeling of Elastoplastic coupling of Reinforcement with Concrete] // Izvestiya vuzov. Stroitel'stvo, 2015, No. 2, pp. 103-109.
16. **Sokolov B.S.** Teoriya Silovogo Soprotivleniya Anizotropnykh Materialov Szhatiyu i yeye Prakticheskoye Primeneniye [Theory of force resistance of anisotropic materials to compression and its practical application: monograph]. Moscow, Izd-vo ASV, 2011, 160 pages.

СПИСОК ЛИТЕРАТУРЫ

1. Патент 141473 Российская Федерация, МПК E04B1/20 U1. Универсальная индустриальная каркасная система строительства - Татарстан (УИКСС-Татарстан) / Соколов Б.С.; заявитель и патентообладатель Соколов Б.С. – №2013128714/03; заявл. 24.06.2013; опубл. 10.06.2014, Бюл. №16. – 2 с.
2. **Соколов Б.С., Фабричная К.А.** К строительству экошкол с использованием универсальной индустриальной каркасной системы строительства УИКСС-Татарстан. // Жилищное строительство, 2015, №2, с. 9-13.
3. **Соколов Б.С., Фабричная К.А.** Применение каркасной системы УИКСС при реконструкции зданий. // Вестник гражданских инженеров, 2015, №6(53), с. 45-51.
4. **Соколов Б.С., Трошков Е.О.** Деформативность штепсельных стыков сборных железобетонных плит перекрытий с колоннами в несущей системе УИКСС. // Вестник гражданских инженеров, 2017, № 3(62), с. 32-39.
5. **Соколов Б.С., Трошков Е.О.** Сравнение результатов компьютерного моделирования и экспериментальных исследований штепсельных стыков сборных железобетонных колонн с плитами перекрытий. // Жилищное строительство, 2017, № 7, с. 41-46.
6. **Евдокимова Т.С., Морозов В.И.** Экспериментальные исследования кососжимаемых железобетонных и фиброжелезобетонных элементов. // Вестник гражданских инженеров, 2015, №6 (53), с. 37-41.
7. **Евдокимова Т.С.** Практический метод расчета кососжимаемых фиброжелезобетонных элементов. // Вестник гражданских инженеров, 2015, №3 (50), с. 68-74.
8. **Гениев Г.А., Киссюк В.Н., Тюпин Г.А.** Теория пластичности бетона и железобетона. – М.: Стройиздат, 1974, 316 с.
9. СП 63.13330-2012. Бетонные и железобетонные конструкции. Основные положения. Актуализированная редакция СНиП 52-01-2003. – М.: НИИЖБ, 2012. – 153 с.
10. **Холмянский М.М.** Бетон и железобетон: Деформативность и прочность. – М.: Стройиздат, 1997. – 576 с.
11. **Ржаницын А.Р.** Составные стержни и пластинки. – М.: Стройиздат. 1986.– 316 с.
12. **Матков Н.Г.** Бессварные стыки внецентренно сжатых колонн с обжатием и анкеровкой арматуры растворами. // Бетон и железобетон, 1998, № 1.
13. **Бенин А.В., Семенов А.С., Семенов С.Г., Мельников Б.Е**. Математическое моделирование процесса разрушения сцепления арматуры с бетоном. Часть 1. Модели с учетом несплошности соединения // Инженерно-строительный журнал, 2013, №5, с. 86-99.
14. **Бенин А.В. Семенов А.С., Семенов С.Г., Мельников Б.Е**. Математическое моделирование процесса разрушения сцепления арматуры с бетоном. Часть 2. Модели без учета несплошности соединения // Инженерно-строительный журнал, 2014, №1, с. 23-40.
15. **Тихомиров В.М., Астахов Ю.В., Самошкин А.С.** Моделирование упругопластического сцепления арматуры с бетоном. // Известия вузов. Строительство, 2015, №2, с. 103-109.
16. **Соколов Б.С.** Теория силового сопротивления анизотропных материалов сжатию и ее практическое применение: монография. – М.: Изд-во АСВ, 2011. – 160 с.

Boris S. Sokolov, Corresponding Member of Russian Academy of Architecture and Construction Sciences, Dr.Sc., Professor; scientific consultant of JSC "Kazan Giproniaviaprom"; 1, Ul. Dementyeva, 420127, Kazan, Russia; phone +7(919) 636-04-74;

Dissipative Systems Computer Modelling of the Stress-Strain State of Plug-In Connections of Reinforced Concrete Columns with the Coverage Plates Under the Out-of-Square Eccentric Compression

E-mail: sbs.1942@mail.ru.

Evgeniy O. Troshkov, Candidate of Engineering Sciences; Senior Lecturer of Volga State University of Technology; 3, Pl. Lenina, 424000, Yoshkar-Ola, Russia; phone +7 (987) 711-57-87;
E-mail: troshkoveo@mail.ru.

Соколов Борис Сергеевич, член-корреспондент РА-АСН, профессор, доктор технических наук; научный консультант АО «Казанский Гипрониавиапром»; 420127, Россия, Республика Татарстан, г. Казань, ул. Дементьева, 1; тел. +7(919) 636-04-74;
E-mail: sbs.1942@mail.ru.

Трошков Евгений Олегович, кандидат технических наук; старший преподаватель, Поволжский государственный технологический университет; 424000, Россия, Республика Марий Эл, г. Йошкар-Ола, пл. Ленина, дом 3; тел. +7 (987) 711-57-87;
E-mail: troshkoveo@mail.ru.

DOI:10.22337/2587-9618-2018-14-3-136-141

BOLTS PULLING TEST. REVERSER FOR BOLTS TESTING

Mark P. Son
Perm National Research Polytechnic University, Perm, RUSSIA

Abstract: The article describes developed device for performing pulling tests of bolts, including high-strength. Principle of reverser operation is change of sign of applied load – compression of press causes stretching of a bolt. Advantages of presented reverser are: reliability, mobility, small size, economical operation and simpleness. Reverser designs permit to perform bolt tests at any hydraulic press. Using the developed device, deformation diagrams were obtained for bolts of different strength class 8.8 steel 40Kh and 20G2R and 10.9 steel 40Kh. These diagrams may serve as basis for numerical modeling of bolts in software packages, and also manual calculation of yielding. Tests revealed a number of advantages of bolts made of steel 20G2R over 40Kh, due to which application of bolts made of steel 20G2R is recommended in assemblies of any level of responsibility.

Keywords: reverser, bolt,deformation diagrams,mechanical properties, yielding

ИСПЫТАНИЕ БОЛТОВ НА РАСТЯЖЕНИЕ. РЕВЕРСОР ДЛЯ ИСПЫТАНИЯ БОЛТОВ

М.П. Сон
Пермский национальный исследовательский политехнический университет, г. Пермь, РОССИЯ

Аннотация: В статье описывается разработанное устройство для испытаний болтов, включая высокопрочные, на растяжение. Принцип работы реверсора заключается в смене знака прикладываемого усилия - сжатие пресса вызывает растяжение болта. К достоинствам представленного реверсора относятся: надежность, мобильность, компактность, экономичность и простота. Конструкция реверсора позволяет проводить испытания болтов на любом гидравлическом прессе. При помощи разработанного устройства были получены диаграммы деформирования для болтов класса прочности 8.8 сталей 40Х и 20Г2Р и 10.9 стали 40Х. Данные диаграммы могут служить основой для численного моделирования болтов в программных комплексах, а также ручного расчета податливости. Испытания выявили ряд преимуществ болтов из стали 20Г2Р в сравнении с 40Х, в связи с чем, рекомендуется применение болтов из стали 20Г2Р в узлах любого уровня ответственности.

Ключевые слова: реверсор, болт, диаграммы деформирования, механические свойства, податливость

Bolt joints of beams and columns, high pressure vessels and other structures are critical components often determining reliability of the whole structure. To increase reliability of this type of joints it is necessary to apply design and calculation methods, based on consistent tests [7].

At present, there exists a large number of works dedicated to study of mechanical behavior of bolt and flange s joints, for example, study of operation of T-shaped flanges [6]. Article [1] presents variants of bolt joints of beams and columns. Work [2] presents results of series tests of full-scale samples. Sample consisting of column and adjacent beam was loaded with bending moment applied to beam until destruction of the joint, with varied plate size and number of connecting bolts. Study [3] shows that reinforcement of flange with additional stiffening ribs leads to increase of strength but decreases joint deformability. Share of plastic deformations in reinforced joint decreases and consequently decreases ability of the joint to disperse oscillations caused by seismic loads. Experimental and theoretical study of bolt joint "column - column" [4]

performs detailed mathematic modeling of the assembly with regard to dimensional geometry of columns, flanges and bolts. Contact condition is given for flanges, implementing dry friction, preliminary tensioning of bolts is taken into account. Analysis of structure consisting of large number of bolted beams is given in work [5]. Structure behavior in case of exclusion of one bolt of flange joint is modeled.

Large number of studies are aimed to study bolt joints, while omitting the bolts themselves from the analysis. It is the bolt breakage which may constitute breakage of the assembly and the structure in whole. Calculations of bolt joints, of all mechanical bolt properties, use only design strength corresponding to strength class. In reality bolts of same strength class may be made of different steel grades, and consequently differ in relative elongation at failure and variation of mechanical properties.

Loads on assemblies and joints are mainly oscillatory. To increase fatigue strength bolts are pretensioned to value Fo. After application of external force F compression stress of joined flanges decreases and bolt receives additional force χF, and part of force equal to $(1- \chi)F$ decreases initial compression of flanges. Final loads in bolt and flanges may be determined according to formulas 1.

$$F_b = Fo + \chi F$$
$$F_f = - Fo + (1- \chi)F \qquad (1)$$

where F_b – full stress in bolt, F_f- flanges compression stress, χ – main load factor.

Factor χ, determining share of external stretching force additionally loading the bolt, is of special importance in calculation of joints operating under oscillatory loads. Main load factor depends on stiffness of flanges and bolt and may be found according to formula 2:

$$\chi = \lambda_f/(\lambda_b+ \lambda_f) \qquad (2)$$

where λ_b – axial yield of bolt, λ_f – axial yield of flanges (clamped parts).

In clamping flange package maximal compressing stresses are in points near opening under bolt head and nut. These stresses decrease to middle of the clamped package, forming cone of pressure (Figure 1). It is considered that base of cone does not depend on external load value and consequently compressed flanges operate as stem with cone-like section with opening until load reaches value $Fo/(1-\chi)$ when flanges will open. Such model describes actual operation of thick thickness flanges with enough exactness. For thin (flexible flanges) calculation agrees with the experiments at large values of tightening stress $б_0=(0,5\text{-}0,7)б_т$ and such external load which causes just slight opening of joint. Angle of inclination of cone generatrix is considered equal to 30^o, consequently having calculated average cone diameter it is possible to obtain yield of flanges λ_f.

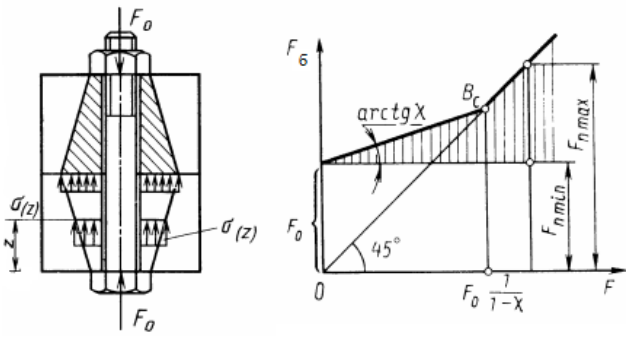


Figure 1. Distribution of stresses in compressed flanges over cone of pressure.

Yield of bolt may be determined as sum of yields pf its parts: cylindrical part of bolt and threaded part of bolt (where l, A, E – length, area and elasticity modulus). Calculation of λ_b is of no difficulties, but for short bolts ($l < 6d$) yield of bolt head (λ_h), and also of thread (λ_t) within limits of nut coupling should be considered. There are empiric formulas for calculation of λ_h, λ_t, but as V.B. Kuklin has showed, yield of thread strongly depends on tolerance ranges and angle of profile of thread and nuts. Also V.B. Kuklin has found that contact deformations of operating surfaces of thread have significant influence on thread yield, which may 2-4 times surpass own yield of turns.

Each bolt, following to GOST, should be marked with designation of strength class, which is determined according to results of bolt tests.
Bolts are testes at tensile testing machines equipped with special bolt grips. A bolt is «dressed» into an insert which is installed into a grip, which in turn is fastened to tensile machine rod.

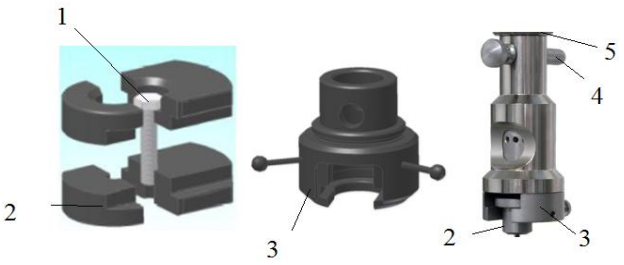


Figure 2. Attachment for testing bolts at tensile machine. 1 - bolt, 2 - inserts, 3 - grip, 4 – bush for fixing grip onto rod, 5 – rod of tensile machine.

Common main drawbacks for all types of these grips are:

1) High cost, grips for stretching bolts are not included into main kit of tensile machine and should be bought separately.
2) Possibility of using grips only in tensile machines made by same manufacturer.
3) Limited carrying capacity of grip. For example, grips for bolts Zwick/Roell for test machine line All round Line are limited to load of 250 kN, while temporary load on bolt may reach 2000 kN (for bolts M48 strength class 12.9).

To eliminate the described drawbacks the author of this article has developed reverser for testing bolts. The device belongs to accessories for fixing and mechanical testing of bolts and high-strength bolts. Reverser consists of two same U-shaped metallic parts (Figure 3) with round opening in shelf of a part for bolt installation. Axis of opening coincides with axis of bolt and direction of stress. U-shaped parts are located orthogonally, connected with stands to each other until alignment of openings, after which connected by a bolt (high-strength bolt). Nut is screwed on threaded end of bolt. Connected parts are installed into a press. Compression of press makes them to spread, causing stretching stress on a bolt. So, principle of reverser operation is change of sign of applied stresses – compression of press causes stretching of bolt.

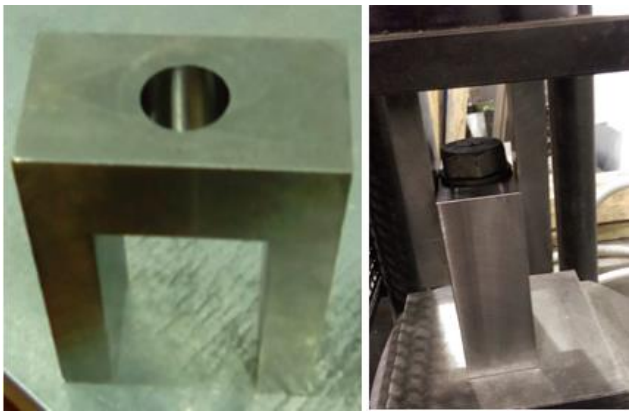


Figure 3. On the left – part of reverser, on the right – bolt test in press, using reverser.

Reverser compares favorably to grips, its main advantages are:
Universality – reverser may be installed and bolts testes at any press.
Reliability.
Mobility (transferability) is attained by small reverser weight.
Small size – reverser size is determined by diameter of bolts being tested.
Safety at break of bolt is achieved by the fact that bolt body is fully covered by the reverser itself (one U-shaped part from 2 sides, second part from 2 sides), which excludes possible shrapnel and bolt parts coming into personnel.
Economic operation – reverser is made from sheet metal using plasma cutting and has no expensive parts.
Simpleness – preparation process includes installation of bolt with turning on reverser, with following installation to press plate. Bolt is centered automatically, its preparation to test takes about 30 seconds.
Using this reverser, were tested bolts M24 from different steels, lots and strength classes. Tests were performed at hydraulic 500 t press. Technical characteristics of press: load accuracy – 16 kg, deformation accuracy - 0,0036 mm,

loading speed 133 kN/min. Bolt stretching diagrams were received (Figure 4-5).

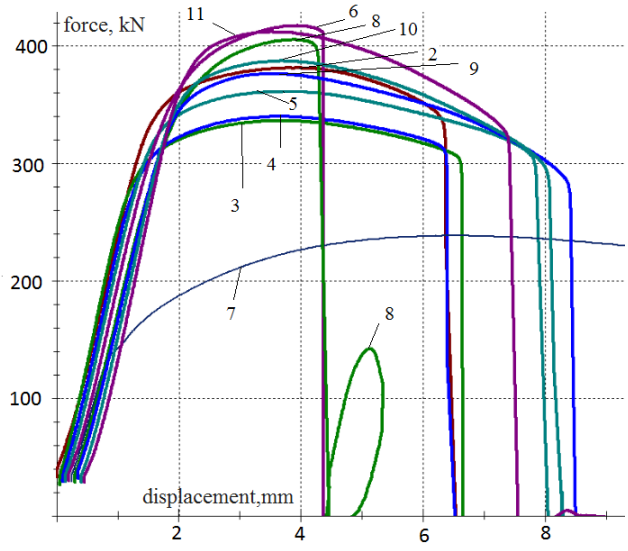


Figure 4. Diagrams of testing bolts of steel 40Kh.

Diagrams 2-4 are built for bolts strength class 8.8 from steel 40Kh. According to test results tensile strength of bolts was Rbun=950-1090 MPa.

Diagrams 5-11 are built for bolts strength class 10.9 from steel 40Kh «select». According to test results tensile strength of bolts was Rbun=1040-1200 MPa, except for bolt № 7, which experienced maximal load 238,5kN (б=676 MPa) and showed deformation diagram drastically different from other bolts, this product is considered defective. Also bolt № 8 may be considered defective, though it showed R_{bun}=1165 MPa, but destruction was by thread stripping, and according to GOST a test is considered satisfactory if breakdown happens in rod or free threaded part of bolt.

In other cases (tests 2-6, 9-11) destruction was brittle, bolts were broken at normal in threaded part by tearing off.

Also were tested bolts 8.8 from boron steel 20G2R. Deformation diagrams of 4 tested bolts (Figure 5) are practically identical. Maximal load on bolts was 339-343 kN, which corresponds to stresses б=960-970MPa. Bolts showed greater plasticity comparing to bolts from steel 40Kh. Destruction was ductile, with formation of sloping planes and characteristic tapering neck (Figure 6).

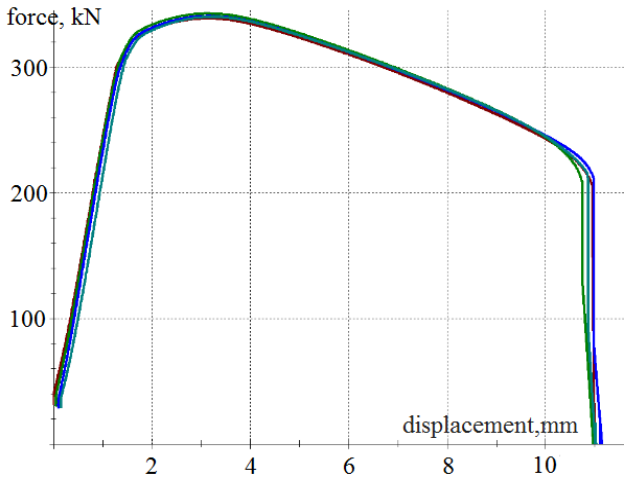


Figure 5. Diagrams of testing bolts from steel 20G2R.



Figure 6. Characteristic destruction of bolts. On the left – bolts 10.9 from steel 40Kh, on the right – bolts 8.8 from steel 20G2R.

CONCLUSION

For calculation of bolt joints it is necessary to know actual diagrams of bolts operation, as their yield consists of yield of bolt body, yield of head and yield of thread. Using the developed device for mechanical stretch testing of bolts – reverser, deformation diagrams for bolts strength class 8.8 steels 40Kh and 20G2R, and 10.9 steel 40Kh were obtained. These diagrams may serve as basis for numeric modeling of bolts in software packages, and also for calculation of share of main load according to formula 2. At present in Russia it is customary to design critical assemblies using bolts from steel 40Kh, which is based on obsolete recommendations on design.Test revealed number of advantages of bolts from steel 20G2R comparing to 40Kh. First, greater relative elongation at rupture.Second, smaller variation of mechanical properties. Also bolts 8.8 from steel 20G2R showed temporary resistance of 960-970 MPa, which is higher than 800 MPa assigned for the class, while bolts from steel 40Kh in some cases showed unacceptable strength or destruction scenario (in the thread) and were considered defective. So we recommend using bolts made of boron steel 20G2R in assemblies of any level of responsibility.

REFERENCES

1. **Ghindea M., Ballok R.** State-of-the-art Review on Bolted Steel Beam-to-Column Connections // Bulletin of the Transilvania University of Braşov, 2015, Volume 8(57), Special Issue No. 1.
2. **Prinz G.S.**, **Nussbaumer A., Borges L., Khadka S.** Experimental Testing and Simulation of Bolted Beam-column Connections Having Thick Extended Endplates and Multiple Bolts per Row. // Engineering Structures, 2014, 59, pp. 434-447.
3. **Abidelah A., Bouchair A., Kerdal D.E.** Experimental and Analytical Behavior of Bolted End-Plate Connections with or Withour Stiffeners. // J Constr Steel Res, 2012, No. 76, pp. 13-27.
4. **Liu X.C., He X.N., Wang H.X., Zhang A.L.** Compression-Bend-Shearing Performance of Column-to-Column Bolted-Flange Connections in Prefabricated Multi-High-Rise Steel Structures.// Engineering Structures, 2018, Volume 160, pp. 439-460.
5. **Blachowski** B.**, Gutkowski W.** Effect of Damaged Circular Flange-Bolted Connections on Behaviour of Tall Towers, Modelled by Multilevel Substructuring. // Engineering Structures, 2016, Volume 111, pp. 93-103.
6. **Swanson J.** Ultimate Strength Prying Models for Bolted T-stub Connections. // Engineering journal, Third quarter, 2002, pp. 136-147.
7. **Baker M**. Is There a Reproducibility crisis? // Nature, 2016, Volume 533, pp. 452-454.

СПИСОК ЛИТЕРАТУРЫ

1. **Ghindea M., Ballok R.** State-of-the-art Review on Bolted Steel Beam-to-Column Connections // Bulletin of the Transilvania University of Braşov, 2015, Volume 8(57), Special Issue No. 1.
2. **Prinz G.S.**, **Nussbaumer A., Borges L., Khadka S.** Experimental Testing and Simulation of Bolted Beam-column Connections Having Thick Extended Endplates and Multiple Bolts per Row. // Engineering Structures, 2014, 59, pp. 434-447.
3. **Abidelah A., Bouchair A., Kerdal D.E.** Experimental and Analytical Behavior of Bolted End-Plate Connections with or Withour Stiffeners. // J Constr Steel Res, 2012, No. 76, pp. 13-27.
4. **Liu X.C., He X.N., Wang H.X., Zhang A.L.** Compression-Bend-Shearing Performance of Column-to-Column Bolted-

Flange Connections in Prefabricated Multi-High-Rise Steel Structures.// Engineering Structures, 2018, Volume 160, pp. 439-460.
5. **Blachowski** B.**, Gutkowski W.** Effect of Damaged Circular Flange-Bolted Connections on Behaviour of Tall Towers, Modelled by Multilevel Substructuring. // Engineering Structures, 2016, Volume 111, pp. 93-103.
6. **Swanson J.** Ultimate Strength Prying Models for Bolted T-stub Connections. // Engineering journal, Third quarter, 2002, pp. 136-147.
7. **Baker M**. Is There a Reproducibility crisis? // Nature, 2016, Volume 533, pp. 452-454.

Mark P. Son, Candidate of Technical Sciences, associate Professor, Department of Building structures and computational mechanics, Perm National Research Polytechnic University; 29-a, Komsomolsky prospect, Perm, 614600, Russia; fax: + 7(342) 2-453-440,
E-mail: mark-son.mail.ru.

Сон Марк Петрович, кандидат технических наук, доцент кафедры строительной механики и вычислительных технологий Пермского национального исследовательского политехнического университета; 614990, Россия, г. Пермь, Комсомольский пр., д. 29; факс: + 7(342) 2-453-440,
E-mail: mark-son.mail.ru.

DOI:10.22337/2587-9618-2018-14-3-142-152

RELIABILITY ANALYSIS OF REINFORCED CONCRETE ELEMENTS WITH NORMAL CRACKS (ON RC BEAM EXAMPLE)

Vladimir S. Utkin, Sergey A. Solovyev
Vologda State University, Vologda, RUSSIA

Abstract: The purpose of research is development of methods for reliability analysis of structural reinforced concrete elements (on example of reinforced concrete beam) according to criterion of the normal cracks length in tensile zone of concrete. Cracks in tensile zone of concrete in beams leads to displacement of the beam's neutral axis towards the compressed part of the concrete, thereby increasing the compression stress in the concrete, to the increasing of the stress in the reinforcement bars on the crack width, to the growth of corrosion processes, etc. This leads to the decreasing of beams mechanical safety and reliability (as a quantitative measure of mechanical safety). The main parameters, which reduce the strength and stiffness of the beam, of the cracks is the length and width of the crack. The article describes the influence of the cracks length on the reliability of reinforced concrete elements. The article differs from existing approaches in that is it built on a limited statistical data of controlled parameters in mathematical models of limit state. The article also considers the influence of cracks in the structural element. The methods of reliability analysis allow to assess the mechanical safety of reinforced concrete elements and to make appropriate decisions about the safety, strengthening or replacement of the reinforced concrete element.

Keywords: reliability, normal cracks, beam, safety, failure probability, fuzzy variable, random set theory

РАСЧЕТ НАДЕЖНОСТИ ЖЕЛЕЗОБЕТОННЫХ ЭЛЕМЕНТОВ С НОРМАЛЬНЫМИ ТРЕЩИНАМИ НА ПРИМЕРЕ ЖЕЛЕЗОБЕТОННОЙ БАЛКИ

В.С. Уткин, С.А. Соловьев
Вологодский государственный университет, г. Вологда, РОССИЯ

Аннотация: Цель работы – разработка методов расчета надежности несущих железобетонных элементов на примере железобетонной балки по критерию длины серии нормальных трещин в растянутой зоне бетона балки. Трещины в растянутой зоне бетона балки приводит к смещению нейтральной оси балки в сторону сжатой части балки, повышая тем самым напряжения сжатия в бетоне, повышают деформации в арматуре на ширине раскрытия трещины, способствуют развитию коррозионных процессов и т.д. Это приводит к снижению механической безопасности балки, в качестве количественной меры которой используется надежность. Основными параметрами трещины, приводящими к снижению прочности и жесткости балки, является длина и ширина раскрытия трещины. Статья посвящена учету влияния длины серии нормальных трещин на надежность железобетонных элементов. Статья отличается от существующих подходов тем, что построена на ограниченном объеме статистической информации о контролируемых параметрах в математических моделях предельных состояний, а также учету влияния нескольких трещин в несущем элементе. Предложенные методы расчетов надежности позволяют оценить механическую безопасность несущих железобетонных элементов и принять адекватные решения о безопасности эксплуатации, усилению или замене балки.

Ключевые слова: надежность, нормальные трещины, балка, безопасность, вероятность отказа, нечеткая переменная, теория случайных множеств

1. INTRODUCTION

The Russian Federal Law No. 384 "Technical regulation for buildings and structures safety" came to force in 2010. Interstate Standard GOST 27751-2014 "Reliability of structures and foundations" came to force in 2015 on the basis of the Law No. 384. One of the main purposes of the Law is the provision of mechanical (structural) safety of buildings and structures during their operation. "Mechanical safety" is the state of structure in which there is no inadmissible risk of failure and harm to the life and health of citizens. Quantitative assessment of the mechanical safety may be the reliability (safety) of the structure or structural element. According to the European Standard Eurocode 0 "Basis of structural design", the reliability – is an ability of a structure or a structural member to fulfill the specified requirements, including the design working life, for which it has been designed. Reliability is usually expressed in probabilistic terms. The measure of reliability is probability of failure or probability of non-failure. General principles of structural reliability are regulated by Eurocode 0 and International Standard ISO 2394:2015 «General principles on reliability of structures». Interstate Standard GOST 27751-2014 regulates the general principles of structural reliability in Russian Federation.

2. LITERATURE REVIEW

Probabilistic-statistical methods of reliability analysis were studied by many researches: [1, 2, 3 etc.]. Most of the work for the reliability analysis by probabilistic method is currently based on the hypothesis of normal distribution of random variables in mathematical models of limit state. The paper [4] presents the comparison between FORM (First Order Reliability Method) and ISM (The Importance Sampling Method) in reliability analysis of reinforced concrete buildings (including RC beams). Both methods are only used with a large amount of statistical data, which in practice may cause some difficulties. The article [5] describes the reliability analysis methods for triangular and T-reinforced concrete beams. The method of reliability analysis also based on probabilistic methods. The article [6] presents reliability analysis of reinforced concrete beam exposed to fire using Monte Carlo simulation. The article [7] presents the reliability analysis of a corroded RC beam based on Bayesian updating of the corrosion model.

However, the vulnerability of probabilistic methods of reliability analysis appears in its practical use for individual structural elements in condition of limited time for inspection, the high cost of individual tests, inaccessibility or inability of the study to some parameters, and other reasons. In this regard, new methods of reliability analysis based on new mathematical theories: possibility theory [8], fuzzy set theory [9], theory of random sets [10, 11] etc., has been developed. The new methods allow to take into account the limited statistical information of controlled parameters in mathematical models of limit state in the reliability analysis, of course with the reducing the information content of the result. There is no theory to make up for the lack of statistical data in the reliability analysis.

So, Dubois and Prad [8] notes that "the probability, on the one hand, and a pair of "possibility – necessity" correspond to the two extreme, and so the ideal, situations". It is also noted that a probability measure in a natural way synthesize database of accurate and differentiated knowledge, then as a measure of possibility is the essence of reflection is inaccurate, but coherent (i.e. corroborative) knowledge.

3. PROBLEM STATEMENT

A special problem occurs in assessing the safety level in reinforced concrete beams with normal cracks in the tensile zone of concrete, when statistical data of the controlled parameters is always individual and limited. In this case, the application of probabilistic and statistical

methods is not correct. The Figure 1 shows an example of a reinforced concrete beam with normal cracks. Without considering the reasons for the formation of cracks and their impact on the reduction of the RC beam strength and stiffness, let's consider the method of reliability analysis of RC beam with normal cracks on crack length criterion for subsequent decision-making about the possibility of further operation, strengthening or even replacing.

The relevance and novelty of the problem lies in the fact that in the standards of reinforced concrete elements design there are no requirements on the design RC elements according to the crack length criterion and guidelines for the reliability analysis consequently. At the same time, it is known [12] that the cracks in reinforced concrete beams reduces their reliability, and the critical crack length leads to it spontaneous self-growth and to the possibly failure. Piradov K.A. and Savitchkiy N.V. convincingly demonstrate in [13] the necessity for a transition to reinforced concrete structures design by fracture mechanics methods.

So, it is proposed to consider the methods of reliability analysis of reinforced concrete beams with normal cracks (Figure 1), with different types of statistical data about controlled parameters in the design mathematical models of limit state.

The reinforced concrete beam failure may occur according to various criteria of limit state (strength of concrete and rebar, the deflection, the cracks width, etc.). In this sense, the RC beam is a coherent mechanical system in terms of reliability theory. Cracks in RC beams are caused by tensile stresses and are characterized by width a_{crc} and length l_{crc}.

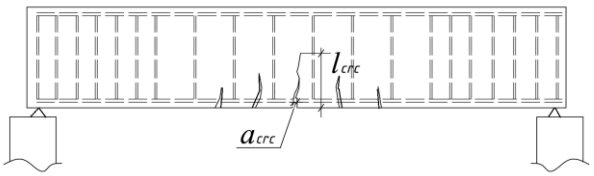


Figure 1. Reinforced concrete beam with normal cracks.

4. RELIABILITY ANALYSIS

The article [14] presents the method of reliability analysis of reinforced concrete beam with one crack by crack length with the mathematical model of limit state:

$$\tilde{l}_{crc} \le l_{crc,ult} = 0{,}3h_0, \text{ or } X \le k, \qquad (1)$$

where $X=\tilde{l}_{crc}$ – length controlled (measured) crack the greatest length in the beam cross-section; $k=l_{crc,ult} = 0{,}3h_0$ – critical crack length (adopted as an option by [12]), which is deterministic value in this case; h_0 - distance from extreme compression fiber to centroid of longitudinal tension reinforcement.

There are other proposals about the critical length of cracks in reinforced concrete beams, for example $l_{crc,ult} = 0{,}5h$ [15]. Not discussing the problem of the size of the critical crack length, let's assume that it is known, and in the general case depends on the critical value of stress intensity factor K_{IC}. Evaluation of K_{IC} for reinforced concrete beams described in [16].

Every crack reduces the reliability of the beam. If to take the lack of interaction between cracks length (for simplicity), and the failure of the beam by the any of cracks leads to failure of the entire beam, then the beam with cracks can be seen as a coherent mechanical system in terms of reliability theory. In the reliability analysis by possibilistic methods for each criterion of limit state, and for the considered task for each normal crack, the possibility *R* and the necessity *N* non-failure of the RC beam as a coherent system [17] will be determined by the interval $[N_{\text{i, min}}; R_{\text{i, min}}]$.

Measurement of the crack length in reinforced concrete beams is challenging, since its length is determined not only by visible part, but by a part of loosened concrete at the crack tip [12]. It is proposed to use the method described in the patent [18] to measure the crack length (Figure 2).

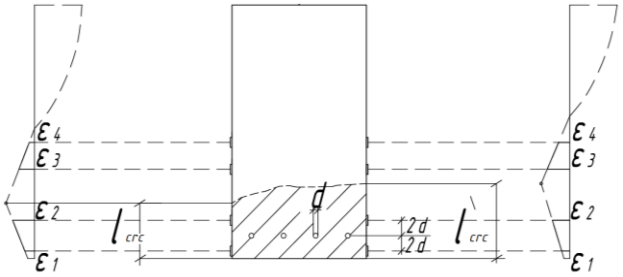


Figure 2. Method for measurement of crack length by [18].

As noted above, the reliability analysis of RC beam will be carried out on the basis of possibility theory [8, 9]. In this case, fuzzy variable described by the distribution function of possibilities $\pi_X(x)$. The most widely used in practice of reliability analysis of structural elements received a distribution function of possibilities with the analytical view:

$$\pi_X(x) = \exp\left[-\left(\frac{x-a_x}{b_x}\right)^2\right], \qquad (2)$$

where

$$a_x = 0{,}5\cdot(X_{\max} + X_{\min})$$

– "conditional mean";

$$b_x = 0{,}5(X_{\max} - X_{\min})/\sqrt{-\ln\alpha}$$

– measure of "dispersion", $X_{\max}$ и $X_{\min}$ - the maximum and minimum value in the set of values $\{x\}$ of fuzzy variable X; $\alpha \in [0;1]$ - cut (risk) level, the value of which is set.

The choice of distribution function has an impact on the result of reliability analysis, including the width of the confidence interval $[N; R]$, which is the results of reliability analysis. There are no rules for functions choices and checking them such Pearson' chi-squared test.

Cut level α can be considered as an indicator (measure) of uncertainty of the distribution functions sets of random variables with their distribution in the shaded areas.

The reliability analysis of RC beam with one crack by possibilistic method carry out by the result of several measurements of crack length by mathematical model (1). We set α, and calculate the parameters a_x and b_x. If $a_x \le k$ (that usually corresponds to the operational stage), then R=1. Possibility of failure Q calculated as

$$Q = \exp\left[-\left(\frac{k-a_x}{b_x}\right)^2\right].$$

Reliability will be characterized by the interval $[N=1-Q; R]$.

Example 1. Let $X = \{17;20;23\}$ mm and $k = 24$ mm. Let's find parameters of $\pi_X(x)$ with different values of α. By (2): $a_x = 0{,}5\cdot(23+17) = 20$ mm and $b_x = 0{,}5(23-17)/\sqrt{-\ln\alpha}$ mm. As $a_x = 20 \le k = 24$ mm, then R=1. Results of Q with different values of α shown in table 1. Figure 3 shows a graph of the dependence of possibility of failure Q and the cut level α:

$$Q(\alpha) = \exp\left[-\left(\frac{24-20}{0{,}5(23-17)/\sqrt{-\ln\alpha}}\right)^2\right]$$

according to the Example 1.

Table 1. Given Data.

Cut level α	b_x, mm	Q
0,01	1,398	$2{,}78*10^{-4}$
0,05	1,733	$4{,}865*10^{-3}$
0,1	1,977	$1{,}677*10^{-2}$
0,2	2,365	0,057
0,4	3,134	0,196

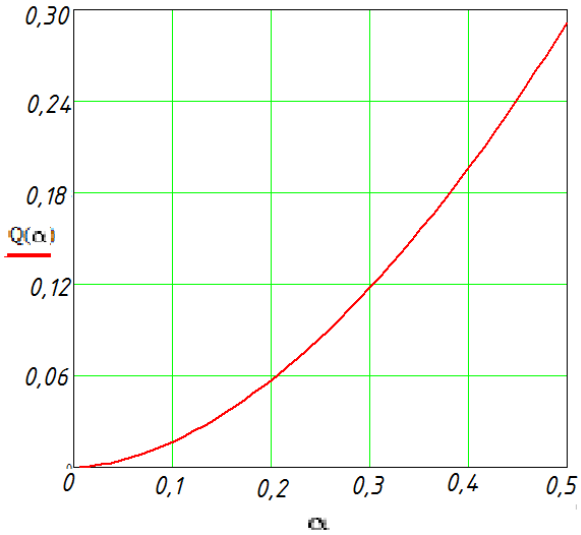


Figure 3. Dependence of possibility of failure Q and the cut level α .

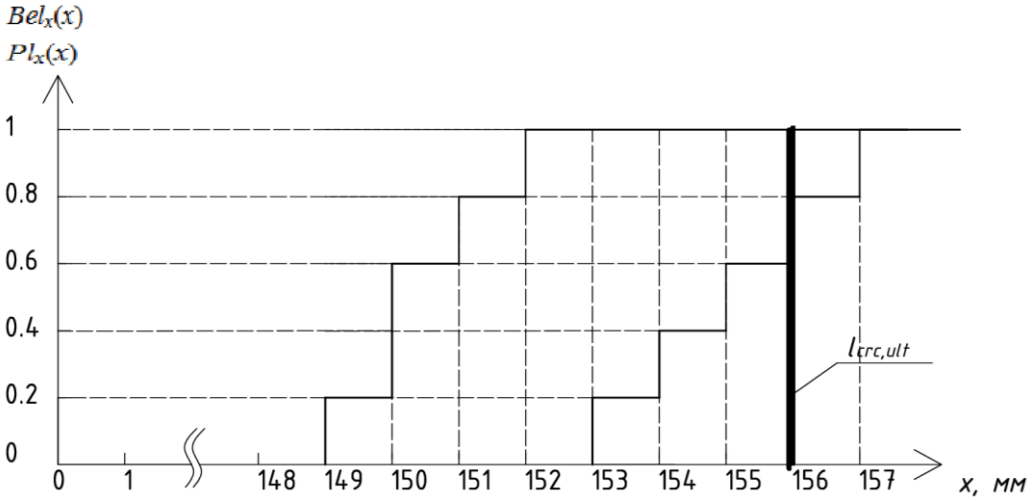


Figure 4. Graphs of belief function Belx(x) and plausibility function Plx(x) for $X = \tilde{l}_{crc}$.

From the above values of Q in the table 1 and from the graph (Figure 4) we can see, that the intensity of the impact of the cut (risk) level for the Q increases with growth α . At small values of $\alpha < 0{,}05$, the effect on Q is more subtle. Q increases dramatically with $\alpha > 0{,}1$. These results show the reduction of information content of the reliability result in the form of a confidence interval with increasing α values. That is a disadvantage of possibilistic method of reliability analysis for an individual object.

In this regard, the possibilistic method of reliability analysis is preferred in the comparative analysis of two or more objects by reliability index. And value of α it is recommended to take in the interval [0,01; 0,1], where α impact on the value of Q is relatively small. Provides information on the reliability analysis of reinforced concrete beams can be used to assess the level of safety of one beam and a series of such beams in order to compare them by reliability indexes.

5. RANDOM SET THEORY APPROACH

Let's consider the second approach to reliability analysis of reinforced concrete beam with normal

cracks on the basis of known theory of random sets (theory of evidence of Dempster-Shafer) [10, 11], in which there are no parameters and therefore their influence on the result of the reliability analysis. Reliability analysis of reinforced concrete beam we will still spend on the criterion of crack length for the mathematical model (1) by method based on the theory of random sets [19] with the data about X in the form of sub-intervals set of the measurement results of the controlled parameter X.

Example 2. Let $X = \tilde{l}_{crc}$ in interval form at different points in time during the operation process of reinforced concrete beam as: X = {[150; 154], [151; 155], [150; 156], [152; 157], [149; 153]} mm and $l_{crc,ult} = k = 156$ mm. In accordance with the theory of random sets [19], Figure 4 shows graphs of belief function $Bel_x(x)$ and plausibility function $Pl_x(x)$ for $X = \tilde{l}_{crc}$, which does not contain parameters to set.

The upper $\overline{P}$ and lower $\underline{P}$ boundaries of the probability of non-failure interval is estimated by [19, 20] Fig. 4. with $l_{crc,ult} = k = 156$ mm as interval [0,80; 1].

Example 3. Let's consider another feature of reliability analysis based on the theory of random sets. With the original data of the above example and with $k = 158$ mm, the interval of reliability is [1; 1], i.e. the probability of failure is equal to 0, which is statistically incorrect.

Thus, the reliability analysis of structural elements based on the theory of evidence (or theory of random sets) can be used in practice without the involvement of functions of random variables (and parameters definitions). However, the small amount of statistical data as sub-intervals sets and for large values of the non-failure probability of structural element this method may be inconclusive, since the probability of failure may be equal to one.

There is another variant for the reliability analysis with a small amount of statistical data in form of intervals subset. So, it is proposed [20] to use the advanced functions of belief and plausibility through the use of a imprecise Dirichlet model (IDM) as one of the types of robust models. In this case, the upper and lower bounds of probability of non-failure can be written as:

$$\underline{P}(A \mid c, s) = \frac{N \cdot Bel(A)}{N + s} = \chi Bel(A) \text{ and}$$
$$\overline{P}(A \mid c, s) = \frac{N \cdot Pl(A) + s}{N + s} = 1 - \chi[1 - Pl(A)], \quad (6)$$

where N – the number of tests (observations); s – the parameter characterizing the extent of «uncertainty», the value of which is set, where is the notation

$$\chi = (1 + s / N)^{-1}$$

and $\chi \in [0; 1]$. Let's consider the algorithm of calculation by this method with an example.

We use the statistical data in the first example, but with introducing the advanced belief and plausibility functions. Parameter s=2 as the most safe solution [21]. When N=5, extent of contamination is

$$\chi = (1 + s / N)^{-1} = (1 + 2/5)^{-1} = 0.714.$$

Then

$$\underline{P}(A \mid c, s) = \chi \cdot 0.80 = 0.571$$

and

$$\overline{P}(A \mid c, s) = 1 - \chi[1 - 1] = 1.$$

Reliability characterized by interval [0.571; 1], which is wider then interval [0.800; 1] in above example.

Figure 5 shows that the parameter s changes the lower bound of the non-failure probability within [0,571; 0,800], in contrast to the parameter in possibilistic method, which causes the possibility of failure Q in the larger range [0; 1].

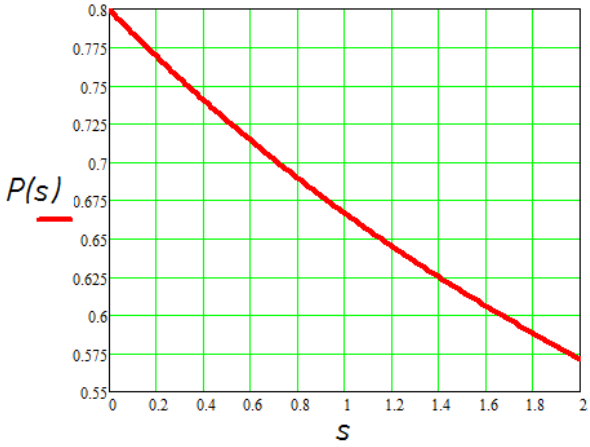


Figure 5. Probability of failure $\underline{P}$ - parameter of «uncertainty» s graph.

Therefore, a volitional decision on the appointment of the parameter *s* to a lesser extent affects on the final result of reliability analysis. And this result can be considered as more credible.

Let's use the data from the example 3 (with $k = 158$ mm), but with the advanced functions of belief and plausibility. Let *s*=1, given the higher confidence in test results and greater the credibility of the expert values and thus a lower "uncertainty" of the statistical data. With *N*=5 we calculate:

$$\chi = (1 + s/N)^{-1} = (1 + 1/5)^{-1} = 0{,}833.$$

Then

$$\underline{P}(A \mid c, s) = \chi \cdot 1 = 0{,}833$$

and

$$\overline{P}(A \mid c, s) = 1 - \chi[1 - 1] = 1.$$

Reliability is characterized by the interval [0,833; 1], which more correct then interval [1; 1] in Example 3.

Thus, using of advanced functions of belief and plausibility using the imprecise Dirichlet model and random sets theory allow us to obtain more conclusive results of reliability analysis for a single crack in the concrete. But the advanced functions are parametric (including parameter *s*).

As a result of using the advanced functions of belief and plausibility, we can get the expanded boundaries of the mathematical expectation of a random variable *X*:

$$\underline{F}(x \mid c, s) = \underline{P}(\{w \le x\} \mid c, s) = \\ = \begin{cases} (N+s)^{-1} \sum\limits_{i:\sup\ A_i \le x} c_i, & x < \Omega_* \\ 1, & x = \Omega_*; \end{cases}$$

$$\overline{F}(x \mid c, s) = \overline{P}(\{w \le x\} \mid c, s) = \\ = \begin{cases} (N+s)^{-1} \left(s + \sum\limits_{i:\sup\ A_i \le x} c_i, x \right) > \Omega_* \\ 0, \quad x = \Omega_*. \end{cases}$$

By [20], bounds of the mathematical expectation of a random variable *X* represented by intervals (such as probability of non-failure) can be found as:

$$\underline{E}X = \int_{\Omega} \omega d\overline{F}(\omega \mid c, s) = \\ = (N+s)^{-1} \left(s \cdot \Omega_* + \sum_{i=1}^{n} c_i \inf\ A_i \right);$$

$$\overline{E}X = \int_{\Omega} \omega d\underline{F}(\omega \mid c, s) = \\ = (N+s)^{-1} \left(s \cdot \Omega^* + \sum_{i=1}^{n} c_i \sup\ A_i \right).$$

Let conventionally known intervals, which characterizing the reliability of a reinforced concrete beam according to the criterion of crack length: [0,995; 1], [0,997; 1], [0,994; 1], [0,995; 1]. It is known that the reliability of changes in the boundaries of the interval $[\Omega_{*}=0;\ \Omega^{*}=1]$. Take s=0.4. Then:

$$\underline{E}X = (4+0{,}4)^{-1}(0{,}4\cdot 0 + 0{,}995 + \\ + 0{,}997 + 0{,}994 + 0{,}995) = 0{,}9,$$
$$\overline{E}X = (4+0{,}4)^{-1}(0{,}4\cdot 1 + 1 + 1 + 1 + 1) = 1.$$

Subject to uncertainty *s*=0,4 of source data, the mathematical expectation of the reliability of reinforced concrete beam according to the criterion of crack length is characterized by the interval [0.905; 1]. In the absence of "uncertainty " (when *s*=0):

$$\underline{E}X = (4+0)^{-1}(0\cdot 0 + 0{,}995 + \\ + 0{,}997 + 0{,}994 + 0{,}995) = 0{,}9953,$$
$$\overline{E}X = (4+0)^{-1}(0\cdot 1 + 1 + 1 + 1 + 1) = 1,$$

statistical mathematical expectation of the reinforced concrete beam reliability according to the criterion of crack length is characterized by the interval [0,9953; 1].

Thus, advanced functions of belief and plausibility can be used in practice of reliability analysis, having the advantage over methods based on the theory of possibilities, that the *s* parameter is lesser affects on the results of reliability compared with the parameter (cut level α) in possibilisitc method.

Returning to the cracks system in reinforced concrete beams and reliability analysis using the theory of random sets, with the conditions of independence in the interaction between cracks, the reliability analysis of reinforced concrete beam produced by each crack of the beam with the results by the lower and upper values of probabilities, and the reliability of the beam as system according to the criterion of crack length is characterized by [20] interval

$$\left[\prod_{i=1}^{n}\underline{P}_i;\ \prod_{i=1}^{n}\overline{P}_i\right],\quad i=1,\ldots,n,$$

where *n* is the number of cracks in the beam.

Possibilistic method of reliability analysis may be recommended in case of a very small amount of statistical data in the form of individual values. In this case, it should carefully consider the purpose of the cut (risk) level α and take it on the recommendations and in the interval [0,01; 0,1], or other reasonable methods depending on the level of safety. Parameter "*s*" also is subject to additional research.

6. CONCLUSIONS

1. The article describes the method of reliability analysis of structural RC elements on example of RC beams with a series of normal cracks on the basis of the possibility theory;
2. Some recommendations are given for the appointment of the cut (risk) level in possibilistic methods of reliability analysis of structural elements;
3. The article presents the methods of reliability analysis of reinforced concrete beams with a series of normal cracks on the basis of the random set theory and on the advanced functions of belief and plausibility on the imprecise Dirichlet model;
4. The developed methods can be used in the reliability analysis of other structural elements for the requirements of standards on safety of structures and foundations.

REFERENCES

1. **Keshtegar B., Kisi O.** M5 Model Tree and Monte Carlo Simulation for Efficient Structural Reliability Analysis. // Applied Mathematical Modelling, 2017, Volume 48, pp. 99-910.
2. **Krejsa M., Janas P., Krejsa V.** Structural Reliability Analysis Using DOProC

Method. // Procedia Engineering, 2016, Volume 142, pp. 34-41.
3. **Olmati P., Sagaseta J., Cormie D., Jones A.E.K.** Simplified Reliability Analysis of Punching in Reinforced Concrete Flat Slab Buildings Under Accidental Actions. // Engineering Structures, 2017, Volume 130, pp. 83-98.
4. **El Ghoulbzouri A., Kissi B., Khamlichi A.** Reliability Analysis of Reinforced Concrete Buildings: Comparison between FORM and ISM. // Procedia Engineering, 2015, Volume 114, pp. 650-657.
5. **Al-Ansari M.S.** Reliability and Flexural Behavior of Triangular and T-reinforced Concrete Beams. // International Journal of Advanced Structural Engineering, 2015, Volume 7, Issue 4, pp. 377-386.
6. **Eamon C.D., Jensen E.** Reliability Analysis of Prestressed Concrete Beams Exposed to Fire. // Engineering Structures, 2012, Volume 43, pp. 69-77.
7. **Faroz S.A., Pujari N.N., Ghosh S.** Reliability of a Corroded RC Beam Based on Bayesian Updating of the Corrosion Model. // Engineering Structures, 2016, Volume 126, pp. 457-468.
8. **Dubois D., Prade H.** Possibility Theory. Plenum, New York Press, 1988, 263 pages.
9. **Zadeh L.A.** Fuzzy sets. // Information and Control, 1965, Volume 8, Issue 3, pp. 338-353.
10. **Dempster A.P.** Upper and Lower Probabilities Induced by Multivalued Mapping. // Annals of Mathematical Statistic, 1967, Volume 38, No. 2, pp. 325-329.
11. **Shafer G.A.** Mathematical Theory of Evidence. Princeton: Princeton university press, 1976, 297 pages.
12. **Zaytsev Yu.V.** Mekhanika Razrusheniia Dlia Stroitelei [Mechanics of Destruction for Builders]. Moscow, Vysshaya shkola, 1991, 287 pages.
13. **Piradov K.A., Savitskiy N.V.** Mekhanika Razrusheniya i Teoriya Zhelezobetona [Fracture Mechanics and Theory of Reinforced Concrete]. Concrete and reinforced concrete, 2014, No. 4, pp. 23-25.
14. **Utkin V.S., Solovyev S.A.** Reliability Analysis of Existing Reinforced Concrete Beams on Normal Crack Length Criterion. // International Journal for Computational Civil and Structural Engineering, 2017, No. 2, pp. 56-63.
15. **Gvozdev A.A.** Novoe v Proektirovanii Betonnykh i Zhelezobetonnykh Konstruktsii [New in the Design of Concrete and Reinforced Concrete Structures]. Moscow, Stroyizdat, 1978, 158 pages.
16. **Varlamov A.A., Krutsiljak M.M., Krutsiljak Yu.M**. Sposob Opredeleniia Kriticheskogo Koeffitsienta Intensivnosti Napriazheniia v Izdelii [Patent No. RF 2324916, MPK. Technique for determining critical stress intensity coefficient in a body]. Patent holder MGTU im. G.I. Nosova, 2012.
17. **Gurov S.V., Utkin L.V.** Nadezhnost' Sistem pri Nepolnoi Informatsii [Reliability of Systems under Incomplete Information]. Sankt Petersburg, Lubavich, 1999, 166 pages.
18. **Utkin V.S., Solov'ev S.A., Kaberova A.A. et al.** Patent No. RF 2596694, MPK G01B 7/00. Sposob Izmereniya Dliny Treshchiny i Skorosti ee Razvitiya Izgibaemykh i Rastyagivaemykh Elementov Konstruktsiy [Patent No. RF 2596694, MPK G01B 7/00. Crack Length Measurement Method and Rate of Crack Propagation of Bending and Tensile Structural Elements]. Patent holder Vologodsky State University, no. 2015131233/28; appl. 27.07.2015; publ. 10.09.2016, bulletin no. 25.
19. **Utkin V.S., Solov'ev S.A.** Opredelenie Nadezhnosti i Nesushchei Sposobnosti Elementov Konstruktsii s Ispol'zovaniem Teorii Svidetel'stv Dempstera-Shefera [Calculation of Reliability and Bearing Capacity of Structures Using Evidence Theory]. // Structural Mechanics and

Analysis of Constructions, 2015, No. 5, pp. 38-45.
20. **Utkin L.V.** Analiz Riska i Priniatie Reshenii pri Nepolnoi Informatsii [Risk Analysis and Decision Making under Incomplete Information]. Saint-Petersburg, Nauka, 2007, 404 pages.
21. **Bernard J.M.** Analysis of Local or Asymmetric Dependencies in Contingency Tables using the Imprecise Dirichlet Model. // International Symposium on Imprecise Probabilities and Their Applications, 2003, pp. 46-62.

СПИСОК ЛИТЕРАТУРЫ

1. **Keshtegar B., Kisi O.** M5 Model Tree and Monte Carlo Simulation for Efficient Structural Reliability Analysis. // Applied Mathematical Modelling, 2017, Volume 48, pp. 99-910.
2. **Krejsa M., Janas P., Krejsa V.** Structural Reliability Analysis Using DOProC Method. // Procedia Engineering, 2016, Volume 142, pp. 34-41.
3. **Olmati P., Sagaseta J., Cormie D., Jones A.E.K.** Simplified Reliability Analysis of Punching in Reinforced Concrete Flat Slab Buildings Under Accidental Actions. // Engineering Structures, 2017, Volume 130, pp. 83-98.
4. **El Ghoulbzouri A., Kissi B., Khamlichi A.** Reliability Analysis of Reinforced Concrete Buildings: Comparison between FORM and ISM. // Procedia Engineering, 2015, Volume 114, pp. 650-657.
5. **Al-Ansari M.S.** Reliability and Flexural Behavior of Triangular and T-reinforced Concrete Beams. // International Journal of Advanced Structural Engineering, 2015, Volume 7, Issue 4, pp. 377-386.
6. **Eamon C.D., Jensen E.** Reliability Analysis of Prestressed Concrete Beams Exposed to Fire. // Engineering Structures, 2012, Volume 43, pp. 69-77.
7. **Faroz S.A., Pujari N.N., Ghosh S.** Reliability of a Corroded RC Beam Based on Bayesian Updating of the Corrosion Model. // Engineering Structures, 2016, Volume 126, pp. 457-468.
8. **Dubois D., Prade H.** Possibility Theory. Plenum, New York Press, 1988, 263 pages.
9. **Zadeh L.A.** Fuzzy sets. // Information and Control, 1965, Volume 8, Issue 3, pp. 338-353.
10. **Dempster A.P.** Upper and Lower Probabilities Induced by Multivalued Mapping. // Annals of Mathematical Statistic, 1967, Volume 38, No. 2, pp. 325-329.
11. **Shafer G.A.** Mathematical Theory of Evidence. Princeton: Princeton university press, 1976, 297 pages.
12. **Зайцев Ю.В.** Механика разрушения для строителей. – М.: Высшая школа, 1991. – 287 с.
13. **Пирадов К.А., Савицкий Н.В.** Механика разрушения и теория железобетона. // Бетон и железобетон, 2014, №4, с. 23-25.
14. **Utkin V.S., Solovyev S.A.** Reliability Analysis of Existing Reinforced Concrete Beams on Normal Crack Length Criterion. // International Journal for Computational Civil and Structural Engineering / Международный журнал по расчету гражданских и строительных конструкций, 2017, No. 2, pp. 56-63.
15. **Гвоздев А.А.** Новое в проектировании бетонных и железобетонных конструкций. – М.: Стройиздат, 1978. - 158 с.
16. Патент РФ №2324916. МПК G01N3. Способ определения критического коэффициента интенсивности напряжения в изделии. Авторы: Варламов А.А., Круциляк М.М., Круциляк Ю.М. Патентообладатель: МГТУ им. Г.И. Носова. – 2012.
17. **Гуров С.В., Уткин Л.В**. Надежность систем при неполной информации. СПб: Любавич, 1999. – 166 с.

18. Патент РФ 2596694. МПК G01B7/00. Способ измерения длины трещины и скорости ее развития в изгибаемых и растянутых элементах конструкций. – Авторы: Уткин В.С., Соловьев С.А., Каберова А.А., Русанов В.В. – Патентообладатель: ФГБОУ ВО «ВоГУ». – 2015.
19. **Уткин В.С., Соловьев С.А.** Определение надежности и несущей способности элементов конструкций с использованием теории свидетельств Демпстера-Шефера. // Строительная механика и расчет сооружений, 2015, №5, с. 38-45.
20. **Уткин Л.В.** Анализ риска и принятие решений при неполной информации. – СПб.: Наука, 2007. – 404 с.
21. **Bernard J.M.** Analysis of Local or Asymmetric Dependencies in Contingency Tables using the Imprecise Dirichlet Model. // International Symposium on Imprecise Probabilities and Their Applications, 2003, pp. 46-62.

Vladimir S. Utkin, Dr. Sc., Professor, Department of Industrial and Civil Engineering, Vologda State University; 15, Lenin Street, Vologda, 160000, Russia; phone/fax: +7 (8172) 51-83-96;
E-mail: utkinvogtu@mail.ru.

Sergey A. Solovyev, Ph.D. Student, Department of Industrial and Civil Engineering, Vologda State University; 15, Lenin Street, Vologda, 160000, Russia; phone/fax: +7 (8172) 51-83-96;
E-mail: ser6sol@yandex.ru.

Уткин Владимир Сергеевич, доктор технических наук, профессор кафедры промышленного и гражданского строительства Вологодского государственного университета; 160000, Россия, г. Вологда, ул. Ленина, д. 15; тел. +7 (8172) 51-83-96;
E-mail: utkinvogtu@mail.ru.

Соловьев Сергей Александрович, аспирант кафедры промышленного и гражданского строительства Вологодского государственного университета; 160000, Россия, г. Вологда, Набережная 6 Армии, д. 201, тел. +7 (8172) 27-32-82;
E-mail: ser6sol@yandex.ru.

DOI:10.22337/2587-9618-2018-14-3-153-160

STUDY AND SIMULATION OF HEAT TRANSFER PROCESSES DURING FOAM GLASS HIGH TEMPERATURE PROCESSING

Sergey V. Fedosov [1], Maksim O. Bakanov [2], Sergey N. Nikishov [1, 2]

[1] Ivanovo State Polytechnic University, Ivanovo, RUSSIA

[2] Ivanovo Fire Rescue Academy of State Firefighting Service of Ministry of Russian Federation for Civil Defense, Emergencies and Elimination of Consequences of Natural Disasters, Ivanovo, RUSSIA

Abstract: The paper presents basic aspects of simulation of pores formation and growth in the foam glass structure process during raw material mixture high temperature processing. The key mathematical approaches to heat transfer processes simulation and the dynamics of the pores radius growth in the raw material mixture structure are presented. The key assumptions and restrictions allowing representing the most adequate research outcomes at this stage of the subject development are outlined.

Keywords: foam glass, heat treatment, mathematical simulation, temperature patterns, surface tension, viscosity

ИССЛЕДОВАНИЕ И МОДЕЛИРОВАНИЕ ПРОЦЕССОВ ТЕПЛОПЕРЕНОСА ПРИ ВЫСОКОТЕМПЕРАТУРНОЙ ОБРАБОТКЕ ПЕНОСТЕКЛА

С.В. Федосов [1], М.О. Баканов [2], С.Н. Никишов [1, 2]

Ивановский государственный политехнический университет», г. Иваново, РОССИЯ

[2] Ивановская пожарно-спасательная академия Государственной противопожарной службы Министерства Российской Федерации по делам гражданской обороны, чрезвычайным ситуациям и ликвидации последствий стихийных бедствий, г. Иваново, РОССИЯ

Аннотация: в работе представлены основные аспекты моделирования процесса формирования и роста пор в структуре пеностекла при высокотемпературной обработке сырьевой смеси. Показаны ключевые математические подходы к моделированию процессов теплопереноса и динамики роста радиуса поры в структуре сырьевой смеси. Обозначены основные допущения и ограничения, позволяющие на данном этапе разработки темы представить наиболее адекватные результаты исследования.

Ключевые слова: пеностекло, термическая обработка, математическое моделирование, температурные поля, поверхностное натяжение, вязкость

1. INTRODUCTION

Improvement of the buildings thermal insulation and housing and utilities infrastructure energy efficiency constitutes one of the energy saving directions. Modern requirements related to building envelopes energy saving determine the use of high-tech materials and systems enabling to solve the issue of the buildings effective thermal protection.

Despite the fact that in recent years the issues of thermal insulating materials range expanding and quality improving has attracted considerable attention the construction market continue to experience shortage in this product.

Insufficient attention is given to assessing the reliability of newly developed materials in buildings envelopes which are often not interlinked with climatic, inventory and logistics and economic conditions of separate regions of our country.

Pursuant thereto, elaboration of physic-and-engineering and structural-and-technological basis for energy-efficient materials creation constitutes relevant objective for the construction industry. High-performance thermal insu-

lating material characterized with cellular structure - foam glass [1] - is gaining increasing urgent imperative.

Foam glass is a highly porous material (80-95%), consisting of closed or intercommunicating pores separated by vitrifaction separating partitions [2, 3]. Conventionally, foam glass is produced on the basis of secondary glass cullet or specially welded glass (finely crushed glass), with its full or partial introduction into the raw material mixture composition [4].

Several research directions within which scientists actively conduct their survey are visible in the foam glass technology. One of the directions is to optimize the raw material mixture heat treatment for foamed glass production. The key research method of this direction is the mathematical simulation of thermal processing operations during the foam glass production.

2. RESEARCH METHODS. PROBLEM STATEMENT

Thermal processing operations simulation is executed on the basis of heat transfer theory which allows considering intercorrelation of macrophysical characteristics of foamed glass production engineering operation.

Consideration of the process physical foundations is not insignificant because the end material thermal insulating properties are depend directly on other physic-and-engineering characteristics, which change over time and under temperature modification [6].

During the simulation we take the primary environment as the raw material mixture backfilling for foamed glass production in the foaming mold, where the microdomains not filled with crushed glass and gas-forming agents act as pores. The primary system is a chaotic structure, which causes certain difficulties in the process mathematical description, so the necessity in elaboration of the arranged mathematical model reflecting all the primary structure major peculiarities appears.

It is obligatory to formalize both the heat transfer processes and the physical processes taking place when changing the heat treatment modes.

With temperature increasing, existing moisture in the raw material mixture starts to evaporate and exits to the furnace chamber for foaming. When the temperature values in the furnace chamber are close to the values when the glass grains melting starts, the backfilling near-surface layers that are in the immediate contact with the foaming mold metal bezels start to melt first, and somewhat later (in terms of time) the layer, which is heated through convection. The process of backfilling near-surface melting (raw material mixture) takes place – the backfilling central areas are still not heated (due to the surrounding material low thermal conductivity). As a result thereof, the gas-emission sources in these pores do not operate, while the glass particles surrounding this center are already being foamed, and pore radius growth continues in it. Thus, the pore formation material of the charge is formed unevenly, which affects the end product thermal and physical properties quality.

In cases where the temporal parameters for the raw material mixture conditioning during foaming are not sufficient to enable the glass grains melting over the backfill entire volume, the raw material mixture centers need more time for melting, and thus remain not porous. In cases where the foaming period is considerably exceeding the glass grains melting period, fusing of the backfilling near-surface layers takes place since gas production sources completely burn up through warming up, and the glass viscosity decreases, and the molten glass surface tension does not allow delaying a dedicated gas phase in the formed pores spheres, which exits to the furnace chamber for foaming. In such cases, the raw material mixture central part becomes more porous compared to the raw material mixture surface layers.

Thus, we assume that the distribution of temperature patterns over the backfilling of the raw material mixture passes from near-surface areas to the center. The first objective of the research was to determine and describe the temperature

patterns distribution in the raw material mixture backfilling volume and to identify the patterns of the pore radius growth as a result of its high temperature processing.

The second objective was to determine the conditions for the pores uniform formation over the material volume. Such conditions can be created, for example, through various technical means and technologies, allowing to influence the raw material mixture in real-time, for example, the vibration platforms or ultrasonic treatment application as well as application of powders with different gas-yielding properties (activity), combination of these and other technological influences is possible.

Difficulties which solution requires the heat transfer simplified (or approximate) mathematical models application appear when developing the unified mathematical model able to take into consideration all the above mentioned factors.

As a rule, mathematical physics methods are used for the differential equations solution. In some specific cases, these equations can be solved through numerical methods using computer. However, difficulties related to computational nature arise herewith.

In general case, the heat and substance mass transfer boundary problem can be represented with parabolic type non-linear non-homogeneous differential equations in particular derivatives:

- heat conductivity boundary problem:

$$\rho(u,t)\cdot c(u,t)\frac{\partial t(x,\tau)}{\partial \tau}=\frac{\partial}{\partial x}\left[\lambda(u,t)\frac{\partial t(x,\tau)}{\partial x}\right], \quad (1)$$

where $\rho(u,t), c(u,t), \lambda(u,t)$ - is the thermal properties of the foam glass charge material (density, heat capacity, thermal conductivity), in general case depending on the moisture content and temperature;

- initial condition:

$$t(x,\tau)\big|_{\tau=0}=t_0(x) \quad (2)$$

- boundary conditions:

$$t(x,\tau)\big|_{x=0}=f_н(\tau) \quad (3)$$

$$\left.\frac{\partial t(x,\tau)}{\partial x}\right|_{x=\frac{L}{2}}=0 \quad (4)$$

The initial condition (5) demonstrates that foam glass charge material is characterized with an arbitrary temperature distribution on a coordinate at the moment taken for the reference point.

The boundary condition (6) demonstrates that we have assumed the equality of the mold temperature and material values from which the coordinate x is calculated in the walls contact zone of the metal mold for foaming. Condition (7) indicates that the objective can be considered as a symmetrical one.

It is obligatory to set the boundary conditions and solve the plane problem for one of the coordinates in the modeling early stages. Figure 1 shows the boundary problem of heat transfer in foam glass charge material for the metal mold on the ***x*** coordinate.

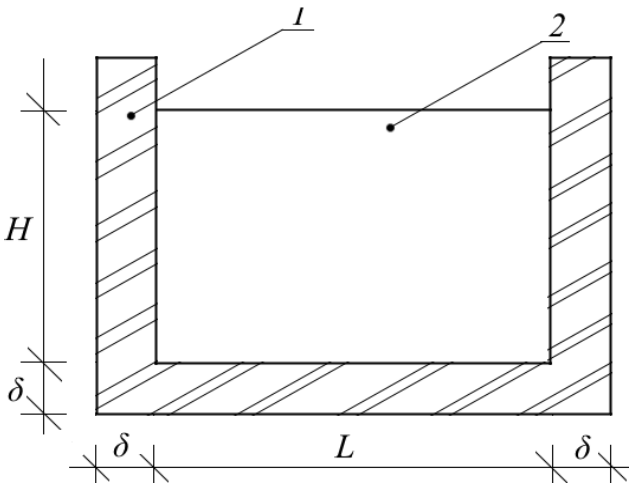


Figure 1. The raw material mixture model (2) – metal mold (1).

Under these conditions the boundary problem of heat transfer in the raw material mixture in metal mold shall be recorded as follows:

$$\rho c\frac{\partial t(x,\tau)}{\partial \tau}=\lambda\frac{\partial^2 t(x,\tau)}{\partial x^2};\ \tau>0;\ 0\le x\le\frac{L}{2}, \quad (5)$$

$$t(x,\tau)\big|_{\tau=0} = t_0(x), \quad (6)$$

$$t(x,\tau)\big|_{x=0} = t_н, \quad (7)$$

$$\frac{\partial t(x,\tau)}{\partial x}\bigg|_{x=\frac{L}{2}} = 0, \quad (8)$$

Here: ρ, c, λ – respectively: the raw material mixture density, heat capacity and thermal conductivity.

Let us introduce dimensionless variables:

$$T\left(\bar{x}, Fo\right) = \frac{t(x,\tau)-t_0}{t_н - t_0}; \; Fo = \frac{a\tau}{(L/2)^2}; \; \bar{x} = \frac{x}{(L/2)}; \quad (9)$$

And then the problem (5)-(8) assumes the view:

$$\frac{\partial T\left(\bar{x}, Fo\right)}{\partial Fo} = \frac{\partial^2 T\left(\bar{x}, Fo\right)}{\partial \bar{x}^2}; \; Fo > 0; \; 0 \le \bar{x} \le 1; \quad (10)$$

$$T\left(\bar{x}, Fo\right) = \frac{t(x,\tau)-t_0}{t_н - t_0} = T_0\left(\bar{x}\right); \quad (11)$$

$$T\left(\bar{x}, Fo\right)\big|_{\bar{x}=0} = \frac{t_н - t_0}{t_н - t_0} = 1; \quad (12)$$

$$\frac{\partial T\left(\bar{x}, Fo\right)}{\partial \bar{x}}\bigg|_{\bar{x}=1} = 0. \quad (13)$$

3. RESEARCH OUTCOMES

Omitting ordinary but cumbersome conversions, we provide the final solution of the boundary problem in the originals area:

$$T\left(\bar{x}, Fo\right) = 1 - \frac{4}{\pi}\sum_{n=1}^{\infty}\frac{1}{(2n-1)}\sin\left[\frac{\pi}{2}(2n-1)\bar{x}\right]\cdot$$
$$\cdot\exp\left[-\frac{\pi^2}{4}(2n-1)^2 Fo\right] +$$
$$+ 2\sum_{n=1}^{\infty}\sin\left[\frac{\pi}{2}(2n-1)\bar{x}\right]\cdot\int_0^1 T_0(\xi)\cdot$$
$$\cdot\sin\left[\frac{\pi}{2}(2n-1)\xi\right]d\xi\cdot\exp\left[-\frac{\pi^2}{4}(2n-1)^2 Fo\right] \quad (14)$$

Calculation results according to the equation (14) are shown in Figure 2 as curves illustrating the dimensionless temperature change on the dimensionless coordinate depending on the dimensionless process time.

Thus, the equations system (5–8) with initial (2) and boundary (3–4) conditions is called the heat transfer boundary problem and in general demonstrates the temperature patterns distribution in the raw material mixture.

Researchers [7] proposed the model based on the processes time scales during the required porous structure formation in order to describe the pores formation physical process in the raw material mixture melt:

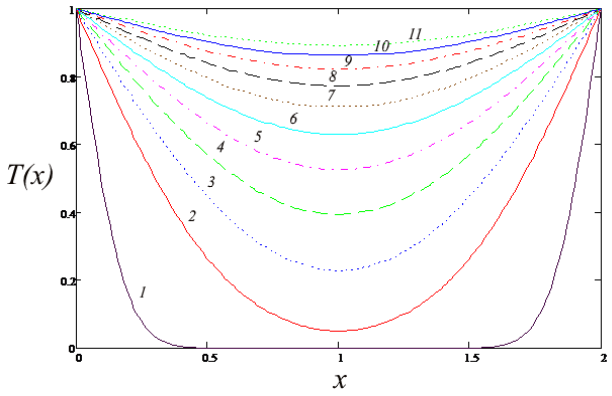


Figure 2. Illustration of calculations to the equation. Fo: 1) 0.01; 2) 0.1; 3) 0.2; 4) 0.3; 5) 0.4; 6) 0.5; 7) 0.6; 8) 0.7; 9) 0.8; 10) 0.9 11) 1.

$$\tau_1 = \frac{h^2}{a}, \quad (15)$$

where τ_1 – the crushed glass heating period to chalk decomposition temperatures range; a, m^2/s - the mixture thermal diffusivity factor; h, m – the typical length scale in the mold volume.

Pores formation due to the gas pressure increase by gas-emission sources takes place in the process second stage:

$$\tau_2 = \frac{P_0}{a}R^3, \quad (16)$$

where α' – gas-emission source power factor, J/s; P_0 – atmospheric pressure, Pa; R – pore radius, m.

In describing the second simulation stage the authors used the motion equation of a viscous incompressible fluid (Navier–Stokes) and continuity equation in spherical coordinates, simultaneously noting that the υ liquid rate around a bubble has only a radial component, and due to spherical symmetry depends only on R – distance from the pore center (pore radius) and t – process time: $\upsilon=\upsilon(R,t)$. The process second stage model represents a nonlinear differential equation for pores radius $R(t)$ growth over time:

$$-\frac{3}{2}\left(\frac{dR}{dt}\right)^2 - R(t)\frac{d^2R}{dt^2} = \frac{1}{\rho}\left(P_0 + \frac{\sigma}{R}\right) - \frac{1}{\rho}\cdot\frac{\beta' + \alpha' t}{R^3} + \nu\left[\frac{1}{\left(\frac{dR}{dt}\right)}\frac{d^2R}{dt^2} + \frac{4}{3R}\left(\frac{dR}{dt}\right)\right], \quad (17)$$

where ρ – melt density of cellular glass charge stock, [kg/m^3]; $R(t)$ – the function of cell radius increase over time; α' – power factor of gas generating source, [J/s]; β' – initial conditions factor, [J]; R – cells radius [m]; P_0 – atmospheric pressure, [PA]; σ – melt surface tension factor of the cellular glass charge stock, [N/m].

Analysis of the work outcomes related to foam glass porous structure formation suggests using equation (18), which describes the single pore growth:

$$\frac{\partial R_1}{\partial t} = \frac{\frac{3V_l}{4\pi} + R_1^3}{\mu\frac{3V_l}{\pi}}((p_{\text{int.}} - p_{ext.})\cdot R_1 - 2\sigma\ , \quad (18)$$

where R_1 – is the pores inner radius [m]; V_l – molten glass volume within the pores shell; σ – surface tension factor, [N/m]; μ – fluid dynamic viscosity factor [PA·s]; $p_{int.}$ – gas pressure inside pore, [PA]; $p_{ext.}$ – pressure on the glass melt external (outer) boundary, [Pa].

The Runge–Kutta fourth-order method [8] in the MathCAD program was used for calculations and equation graphical interpretation (18).

Four function values for two intermediate points were used on the following step: two values in the center of the step and the two values at the ends of the step:

$$k_1 = h\cdot f(t_i\cdot R_i); \quad (19)$$

$$k_2 = f(t_i\cdot\frac{1}{2}\cdot h, R_i + k_1\cdot\frac{1}{2}\cdot\Delta R_i); \quad (20)$$

$$k_3 = f(t_i\cdot\frac{1}{2}\cdot h, R_i + k_2\cdot\frac{1}{2}\cdot\Delta R_i); \quad (21)$$

$$k_4 = f(t_i\cdot h, R_i + k_3\cdot\Delta R_i); \quad (22)$$

$$R_{i+1} = R_i + (k_1 + 2k_2 + 2k_3 + k_4)\cdot\frac{1}{6}\Delta R_i\ . \quad (23)$$

Values μ and σ at calculations are taken as variables.

Changing the values of dynamic viscosity was calculated by the formula [9, 10]:

$$\mu = \mu_0\cdot 10^{A\cdot\frac{T_0 - T}{(T - B)\cdot(T_0 - C)}}, \quad (24)$$

where μ_0 – factor of dynamic viscosity at the initial moment of time [Pa·s], To – temperature at initial moment of time [K], T – temperature [K], A and B – empirical factors.

Changing the values of surface tension factor calculated by the formula [11]:

$$\sigma = \sigma_0 - 0{,}004\cdot\frac{T - 1173}{100}\ , \quad (25)$$

where σ_0 – factor of surface tension at the initial moment of time [N/m].

Temperature change over time was prescribed as follows:

$$T = T_0 + k\cdot t\ , \quad (26)$$

where k – factor taking into account the heating rate, t – time [sec].

Calculations results are presented in Figure 3.

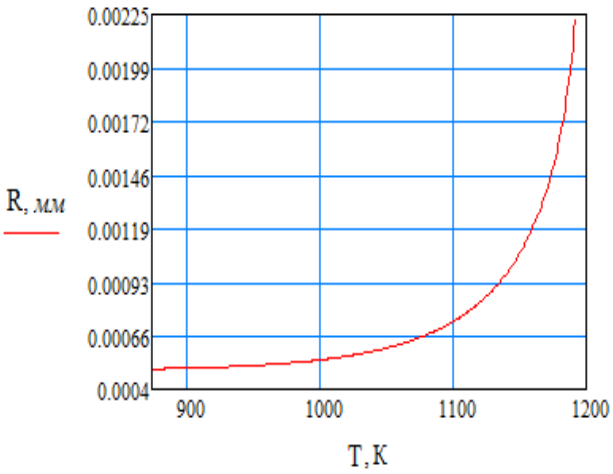


Figure 3. Diagram of pores radius growth depending on the temperature.

4. OUTCOMES DISCUSSION

Application of the equation (18) is admissible when making a number of assumptions and allows creating a shared understanding of the foam glass foaming process, since glass melt viscosity indices exert the greatest influence on the bubble growth rate and radius of all the used variables, as the start and end values are characterized by changes from 10^{12} to 10. Glass viscosity value depends on the primary raw material and pursuant to [12] considerably changes in the foaming process (Figure 4).

5. CONCLUSIONS

Adequate methods enabling to analytically determine the dependence of the glass melt viscosity on temperature is currently not available, so it is necessary to conduct experimental studies ultimately limiting the mathematical model application only for the particular primary raw materials used in the experiment.

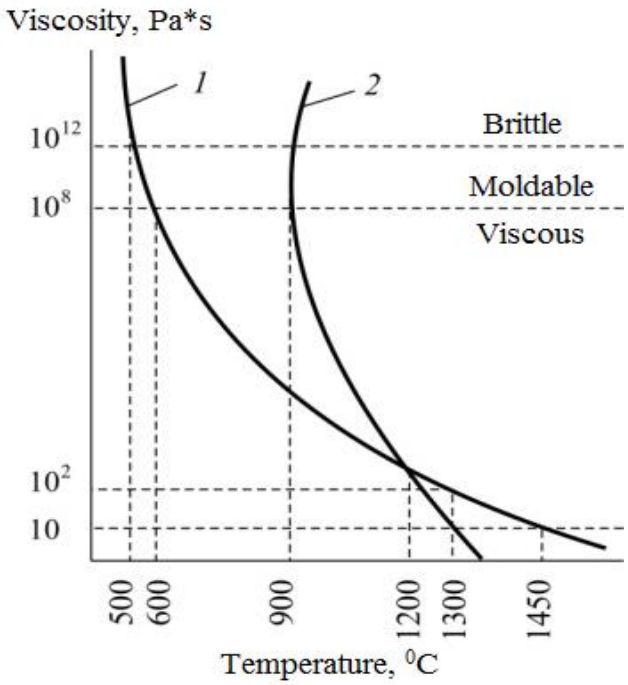


Figure 4. Dependence of the glass melt viscosity on the glass temperature and class: 1 – "Long" glass; 2 – "Short" glass.

The above mentioned suggests that there exists the necessity in mathematical models elaboration capable, with a sufficiently high accuracy, to describe the phenomena occurring at the foam glass porous structure formation during its production, based not only on the thermophysical, but engineering, economic and other factors.

REFERENCES

1. **Minko N.I., Beam O.V., Evtushenko E.I., Arzew V.M., Sergeev S.V.** Penosteklo – Sovremennyj Jeffektivnyj Neorganicheskij Teploizoljacionnyj Material [Foam Glass is a Modern Effective Inorganic Thermal Insulating Material]. // Fundamental research, 2013, No. 6-4, pp. 849-854.
2. **Bobrov Y.L., Ovcharenko E.G., Shoikhet B.M., Petukhova E.Yu.** Teploizoljacionnye Materialy i Konstrukcii [Thermal Insulating Materials and Con-

structions]. Moscow, Infra-Moscow, 2003, 268 pages.
3. **Will P.A., Alekseev S.V., Shutov A.I., Mospan V.I.** Penosteklo **[**Foam Glass]. Belgorod, Publishing house of Belgorod State Technological University, 2009, 109 pages.
4. **Sigaev, V.N., Zhakipbaev B.E., Spiridonov Iu.A.** Ispol'zovanie Gornyh Porod Dlja Poluchenija Penostekla [Rocks Application for Foam Glass Production]. // Glass and Ceramics, 2013, No. 4, pp. 47-50.
5. **Fedosov S.V., Bakanov M.O., Nikishov S.N.** Variativnost' Podhodov k Matematicheskomu Modelirovaniju Processov Termicheskoj Obrabotki Penostekol'noj Shihty [Variability of Approaches to Mathematic Simulation of Foam Glass Charge Stock Thermal Processing]. // Academic Journal Bulletin of BSTU named after V.G. Shukhov, 2017, No. 11, pp. 110–116.
6. **Tsoi P.V.** Metody Rascheta Otdel'nyh Zadach Teplomassoperenosa [Calculation Methods of the Heat and Mass Transfer Individual Problems]. Moscow, Energia, 1971, 384 pages.
7. **Fedosov S.V., Bakanov M.O., Volkov A.V. Sokol, A.I., Shapochkina Y.A.** Matematicheskaja Model' Dinamiki Processa Poroobrazovanija pri Termicheskoj Obrabotke Penostekol'noj Shihty [Mathematical Model of the Pore Formation Dynamics Owing to Heat Treatment of the Foam Glass Batc]. // Journal of Higher Educational Establishments. Chemistry and Chemical Technology, 2014, Vol. 57, Ed. 3, pp. 73-79.
8. **Bakhvalov N.S.** Chislennye Metody (Analiz, Algebra, Obyknovennye Differencial'nye Uravnenija) [Numerical Methods (Analysis, Algebra, Ordinary Differential Equations)]. Moscow, Nauka, 1975, 632 pages.
9. **Sangadiev S.Sh., Munkueva S.B., Sanditov D.S.** Opredelenie Parametrov Uravnenija Fogelja-Ful'chera-Tammana Dlja Temperaturnoj Zavisimosti vjazkosti v Oblasti Perehoda Zhidkost'-Steklo [Determination of the Vogel-Fulcher-Tammann Equation Parameters for Viscosity Temperature Dependence in the Liquid-Glass Transition Area]. // Bulletin of the Buryat State University, 2009, No. 3, pp. 153-156.
10. **Lakatos T., Johansson L.-G., Simmingskold B.** Viscosity Temperature Relation in the Glass System SiO_2-Al_2O_3-Na_2O-K_2O-CaO-MgO in the Composition Range of Technical Glasses. // Glass Technol., 1972, No. 13(3), pp. 88-95.
11. **Scholze H.** Glas Natur, Struktur und Eigenschaften. Springer – Verlag, Berlin Heidelberg New York, 1988.
12. **Semeinykh N.S. Sapegin G.V.** Analiz Ispol'zovanija Razlichnyh Syr'evyh Komponentov v Proizvodstve Granulirovannogo Penostekla [Analysis of Different Raw Materials Components Application in the Granulated Foam Glass Production]. // Bulletin of Perm National Research Polytechnic University. Construction and architecture, 2017, Vol. 8, No. 1, pp. 60-74.

СПИСОК ЛИТЕРАТУРЫ

1. **Минько Н.И., Пучка О.В., Евтушенко Е.И., Нарцев В.М., Сергеев С.В.** Пеностекло – современный эффективный неорганический теплоизоляционный материал. // Фундаментальные исследования, 2013, №6-4, с. 849-854.
2. **Бобров Ю.Л., Овчаренко Е.Г., Шойхет Б.М., Петухова Е.Ю.** Теплоизоляционные материалы и конструкции. – М.: Инфра-М, 2003. – 268 с.
3. **Воля П.А., Алексеев С.В., Шутов А.И., Мосьпан В.И.** Пеностекло. – Белгород: Изд-во БГТУ, 2009. – 109 с.
4. **Сигаев В.Н., Жакипбаев Б.Е., Спиридонов Ю.А.** Использование горных пород для получения пеностекла. // Стекло и керамика, 2013, №4, с. 47-50.

5. **Федосов С.В., Баканов М.О., Никишов С.Н.** Вариативность подходов к математическому моделированию процессов термической обработки пеностекольной шихты. // Вестник БГТУ им. В.Г. Шухова, 2017, № 11, с. 110-116.
6. **Цой П.В.** Методы расчета отдельных задач тепломассопереноса. – М.: Энергия, 1971. – 384 с.
7. **Федосов С.В., Баканов М.О., Волков А.В. Сокольский А.И., Щепочкина Ю.А.** Математическая модель динамики процесса порообразования при термической обработке пеностекольной шихты. // Известия ВУЗов. Химия и химическая технология, 2014, Том 57, Вып. 3, с. 73-79.
8. **Бахвалов Н.С.** Численные методы (анализ, алгебра, обыкновенные дифференциальные уравнения). – М.: Наука, 1975. – 632 с.
9. **Сангадиев С.Ш., Мункуева С.Б., Сандитов Д.С.** Определение параметров уравнения Фогеля-Фульчера-Таммана для температурной зависимости вязкости в области перехода жидкость-стекло. // Вестник бурятского государственного университета, 2009, №3, с. 153-156.
10. **Lakatos T., Johansson L.-G., Simmingskold B.** Viscosity Temperature Relation in the Glass System SiO_2-Al_2O_3-Na_2O-K_2O-CaO-MgO in the Composition Range of Technical Glasses. // Glass Technol., 1972, No. 13(3), pp. 88-95.
11. **Scholze H.** Glas Natur, Struktur und Eigenschaften. Springer – Verlag, Berlin Heidelberg New York, 1988.
12. **Семейных Н.С., Сопегин Г.В.** Анализ использования различных сырьевых компонентов в производстве гранулированного пеностекла. // Вестник Пермского национального исследовательского политехнического университета. Строительство и архитектура, 2017, Том 8, №1, с. 60-74.

Sergey V. Fedosov, Full Member of the Russian Academy of Architecture and Construction Science (RAACS), president of the Ivanovo state Polytechnic University; Ivanovo State Politechnical University; 20, Ul. 8 Marta, Ivanovo, 153037, Russia;
phone + 7(4932) 32-85-40; fax +7(4932) 37-19-42;
E-mail: fedosov-academic53@mail.ru.

Maxim O. Bakanov, Candidate of technical Sciences, head of Department, Ivanovo Fire Rescue Academy of State Firefighting Service of Ministry of Russian Federation for Civil Defense, Emergencies and Elimination of Consequences of Natural Disasters; 33, Prospekt Stroiteley, Ivanovo, 153040, Russia;
phone +7(4932)34-37-09; e-mail: mask-13@mail.ru.

Sergey N. Nikishov, PhD student, Ivanovo State Politechnical University; Senior Teacher, Ivanovo Fire Rescue Academy of State Firefighting Service of Ministry of Russian Federation for Civil Defense, Emergencies and Elimination of Consequences of Natural Disasters; 33, Prospekt Stroiteley, Ivanovo, 153040, Russia;
phone +7 (4932)34-37-09; e-mail: mordov5988@mail.ru.

Федосов Сергей Викторович, академик Российской академии архитектуры и строительных наук (РААСН), профессор, доктор технических наук, президент Ивановского государственного политехнического университета; 153037, Россия, Ивановская область, г. Иваново, ул. 8 Марта, д. 20;
тел. + 7(4932) 32-85-40; факс +7(4932) 37-19-42;
E-mail: fedosov-academic53@mail.ru.

Баканов Максим Олегович, кандидат технических наук, начальник кафедры, Ивановская пожарно-спасательная академия Государственной противопожарной службы Министерства Российской Федерации по делам гражданской обороны, чрезвычайным ситуациям и ликвидации последствий стихийных бедствий; 153040, Россия, Ивановская область, г. Иваново, проспект Строителей, д. 33;
тел. +7(4932)34-37-09; e-mail: mask-13@mail.ru.

Никишов Сергей Николаевич, аспирант, Ивановский государственный политехнический университет; старший преподаватель, Ивановская пожарно-спасательная академия Государственной противопожарной службы Министерства Российской Федерации по делам гражданской обороны, чрезвычайным ситуациям и ликвидации последствий стихийных бедствий; 153040, Россия, Ивановская область, г. Иваново, проспект Строителей, д. 33;
тел. +7(4932)34-37-09; e-mail: mordov5988@mail.ru.

DOI:10.22337/2587-9618-2018-14-3-161-168

MATHEMATICAL MODELING OF DIFFUSION PROCESSES OF MASS TRANSFER OF "FREE CALCIUM HYDROXIDE" DURING CORROSION OF CEMENT CONCRETES

Sergey V. Fedosov, Varvara Eu. Roumyantseva, Viktoriya S. Konovalova, Svetlana A. Loginova
Ivanovo State Polytechnic University, Ivanovo, RUSSIA

Abstract: The paper presents a mathematical model of mass transfer in the processes of corrosion of the first type of cement concrete at the level of phenomenological equations for a closed reservoir-liquid system. A step-by-step transition to the recording of the boundary value mass conduction problem in dimensionless coordinates is shown. The solutions of the boundary value mass conduction problem for the region of large and small values of Fourier numbers are obtained.

Keywords: cement concrete, corrosion, mathematical model, mass transfer, concentration of "free calcium hydroxide"

МАТЕМАТИЧЕСКОЕ МОДЕЛИРОВАНИЕ ДИФФУЗИОННЫХ ПРОЦЕССОВ МАССОПЕРЕНОСА «СВОБОДНОГО ГИДРОКСИДА КАЛЬЦИЯ» ПРИ КОРРОЗИИ ЦЕМЕНТНЫХ БЕТОНОВ

С.В. Федосов, В.Е. Румянцева, В.С. Коновалова, С.А. Логинова
Ивановский государственный политехнический университет, г. Иваново, РОССИЯ

Аннотация: В статье представлена математическая модель массопереноса в процессах коррозии первого вида цементных бетонов на уровне феноменологических уравнений для замкнутой системы «резервуар-жидкость». Показан пошаговый переход к записи краевой задачи массопроводности в безразмерных координатах. Получены решения краевой задачи массопроводности для области больших и малых значений чисел Фурье.

Ключевые слова: цементный бетон, коррозия, математическая модель, массоперенос, концентрация «свободного гидроксида кальция»

1. INTRODUCTION

Durability of buildings and structures can be provided by the use of corrosion-resistant materials. Forecasting the service life of concrete and reinforced concrete structures is a complex analytical process [1]. In most cases, the main causes of damage are corrosion processes caused by adverse environmental effects.

Reliable prediction of durability of building structures is impossible without experimental analysis and theoretical developments [2] aimed at creating mathematical models of processes occurring at all stages of production and operation [1, 2].

One of the directions of the scientific school, which works fruitfully at Ivanovo state Polytechnic University, is the theoretical study and mathematical modeling of corrosion processes of concretes proceeding along the mechanisms of the first and second types [3-9]. To date, the authors of the article have developed a complex of mathematical models of

corrosion processes in different environments, and proposed ways to combat corrosion destruction [6-9].

First of all, calcium oxide is responsible for the strength of concrete, which is part of the main minerals of Portland cement [1, 10]. The decrease in the content of "free calcium hydroxide", which is the main component that determines mass transfer, causes a change in the phase and thermodynamic equilibrium in the system, leads to the decomposition of the main components of the cement stone, and as a result, to the loss of the strength properties of concrete.

2. MATHEMATICAL MODEL OF MASS TRANSFER IN CORROSION PROCESSES OF THE FIRST TYPE AT THE LEVEL OF PHENOMENOLOGICAL EQUATIONS FOR A CLOSED "RESERVOIR-LIQUID" SYSTEM

Mass transfer in the "reservoir-liquid" system according to the first type of corrosion is determined by the boundary value problem of mass conductivity of the type [3, 4]:

$$\frac{\partial C(x,\tau)}{\partial \tau} = k\frac{\partial^2 C(x,\tau)}{\partial x^2},\ \tau > 0,\ 0 \le x \le \delta. \qquad (1)$$

Initial condition:

$$C(x,\tau)|_{\tau=0} = C(x,0) = C_0. \qquad (2)$$

Border conditions:

$$\frac{\partial C(0,\tau)}{\partial x} = 0, \qquad (3)$$

$$k\frac{\partial C(\delta,\tau)}{\partial x} = \beta[C_e(\tau) - C(\delta,\tau)]. \qquad (4)$$

where: $C(x,\tau)$ is concentration of "free calcium hydroxide" in concrete at a time τ at an arbitrary point with x coordinate, in terms of CaO, kg CaO / kg of concrete; $C_0(x)$ is concentration of "free calcium hydroxide" in concrete at the initial moment of time at any point with x coordinate, in terms of CaO, kg CaO / kg of concrete; k is mass conductivity coefficient in solid phase, m^2/s; δ is wall thickness of the structure, m.

The value of the equilibrium concentration on the surface of the solid C_e is not constant, but depends on the concentration of the component in the liquid phase:

$$C_e(\tau) = f[C_{liq}(\tau)].. \qquad (5)$$

The simplest form of this dependence is Henry's law [9]:

$$C_e(\tau) = mC_{liq}(\tau), \qquad (6)$$

where: m is Henry's constant, kg of liquid / kg of concrete.

According to the law of mass conservation, the mass flow of substance emerging from the concrete surface should be equal to the amount of substance arriving in the liquid phase.

$$-S\rho_{con}k\frac{\partial C(\delta,\tau)}{\partial x} = V_{liq}\rho_{liq}\frac{\partial C_{liq}(\tau)}{\partial \tau}, \qquad (7)$$

where: S is internal surface of the tank, m^2; V_{liq} is tank volume m^3; ρ_{con}, ρ_{liq} are densities of concrete and liquid, respectively, kg/m^3.

To obtain generalized solutions suitable for qualitative analysis of corrosion processes, we introduce dimensionless variables of the form:

$$Z(\bar{x}, Fo_m) = \frac{C_0 - C(x,\tau)}{C_0}, \bar{x} = \frac{x}{\delta}, \quad Fo_m = \frac{k\tau}{\delta^2}. \qquad (8)$$

We transform the equation (1) with regard to (8):

$$\frac{\partial C[C_0 - C(x,\tau)]}{\partial \tau \cdot C_0} = \\ = k \frac{\partial^2 C[C_0 - C(x,\tau)]}{\partial x^2 \cdot C_0}. \quad (9)$$

This implies:

$$\frac{\partial Z(\bar{x}, Fo_m)}{\partial \tau} = k \frac{\partial^2 Z(\bar{x}, Fo_m)}{\partial x^2}. \quad (10)$$

Multiply by δ^2 and divide by k both parts of the equation:

$$\frac{\partial Z(\bar{x}, Fo_m)\delta^2}{\partial \tau \cdot k} = \frac{\partial^2 Z(\bar{x}, Fo_m)\delta^2}{\partial x^2}. \quad (11)$$

In dimensionless coordinates, the boundary value problem (1)-(4) is transformed to the form [5]:

$$\frac{\partial Z(\bar{x}, Fo_m)}{\partial Fo_m} = \frac{\partial^2 Z(\bar{x}, Fo_m)}{\partial \bar{x}^2}, \quad (12)$$

$Fo_m > 0$, $0 \le \bar{x} \le 1$.

Initial condition:

$$Z(\bar{x}, 0) = 0. \quad (13)$$

Border conditions:

$$\frac{\partial Z(0, Fo_m)}{\partial \bar{x}} = 0. \quad (14)$$

$$\frac{1}{Bi_m} \cdot \frac{\partial Z(1, Fo_m)}{\partial \bar{x}} = \\ = [Z_e(Fo_m) - Z(1, Fo_m)]. \quad (15)$$

where:

$$Bi_m = \beta \cdot \frac{\delta}{k}$$

is Bio mass transfer criterion;

$$Fo_m = k \cdot \frac{\tau}{\delta^2}$$

is Fourier mass transfer criterion.

We transform the equation (7) by multiplying the summands on the left by

$$\frac{\delta}{\delta},$$

and on the right by

$$\frac{\delta^2}{\delta^2}:$$

$$-S\rho_{con} k \frac{\partial [C_0 - C(\delta,\tau)]\delta}{C_0 \partial x \cdot \delta} = \\ = V_{liq}\rho_{liq} \frac{\partial C_{liq}(\tau)\delta^2}{\partial \tau \cdot C_0 \delta^2}. \quad (16)$$

Assuming that the equilibrium in the system obeys Henry's law (6), we write:

$$\frac{S}{V} \cdot \frac{\rho_{con}}{\rho_{liq}} \cdot \frac{k}{\delta} \cdot \frac{\partial Z(0, Fo_m)}{\partial \bar{x}} = \\ - \frac{\partial Z[C_0 - mC_{liq}(\tau)]}{m\partial\left(\frac{\tau}{\delta^2}\right) C_0 \delta^2} = \\ = - \frac{\partial Z_{liq}(Fo_m)}{m\partial\left(\frac{\tau}{\delta^2}\right)\delta^2}. \quad (17)$$

Divide by k:

$$\frac{S}{V} \cdot \frac{\rho_{con}}{\rho_{liq}} \cdot \frac{1}{\delta} \cdot \frac{\partial Z(1, Fo_m)}{\partial \bar{x}} = \\ = - \frac{\partial Z_{liq}(Fo_m)}{m\partial\left(\frac{k\tau}{\delta^2}\right)\delta^2}. \quad (18)$$

The last expression denotes:

$$Z_{liq}(Fo_m) = \frac{C_0 - mC_{liq}(\tau)}{C_0}. \quad (19)$$

We denote that:

$$K_m = \frac{mS\delta}{V_{liq}} \cdot \frac{\rho_{con}}{\rho_{liq}} = \frac{mG_{con}}{G_{liq}}, \quad (20)$$

where: *Km* is coefficient considering phase characteristics; G_{con} is the mass of the concrete tank, kg; G_{liq} is the mass of liquid in the tank, kg.

In the accepted variables equation (7) will take the form:

$$-\frac{\partial Z_{liq}(Fo_m)}{\partial Fo_m} = K_m \frac{\partial Z(1, Fo_m)}{\partial \bar{x}}. \quad (21)$$

We transform the equation (6):

$$\frac{C_0 - C_e(\tau)}{C_0} = \frac{C_0 - mC_{liq}(\tau)}{C_0}. \quad (22)$$

In this case, the boundary value problem of mass conductivity will take the form:

$$\frac{\partial Z(\bar{x}, Fo_m)}{\partial Fo_m} = \frac{\delta^2 Z(\bar{x}, Fo_m)}{\partial \bar{x}^2}. \quad (23)$$

The initial and boundary conditions of expression (23) are expressions (13)-(15). In equation (15), $Z_e(Fo_m)$ is the same as $Z_{liq}(Fo_m)$.

The solution of the equation (23) obtained by the Laplace integral transformation takes the form [5, 6]:

$$\mathrm{Z}(\bar{\mathrm{x}}, \mathrm{s}) = \mathrm{Ach}\left(\sqrt{\mathrm{s}}\bar{\mathrm{x}}\right) + \mathrm{Bsh}\left(\sqrt{\mathrm{s}}\bar{\mathrm{x}}\right), \quad (24)$$

$$\frac{dZ(\bar{x}, s)}{\partial \bar{x}} = A\sqrt{s}sh\left(\sqrt{s}\bar{x}\right) + B\sqrt{s}ch\left(\sqrt{s}\bar{x}\right), \quad (25)$$

$$\frac{1}{Bi_m}\left[A\sqrt{s}sh\sqrt{s}\right] + \frac{K_m}{s}\left[A\sqrt{s}sh\sqrt{s}\right] = \frac{Z_{liq}(0)}{s} - Ach\sqrt{s}, \quad (26)$$

$$A = \frac{Bi_m\sqrt{s}Z_{liq}(0)}{s\left[ssh\sqrt{s} + K_m sh\sqrt{s} + Bi_m\sqrt{s}ch\sqrt{s}\right]} \quad (27)$$

$$Z(\bar{x}, s) = \frac{Bi_m Z_{liq}(0)ch\left(\sqrt{s}\bar{x}\right)}{s\left[ssh\sqrt{s} + Bi_m K_m sh\sqrt{s} + Bi_m\sqrt{s}ch\sqrt{s}\right]}. \quad (28)$$

The final solution of the boundary value problem (23) for the region of large values of Fourier numbers (for Fo_m > 0,1) has the form [5]:

$$Z(\bar{x}, Fo_m) = \frac{Z(0)}{1 + K_m} - 2Bi_m Z_{liq}(0)\sum_{n=1}^{\infty}\frac{\cos(\mu_m\bar{x})}{\psi'(\mu_m)}\exp(-\mu_m^2 Fo_m), \quad (29)$$

$$\psi`(\mu_\mathrm{m}) = \sin\mu_\mathrm{m}\left[3\mu_\mathrm{m}^2 + \mathrm{Bi_m}\left(\mu_\mathrm{m}^2\text{-}\mathrm{K_G b}\right)\right] + \mu_\mathrm{m}\cos\mu_\mathrm{m}\left[\mu_\mathrm{m}^2\text{-}(\mathrm{Bi_m K_G b} + 2)\right]. \quad (30)$$

The characteristic equation for finding the roots of μ_m is:

$$tg\mu_m = \frac{Bi_m\mu_m}{\mu_m^2 - K_m Bi_m}, \quad (31)$$

For the average concentration, we write:

$$Z_{mid}(Fo_m) = \frac{Z_{liq}(0)}{1 + K_m} - 2Bi_m Z_{liq}(0)\sum_{n=1}^{\infty}\frac{sin\mu_m}{\mu_m\psi'(\mu_m)}\exp(-\mu_m^2 Fo_m), \quad (32)$$

$$Z_{liq}(Fo_m) = \\ = Z_{liq}(0)\left\{1 + 2Bi_m K_m \sum_{n=1}^{\infty} \frac{sin\mu_m}{\mu_m \psi'(\mu_m)} [\exp(-\mu_m^2 Fo_m - 1]\right\}. \quad (33)$$

In cases where the condition $Fo_m \leq 0{,}1$ is satisfied, it is advisable to obtain solutions using hyperbolic functions for large values of arguments (small Fourier numbers).

The final solution of the equation (23) for the region of small values of Fourier numbers has the form:

$$\frac{Z(\bar{x}, Fo_m)}{Z_{liq}(0)} = \\ = -\frac{Bi_m}{\sqrt{Bi_m^2 - 4K_m}} \sum_{i=1}^{2} (-1)^i exp[-a_i(1 - \bar{x}) + a_i^2 Fo_m] \, erfc\left(\frac{1-\bar{x}}{2\sqrt{Fo_m}} - a_i\sqrt{Fo_m}\right), \quad (34)$$

$$a_i = \frac{-a \pm \sqrt{D}}{2}, \quad (35)$$

$$\mathrm{Z_{mid}(Fo_m)} = \int_0^1 \mathrm{Z(\bar{x}, Fo_m)} d\bar{x}, \quad (36)$$

$$\frac{Z_{liq}(Fo_m)}{Z_{liq}(0)} = 1 - \\ - \frac{K_m Bi_m}{\sqrt{Bi_m^2 - 4K_m Bi_m}} \sum_{i=1}^{2} (-1)^{i+1} \left\{ 2\sqrt{\frac{Fo_m}{\pi}} + a_i \int_0^{Fo_m} exp(a_i^2 Fo_m) erfc\left(-a_i\sqrt{Fo_m}\right) dFo_m \right\}. \quad (37)$$

The obtained expressions allow to calculate the concentration fields of the transferred component along the thickness of the structure, to find the average concentration at any time, and to determine the value of the concentration of the "target" component in the liquid phase. Some results of calculations [5-7] are shown in Figures 1 and 2.

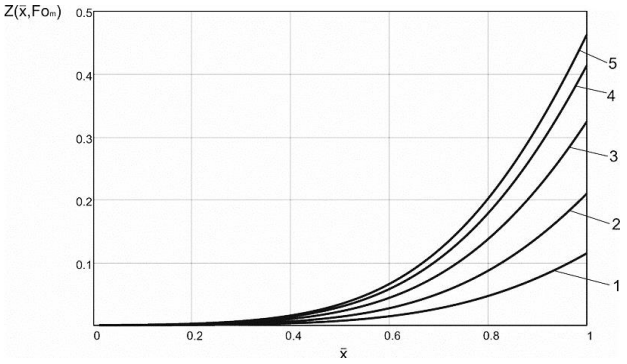


Figure 1. Profiles of the dimensionless concentrations on the thickness of the concrete at Fo_m = 0.05 at various values of Bi_m: 1 – 0.5; 2 - 1; 3 – 1.75; 4 – 2.5; 5 – 3.

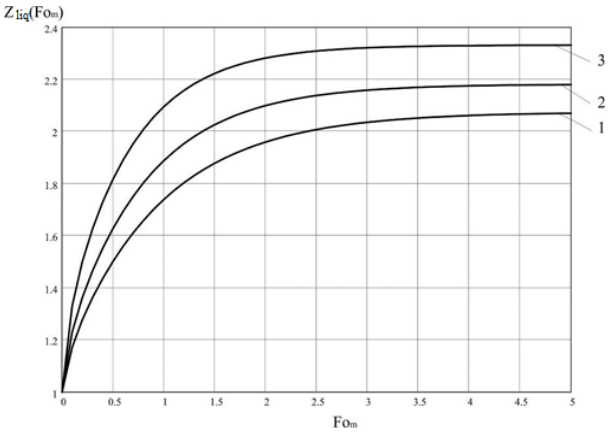


Figure 2. Concentration of the transferred component in the liquid phase at Fo_m = 0÷5; Km = 0.1; Bi_m: 1 – 0.5; 2 – 1; 3 – 1.5.

A necessary condition for the implementation of calculations is the availability of data on static and kinetic characteristics of the process, which can be obtained only on the basis of experimental studies.

3. CONCLUSION

Development of mathematical models is impossible without a clear understanding of the mechanism of the processes, experimental data characterizing the influence of various factors

on the kinetics and dynamics of processes and verification of the correctness of the forecast methodology in full-scale conditions [6, 8].

The joint analysis of the results of numerical and experimental studies confirms the adequacy of the developed mathematical models of mass transfer in the systems under study and makes it possible to use the developed mathematical models and the proposed methods for calculating the mass transfer process at the corrosion of the first and second types on real objects.

REFERENCES

1. **Moskvin V.M.** Korroziya Betona [Corrosion of Concrete]. Moscow, Gosstrojizdat, 1952, 342 pages.
2. **Stepanova V.F., Sokolova S.E., Polushkin A.L.** Problemy Dolgovechnosti Betonnyh i Zhelezobetonnyh Konstrukcij v Sovremennom Stroitel'stve [Problems of Durability of Concrete and Reinforced Concrete Structures in Modern Construction] // Bulletin of SIC Construction, 2017, No. 1(12), pp. 126-133.
3. **Fedosov S.V., Rumyanceva V.E., Kas'yanenko N.S., Krasil'nikov I.V.** Teoreticheskie i Ehksperimental'nye Issledovaniya Processov Korrozii Pervogo Vida Cementnyh Betonov pri Nalichii Vnutrennego Istochnika Massy [Theoretical and Experimental Studies of Corrosion Processes of the First Type of Cement Concrete in the Presence of an Internal Source of Mass] // Building materials. 2013. No. 6. pp. 44-47.
4. **Rumyanceva V.E., Loginova S.A.** Matematicheskoe Modelirovanie Korrozionnyh Processov Betona i Zhelezobetona [Mathematical Modeling of Corrosion Processes of Concrete and Reinforced Concrete]. // Issues of modern science and practice. University of V.I. Vernadsky, 2015, No. 1(55), pp. 235-244.
5. **Fedosov S.V., Fedosova N.L., Rumyanceva V.E., Krasil'nikov I.V.** Issledovanie Diffuzionnyh Processov Massoperenosa pri Zhidkostnoj Korrozii Pervogo Vida Cementnyh Betonov [Investigation of Diffusion Processes of Mass Transfer During Liquid Corrosion of the First Type of Cement Concretes]. // Proceedings of High Schools. Chemistry and Chemical Technology, 2015, Vol. 58, No. 1, pp. 99-104.
6. **Fedosov S.V., Rumyanceva V.E., Krasil'nikov I.V., Konovalova S.V., Karavaev I.V.** Opredelenie Resursa Bezopasnoj Ehkspluatacii Konstrukcij iz Betona, Soderzhashchego Gidrofobiziruyushchie Dobavki [Determination of Safe Service Life of Structures Made of Concrete Containing Hydrophobic Additives]. // Proceedings of high schools. Technology of the textile industry, 2017, No. 6(372), pp. 268-276.
7. **Fedosov S.V., Rumyanceva V.E., Krasil'nikov I.V., Loginova S.A.** Issledovanie Vliyaniya Processov Massoperenosa na Nadezhnost' i Dolgovechnost' Zhelezobetonnyh Konstrukcij, Ehkspluatiruemyh v Zhidkih Agressivnyh Sredah [Investigation of the Influence of Mass Transfer Processes on the Reliability and Durability of Reinforced Concrete Structures Operated in Liquid Aggressive Media]. // Building materials, 2017, No. 12, pp. 52-57.
8. **Fedosov S.V., Rumyanceva V.E., Konovalova S.V., Karavaev I.V.** ZHidkostnaya Korroziya Betonov v Srede s Razlichnoj Stepen'yu Agressivnosti [Liquid Corrosion of Concrete in the Environment with Various Degree of Aggressiveness] // Bulletin of Civil Engineers, 2017, No. 4(62), pp. 113-118.
9. **Fedosov S.V., Rumyanceva V.E., Konovalova S.V.** Issledovanie Processov Korrozionnoj Destrukcii Zhelezobetonnyh Izdelij v Agressivnyh Sredah s Hlorid-ionami [Study of the Processes of a

Corrosion Destruction of Reinforced Concrete Products in Aggressive Environments Containing Chloride Ions]. // Bulletin of civil engineers, 2016, No. 5(58), pp. 61-67.

10. **Liang Ming-Te, Shien-Min Lin.** Mathematical Model and Applications for Concrete Carbonation. // Journal of Marine Science and Technologic, 2003, Vol. 11, No. 1, pp. 20-30.

СПИСОК ЛИТЕРАТУРЫ

1. **Москвин В.М.** Коррозия бетона. – М.: Госстройиздат, 1952. – 342 с.
2. **Степанова В.Ф., Соколова С.Е., Полушкин А.Л.** Эффективные способы вторичной защиты для повышения долговечности зданий и сооружений. // Вестник НИЦ Строительство, 2017, №1(12), с. 126-133.
3. **Федосов С.В., Румянцева В.Е., Касьяненко Н.С., Красильников И.В.** Теоретические и экспериментальные исследования процессов коррозии первого вида цементных бетонов при наличии внутреннего источника массы. // Строительные материалы, №6, 2013, с. 44-47.
4. **Румянцева В.Е., Логинова С.А.** Математическое моделирование коррозионных процессов бетона и железобетона. // Вопросы современной науки и практики. Университет им. В.И. Вернадского, 2015, №1(55), с. 235-244.
5. **Федосов С.В., Федосова Н.Л., Румянцева В.Е., Красильников И.В.** Исследование диффузионных процессов массопереноса при жидкостной коррозии первого вида цементных бетонов. // Известия вузов. Химия и химическая технология, 2015, Том 58, Вып. 1, с. 99-104.
6. **Федосов С.В., Румянцева В.Е., Красильников И.В., Коновалова С.В., Караваев И.В.** Определение ресурса безопасной эксплуатации конструкций из бетона, содержащего гидрофобизирующие добавки. // Известия вузов. Технология текстильной промышленности, 2017, №6(372), с. 268-276.
7. **Федосов С.В., Румянцева В.Е., Красильников И.В., Логинова С.А.** Исследование влияния процессов массопереноса на надежность и долговечность железобетонных конструкций, эксплуатируемых в жидких агрессивных средах. // Строительные материалы, 2017, №12, с. 52-57.
8. **Федосов С.В., Румянцева В.Е., Коновалова С.В., Караваев И.В.** Жидкостная коррозия бетонов в среде с различной степенью агрессивности. // Вестник гражданских инженеров, 2017, №4(62), с. 113-118.

Sergey V. Fedosov, Full Member of the Russian Academy of Architecture and Construction Sciences, Professor, Doctor of Technical Sciences, head of the Department of "Technosphere safety" Ivanovo State Polytechnical University; 153037, Russia, Ivanovo region, Ivanovo, St. 8th March, 20;
phone +7(4932) 32-85-40; fax +7(4932) 37-19-42;
E-mail: fedosov-academic53@mail.ru.

Varvara E. Roumyantseva, Advisor to the Russian Academy of Architecture and Construction Sciences, Professor, Doctor of Technical Sciences, Director of the Institute of information technologies and natural Sciences and Humanities, head of the Department of nanotechnology, physics and chemistry, Ivanovo State Polytechnical University; 153037, Russia, Ivanovo region, Ivanovo, St. 8th March, 20;
phone +7(4932) 41-75-09; +7(906)617-17-84;
E-mail: varrym@gmail.com.

Viktoriya S. Konovalova, Candidate of Technical Sciences, senior lecturer of the Department of nanotechnology, physics and chemistry, Ivanovo State Polytechnical University; 153037, Russia, Ivanovo region, Ivanovo, St. 8th March, 20;
phone +7(910)997-02-68; e-mail: kotprotiv@yandex.ru.

Svetlana A. Loginova, assistant Professor of the Department of nanotechnology, physics and chemistry,

Ivanovo State Polytechnical University; 153037, Russia, Ivanovo region, Ivanovo, St. 8th March, 20;
phone +7(906)617-12-27;
E-mail: sl79066171227@yandex.ru.

Федосов Сергей Викторович, академик Российской академии архитектуры и строительных наук (РААСН), профессор, доктор технических наук, заведующий кафедрой «Техносферная безопасность» Ивановского государственного политехнического университета; 153037, Россия, Ивановская область, г. Иваново, ул. 8 Марта, д. 20; тел. +7(4932) 32-85-40; факс +7(4932) 37-19-42;
E-mail: fedosov-academic53@mail.ru.

Румянцева Варвара Евгеньевна, советник Российской академии архитектуры и строительных наук (РААСН), профессор, доктор технических наук, директор Института информационных технологий и естественно-гуманитарных наук, заведующая кафедрой нанотехнологий, физики и химии Ивановского государственного политехнического университета; 153037, Россия, Ивановская область, г. Иваново, ул. 8 Марта, д. 20; тел. +7(4932) 41-75-09; +7(906)617-17-84; e-mail: varrym@gmail.com.

Коновалова Виктория Сергеевна, кандидат технических наук, старший преподаватель кафедры нанотехнологий, физики и химии Ивановского государственного политехнического университета; 153037, Россия, Ивановская область, г. Иваново, ул. 8 Марта, д. 20; тел. +7(910)997-02-68;
E-mail: kotprotiv@yandex.ru.

Логинова Светлана Андреевна, ассистент кафедры нанотехнологий, физики и химии Ивановского государственного политехнического университета; 153037, Россия, Ивановская область, г. Иваново, ул. 8 Марта, д. 20; тел. +7(906)617-12-27;
E-mail: sl79066171227@yandex.ru.



К ЮБИЛЕЮ ВИТАЛИЯ ИВАНОВИЧА СОЛОМИНА

16 июля 2018 года исполнилось 90 лет академику Российской академии архитектуры и строительных наук, профессору, доктору технических наук Виталию Ивановичу Соломину.

Трудовая и творческая деятельность В.И. Соломина на протяжении более чем семи десятилетий – достойный пример для подражания молодому поколению, воспитанию которого он всегда уделял и уделяет большое внимание.

Мы знаем Виталия Ивановича как крупного, признанного в России и за рубежом ученого в области строительной механики, получившего выдающиеся результаты, связанные с решением нелинейных задач расчета и оптимального проектирования фундаментных конструкций и их оснований, основателя и руководителя крупной научной школы, работа которой традиционно была направлена на совершенствование методов расчета и принципов конструирования фундаментных конструкций, опытного организатора науки, образования и просветительской деятельности.

Профессиональная деятельность В.И. Соломина была неоднократно отмечена высокими государственными наградами и почетными званиями, в числе которых орден «Знак Почета», нагрудный знак Министерства высшего образования СССР «За отличные успехи в работе», медаль «50 лет Победы в Великой Отечественной войне», звания Лауреат Государственной премии СССР за заслуги в области науки и техники, Почетный строитель России, Заслуженный деятель науки и техники РСФСР, Почетный гражданин г. Челябинска и другие.

Желаем Вам, Виталий Иванович, крепкого здоровья, благополучия, большого счастья и дальнейших творческих успехов!

Редакционный Совет международного научного журнала
“International Journal for Computational Civil and Structural Engineering”

О ПРОВЕДЕНИИ ОБЩЕГО СОБРАНИЯ ЧЛЕНОВ РОССИЙСКОЙ АКАДЕМИИ АРХИТЕКТУРЫ И СТРОИТЕЛЬНЫХ НАУК В 2019 ГОДУ

На основании Устава федерального государственного бюджетного учреждения «Российская академия архитектуры и строительных наук», утвержденного постановлением Правительства Российской Федерации 28 мая 2014 г. №488, выборы президента Российской академии архитектуры и строительных наук (РААСН) и президиума РААСН будут проведены на Общем собрании членов РААСН 17-19 апреля 2019 года (Москва, Центральный дом архитектора).

Право выдвижения кандидатов на должность президента РААСН, первого вице-президента РААСН, вице-президентов РААСН (по направлениям «Архитектура», «Градостроительство», «Строительные науки», «Инновации»), академиков-секретарей отделений РААСН (архитектуры, градостроительства, строительных наук) предоставляется членам РААСН.

Выдвижение кандидатур на указанные должности осуществляется не позднее, чем за 2 (два) месяца до даты проведения Общего собрания членов РААСН.

В соответствии с постановлением президиума РААСН от 26 сентября 2018 г. №10 выборы членов РААСН (академиков РААСН и членов-корреспондентов РААСН) в 2019 году проводиться не будут.